Universiteit Leiden
The Netherlands

On preoperative systemic treatment of muscle-invasive bladder cancer
Dorp, J. van

Citation

Dorp, J. van. (2025, January 10). *On preoperative systemic treatment of muscle-invasive bladder cancer*. Retrieved from https://hdl.handle.net/1887/4175499

ON PREOPERATIVE SYSTEMIC TREATMENT OF MUSCLE-INVASIVE BLADDER CANCER

Jeroen van Dorp

On preoperative systemic treatment of muscle-invasive bladder cancer

Jeroen van Dorp

About the cover:

This classic image from *Star Wars: Episode IV - A new Hope* (1977), depicts the main character *Luke Skywalker* looking at the binary sunset on his home planet of *Tatooine*, symbolizing the beginning of his journey that will lead him to become a jedi knight and to eventually confront *Darth Vader*. The silhouette of *Luke Skywalker* has been changed to that of the author, metaphorically pondering over the molecular events that are taking place when a cancer patient is treated with immune checkpoint inhibitors. The darker sun symbolizes a tumor cell that uses multiple immune checkpoints to prevent recognition by the immune system. The bright sun symbolizes an activated T-cell with blocked CTLA-4 and PD-1 molecules, preventing inhibition by the tumor cell and allowing for recognition and eventually killing of the tumor cell.

On preoperative systemic treatment of muscle-invasive bladder cancer

Proefschrift

ter verkrijging van
de graad van doctor aan de Universiteit Leiden,
op gezag van rector magnificus prof.dr.ir. H. Bijl,
volgens besluit van het college voor promoties
te verdedigen op vrijdag 10 januari 2025
klokke 13:00 uur

door
Jeroen van Dorp

TABLE OF CONTENTS

CHAPTER 1

General introduction and outline of thesis

EPIDEMIOLOGY OF BLADDER CANCER

Urothelial carcinoma of the bladder, more commonly described as bladder cancer (BC), is the 10th most common cancer worldwide[1,2]. In approximately 75% of BC cases, patients present with non-muscle invasive disease, confined to the mucosa (Ta or carcinoma *in situ*) or submucosa (T1). The main clinical risk is progression to muscle-invasive disease, with chances of progression within ten years varying from 3.7% to 53% depending on stage and grade of the disease[3].

In approximately 25% of BC cases, patients present with muscle-invasive disease, characterized by invasion of tumor cells into the musclaris propria layer of the urothelium. Despite optimal treatment, muscle-invasive BC carries a poor prognosis, which is strongly correlated to primary tumor stage (T-stage) and nodal stage (N-stage). Tumors invading the superficial (T2a) or deep (T2b) layers of the bladder have a relatively good prognosis, while tumors growing through the bladder wall into the perivescial fat (T3) or into adjacent organs (T4a) or the abdominal or pelvic wall (T4b) have a worse prognosis and are associated with a higher chance of lymph node metastases or distant metastases.

LOCALIZED TREATMENT OF MUSCLE-INVASIVE BLADDER CANCER

Standard treatment for muscle-invasive BC (cT2-4aN0M0) consists of radical cystectomy including removal of the locoregional lymph nodes[4-6]. This treatment should also be considered for patients with recurring disease despite intravesical instillations with *Bacillus Calmette-Guerin* and/or for patients with very high-risk non-muscle-invasive BC. Progression-free survival (PFS) and overall survival (OS) in a large population-based study was 35% and 58% at ten years, respectively[7]. However, OS drops to only 18% at five years for patients that underwent cystectomy with lymph node-positive disease[8].

An alternative strategy is to treat patients with a bladder-sparing approach. A transurethral resection of the bladder tumor (TUR-BT) with curative intent is only an option when tumor invasion is limited to the superficial muscle layer and if re-staging biopsies are negative for residual (invasive) tumor and is generally not recommended as a definitive therapy[9]. External beam radiotherapy (EBRT; total target dose of 64-66 Gy) has shown inferior OS compared to radical cystectomy alone and should only be offered as primary therapy for muscle-invasive BC patients unfit for radical cystectomy[10]. Cisplatin-based chemotherapy should not be used as a primary treatment for muscle-invasive BC, however this treatment plays a pivotal role as neoadjuvant therapy in muscle-invasive or in metastatic urothelial cancer (mUC), as discussed in more details below[11].

Trimodality therapy combines TUR-BT, chemotherapy and EBRT. There are no successfully completed randomized controlled trials comparing the outcome of this combination treatment with radical cystectomy. However, long-term outcomes of trimodality bladder-preserving treatment seem to be comparable to those of radical cystectomy according to a number of retrospective multi-center trials[12-14]. These results would suggest that trimodality therapy should be offered to all suitable candidates with muscle-invasive bladder cancer.
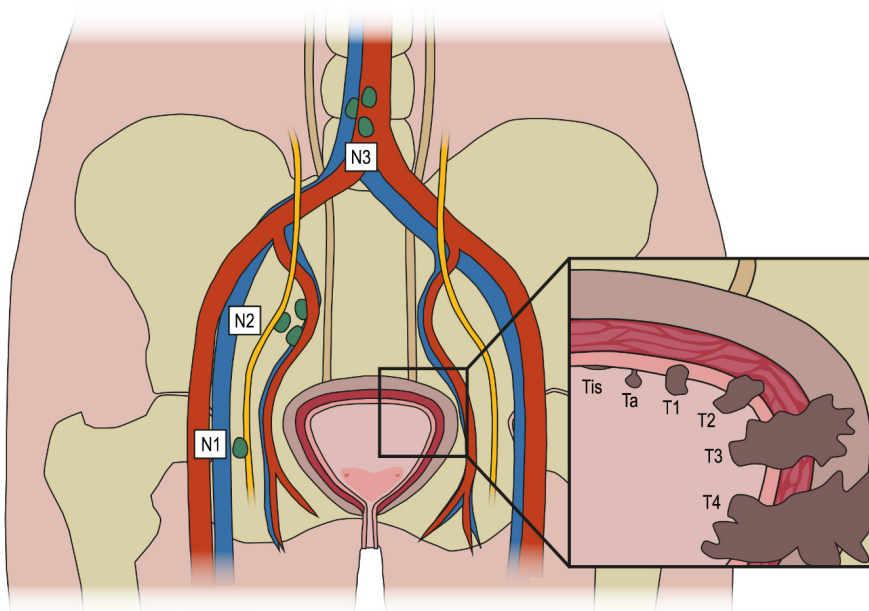
Figure 1 | Graphic overview of bladder cancer TNM staging. Box on the right shows the different tumor stages. Tis: Carcinoma *in situ*: "flat tumor"; Ta: Non-invasive papillary carcinoma; T1: Tumor invades subepithelial connective tissue; T2 Tumour invades muscularis propria layer; T3: Tumor invades perivesical tissue; T4: Tumor invades any of the following: prostate stroma, seminal vesicles, uterus, vagina, pelvic wall, abdominal wall. Nodal stages are shown on the left. N1: Metastasis in a single lymph node in the true pelvis (hypogastric, obturator, external iliac, or presacral); N2: Metastasis in multiple regional lymph nodes in the true pelvis (hypogastric, obturator, external iliac, or presacral); N3: ≥1 metastasis in a common iliac lymph node(s).

PLATINUM-BASED CHEMOTHERAPY FOR LOCALIZED BLADDER CANCER

To improve outcomes for patients with muscle-invasive disease, eligible patients are treated with neoadjuvant cisplatin-based chemotherapy prior to radical cystectomy. Cisplatin can be considered the driving force of neoadjuvant chemotherapy in muscle-invasive BC. However, the efficacy of cisplatin as monotherapy is limited. Instead, cisplatin is administered in the

neoadjuvant setting in combination with gemcitabine or together with methotrexate, vinblastine and adriamycin (MVAC)[15-17]. Neoadjuvant cisplatin-based chemotherapy followed by radical cystectomy leads to a pathological complete response (ypT0N0) in up to 42% of patients[17]. OS is improved by 5-8% for the group as a whole, with most benefit for patients that had a good response after chemotherapy[18]. It was shown in the randomized phase III VESPER trial that (dose-dense) MVAC leads to a superior pathological complete response rate compared to cisplatin with gemcitabine (42% versus 36%)[17]. Other neoadjuvant chemotherapy regimens, such as carboplatin-based combinations or platinum monotherapies have not been tested in randomized controlled trials and are likely inferior to neoadjuvant cisplatin-based combinations[19-21].

Chemotherapy can also be given in the adjuvant setting. When compared to neo-adjuvant chemotherapy trials, the path to show benefit of adjuvant chemotherapy has been more complicated. Reasons for inconsistent results have included inability to fully enroll randomized trials and higher rates of ineligibility to receive and/or complete chemotherapy treatment, which often arises after surgery and is less of a problem in the neoadjuvant setting[22-24]. There is still a place for adjuvant cisplatin-based chemotherapy for patients who were treated with a direct cystectomy, did not receive neoadjuvant chemotherapy and are fit enough to undergo treatment, yielding improved OS compared to deferred platinum-based treatment in the metastatic setting[25-27].

BIOMARKERS FOR PREDICTING RESPONSE TO NEOADJUVANT CHEMOTHERAPY

Different molecular and pathological biomarkers have been described to predict response and survival after treatment with neoadjuvant chemotherapy in BC. However, for a number of biomarkers there are conflicting reports and they often are not validated in larger cohorts. Consequently, these biomarkers have no place in current clinical practice. With more treatments and potential combination strategies coming available, it will be more important to select the best treatment for every individual treatment with the help of biomarkers.

Various genomic alterations have previously been suggested to correlate to response after platinum-based chemotherapy. Most notably, mutations in *ERBB2*, *ERCC2*, *ATM*, F*ANCC*, *RB1* and in genes related to DNA damage repair[28-30]. However, these (combination of) genes have mostly been studied in small-scale studies and have not been validated in larger cohorts. One study retrospectively evaluated mutations in genes potentially related to response to platinum-based chemotherapy including *ERCC2*, *ATM*, *FANCC*, *RB1* in 48 patients which were subsequently treated with neoadjuvant cisplatin-based chemotherapy followed by radical cystectomy[31]. Tumor mutation status was not associated with pathological response and survival status[31]. In addition, this study investigated 114 patients undergoing a diagnostic TUR-BT after neoadjuvant cisplatin-based chemotherapy and prior to radical cystectomy to predict if patients could be selected

to potentially forego radical cystectomy. However, only 25 (47%) patients with a pathological complete response after TUR-BT also showed a pathological complete response after radical cystectomy. Of note, twelve (23%) of the remaining patients still had muscle-invasive disease after radical cystectomy. Taken together, there is currently not enough evidence to support routine molecular testing to select patients that will benefit from neoadjuvant chemotherapy. In addition, there is currently no effective method to select patients that have a pathological complete response after neoadjuvant cisplatin-based chemotherapy prior to radical cystectomy.

IMMUNE CHECKPOINT INHIBITORS

The physiological role of immune checkpoints is to maintain self-tolerance and regulate the extent and duration of inflammatory processes. However, these pathways are used by tumors in an attempt to escape from an anti-tumor immune response[32,33]. The mechanism of action of immune checkpoint inhibitors (ICI) is complex and dependent on the pre-existing Tumor-immune micro-environment (TIME), such as the abundance and activation state of CD8^{+} T-cells, the presence of other immune cell subsets and local cytokine signaling. In addition, treatment with ICI directly influences and changes the TIME, resulting in a delicate interplay. The best known immune checkpoints are CTLA-4 and PD-1/PD-L1. However, other immune checkpoints are currently being investigated, including TIGIT, TIM3 and LAG3[34].

CTLA-4 is expressed by T-cells where it competes with CD28 for binding with the CD80/CD86 dimer expressed primarily by antigen-presenting cells. Binding of CD80/CD86 with CD28 elicits a signaling cascade eventually leading to T-cell activation[33,35]. CTLA-4 has a higher affinity for CD80/CD86 and binding results in an inhibitory response. By blocking the CTLA-4 receptor with monoclonal antibodies such as ipilimumab and tremelimumab, this inhibitory response can be negated, allowing for binding of CD80/86 with CD28 to co-stimulate T-cell activation[33,36]. Ipilimumab and tremelimumab have been used in numerous clinical trials as monotherapy and in combination with other ICI.

PD-1 is expressed by antigen-experienced T-cells and helps to regulate and control immune responses by binding to PD-L1 and PD-L2, which are expressed by antigen-presenting cells and tumor cells. Binding eventually results in T-cell inhibition and chronic stimulation leads to an exhausted T-cell phenotype[32,33]. Multiple monoclonal inhibitory antibodies have been developed that target either PD-1 (nivolumab, pembrolizumab) or PD-L1 (durvalumab, avelumab and atezolizumab). These antibodies have been tested elaborately in multiple cancer types, including urothelial cancer, either as monotherapy or in combination with other ICI or other anti-cancer drugs.
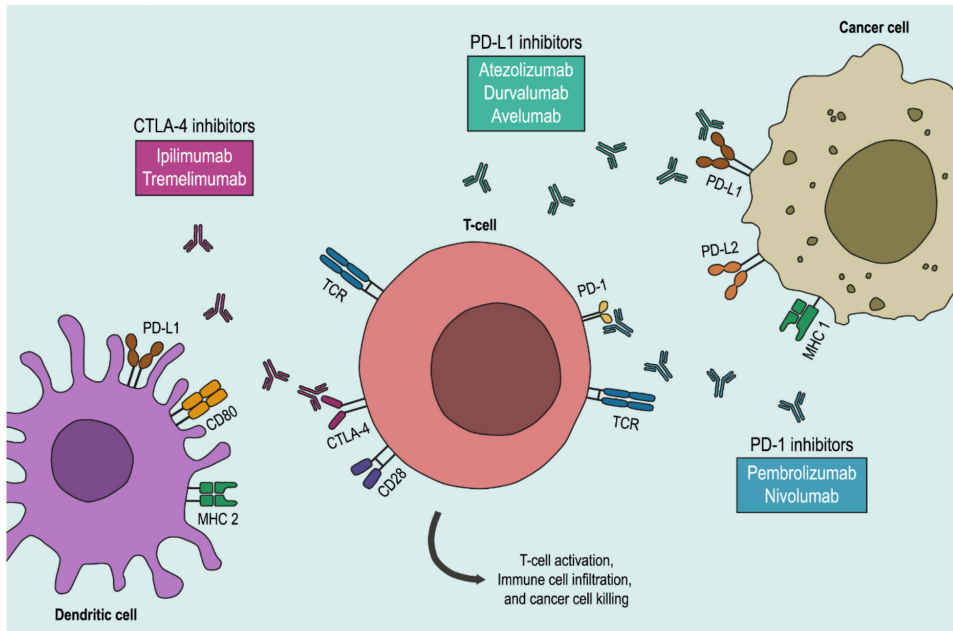
Figure 2 | Schematic overview of immune cell activation during treatment with immune checkpoint inhibition. Cancer cell (neo-)antigens are presented to T-cells by MHC class 2 molecules present on dendritic cells. PD-L1 (and to a lesser extent, also PD-L2) expressed by cancer cells binds to PD-1 that is expressed by T-cells, ultimately inhibiting T-cell activation. PD-1/PD-L1/PD-L2 inhibitors prevent this interaction, thereby preventing the inhibitory signal. CD80, expressed by dendritic cells, binds to CTLA-4 expressed by T-cells inhibiting T-cell activation. By inhibiting CTLA-4, CD80 instead binds to CD28 expressed by T-cells, stimulating T-cell activation, immune cell infiltration and cancer cell killing. *TCR: T-cell receptor; MHC: Major histocompatibility complex; Illustration inspired by Roviello and colleagues[37]*

IMMUNE CHECKPOINT INHIBITION IN BLADDER CANCER

Standard first-line therapy for mUC is cisplatin-based combination chemotherapy[38,39]. Carboplatin can be considered as an alternative for patients ineligible for cisplatin[38,39]. Following the success in other cancer types, such as melanoma, renal cell carcinoma and non-small cell lung cancer, ICIs were tested in multiple trials in platinum-refractory mUC[40,41]. An improved OS was observed for pembrolizumab (PD-1 inhibitor) compared to chemotherapy in platinum-refractory mUC in the KEYNOTE-045 trial[40]. These results led to the approval of pembrolizumab for the treatment of platinum-refractory mUC patients. The IMvigor211 trial explored atezolizumab as second-line therapy in mUC and showed improved OS for the intention-to-treat population. However, the primary endpoint of this trial (improved OS in patients with tumors with high PD-L1 expression) was not met[41].

A number of phase 3 trials have been conducted to investigate the effect of first-line treatment with PD-1/PD-L1 inhibition compared to standard platinum-based chemotherapy. These trials include

the KEYNOTE-361 (pembrolizumab), DANUBE (durvalumab) and the IMvigor130 (atezolizumab) trials. No meaningful improvement in clinical benefit for anti-PD(L)-1 monotherapy versus standard first-line platinum-based chemotherapy treatment has been observed in either of these trials[42-44]. The KEYNOTE-361 and IMvigor130 as well as the CheckMate-901 (nivolumab) also tested the effect of combined platinum-based chemotherapy and PD-1/PD-L1 inhibition as a first-line treatment option. In both the KEYNOTE-361 and IMvigor130 the combination treatment did not confer a significant benefit over standard treatment with chemotherapy in the intention-to-treat analysis[42,45]. However, the recently published results of the CheckMate-901 have shown both an improved PFS as well as an improved OS for patients treated with nivolumab combined with cisplatin-based chemotherapy compared to cisplatin-based chemotherapy alone[46].

The DANUBE and CheckMate-901 trials evaluate the combination of PD-1/PD-L1 inhibition with CTLA-4 inhibition in urothelial cancer[43,44]. The DANUBE trial did not reach its primary endpoint(s). However, a numerical difference can be observed in favor of combined treatment with durvalumab plus tremelimumab compared to durvalumab monotherapy, especially in the PD-L1+ population[44]. As described above, significant clinical benefit was observed for patients that were treated with nivolumab in addition to cisplatin/gemcitabine compared to cisplatin/gemcitabine monotherapy in the Checkmate-901 study. Another arm in the study investigated the effect of ipilimumab plus nivolumab in first-line advanced urothelial cancer patients. Whereas one of the endpoints, OS in patients with high PD-L1 expression was not met, the results for the other primary endpoint in cisplatin-ineligible patients are still pending.

CHECKPOINT INHIBITION AS PERIOPERATIVE TREATMENT IN BLADDER CANCER

In addition to trials investigating the feasibility in the metastatic setting, a number of phase 1/2 trials investigated ICI in the neoadjuvant setting, primarily to offer an alternative for patients who refused cisplatin or were ineligible. Preoperative pembrolizumab was investigated in the PURE-01 trial[47,48]. In total, 143 patients with cT2-4N0 BC were treated with three cycles of pembrolizumab, followed by radical surgery. A pCR rate of 38.5% was observed[47,48]. In the ABACUS trial, preoperative atezolizumab was investigated in cT2N0-cT4aN0 BC patients[49]. This trial yielded a response rate of 31%[49].

Following up on the success of these trials, two neoadjuvant trials were initiated using a combination of CTLA-4 inhibition and PD-1/PD-L1 inhibition[50,51]. In cohort 1 of the NABUCCO trial, 24 patients with locally advanced BC were treated with a combination of ipilimumab plus nivolumab followed by radical surgery[50]. Here, a pCR was observed in 46% of patients. In addition, 58% of patients had no remaining residual muscle-invasive disease after surgery (ypT0/Tis/Ta/T1N0)[50]. The group of Gao and colleagues conducted a trial with two cycles tremelimumab plus

durvalumab in locally advanced BC. A pCR was observed in 38% of patients that underwent surgery, which is comparable to platinum-based chemotherapy regimens in locally advanced disease[17,51].

In defining the optimal setting for ICI, some recent trials suggest there is a place for checkpoint inhibition in the adjuvant setting in BC. Two phase 3 trials have explored the efficacy and clinical benefit of adjuvant nivolumab (CheckMate-274) and atezolizumab (IMvigor010) in patients with residual muscle-invasive disease after radical surgery[52,53]. Only the trial with nivolumab met its primary endpoint of improved PFS in the intention-to-treat population, as well as in the PD-L1[high] population[52]. However, as PD-1/PD-L1 inhibition is approved as second-line treatment for urothelial cancer, it is possible that the group that did not receive adjuvant nivolumab will eventually benefit from checkpoint blockade in a later disease stage, as the disease would still be naive to exposure to checkpoint inhibition. Therefore, OS data are needed to fully assess clinical benefit.

MODULATING THE TUMOR IMMUNE MICRO-ENVIRONMENT TO IMPROVE RESPONSE TO CHECKPOINT INHIBITION

Adding conventional chemotherapy to ICI treatment may alter the TIME to be more susceptible to respond to ICI treatment. The initial results of combination strategies did not show a survival benefit compared to platinum-based chemotherapy in mUC patients in both the KEYNOTE-361 (pembrolizumab) and in the IMvigor130 (atezolizumab) trials[42,45]. However, as discussed prior, the recently published results of the CheckMate-901 have shown both an improved PFS as well as an improved OS for patients treated with nivolumab combined with cisplatin-based chemotherapy compared to cisplatin-based chemotherapy alone[46]. Potentially, the discrepancy between the results of the CheckMate-901 (nivolumab) trial and the other two trials can be (partially) explained by the fact that the former addressed the benefit of adding PD-1 inhibition to cisplatin-based chemotherapy specifically, whereas patients in the other phase 3 trials were treated with PD-1/PD-L1 inhibition combined with investigator's choice platinum-based regimens, which consisted of carboplatin in the majority of patients. Indeed, exploratory analyses performed in both the KEYNOTE-361 and IMvigor130 showed improved PFS (and OS in IMvigor130) in patients receiving PD-1/PD-L1 inhibition in patients treated with cisplatin-based therapy but not in those treated with carboplatin-based therapy[42,45,46].

Potentially, an improved synergistic or additive effect of combining chemotherapy and ICI therapy can be achieved by a sequential approach. Indeed, this hypothesis is supported by the improved results for adjuvant nivolumab in the subset of patients who received neoadjuvant chemotherapy in the CheckMate-274 trial[52]. In addition, the JAVELIN Bladder 100 trial showed an improved OS after maintenance treatment with avelumab (PD-L1 inhibitor) after initial treatment with platinum-based chemotherapy[54].

Traditionally, chemotherapy has been regarded as immuno-suppressive, depleting immune cell subsets and leading to an increased rate of infections[55]. However, it has been shown in numerous preclinical and clinical studies that treatment with chemotherapy can also have immunostimulatory effects[56,57]. One of the direct effects of chemotherapy is the induction of immunogenic cell death, a form of cell death that is being preceded by a cellular stress-response. Via complex intracellular pathways, phagocytosis of tumor cells (or portions thereof) by dendritic cells is facilitated[58]. Processing of this cellular debris by dendritic cells eventually leads to presentation of neoantigens[59,60]. In addition to the induction of immunogenic cell death, chemotherapy treatment also affects regulatory T-cells, tumor-associated macrophages and myeloid derived suppressor cells[61,62]. This phenomenon could be further exploited when used in conjunction with ICI especially with a sequential approach. Priming the TIME and allowing recovery of immune cell populations to subsequently further improve the anti-tumor response with ICI treatment[63].

CTDNA AS A BIOMARKER TO PREDICT RESPONSE AFTER TREATMENT WITH CHECKPOINT INHIBITION

Circulating tumor DNA (ctDNA) from plasma can be utilized as a minimally-invasive biomarker to monitor tumor status[64,65]. Specifically in BC, ctDNA can also be collected from urine, as a non-invasive liquid biopsy, to assess tumor status[66]. Based on a panel-based approach, it was found previously that ctDNA is detectable is both urine and plasma in patients with muscle-invasive BC and that detectable ctDNA during neoadjuvant chemotherapy is associated with early disease recurrence[66]. Since then, methods to assess ctDNA have evolved and individualized tumor-specific panels based on differences derived from whole-exome data[67-70].

CtDNA in plasma (based on individualized tumor-specific panels) was also assessed in the phase 3 trial with adjuvant atezolizumab (IMvigor010) in patients with residual muscle-invasive disease after radical surgery[53,67]. The subgroup of patients with detectable ctDNA in plasma after surgery had a significant OS benefit after treatment with adjuvant atezolizumab, this benefit was not observed in patients without detectable ctDNA[53,67]. In addition, a similar ctDNA assessment was done in the ABACUS trial, were patients were treated with preoperative atezolizumab[49,68]. Absence of ctDNA after surgery was strongly associated with PFS[68]. Currently, ctDNA is used both to monitor response to treatment and to detect minimal residual disease to predict disease recurrence. While the optimal way to utilize ctDNA for the treatment of urothelial cancer remains elusive, this biomarker will potentially be a helpful clinical tool.

CHECKPOINT INHIBITION FOR PROSTATE CANCER

ICI has demonstrated impressive results in different disease stages in BC. However, the first trials with checkpoint inhibition in prostate cancer (PCa) showed only limited clinical benefit[71,72]. Currently, only pembrolizumab is approved for metastatic PCa for patients after progression on docetaxel and hormonal therapy with tumors with high microsatellite instability, deficient mismatch repair or a tumor mutational burden ≥10 mut/Mb only[73]. In the CheckMate-650 trial, encouraging results in PCa were observed by combining nivolumab and ipilimumab in the showing an overall response rate of 25.0% in chemotherapy-naïve metastatic castration-resistant PCa patients[74]. Specifically, patients in this trial with a AR-V7 mutation seem to benefit from treatment with combined ipilimumab and nivolumab[74].

OUTLINE OF THESIS

This thesis focuses on systemic preoperative treatment strategies for muscle-invasive BC. With the encouraging results of ICI in recent years, the treatment landscape of BC is rapidly changing. In addition, it is becoming clear that the effect of ICI is highly dependent on the interaction between tumor cells and the TIME. In **Chapter 2** we reviewed the recent advancements in ICI treatment in BC and its relation with the TIME.

In **Chapter 3**, we look primarily at predicting pathological response after neoadjuvant platinum-based chemotherapy based on genomic biomarkers. Several genomic biomarkers have been suggested to correlate with pathological response including mutations in *ERBB2*, *ERCC2* and in any of *ATM*, *RB1* and/or *FANCC* genes. However, these results have been obtained in small explorative studies and the results have never been validated in larger cohorts, hindering their current clinical application. We have assessed sequencing data from a large cohort of 165 patients from five different hospitals in an attempt to validate the relation to the aforementioned biomarkers.

In **Chapter 4**, we retrospectively investigated a cohort of muscle-invasive BC patients that were treated with neoadjuvant chemotherapy followed by radical cystectomy. We collected TUR-BT tumor material from before start of neoadjuvant treatment and from the radical cystectomy specimen and performed RNA sequencing and multiplex immunofluorescence on tissue to identify changes induced by neoadjuvant chemotherapy that could potentially influence the subsequent effect of ICI treatment.

Following up on the results of the NABUCCO trial cohort 1, we set out to find the optimal dose of preoperative ipilimumab and nivolumab for patients with locoregionally advanced urothelial cancer. In **Chapter 5**, we look in detail at the results from the NABUCCO trial, cohort 2. Here, patients were randomized to receive either two cycles of ipilimumab 3 mg/kg plus nivolumab

1 mg/kg (cohort 2A) or two cycles of ipilimumab 1 mg/kg plus nivolumab 3 mg/kg (cohort 2B), followed in both cohorts by a third cycle of nivolumab 3 mg/kg. In addition, we set out to predict pathological response and clinical outcome based on ctDNA in plasma and urine in patients treated in NABUCCO cohort 1 and 2.

Historically, it has been described that incidental prostate cancer is found in a number of patients that undergo radical cystoprostatectomy for BC, allowing for the opportunity to look at the effect of ipilimumab plus nivolumab in (incidental) prostate cancer. In **Chapter 6**, we retrospectively assessed the prostate tissue that was part of the radical cystoprostatectomy specimens from NABUCCO cohort 1 and compare this to a control cohort of patients that were not treated with combined ipilimumab and nivolumab.

REFERENCES

1. Powles, T., *et al.* Bladder cancer: ESMO Clinical Practice Guideline for diagnosis, treatment and follow-up. *Ann Oncol* 33, 244-258 (2022).

2. Bray, F., *et al.* Global cancer statistics 2018: GLOBOCAN estimates of incidence and mortality worldwide for 36 cancers in 185 countries. *CA Cancer J Clin* 68, 394-424 (2018).

3. Sylvester, R.J., *et al.* European Association of Urology (EAU) Prognostic Factor Risk Groups for Non-muscle-invasive Bladder Cancer (NMIBC) Incorporating the WHO 2004/2016 and WHO 1973 Classification Systems for Grade: An Update from the EAU NMIBC Guidelines Panel. *Eur Urol* 79, 480-488 (2021).

4. Stein, J.P., *et al.* Radical cystectomy in the treatment of invasive bladder cancer: long-term results in 1,054 patients. *J Clin Oncol* 19, 666-675 (2001).

5. Dalbagni, G., *et al.* Cystectomy for bladder cancer: a contemporary series. *J Urol* 165, 1111-1116 (2001).

6. Stein, J.P. & Skinner, D.G. Radical cystectomy for invasive bladder cancer: long-term results of a standard procedure. *World J Urol* 24, 296-304 (2006).

7. Fahmy, O., *et al.* A systematic review and meta-analysis on the oncological long-term outcomes after trimodality therapy and radical cystectomy with or without neoadjuvant chemotherapy for muscle-invasive bladder cancer. *Urol Oncol* 36, 43-53 (2018).

8. Darwish, C., Sparks, A., Amdur, R., Reddy, A. & Whalen, M. Trends in Treatment Strategies and Comparison of Outcomes in Lymph Node Positive Bladder Cancer: An Analysis of the National Cancer Database. *Urology* 146, 168-176 (2020).

9. Herr, H.W. Conservative management of muscle-infiltrating bladder cancer: prospective experience. *J Urol* 138, 1162-1163 (1987).

10. Shelley, M.D., Barber, J., Wilt, T. & Mason, M.D. Surgery versus radiotherapy for muscle invasive bladder cancer. *Cochrane Database Syst Rev*, CD002079 (2002).

11. Audenet, F., *et al.* Effectiveness of Transurethral Resection plus Systemic Chemotherapy as Definitive Treatment for Muscle Invasive Bladder Cancer in Population Level Data. *J Urol* 200, 996-1004 (2018).

12. Cahn, D.B., *et al.* Contemporary use trends and survival outcomes in patients undergoing radical cystectomy or bladder-preservation therapy for muscle-invasive bladder cancer. *Cancer* 123, 4337-4345 (2017).

13. Williams, S.B., *et al.* Comparing Survival Outcomes and Costs Associated With Radical Cystectomy and Trimodal Therapy for Older Adults With Muscle-Invasive Bladder Cancer. *JAMA Surg* 153, 881-889 (2018).

14. Zlotta, A.R., *et al.* Radical cystectomy versus trimodality therapy for muscle-invasive bladder cancer: a multi-institutional propensity score matched and weighted analysis. *Lancet Oncol* 24, 669-681 (2023).

15. Zargar, H., *et al.* Neoadjuvant Dose Dense MVAC versus Gemcitabine and Cisplatin in Patients with cT3-4aN0M0 Bladder Cancer Treated with Radical Cystectomy. *J Urol* 199, 1452-1458 (2018).

16. Galsky, M.D., *et al.* Comparative effectiveness of gemcitabine plus cisplatin versus methotrexate, vinblastine, doxorubicin, plus cisplatin as neoadjuvant therapy for muscle-invasive bladder cancer. *Cancer* 121, 2586-2593 (2015).

17. Pfister, C., *et al.* Randomized Phase III Trial of Dose-dense Methotrexate, Vinblastine, Doxorubicin, and Cisplatin, or Gemcitabine and Cisplatin as Perioperative Chemotherapy for Patients with Muscle-invasive Bladder Cancer. Analysis of the GETUG/AFU V05 VESPER Trial Secondary Endpoints: Chemotherapy Toxicity and Pathological Responses. *Eur Urol* 79, 214-221 (2021).

18. Advanced Bladder Cancer Meta-analysis, C. Neoadjuvant chemotherapy in invasive bladder cancer: update of

a systematic review and meta-analysis of individual patient data advanced bladder cancer (ABC) meta-analysis collaboration. *Eur Urol* 48, 202-205; discussion 205-206 (2005).

19. Sherif, A., *et al.* Neoadjuvant cisplatin-methotrexate chemotherapy for invasive bladder cancer -- Nordic cystectomy trial 2. *Scand J Urol Nephrol* 36, 419-425 (2002).

20. Sengelov, L., *et al.* Neoadjuvant chemotherapy with cisplatin and methotrexate in patients with muscle-invasive bladder tumours. *Acta Oncol* 41, 447-456 (2002).

21. Murasawa, H., *et al.* The utility of neoadjuvant gemcitabine plus carboplatin followed by immediate radical cystectomy in patients with muscle-invasive bladder cancer who are ineligible for cisplatin-based chemotherapy. *Int J Clin Oncol* 22, 159-165 (2017).

22. Cohen, S.M., Goel, A., Phillips, J., Ennis, R.D. & Grossbard, M.L. The role of perioperative chemotherapy in the treatment of urothelial cancer. *Oncologist* 11, 630-640 (2006).

23. Sylvester, R. & Sternberg, C. The role of adjuvant combination chemotherapy after cystectomy in locally advanced bladder cancer: what we do not know and why. *Ann Oncol* 11, 851-856 (2000).

24. Donat, S.M., *et al.* Potential impact of postoperative early complications on the timing of adjuvant chemotherapy in patients undergoing radical cystectomy: a high-volume tertiary cancer center experience. *Eur Urol* 55, 177-185 (2009).

25. Leow, J.J., *et al.* Adjuvant chemotherapy for invasive bladder cancer: a 2013 updated systematic review and meta-analysis of randomized trials. *Eur Urol* 66, 42-54 (2014).

26. Galsky, M.D., *et al.* Effectiveness of Adjuvant Chemotherapy for Locally Advanced Bladder Cancer. *J Clin Oncol* 34, 825-832 (2016).

27. Sternberg, C.N., *et al.* Immediate versus deferred chemotherapy after radical cystectomy in patients with pT3-pT4 or N+ M0 urothelial carcinoma of the bladder (EORTC 30994): an intergroup, open-label, randomised phase 3 trial. *Lancet Oncol* 16, 76-86 (2015).

28. Plimack, E.R., *et al.* Defects in DNA Repair Genes Predict Response to Neoadjuvant Cisplatin-based Chemotherapy in Muscle-invasive Bladder Cancer. *Eur Urol* 68, 959-967 (2015).

29. Van Allen, E.M., *et al.* Somatic ERCC2 mutations correlate with cisplatin sensitivity in muscle-invasive urothelial carcinoma. *Cancer Discov* 4, 1140-1153 (2014).

30. Groenendijk, F.H., *et al.* ERBB2 Mutations Characterize a Subgroup of Muscle-invasive Bladder Cancers with Excellent Response to Neoadjuvant Chemotherapy. *Eur Urol* 69, 384-388 (2016).

31. Becker, R.E.N., *et al.* Clinical Restaging and Tumor Sequencing are Inaccurate Indicators of Response to Neoadjuvant Chemotherapy for Muscle-invasive Bladder Cancer. *Eur Urol* 79, 364-371 (2021).

32. Keir, M.E., Butte, M.J., Freeman, G.J. & Sharpe, A.H. PD-1 and its ligands in tolerance and immunity. *Annu Rev Immunol* 26, 677-704 (2008).

33. Pardoll, D.M. The blockade of immune checkpoints in cancer immunotherapy. *Nat Rev Cancer* 12, 252-264 (2012).

34. Walsh, R.J., Sundar, R. & Lim, J.S.J. Immune checkpoint inhibitor combinations-current and emerging strategies. *Br J Cancer* 128, 1415-1417 (2023).

35. Krummel, M.F. & Allison, J.P. CD28 and CTLA-4 have opposing effects on the response of T cells to stimulation. *J Exp Med* 182, 459-465 (1995).

36. Linsley, P.S., *et al.* CTLA-4 is a second receptor for the B cell activation antigen B7. *J Exp Med* 174, 561-569 (1991).

37. Roviello, G., *et al.* Immune Checkpoint Inhibitors in Urothelial Bladder Cancer: State of the Art and Future Perspectives. *Cancers (Basel)* 13(2021).

38. von der Maase, H., *et al.* Gemcitabine and cisplatin versus methotrexate, vinblastine, doxorubicin, and cisplatin in advanced or metastatic bladder cancer: results of a large, randomized, multinational, multicenter, phase III study. *J Clin Oncol* 18, 3068-3077 (2000).

39. De Santis, M., *et al.* Randomized phase II/III trial assessing gemcitabine/carboplatin and methotrexate/carboplatin/ vinblastine in patients with advanced urothelial cancer who are unfit for cisplatin-based chemotherapy: EORTC study 30986. *J Clin Oncol* 30, 191-199 (2012).

40. Bellmunt, J., *et al.* Pembrolizumab as Second-Line Therapy for Advanced Urothelial Carcinoma. *N Engl J Med* 376, 1015-1026 (2017).

41. Powles, T., *et al.* Atezolizumab versus chemotherapy in patients with platinum-treated locally advanced or metastatic urothelial carcinoma (IMvigor211): a multicentre, open-label, phase 3 randomised controlled trial. *Lancet* 391, 748-757 (2018).

42. Powles, T., *et al.* Pembrolizumab alone or combined with chemotherapy versus chemotherapy as first-line therapy for advanced urothelial carcinoma (KEYNOTE-361): a randomised, open-label, phase 3 trial. *Lancet Oncol* 22, 931-945 (2021).

43. Galsky, M.D., Powles, T., Li, S., Hennicken, D. & Sonpavde, G. A phase 3, open-label, randomized study of nivolumab plus ipilimumab or standard of care (SOC) versus SOC alone in patients (pts) with previously untreated unresectable or metastatic urothelial carcinoma (mUC; CheckMate 901). *Journal of Clinical Oncology* 36, TPS539-TPS539 (2018).

44. Powles, T., *et al.* Durvalumab alone and durvalumab plus tremelimumab versus chemotherapy in previously untreated patients with unresectable, locally advanced or metastatic urothelial carcinoma (DANUBE): a randomised, open-label, multicentre, phase 3 trial. *Lancet Oncol* 21, 1574-1588 (2020).

45. Galsky, M.D., *et al.* Atezolizumab with or without chemotherapy in metastatic urothelial cancer (IMvigor130): a multicentre, randomised, placebo-controlled phase 3 trial. *Lancet* 395, 1547-1557 (2020).

46. van der Heijden, M.S., *et al.* Nivolumab plus Gemcitabine-Cisplatin in Advanced Urothelial Carcinoma. *N Engl J Med* 389, 1778-1789 (2023).

47. Necchi, A., *et al.* Pembrolizumab as Neoadjuvant Therapy Before Radical Cystectomy in Patients With Muscle-Invasive Urothelial Bladder Carcinoma (PURE-01): An Open-Label, Single-Arm, Phase II Study. *J Clin Oncol* 36, 3353-3360 (2018).

48. Bandini, M., *et al.* Does the administration of preoperative pembrolizumab lead to sustained remission post-cystectomy? First survival outcomes from the PURE-01 study(☆). *Ann Oncol* 31, 1755-1763 (2020).

49. Powles, T., *et al.* Clinical efficacy and biomarker analysis of neoadjuvant atezolizumab in operable urothelial carcinoma in the ABACUS trial. *Nat Med* 25, 1706-1714 (2019).

50. van Dijk, N., *et al.* Preoperative ipilimumab plus nivolumab in locoregionally advanced urothelial cancer: the NABUCCO trial. *Nat Med* 26, 1839-1844 (2020).

51. Gao, J., *et al.* Neoadjuvant PD-L1 plus CTLA-4 blockade in patients with cisplatin-ineligible operable high-risk urothelial carcinoma. *Nat Med* 26, 1845-1851 (2020).

52. Bajorin, D.F., *et al.* Adjuvant Nivolumab versus Placebo in Muscle-Invasive Urothelial Carcinoma. *N Engl J Med* 384, 2102-2114 (2021).

53. Bellmunt, J., *et al.* Adjuvant atezolizumab versus observation in muscle-invasive urothelial carcinoma (IMvigor010): a multicentre, open-label, randomised, phase 3 trial. *Lancet Oncol* 22, 525-537 (2021).

54. Powles, T., *et al.* Avelumab Maintenance Therapy for Advanced or Metastatic Urothelial Carcinoma. *N Engl J Med* 383, 1218-1230 (2020).

55. Vento, S. & Cainelli, F. Infections in patients with cancer undergoing chemotherapy: aetiology, prevention, and treatment. *Lancet Oncol* 4, 595-604 (2003).

56. Bracci, L., Schiavoni, G., Sistigu, A. & Belardelli, F. Immune-based mechanisms of cytotoxic chemotherapy: implications for the design of novel and rationale-based combined treatments against cancer. *Cell Death Differ* 21, 15-25 (2014).

57. Sakai, H., *et al.* Effects of anticancer agents on cell viability, proliferative activity and cytokine production of peripheral blood mononuclear cells. *J Clin Biochem Nutr* 52, 64-71 (2013).

58. Galluzzi, L., *et al.* Consensus guidelines for the definition, detection and interpretation of immunogenic cell death. *J Immunother Cancer* 8(2020).

59. Ott, P.A., *et al.* An immunogenic personal neoantigen vaccine for patients with melanoma. *Nature* 547, 217-221 (2017).

60. Keskin, D.B., *et al.* Neoantigen vaccine generates intratumoral T cell responses in phase Ib glioblastoma trial. *Nature* 565, 234-239 (2019).

61. Wang, Z., Till, B. & Gao, Q. Chemotherapeutic agent-mediated elimination of myeloid-derived suppressor cells. *Oncoimmunology* 6, e1331807 (2017).

62. Roselli, M., *et al.* Effects of conventional therapeutic interventions on the number and function of regulatory T cells. *Oncoimmunology* 2, e27025 (2013).

63. Pfirschke, C., *et al.* Immunogenic Chemotherapy Sensitizes Tumors to Checkpoint Blockade Therapy. *Immunity* 44, 343-354 (2016).

64. Diehl, F., *et al.* Circulating mutant DNA to assess tumor dynamics. *Nat Med* 14, 985-990 (2008).

65. Dawson, S.J., *et al.* Analysis of circulating tumor DNA to monitor metastatic breast cancer. *N Engl J Med* 368, 1199-1209 (2013).

66. Patel, K.M., *et al.* Association Of Plasma And Urinary Mutant DNA With Clinical Outcomes In Muscle Invasive Bladder Cancer. *Sci Rep* 7, 5554 (2017).

67. Powles, T., *et al.* ctDNA guiding adjuvant immunotherapy in urothelial carcinoma. *Nature* 595, 432-437 (2021).

68. Szabados, B., *et al.* Final Results of Neoadjuvant Atezolizumab in Cisplatin-ineligible Patients with Muscle-invasive Urothelial Cancer of the Bladder. *Eur Urol* 82, 212-222 (2022).

69. Christensen, E., *et al.* Early Detection of Metastatic Relapse and Monitoring of Therapeutic Efficacy by Ultra-Deep Sequencing of Plasma Cell-Free DNA in Patients With Urothelial Bladder Carcinoma. *J Clin Oncol* 37, 1547-1557 (2019).

70. Flach, S., *et al.* Liquid BIOpsy for MiNimal RESidual DiSease Detection in Head and Neck Squamous Cell Carcinoma (LIONESS)-a personalised circulating tumour DNA analysis in head and neck squamous cell carcinoma. *Br J Cancer* 126, 1186-1195 (2022).

71. Antonarakis, E.S., *et al.* Pembrolizumab for Treatment-Refractory Metastatic Castration-Resistant Prostate Cancer: Multicohort, Open-Label Phase II KEYNOTE-199 Study. *J Clin Oncol* 38, 395-405 (2020).

72. Beer, T.M., *et al.* Randomized, Double-Blind, Phase III Trial of Ipilimumab Versus Placebo in Asymptomatic or Minimally Symptomatic Patients With Metastatic Chemotherapy-Naive Castration-Resistant Prostate Cancer. *J Clin Oncol* 35, 40-47 (2017).

73. Marabelle, A., *et al.* Efficacy of Pembrolizumab in Patients With Noncolorectal High Microsatellite Instability/Mismatch Repair-Deficient Cancer: Results From the Phase II KEYNOTE-158 Study. *J Clin Oncol* 38, 1-10 (2020).

74. Sharma, P., *et al.* Nivolumab Plus Ipilimumab for Metastatic Castration-Resistant Prostate Cancer: Preliminary Analysis of Patients in the CheckMate 650 Trial. *Cancer Cell* 38, 489-499 e483 (2020).

CHAPTER 2

The bladder cancer immune micro-environment in the context of response to immune checkpoint inhibition

Jeroen van Dorp, Michiel S. van der Heijden

ABSTRACT

Treatment with neoadjuvant cisplatin-based chemotherapy followed by radical cystectomy is the default treatment for muscle-invasive bladder cancer (BC). However, with the encouraging results of immune checkpoint inhibitiors (ICI) directed against PD-1/PD-L1 and CTLA-4 in recent years, the treatment landscape of BC is rapidly changing. In addition, it is becoming clear that the effect of ICI is highly dependent on the interaction between tumor cells and the tumor immune micro-environment (TIME).

Different immune cells are involved in an anti-tumor response in BC. Cytotoxic CD8+ T-cells are the main effector cells, aided by other immune cells including other T-cells, B-cells and pro-inflammatory macrophages. As part of the ongoing anti-tumor immune response, lymphocytes aggregate in clusters called tertiary lymphoid structures (TLS). Tumor mutational burden (TMB) and infiltration of immune cells into the tumor are both important factors for establishing an anti-tumor immune response. In contrast, transforming growth factor beta (TGF-β) signaling in cancer-associated fibroblasts (CAFs) prevents infiltration of lymphocytes and potentially has an immunosuppressive effect.

In conclusion, the effect of ICI seems to be reliant on a combination of tumor-intrinsic and TIME-related parameters. More research is needed to fully understand the underlying biological mechanisms to further improve patient care.

INTRODUCTION

Urothelial carcinoma of the bladder, more commonly described as bladder cancer (BC), is the 10th most common cancer worldwide[1,2]. In approximately 25% of BC cases, patients present with muscle-invasive disease, characterized by invasion of tumor cells into the muscularis propria layer of the urothelium. Standard treatment for muscle-invasive bladder cancer (MIBC) consists of radical cystectomy (RC) including removal of the locoregional lymph nodes[3-5]. However, overall survival (OS) and recurrence-free survival (RFS) after surgery alone are still poor[6,7].

Pre-treating patients with neoadjuvant cisplatin-based chemotherapy (NAC) leads to a pathological complete response (pCR) rate of 20-40% after RC[8]. OS is improved by 5-8% compared to patients treated with a direct cystectomy with most benefit for patients that have a pCR after NAC[9].

Treatment with NAC has been the default treatment for MIBC for many years. However, this might change given the encouraging clinical efficacy of immune checkpoint inhibitors (ICI). It is becoming apparent that treatment with ICI is not a *one size fits all* treatment, but its efficacy is instead highly dependent on characteristics of the tumor and the tumor immune micro-environment (TIME). Here, we will review the research on ICI in MIBC and its reciprocal effects on the TIME.

IMMUNE CHECKPOINT INHIBITORS

The physiological role of immune checkpoints is to maintain self-tolerance and regulate the extent and duration of inflammatory processes. However, these pathways are used by tumors in an attempt to escape from an inevitable immune response[10,11]. The mechanism of action of ICI is complex and dependent on pre-existing factors in the TIME such as the abundance and activation state of CD8^{+} T-cells, the presence of other immune cells and local cytokine signaling. In addition, treatment with ICI directly influences and changes the TIME, resulting in a delicate interplay. The best known immune checkpoints are cytotoxic T-lymphocyte-associated protein 4 (CTLA-4) and programmed cell death protein 1 (PD-1) together with its ligands programmed death-ligand 1 and 2 (PD-L1 and PD-L2). However, more immune checkpoints are currently being investigated, including TIGIT, TIM3 and LAG3[12].

CTLA-4 is expressed by T-cells, where it competes with CD28 for binding with CD80 or CD86, expressed primarily by antigen-presenting cells. Binding with CD28 elicits a signaling cascade eventually leading to T-cell activation[11,13]. Instead, binding of CTLA-4 to CD80 or CD86 results in an inhibitory response. By blocking the CTLA-4 receptor with monoclonal antibodies such as ipilimumab and tremelimumab, this inhibitory response can be negated, allowing for binding of CD80 or CD86 with CD28 to co-stimulate T-cell activation[11,14]. Ipilimumab and tremelimumab have been used in numerous clinical trials as monotherapy and in combination with other ICI. Both

ipilimumab and tremelimumab have been approved by the U.S. Food and Drug Administration (FDA) and the European Medicines Agency (EMA) for clinical use, however neither drug have been approved as a standard treatment option for urothelial cancer specifically.

PD-1 is expressed by T-cells during initial antigen-mediated activation[15]. By engaging its ligands PD-L1 and PD-L2, it functions to counter the activating signals after antigen stimulation, contributing to self-tolerance under physiological conditions[16-18]. The PD-1 pathway is commonly exploited by tumor cells in order to evade the immune system. By inhibiting this pathway with monoclonal antibodies, an effective immune-mediated anti-tumor response can be mounted[19,20]. Multiple monoclonal inhibitory antibodies have been developed that target either PD-1 (nivolumab, pembrolizumab, cemiplimab and dostarlimab) or PD-L1 (durvalumab, avelumab and atezolizumab). These antibodies have been tested elaborately in multiple cancer types, including urothelial cancer, and are all approved by the FDA and EMA for clinical use.

IMMUNE CHECKPOINT INHIBITION IN THE CLINIC

Standard first-line therapy for metastatic urothelial cancer (mUC) is cisplatin-based combination chemotherapy[21,22]. Carboplatin can be considered as an alternative for patients ineligible for cisplatin[21,22]. Following the success in other cancer types, such as melanoma, renal cell carcinoma and non-small cell lung cancer (NSCLC), ICI were tested in multiple trials in platinum-refractory mUC (Table 1)[23,24]. An improved OS was observed for pembrolizumab compared to chemotherapy in platinum-refractory mUC in the KEYNOTE-045 trial[23]. These results led to the approval of pembrolizumab for the treatment of platinum-refractory mUC. The IMvigor211 trial explored atezolizumab as second-line therapy in mUC and showed improved OS for the intention-to-treat (ITT) population. However, this trial did not meet its primary endpoint of improved OS in patients with tumors with high PD-L1 expression[24]. Encouraged by these first results of ICI, a number of phase 3 trials were initiated to investigate the effect of first-line treatment with anti-PD-1/PD-L1 compared to standard platinum-based chemotherapy (Table 1). These included the KEYNOTE-361 (pembrolizumab), DANUBE (durvalumab) and the IMvigor130 (atezolizumab) trials. Unfortunately, no meaningful improvement in clinical benefit for anti-PD-1/PD-L1 monotherapy versus standard first-line platinum-based chemotherapy treatment was observed[25-27]. Both the KEYNOTE-361 and IMvigor130 trials also tested the effect of combined chemotherapy and ICI in this setting. Comparable to treatment with ICI monotherapy, the combination treatment did not confer any benefit over standard treatment with chemotherapy in the ITT analysis[25,28]. The results of another phase 3 trial (CheckMate-901) are still pending. In this trial the investigators assessed the effect of standard cisplatin-based chemotherapy together with nivolumab. A 2023 press release reported a statistically significant improvement in progression-free survival (PFS) and OS for cisplatin/gemcitabine plus nivolumab, in comparison with cisplatin/gemcitabine alone. Interestingly, a subgroup analysis of the IMvigor130 study suggested that the combination of cisplatin-based

chemotherapy with atezolizumab had better synergy than the carboplatin-based combination[28], potentially explaining this phenomenon. The full results of the CheckMate-901 trial are pending and are required to better understand the discrepancies between these results and the results from the other first-line trials with ICI. The DANUBE (durvalumab plus tremelimumab) and CheckMate-901 (ipilimumab plus nivolumab) trials also evaluated the combination of PD-1/PD-L1 inhibition with CTLA-4 inhibition in mUC[26,27]. The DANUBE trial did not reach its primary endpoint(s). However, a numerical difference can be observed in favor of combined treatment with durvalumab plus tremelimumab compared to durvalumab monotherapy, especially in the PD-L1+ population[27]. The formal results of the CheckMate-901 trial are still pending, however, the trial failed to meet one of its (co)primary endpoints of improved OS for ipilimumab plus nivolumab in patients with tumors with high PD-L1 expression, according to a 2022 press release by Bristol Myers Squibb.

In defining the optimal treatment setting, some recent trials suggest there is a place for ICI in the adjuvant setting in MIBC (Table 1). Two phase 3 trials have explored the efficacy and clinical benefit of adjuvant nivolumab (CheckMate-274) and atezolizumab (IMvigor010) in patients with residual muscle-invasive disease after RC[29,30]. Only the trial with nivolumab met its primary endpoint of improved RFS in the ITT population, as well as in the PD-L1high population[29]. However, as PD-1/PD-L1 inhibition is approved as second-line treatment for mUC, it is possible that the group that did not receive adjuvant nivolumab will eventually benefit from checkpoint blockade in a later disease stage, as the disease would still be naïve to exposure to checkpoint inhibition. Therefore, OS data are needed to fully assess clinical benefit. Interestingly, clinical benefit in the CheckMate-274 trial was most prominent in patients that were previously treated with NAC. A potentially similar phenomenon has also been observed in the phase 3 JAVELIN Bladder 100 trial, where patients were treated with avelumab as maintenance therapy after platinum-based treatment in the metastatic setting[31]. Patients treated with avelumab had an improved OS compared to the group receiving best supportive care[31]. In addition to trials investigating the feasibility in the adjuvant or metastatic setting or as maintenance therapy, a number of phase 1/2 trials investigated ICI in the neoadjuvant setting, primarily to offer an alternative for patients who refused cisplatin or were ineligible (Table 1). Preoperative pembrolizumab was investigated in the PURE-01 trial[32,33]. Patients with cT2-4N0 BC were treated with three cycles of pembrolizumab, followed by RC. A pCR rate of 38.5% was observed[32,33]. In the ABACUS trial, preoperative atezolizumab was investigated in cT2-4aN0 BC patients[34]. This trial yielded a response rate of 31%[34].

Following up on the success of these trials, two neoadjuvant trials were initiated using a combination of CTLA-4 inhibition and PD-1/PD-L1 inhibition[35,36]. In the NABUCCO trial, 24 patients with locally advanced BC were treated with a combination of ipilimumab plus nivolumab followed by radical surgery[35]. Here, a pCR was observed in 46% of patients. In addition, 58% of patients had no remaining residual muscle-invasive disease after surgery (ypT0/Tis/Ta/TaN0)[35].

Table 1 | Overview of clinical trials assessing immune checkpoint inhibitors in bladder cancer

Trial reference (ClinicalTrials.gov ID)	Trial title	Therapeutic antibody used	Primary findings	Reference
KEYNOTE-045 (NCT02256436)	A Study of Pembrolizumab (MK-3475) Versus Paclitaxel, Docetaxel, or Vinflunine for Participants With Advanced Urothelial Cancer (MK-3475-045/KEYNOTE-045)	Pembrolizumab	Pembrolizumab was associated with significantly longer OS (by approximately 3 months) than chemotherapy as second-line therapy for platinum-refractory mUC.	[23]
IMvigor211 (NCT02302807)	A Study of Atezolizumab Compared With Chemotherapy in Participants With Locally Advanced or Metastatic Urothelial Bladder Cancer [IMvigor211]	Atezolizumab	Atezolizumab was not associated with significantly longer OS than chemotherapy in patients with platinum-refractory mUC overexpressing PD-L1 (IC2/3).	[24]
KEYNOTE-361 (NCT02853305)	Study of Pembrolizumab With or Without Platinum-based Combination Chemotherapy Versus Chemotherapy Alone in Urothelial Carcinoma (MK-3475-361/ KEYNOTE-361)	Pembrolizumab	The addition of pembrolizumab to first-line platinum-based chemotherapy did not significantly improve efficacy and should not be widely adopted for treatment of advanced urothelial carcinoma.	[25]
DANUBE (NCT02516241)	Study of MEDI4736 (Durvalumab) With or Without Tremelimumab Versus Standard of Care Chemotherapy in Urothelial Cancer	Durvalumab with or without tremelimumab	This study did not meet either of its coprimary endpoints of OS compared between the durvalumab monotherapy versus chemotherapy groups in the population of patients with high PD-L1 expression and between the durvalumab plus tremelimumab versus chemotherapy groups in the ITT population.	[27]
IMvigor130 (NCT02807636)	Study of Atezolizumab as Monotherapy and in Combination With Platinum-Based Chemotherapy in Participants With Untreated Locally Advanced or Metastatic Urothelial Carcinoma (IMvigor130)	Atezolizumab	Addition of atezolizumab to platinum-based chemotherapy as first-line treatment prolonged PFS in patients with mUC. The final OS analysis showed a non-statistically significant OS benefit (HR 0.85, p=0.023). OS for atezolizumab monotherapy vs chemotherapy was negative for the ITT population. An exploratory analysis showed a benefit for atezolizumab monotherapy in the PD-L1–high (IC2/3) group.	[28] ASCO-GU 2023
CheckMate-901 (NCT03036098)	Study of Nivolumab in Combination With Ipilimumab or Standard of Care Chemotherapy Compared to the Standard of Care Chemotherapy Alone in Treatment of Participants With Untreated Inoperable or Metastatic Urothelial Cancer (CheckMate901)	Nivolumab with or without ipilimumab	(2022): Nivolumab plus ipilimumab did not meet the primary endpoint of improved overall survival (OS) in patients with tumors with high PD-L1 expression; (2023): nivolumab in combination with cisplatin-based chemotherapy followed by nivolumab monotherapy demonstrated statistically significant benefits in OS and PFS.	2022/2023 BMS press release

Table 1 | Continued.

Trial reference (ClinicalTrials.gov ID)	Trial title	Therapeutic antibody used	Primary findings	Reference
CheckMate-274 (NCT02632409)	An Investigational Immuno-therapy Study of Nivolumab, Compared to Placebo, in Patients With Bladder or Upper Urinary Tract Cancer, Following Surgery to Remove the Cancer (CheckMate 274)	Nivolumab	Disease-free survival was longer with adjuvant nivolumab than with placebo in the ITT population and among patients with a PD-L1 expression level of 1% or more in patients with high-risk muscle-invasive urothelial carcinoma who were treated with radical surgery.	29
IMvigor010 (NCT02450331)	A Study of Atezolizumab Versus Observation as Adjuvant Therapy in Participants With High-Risk Muscle-Invasive Urothelial Carcinoma (UC) After Surgical Resection (IMvigor010)	Atezolizumab	The trial did not meet its primary endpoint of improved disease-free survival in patients receiving adjuvant atezolizumab over observation.	30
JAVELIN Bladder 100 (NCT02603432)	A Study Of Avelumab In Patients With Locally Advanced Or Metastatic Urothelial Cancer (JAVELIN Bladder 100)	Avelumab	Maintenance avelumab plus best supportive care significantly prolonged OS, as compared with best supportive care alone, among patients with urothelial cancer who had disease that had not progressed with first-line chemotherapy.	31
PURE-01 (NCT02736266)	Neoadjuvant Pembrolizumab for Muscle-invasive Urothelial Bladder Carcinoma	Pembrolizumab	Neoadjuvant pembrolizumab resulted in 42% of patients with pT0 and was safely administered in patients with MIBC.	32
ABACUS (NCT02662309)	Preoperative MPDL3280A in Transitional Cell Carcinoma of the Bladder (ABACUS)	Atezolizumab	The pCR rate was 31% (95% confidence interval: 21–41%), achieving the primary efficacy endpoint.	34
Preoperative durvalumab and tremelimumab (NCT02812420)	Durvalumab and Tremelimumab in Treating Patients With Muscle-Invasive, High-Risk Urothelial Cancer That Cannot Be Treated With Cisplatin-Based Therapy Before Surgery	Durvalumab with tremelimumab	The primary endpoint was safety and we observed 6 of 28 patients (21%) with grade ≥3 immune-related adverse events. We also observed pathological complete response of 37.5% of patients who completed surgery (n = 24).	36
NABUCCO (NCT03387761)	Neo-Adjuvant Bladder Urothelial Carcinoma COmbination-immunotherapy (NABUCCO)	Nivolumab with ipilimumab	All patients were evaluable for the study endpoints and underwent resection, 23 (96%) within 12 weeks (primary endpoint; feasibility). Grade 3-4 immune-related adverse events occurred in 55% of patients. Eleven patients (46%) had a pCR, meeting the secondary efficacy endpoint.	35

Table 1 | Continued.

Trial reference (ClinicalTrials.gov ID)	Trial title	Therapeutic antibody used	Primary findings	Reference
NABUCCO 2 (NCT03387761)	Neo-Adjuvant Bladder Urothelial Carcinoma COmbination-immunotherapy (NABUCCO)	Nivolumab with ipilimumab	A pCR was observed in six (43%) patients in cohort 2A (ipi 3 mg/kg) and in one (7%) patient in cohort 2B (ipi 1 mg/kg). Absence of plasma ctDNA correlated with pCR.	42
CheckMate-032 (NCT01928394)	A Study of Nivolumab by Itself or Nivolumab Combined With Ipilimumab in Patients With Advanced or Metastatic Solid Tumors	Nivolumab with or without ipilimumab	Objective response rate was 25.6%, 26.9%, and 38.0% in the NIVO3, NIVO3+IPI1, and NIVO1+IPI3 arms, respectively. Grade 3 or 4 treatment-related adverse events occurred in 21 (26.9%), 32 (30.8%), and 36 (39.1%) patients treated with NIVO3, NIVO3+IPI1, and NIVO1+IPI3, respectively.	44
EV-101 (NCT02091999)	A Study of Escalating Doses of ASG-22CE Given as Monotherapy in Subjects With Metastatic Urothelial Cancer and Other Malignant Solid Tumors That Express Nectin-4	Enfortumab Vedotin	Single-agent EV was generally well tolerated and provided clinically meaningful and durable responses in patients with mUC.	114
EV-301 (NCT03474107)	A Study to Evaluate Enfortumab Vedotin Versus (vs) Chemotherapy in Subjects With Previously Treated Locally Advanced or Metastatic Urothelial Cancer (EV-301)	Enfortumab Vedotin	Enfortumab vedotin significantly prolonged survival as compared with standard chemotherapy in patients with locally advanced or mUC who had previously received platinum-based treatment and a PD-1 or PD-L1 inhibitor.	115
EV-103 (NCT03288545)	A Study of Enfortumab Vedotin Alone or With Other Therapies for Treatment of Urothelial Cancer (EV-103)	Enfortumab Vedotin and pembrolizumab	Enfortumab vedotin plus pembrolizumab showed a manageable safety profile and promising confirmed objective response rate in cisplatin-ineligible pts with locally advanced or mUC; activity was consistently observed across a range of pre-specified subgroups including those with poor prognosis.	117, 119
EV-302 (NCT04223856)	Enfortumab Vedotin and Pembrolizumab vs. Chemotherapy Alone in Untreated Locally Advanced or Metastatic Urothelial Cancer (EV-302)	Enfortumab Vedotin and pembrolizumab	Pending	118

The group of Gao and colleagues conducted a trial with two cycles of tremelimumab plus durvalumab in locally advanced BC. A pCR was observed in 38% of patients that underwent surgery, which is comparable to platinum-based chemotherapy regimens in locally advanced disease[8,36]. In addition to the results observed in the NABUCCO trial, encouraging results with preoperative ipilimumab plus nivolumab have been observed in multiple other tumor types[37-41]. These studies suggested a lower dose of ipilimumab may be sufficient in the non-metastatic setting. To find the optimal dose of ipilimumab and nivolumab in locally advanced BC, patients in cohort 2 of the NABUCCO trial were randomized to receive either two cycles of 3 mg/kg ipilimumab plus 1 mg/kg of nivolumab or two cycles of 1 mg/kg ipilimumab plus 3 mg/kg of nivolumab in both arms followed by one cycle of 3 mg/kg nivolumab and RC[42]. A pCR was observed in 43% of patients treated with ipilimumab 3 mg/kg in combination with nivolumab, similar to the results from cohort 1 of the NABUCCO trial. In contrast, a pCR was observed in only 7% of patients treated with ipilimumab 1 mg/kg in combination with nivolumab[42]. Similarly, in the CheckMate-032 trial, patients with advanced BC were treated with either nivolumab monotherapy, or in combination with ipilimumab with different dose combinations[43,44]. While this trial was not properly powered to detect a difference in OS, a higher objective response rate was observed for patients treated with plus ipilimumab 3 mg/kg plus nivolumab 1 mg/kg (38.0%) compared to patients treated with ipilimumab 1 mg/kg plus nivolumab 3 mg/kg (26.9%) or nivolumab monotherapy (25.6%)[43]. Taken together, the data in BC suggests that a high dose of CTLA-4 blockade in combination with PD-1/PD-L1 blockade yields better clinical responses compared to a low dose of CTLA-4 blockade. For the locally advanced setting, this could be an alternative treatment especially for cisplatin-ineligible patients.

THE TUMOR IMMUNE MICRO-ENVIRONMENT IN BLADDER CANCER

Across different tumor types, there are certain aspects that impact the general immunogenicity of tumors and the general efficacy of ICI. Tumor mutational burden (TMB) is a metric to indicate the average number of mutations in the DNA of tumor cells compared to healthy cells. Only a small fraction of these mutations are 'driver' mutations, while the majority are 'passenger' mutations with no direct function in tumor development or progression[45,46]. Potentially, these 'passenger mutations' generate aberrant proteins which can be detected by the immune system as neoantigens, triggering an immune response directed against the tumor[47,48]. TMB is a surrogate measure of neoantigen load, which allows it to serve as a predictive biomarker for general immunogenicity and tendency of tumors to respond to ICI[49-51]. TMB varies per individual tumor. However, different tumor types have a different average TMB. Melanoma and other skin cancers typically have the highest TMB. Although not as high as melanoma, average TMB in BC is relatively high, similar to NSCLC[52,53].

TMB has been investigated in a number of BC trials mentioned earlier. In the preoperative setting, it was positively associated with response in the PURE-01 trial (pembrolizumab), and numerically higher in responders compared to non-responders in the ABACUS trial (atezolizumab), NABUCCO trial (ipilimumab plus nivolumab) and in the preoperative trial with tremelimumab and durvalumab[32,34-36]. In addition, changes in the TMB after treatment were assessed in the PURE-01 trial (pembrolizumab) in fourteen patients for which paired tissue samples were available (≥ypT2). Interestingly, TMB was significantly lower compared with the baseline TMB after treatment with pembrolizumab[32]. In addition to an increased TMB, some specific genomic alterations also impact tumor behavior, prognosis and response to ICI. Recently, it was shown that loss of the Y-chromosome is associated with poor prognosis in male BC patients and was related to intratumoral CD8+ T-cell dysfunction and exhaustion. Interestingly, patients with loss of the Y-chromosome exhibited an increased response to PD-1 inhibition in both mice and BC patients[54].

Multiple immune cell subsets are implied to play a role in the TIME. Cytotoxic CD8+ T-cells have been established as one of the major players in the TIME in BC as well as in most other tumor types. Within the CD8+ T-cells, different subsets have been observed with varying degrees of tumor-reactivity. CD8+ T-cells expressing the combination of CD103 (integrin αE) and CD39 (an ectonucleotidase) are enriched for tumor-reactive cells in multiple different tumor types. These cells also efficiently kill autologous tumor cells in a major histocompatibility complex (MHC) class I-dependent manner[55]. Specifically in BC, it has been shown that patients with tumors with high infiltration of CD8+CD103+ tissue-resident memory T-cells are more likely to benefit from ICI and adjuvant chemotherapy[56]. Based on the abundance of CD8+ T-cells and other immune cells and their spatial organization in relation to the tumor, distinct immune phenotypes can be defined[57,58]. *Immune-Inflamed* tumors are considered to be immunologically 'hot' tumors and are characterized by an abundancy of immune cells invading the tumor and the surrounding stroma. Apart from CD8+ T-cells, these include other T-cells, B-cells and pro-inflammatory macrophages. In addition, these tumors are characterized by a type I Interferon gamma (IFN-γ) signature[58]. Tumors that are populated with immune cells but with relatively few cytotoxic T-cells inside the core of the tumor are commonly referred to as tumors with an *immune-excluded* phenotype[57,58]. It is currently not completely understood if these cytotoxic cells are insufficiently stimulated to infiltrate the tumor, or whether tumor infiltration is physically being prevented by interfering fibroblasts or stromal cells or due to other pro-tumorigenic cells[59]. It has been suggested that tumor-associated macrophages along the tumor margins prevent cytotoxic lymphocytes from tumor core infiltration[60]. Tumors with very few immune cells are referred to as immunologically 'cold' tumors or having an *immune-desert* phenotype. These tumors are characterized by a low number of lymphocytes and a high macrophage-to-lymphocyte ratio[61].

Multiple studies have shown that greater infiltration of CD8+ T-cells is related to a more favorable clinical outcome and a better response to ICI in multiple disease stages in BC[34,62-66]. In the ABACUS trial mentioned above, a relatively high proportion of immune-inflamed (73%) tumors was found

based on the abundance and spatial organization of CD8^{+} T-cells. However, the immune-inflamed phenotype did not correlate with response[34]. A CD8/GZMB co-staining was performed to further enrich for tumors with high anti-tumor reactivity. Indeed, the percentage of tumors with an immune-inflamed phenotype that contained CD8^{+}GZMB^{+} cells was higher in responders versus patients that relapsed (87% and 30%, respectively)[34]. In addition, a significant increase in infiltrating CD8^{+} T-cells was observed based on immunohistochemistry when comparing post-treatment tissue to pre-treatment tissue[34]. In the PURE-01 trial mentioned above, the effect of ICI on the TIME was assessed by comparing pre- and post- treatment samples from patients with residual disease after treatment with preoperative pembrolizumab[67]. These findings were compared to patients that were treated with a direct RC, or with NAC followed by RC. It was found that patients with residual tumor after treatment with pembrolizumab and cystectomy showed a high rate of stroma-rich calls with a decreased tumor purity and increased stromal content[67]. In addition, these tumors also expressed luminal markers, distinguishing them from the untreated and tumors that did not respond to NAC. This would suggest that luminal tumors may have an intrinsic resistance to treatment with ICI or that treatment with ICI may select for, or induce, a luminal phenotype[67,68] In another study, immune phenotypes were classified based on CD8^{+} T-cell density in the tumor and stroma compartments in an untreated BC cohort[69]. Immune-inflamed (42%) was the most common immune phenotype, whereas 32% and 26% of tumors were classified as immune-excluded and immune-desert phenotypes, respectively. Although tumors qualified as immune-desert showed a numerically high rate of recurrence (88%), no statistically significant correlation was found[69]. In contrast, in the NABUCCO trial (preoperative ipilimumab plus nivolumab) no correlation was observed between baseline CD8^{+} T-cell density and response to ipilimumab plus nivolumab. In addition, no significant difference was observed in IFN-γ signaling at baseline in responding tumors compared to non-responding tumors. This data suggest that the addition of anti-CTLA-4 to PD-1 blockade can induce a pCR in tumors irrespective of baseline immunity[35]. In addition, the density of CD8^{+}PD1^{+} T-cells in tumors from patients treated with ipilimumab and nivolumab was higher than that of patients treated with a direct cystectomy, regardless of response to ICI[69].

Current efforts to understand anti-tumor immunity are primarily focused on CD8^{+} T-cells. However, there is also a role for CD4^{+} T-cells in the interaction between the tumor and TIME. Regulatory CD4^{+} T-cells in the BC TIME are known for their role in inhibiting or dampening an ongoing immune response by producing anti-inflammatory cytokines like IL-10 and transforming growth factor beta (TGF-β), direct inhibition of dendritic cells and more[70,71]. Regulatory CD4^{+} T-cells in the BC TIME have been associated with adverse outcomes, similar to other tumor types[72]. The exact underlying biological mechanism for this association remains unclear. However one study found overexpression of sphingosine 1 phosphate receptor 1 (S1P1) in BC, promoting production of TGF-β and IL-10 *in vitro* and *in vivo*[73].

In addition to an immunosuppressive role, it was recently found that CD4^{+} T-cells also play an important role in anti-tumor immunity in BC[74]. Based on data from single-cell RNA sequencing,

multiple cytotoxic CD4^{+} T-cell states were identified based on the expression of granzyme B, granzyme K, perforin as well as other granule-associated proteins. These distinct populations were validated by flow cytometry and multiplex immunofluorescence tissue staining. In addition, it was found that cytotoxic CD4^{+} subsets in bladder tumors were clonally expanded, potentially resulting from recognition of bladder tumor antigens. Their functional importance was confirmed by their ability to kill autologous tumors *ex vivo* in a MHC class II-dependent manner. Overall, these findings highlight the importance of CD4^{+} T-cell heterogeneity and the relative balance between activation of cytotoxic CD4^{+} effector cells and inhibitory regulatory cells for killing autologous tumors[74].

Apart from lymphocytes, there is a prominent role for macrophages in the TIME. Macrophages are not a single cell population with a defined phenotype and biological activity but rather a diverse collection of cell types with a wide range of functional roles[75]. Macrophages have been traditionally categorized as either M1 or M2 macrophages, characterized by different markers. M1 macrophages are considered anti-tumorigenic and express high levels of tumor necrosis factor alpha (TNFα), inducible nitric oxide synthase (iNOS) or MHC class II molecules. In contrast, M2 macrophages are considered pro-tumorigenic and express CD163, CD206 and high levels of arginase 1 (ARG1) and IL-10[76]. However, it is becoming clear that a broad spectrum of macrophage phenotypes exists, and using markers to delineate their functional role within the tumor is not straightforward[77]. The majority of the work on macrophages has been done in other tumor types, but a few studies also investigated whether there is an association between macrophage abundance and polarization status (M1-like or M2-like) and prognosis and outcome in BC. One study found that a high intratumoral density of M2 macrophages (based on expression of CD163) was associated with poor outcome in patients with BC[78]. Another study by Sun and colleagues investigated macrophage polarization in relation to response to ICI treatment in the IMvigor210 trial (atezolizumab). It was found that patients with tumors with predominantly M1 macrophages were indeed more sensitive to PD-L1 blockade[79]. Wang and collaborators found that a pro-tumorigenic inflammatory signature was correlated with poor outcome in the IMvigor210 (atezolizumab) and the CheckMate-275 (nivolumab) trials[80]. One preclinical study used a conditional knockout BC mouse model which showed a heterogeneous response to treatment with PD-1 inhibition. Responding tumors showed a higher number of intratumoral macrophages[81]. While the exact mechanism still needs to be unraveled, the number of macrophages and their polarization status seems to be associated with the efficacy of ICI and thus may be relevant to predict which patients respond to treatment.

Similar to other tumor types, multiple other cell types likely also play a role in the TIME in BC. These include, but are not limited to: pericytes, dendritic cells, natural killer cells and eosinophils. While important, limited work has been done in BC specifically.

Tertiary lymphoid structures (TLS) are organized clusters of lymphocytes in chronically inflamed tissue[82]. They resemble secondary lymphoid organs like lymph nodes and have similar functions such as mounting germinal center reactions and priming of antigen-specific T-cells[83,84]. The

density of TLS in the TIME is associated with infiltration of adaptive immune cells and improved clinical outcome in multiple tumor types including in BC[85-87]. However, it is currently unclear what the exact role is of TLS in the anti-tumor immune response and whether they are a prerequisite or rather a consequence of an anti-tumor immune response[86]. It was proposed that TLS mature through different developmental stages with increasing proportions of activated lymphocytes throughout the maturation process[88]. However, another study assessing different BC cohorts found that the proportions of activated B-cells, T-cells and progenitor-like CD8+ T-cells were similar when comparing maturation stages, and seemed to be more dependent on the number of TLS in the TIME[86]. Another study in BC made a distinction between superficial and deep TLS, based on their location relative to the bladder lumen. Superficial TLS were hypothesized to primarily play a role in the immune response against irritative chemicals and microbial pathogens present in the urine. Deep TLS presumably play a more prominent role in anti-tumor immunity. It was found that the density of CD4+ T-cells was higher in superficial TLS and the proportion of follicle-like, mature structures was higher in deep TLS[69]. Two trials that assessed combination ICI as a preoperative strategy in locally advanced BC investigated TLS at baseline as a predictive biomarker. One study testing preoperative tremelimumab plus durvalumab reported a higher density of pretreatment TLS in responders compared to non-responders[36]. In addition, it was observed that a higher density of pretreatment TLS was associated with a longer OS and RFS. In contrast, no difference in pretreatment TLS density was reported in responders compared to non-responders in patients with locally advanced BC treated with preoperative ipilimumab plus nivolumab in the NABUCCO trial[35]. However, the density of TLS after treatment increased in responders, whereas the TLS density decreased in non-responders. In addition, it was found that regulatory T-cells in TLS decreased after treatment with ipilimumab plus nivolumab, showing that this treatment also influences the composition of TLS[35]. In another recent study in BC, an association was found between TLS density and TMB as well as increased T-cell activation. Combining TLS density with TMB into a joint 'TLSTMB' score generated a novel prognostic biomarker that, in contrast to either TLS density of TMB alone, was independent from tumor stage and vascular invasion[86]. The exact role of TLS remains to be elucidated. However, it is clear from multiple studies that TLS play a pivotal role in the anti-tumor immune response in BC.

TGF-β is a cytokine that is involved in multiple different pathways and interactions and is associated with poor clinical outcome in different tumor types[89-91]. It is thought to have a pro-tumorigenic role in advanced cancers by promoting fibroblast activation, immunosuppression, angiogenesis, epithelial-to-mesenchymal transition, and metastasis[92]. In a study by Mariathasan and colleagues, it was found that expression of TGF-β ligand 1 (TGFB1) and TGF-β receptor 2 (TGFBR2) were associated with non-response and reduced OS in patients with mUC who were treated with atezolizumab in the IMvigor210 trial[66]. In addition, the authors speculated that TGF-β signaling in cancer-associated fibroblasts (CAFs) contributed to an immune-excluded TIME. To measure TGF-β signaling specifically in fibroblasts, a pan-fibroblast TGF-β response signature (F-TBRS) was created. Expression of this signature was particularly high in tumors with an inflamed

or excluded phenotype, and low in tumors with an immune desert phenotype. In line with these findings, the F-TBRS was significantly associated with non-response in excluded tumors specifically (Figure 1)[66]. In addition, it was confirmed in an EMT6 mouse mammary carcinoma model that combining PD-L1 blockade and a TGF-β inhibitor led to infiltration of lymphocytes into the tumor and an improved survival, whereas this was not observed upon monotherapy with either inhibitor[66]. In the ABACUS trial, patients were treated with atezolizumab in the preoperative setting. Among the patients that relapsed, the patients with an immune-excluded bladder tumor had a numerically higher expression of the TGF-β response signature, which was not the case for patients that responded. However, no definitive conclusion can be drawn from this study due to lack of statistical power[34]. In the NABUCCO trial (ipilimumab plus nivolumab), a significantly higher expression of the TGF-β response signature was observed in non-responders versus responders at baseline[35]. A number of TGF-β inhibitors have been developed for clinical use and are currently being investigated in early clinical trials[93]. To our knowledge, there are currently two trials investigating TGF-β inhibitors in patients with mUC. In one trial, patients are treated with the oral TGF-β inhibitor vactosertib in combination with durvalumab (NCT04064190), for which results are pending. The other trial tested bintrafusp α (M7824), a bifunctional fusion protein composed of the extracellular domain of a TGF-β receptor fused to PD-L1 antibody (NCT04501094). This trial has been terminated due to low accrual.

MODULATING THE TUMOR IMMUNE MICRO-ENVIRONMENT TO IMPROVE THERAPY RESPONSE

In recent years, encouraging responses to ICI have been observed in BC patients. However, there is still a substantial subset of patients that does not respond to this treatment. This ICI resistance might be explained by various mechanisms, including tumor-intrinsic factors or factors related to the immune micro-environment[50,51,66]. Combining ICI monotherapy with other drugs such as additional ICI or conventional chemotherapy, may alter the TIME to be more susceptible to respond to treatment. Traditionally, chemotherapy has been regarded as immuno-suppressive, depleting immune cell subsets and leading to an increased rate of infections[94]. However, it has been shown in numerous preclinical and clinical studies that treatment with chemotherapy can also have immunostimulatory effects[95,96]. One of the direct effects of chemotherapy is the induction of immunogenic cell death, a form of cell death that is being preceded by a cellular stress-response. Via complex intracellular pathways, phagocytosis of tumor cells (or portions thereof) by dendritic cells is facilitated[97]. Processing of this cellular debris by dendritic cells eventually leads to presentation of neoantigens, as described earlier[47,48].
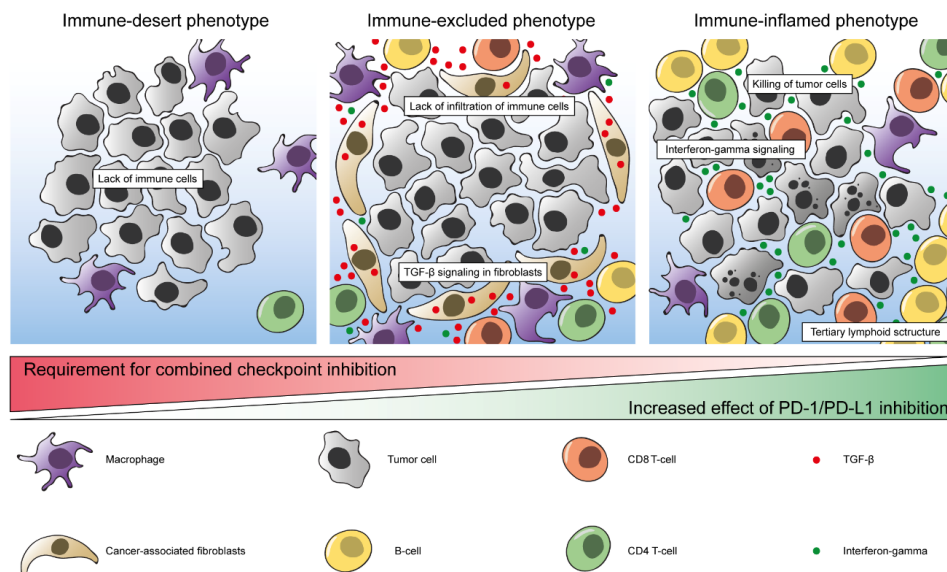
Figure 1 | Model of immune phenotypes in the bladder tumor immune micro-environment. Left: immune-desert phenotype with limited amounts of immune cells. Middle: immune-excluded phenotype with stromal cells, cancer associated fibroblasts and TGF-β signaling preventing infiltration of CD8^{+} T-cells and other immune cells. Macrophages predominantly display an immunosuppressive (M2) phenotype. Right: immune-inflamed phenotype with extensive infiltration of CD8^{+} T-cells and other immune cells. Macrophages are primarily of the M1 phenotype. Bottom: Increased effect of PD-1/PD-L1 inhibition have been observed in tumors with an immune-inflamed phenotype. Addition of CTLA-4 inhibition might be required to mount an effective immune response in tumors without pre-existing immunity.

In addition to the induction of immunogenic cell death, chemotherapy treatment also affects regulatory T-cells, tumor-associated macrophages and myeloid derived suppressor cells[98,99]. This phenomenon could be further exploited when used in conjunction with ICI. Indeed, a synergistic effect of concurrent chemotherapy and ICI has been observed in multiple tumor types, including in NSCLC and in triple-negative breast cancer (TNBC)[100-102]. In BC, one preclinical study assessed the effect of PD-L1 inhibition with or without platinum-based chemotherapy compared to platinum-based chemotherapy alone[103]. The combination strategy was more effective in the MB49 subcutaneous model compared to either platinum-based chemotherapy or PD-L1 inhibition alone. Interestingly, PD-L1 inhibition monotherapy was more effective than the combination strategy in the MBT-2 subcutaneous model, suggesting that combined treatment results are model-dependent[103]. Despite the positive results in other cancer types, no clinical benefit was observed when patients with mUC were treated with PD-1/PD-L1 inhibition or PD-1/PD-L1 inhibition in combination with standard platinum-based chemotherapy over chemotherapy alone in both the KEYNOTE-361 (pembrolizumab) and in the IMvigor130 (atezolizumab) trials[25,28]. However, a 2023 press release of the CheckMate-901 study reported a statistically significant improvement in PFS

and OS for cisplatin/gemcitabine plus nivolumab, in comparison with cisplatin/gemcitabine alone. The full results are pending and are required to better understand the discrepancies between these trial results. Potentially, this might result in the first approved treatment strategy with concurrent chemotherapy and ICI in BC. Theoretically, a sequential approach could be appealing, priming the TIME and allowing recovery of immune cell populations to subsequently further improve the anti-tumor response with ICI treatment[104]. This sequential approach was studied in patients with TNBC, where patients were treated with different types of induction chemotherapy, followed by nivolumab[105]. In metastatic BC, the JAVELIN Bladder 100 trial (avelumab) showed the efficacy of maintenance checkpoint inhibition after initial treatment with platinum-based chemotherapy[31]. The improved results for adjuvant nivolumab in the subset of patients in the CheckMate-274 trial who received NAC similarly supports sequential treatment[29]. Given the accessibility of bladder tumors, the TIME could be modulated by local therapies to improve susceptibility to ICI treatment, without having to expose patients to systemic therapy. For example, intravesical instilments with Bacillus Calmette–Guerin (BCG) or chemotherapeutic agents such as epirubicin or mitomycin can be employed. BCG represents the first type of immunomodulatory treatment approved by the FDA[106]. Despite its proven efficacy in reducing the chance of disease recurrence, its underlying biological mechanism is not fully understood. Generally, BCG is internalized primarily by cancer cells leading to cytokine production and the activation of CD4+ and CD8+ T-cells, leading to the killing of cancer cells[107,108]. Interestingly, one study showed that the efficacy of treatment with BCG is at least partly explained by PD-L1 expression, as the percentage of patients with PD-L1+ tumors at baseline was higher in patients that did not respond to treatment with BCG compared to patients that did respond[109]. Indeed, systemic treatment with pembrolizumab in patients with BCG-unresponsive non-muscle invasive BC was tolerable and showed promising anti-tumor activity in a single-arm phase 2 trial, leading to the approval of pembrolizumab for BCG-unresponsive, high-risk non-muscle invasive BC[110]. Intravesical instilments with ICI could potentially evoke a local immune response with less systemic exposure. Two exploratory trials investigated whether intravesical instilments with pembrolizumab were feasible. In one trial, patients with BCG-unresponsive non-muscle invasive BC were treated with intravesical pembrolizumab. A significant increase in CD4+ T-cells and CD8+ T-cells was found in the urine after a single dose of pembrolizumab as well as an increase in infiltrating CD8+ T-cells in the tumor[111]. Interestingly, even though treatment was only administered locally in the bladder, systemic immune-related adverse events were observed in some patients[111]. In the PemBla trial, six patients were treated with increasing doses of intravesical installments of pembrolizumab after transurethral resection of the bladder, which was well tolerated. These two exploratory trials confirm prior pre-clinical observations in a mouse BC model (MBT-2), where intravesical PD-1 inhibition was used to treat localized BC, and showed a similar effect compared to systemic treatment with PD-1 inhibition and changes in the TIME including increased infiltration of CD8+ T-cells[112]. Enfortumab vedotin (EV) - an antibody-drug conjugate - is directed against nectin-4, a protein which is highly expressed in urothelial cancer cells and is linked to monomethyl auristatin E, an agent that disrupts microtubule formation[113,114]. Encouraging results have been observed when EV was used as

monotherapy in pretreated mUC (Table 1)[115]. In addition, it has also been observed that treatment with EV leads to hallmarks of immunogenic cell death leading to T-cell activation[113,116]. Combined with pembrolizumab, EV has shown promising results and this combination is currently under investigation in a phase 3 study[117-119].

CONCLUSION

We have come to understand that cancer cells rely heavily on their interaction with the surrounding TIME, especially in the context of ICI. It is becoming clear which cell types, pathways and processes are involved in anti-tumor immunity. Taken together, a combination of tumor-intrinsic and microenvironment-related parameters determine the success of therapies targeting immune checkpoints: i) A high TMB and a high rate of neoantigens resulting in aberrant proteins which can be recognized by immune cells to then mount an effective antitumor immune response ii) Pre-existing anti-tumor immunity with infiltrating cytotoxic T-cells, IFN-γ signaling and the formation of TLS; iii) Low expression of TGF-β in CAFs to prevent an immune-excluded immune phenotype (Figure 1)[66,120]. However, despite meeting all of these criteria, some tumors still do not respond well to ICI. This indicates that there are still some missing pieces in the puzzle of adequate immunological cancer treatment. While there are many commonalities across different tumor types, there are also some features related to the TIME that have been found specifically in BC. These include the importance of TGF-β signaling and role of CD4^{+} T-cells and might explain some of the unique clinical findings observed in BC studies. For example, the improved clinical outcome when a high dose of CTLA-4 inhibition is used together with PD1/PD-L1 inhibition and the apparent lack of synergy when treating with a combination of ICI and systemic chemotherapy. Recent findings highlight the rapidly changing treatment landscape of BC. We now understand that cancer cell characteristics are just part of the puzzle for effective cancer treatment. Targeted therapeutic strategies like ICI and antibody-drug conjugates such as EV are highly dependent on the interaction between cancer cells and the TIME. Ultimately, more research is needed to better understand the TIME.

REFERENCES

1. Powles, T., *et al.* Bladder cancer: ESMO Clinical Practice Guideline for diagnosis, treatment and follow-up. *Ann Oncol* 33, 244-258 (2022).

2. Bray, F., *et al.* Global cancer statistics 2018: GLOBOCAN estimates of incidence and mortality worldwide for 36 cancers in 185 countries. *CA Cancer J Clin* 68, 394-424 (2018).

3. Stein, J.P., *et al.* Radical cystectomy in the treatment of invasive bladder cancer: long-term results in 1,054 patients. *J Clin Oncol* 19, 666-675 (2001).

4. Dalbagni, G., *et al.* Cystectomy for bladder cancer: a contemporary series. *J Urol* 165, 1111-1116 (2001).

5. Stein, J.P. & Skinner, D.G. Radical cystectomy for invasive bladder cancer: long-term results of a standard procedure. *World J Urol* 24, 296-304 (2006).

6. Madersbacher, S., *et al.* Radical cystectomy for bladder cancer today--a homogeneous series without neoadjuvant therapy. *J Clin Oncol* 21, 690-696 (2003).

7. Bruins, H.M., *et al.* Clinical outcomes and recurrence predictors of lymph node positive urothelial cancer after cystectomy. *J Urol* 182, 2182-2187 (2009).

8. Pfister, C., *et al.* Randomized Phase III Trial of Dose-dense Methotrexate, Vinblastine, Doxorubicin, and Cisplatin, or Gemcitabine and Cisplatin as Perioperative Chemotherapy for Patients with Muscle-invasive Bladder Cancer. Analysis of the GETUG/AFU V05 VESPER Trial Secondary Endpoints: Chemotherapy Toxicity and Pathological Responses. *Eur Urol* 79, 214-221 (2021).

9. Advanced Bladder Cancer Meta-analysis, C. Neoadjuvant chemotherapy in invasive bladder cancer: update of a systematic review and meta-analysis of individual patient data advanced bladder cancer (ABC) meta-analysis collaboration. *Eur Urol* 48, 202-205; discussion 205-206 (2005).

10. Keir, M.E., Butte, M.J., Freeman, G.J. & Sharpe, A.H. PD-1 and its ligands in tolerance and immunity. *Annu Rev Immunol* 26, 677-704 (2008).

11. Pardoll, D.M. The blockade of immune checkpoints in cancer immunotherapy. *Nat Rev Cancer* 12, 252-264 (2012).

12. Walsh, R.J., Sundar, R. & Lim, J.S.J. Immune checkpoint inhibitor combinations-current and emerging strategies. *Br J Cancer* 128, 1415-1417 (2023).

13. Krummel, M.F. & Allison, J.P. CD28 and CTLA-4 have opposing effects on the response of T cells to stimulation. *J Exp Med* 182, 459-465 (1995).

14. Linsley, P.S., *et al.* CTLA-4 is a second receptor for the B cell activation antigen B7. *J Exp Med* 174, 561-569 (1991).

15. Agata, Y., *et al.* Expression of the PD-1 antigen on the surface of stimulated mouse T and B lymphocytes. *Int Immunol* 8, 765-772 (1996).

16. Freeman, G.J., *et al.* Engagement of the PD-1 immunoinhibitory receptor by a novel B7 family member leads to negative regulation of lymphocyte activation. *J Exp Med* 192, 1027-1034 (2000).

17. Latchman, Y., *et al.* PD-L2 is a second ligand for PD-1 and inhibits T cell activation. *Nat Immunol* 2, 261-268 (2001).

18. Nishimura, H., Nose, M., Hiai, H., Minato, N. & Honjo, T. Development of lupus-like autoimmune diseases by disruption of the PD-1 gene encoding an ITIM motif-carrying immunoreceptor. *Immunity* 11, 141-151 (1999).

19. Iwai, Y., Terawaki, S. & Honjo, T. PD-1 blockade inhibits hematogenous spread of poorly immunogenic tumor cells by enhanced recruitment of effector T cells. *Int Immunol* 17, 133-144 (2005).

20. Hirano, F., *et al.* Blockade of B7-H1 and PD-1 by monoclonal antibodies potentiates cancer therapeutic immunity.

Cancer Res 65, 1089-1096 (2005).

21. von der Maase, H.*, et al.* Gemcitabine and cisplatin versus methotrexate, vinblastine, doxorubicin, and cisplatin in advanced or metastatic bladder cancer: results of a large, randomized, multinational, multicenter, phase III study. *J Clin Oncol* 18, 3068-3077 (2000).

22. De Santis, M.*, et al.* Randomized phase II/III trial assessing gemcitabine/carboplatin and methotrexate/carboplatin/ vinblastine in patients with advanced urothelial cancer who are unfit for cisplatin-based chemotherapy: EORTC study 30986. *J Clin Oncol* 30, 191-199 (2012).

23. Bellmunt, J.*, et al.* Pembrolizumab as Second-Line Therapy for Advanced Urothelial Carcinoma. *N Engl J Med* 376, 1015-1026 (2017).

24. Powles, T.*, et al.* Atezolizumab versus chemotherapy in patients with platinum-treated locally advanced or metastatic urothelial carcinoma (IMvigor211): a multicentre, open-label, phase 3 randomised controlled trial. *Lancet* 391, 748-757 (2018).

25. Powles, T.*, et al.* Pembrolizumab alone or combined with chemotherapy versus chemotherapy as first-line therapy for advanced urothelial carcinoma (KEYNOTE-361): a randomised, open-label, phase 3 trial. *Lancet Oncol* 22, 931-945 (2021).

26. Galsky, M.D., Powles, T., Li, S., Hennicken, D. & Sonpavde, G. A phase 3, open-label, randomized study of nivolumab plus ipilimumab or standard of care (SOC) versus SOC alone in patients (pts) with previously untreated unresectable or metastatic urothelial carcinoma (mUC; CheckMate 901). *Journal of Clinical Oncology* 36, TPS539-TPS539 (2018).

27. Powles, T.*, et al.* Durvalumab alone and durvalumab plus tremelimumab versus chemotherapy in previously untreated patients with unresectable, locally advanced or metastatic urothelial carcinoma (DANUBE): a randomised, open-label, multicentre, phase 3 trial. *Lancet Oncol* 21, 1574-1588 (2020).

28. Galsky, M.D.*, et al.* Atezolizumab with or without chemotherapy in metastatic urothelial cancer (IMvigor130): a multicentre, randomised, placebo-controlled phase 3 trial. *Lancet* 395, 1547-1557 (2020).

29. Bajorin, D.F.*, et al.* Adjuvant Nivolumab versus Placebo in Muscle-Invasive Urothelial Carcinoma. *N Engl J Med* 384, 2102-2114 (2021).

30. Bellmunt, J.*, et al.* Adjuvant atezolizumab versus observation in muscle-invasive urothelial carcinoma (IMvigor010): a multicentre, open-label, randomised, phase 3 trial. *Lancet Oncol* 22, 525-537 (2021).

31. Powles, T.*, et al.* Avelumab Maintenance Therapy for Advanced or Metastatic Urothelial Carcinoma. *N Engl J Med* 383, 1218-1230 (2020).

32. Necchi, A.*, et al.* Pembrolizumab as Neoadjuvant Therapy Before Radical Cystectomy in Patients With Muscle-Invasive Urothelial Bladder Carcinoma (PURE-01): An Open-Label, Single-Arm, Phase II Study. *J Clin Oncol* 36, 3353-3360 (2018).

33. Bandini, M.*, et al.* Does the administration of preoperative pembrolizumab lead to sustained remission post-cystectomy? First survival outcomes from the PURE-01 study(✩). *Ann Oncol* 31, 1755-1763 (2020).

34. Powles, T.*, et al.* Clinical efficacy and biomarker analysis of neoadjuvant atezolizumab in operable urothelial carcinoma in the ABACUS trial. *Nat Med* 25, 1706-1714 (2019).

35. van Dijk, N.*, et al.* Preoperative ipilimumab plus nivolumab in locoregionally advanced urothelial cancer: the NABUCCO trial. *Nat Med* 26, 1839-1844 (2020).

36. Gao, J.*, et al.* Neoadjuvant PD-L1 plus CTLA-4 blockade in patients with cisplatin-ineligible operable high-risk urothelial carcinoma. *Nat Med* 26, 1845-1851 (2020).

37. Amaria, R.N.*, et al.* Neoadjuvant immune checkpoint blockade in high-risk resectable melanoma. *Nat Med* 24, 1649-1654

(2018).

38. Blank, C.U., *et al.* Neoadjuvant versus adjuvant ipilimumab plus nivolumab in macroscopic stage III melanoma. *Nat Med* 24, 1655-1661 (2018).

39. Chalabi, M., *et al.* Neoadjuvant immunotherapy leads to pathological responses in MMR-proficient and MMR-deficient early-stage colon cancers. *Nat Med* 26, 566-576 (2020).

40. Vos, J.L., *et al.* Neoadjuvant immunotherapy with nivolumab and ipilimumab induces major pathological responses in patients with head and neck squamous cell carcinoma. *Nat Commun* 12, 7348 (2021).

41. Cascone, T., *et al.* Neoadjuvant nivolumab or nivolumab plus ipilimumab in operable non-small cell lung cancer: the phase 2 randomized NEOSTAR trial. *Nat Med* 27, 504-514 (2021).

42. van Dorp, J., *et al.* High- or low-dose preoperative ipilimumab plus nivolumab in stage III urothelial cancer: the phase 1B NABUCCO trial. *Nat Med* (2023).

43. Janjigian, Y.Y., *et al.* CheckMate-032 Study: Efficacy and Safety of Nivolumab and Nivolumab Plus Ipilimumab in Patients With Metastatic Esophagogastric Cancer. *J Clin Oncol* 36, 2836-2844 (2018).

44. Sharma, P., *et al.* Nivolumab monotherapy in recurrent metastatic urothelial carcinoma (CheckMate 032): a multicentre, open-label, two-stage, multi-arm, phase 1/2 trial. *Lancet Oncol* 17, 1590-1598 (2016).

45. Hanahan, D. & Weinberg, R.A. Hallmarks of cancer: the next generation. *Cell* 144, 646-674 (2011).

46. McFarland, C.D., *et al.* The Damaging Effect of Passenger Mutations on Cancer Progression. *Cancer Res* 77, 4763-4772 (2017).

47. Ott, P.A., *et al.* An immunogenic personal neoantigen vaccine for patients with melanoma. *Nature* 547, 217-221 (2017).

48. Keskin, D.B., *et al.* Neoantigen vaccine generates intratumoral T cell responses in phase Ib glioblastoma trial. *Nature* 565, 234-239 (2019).

49. Le, D.T., *et al.* PD-1 Blockade in Tumors with Mismatch-Repair Deficiency. *N Engl J Med* 372, 2509-2520 (2015).

50. Samstein, R.M., *et al.* Tumor mutational load predicts survival after immunotherapy across multiple cancer types. *Nat Genet* 51, 202-206 (2019).

51. Goodman, A.M., *et al.* Tumor Mutational Burden as an Independent Predictor of Response to Immunotherapy in Diverse Cancers. *Mol Cancer Ther* 16, 2598-2608 (2017).

52. Chalmers, Z.R., *et al.* Analysis of 100,000 human cancer genomes reveals the landscape of tumor mutational burden. *Genome Med* 9, 34 (2017).

53. Alexandrov, L.B., *et al.* Signatures of mutational processes in human cancer. *Nature* 500, 415-421 (2013).

54. Abdel-Hafiz, H.A., *et al.* Y chromosome loss in cancer drives growth by evasion of adaptive immunity. *Nature* (2023).

55. Duhen, T., *et al.* Co-expression of CD39 and CD103 identifies tumor-reactive CD8 T cells in human solid tumors. *Nat Commun* 9, 2724 (2018).

56. Jin, K., *et al.* CD103(+)CD8(+) tissue-resident memory T cell infiltration predicts clinical outcome and adjuvant therapeutic benefit in muscle-invasive bladder cancer. *Br J Cancer* 126, 1581-1588 (2022).

57. Binnewies, M., *et al.* Understanding the tumor immune microenvironment (TIME) for effective therapy. *Nat Med* 24, 541-550 (2018).

58. Gajewski, T.F., *et al.* Cancer Immunotherapy Targets Based on Understanding the T Cell-Inflamed Versus Non-T Cell-Inflamed Tumor Microenvironment. *Adv Exp Med Biol* 1036, 19-31 (2017).

59. Spranger, S. Mechanisms of tumor escape in the context of the T-cell-inflamed and the non-T-cell-inflamed tumor microenvironment. *Int Immunol* 28, 383-391 (2016).

60. Beatty, G.L., *et al.* Exclusion of T Cells From Pancreatic Carcinomas in Mice Is Regulated by Ly6C(low) F4/80(+) Extratumoral Macrophages. *Gastroenterology* 149, 201-210 (2015).

61. Perez-Romero, K., Rodriguez, R.M., Amedei, A., Barcelo-Coblijn, G. & Lopez, D.H. Immune Landscape in Tumor Microenvironment: Implications for Biomarker Development and Immunotherapy. *Int J Mol Sci* 21(2020).

62. Faraj, S.F., *et al.* Assessment of tumoral PD-L1 expression and intratumoral CD8+ T cells in urothelial carcinoma. *Urology* 85, 703 e701-706 (2015).

63. Krpina, K., Babarovic, E. & Jonjic, N. Correlation of tumor-infiltrating lymphocytes with bladder cancer recurrence in patients with solitary low-grade urothelial carcinoma. *Virchows Arch* 467, 443-448 (2015).

64. Sharma, P., *et al.* CD8 tumor-infiltrating lymphocytes are predictive of survival in muscle-invasive urothelial carcinoma. *Proc Natl Acad Sci U S A* 104, 3967-3972 (2007).

65. Rizvi, H., *et al.* Molecular Determinants of Response to Anti-Programmed Cell Death (PD)-1 and Anti-Programmed Death-Ligand 1 (PD-L1) Blockade in Patients With Non-Small-Cell Lung Cancer Profiled With Targeted Next-Generation Sequencing. *J Clin Oncol* 36, 633-641 (2018).

66. Mariathasan, S., *et al.* TGFbeta attenuates tumour response to PD-L1 blockade by contributing to exclusion of T cells. *Nature* 554, 544-548 (2018).

67. Necchi, A., *et al.* Molecular Characterization of Residual Bladder Cancer after Neoadjuvant Pembrolizumab. *Eur Urol* 80, 149-159 (2021).

68. Kamoun, A., *et al.* A Consensus Molecular Classification of Muscle-invasive Bladder Cancer. *Eur Urol* 77, 420-433 (2020).

69. van Dijk, N., *et al.* The Tumor Immune Landscape and Architecture of Tertiary Lymphoid Structures in Urothelial Cancer. *Front Immunol* 12, 793964 (2021).

70. Li, M.O., Wan, Y.Y. & Flavell, R.A. T cell-produced transforming growth factor-beta1 controls T cell tolerance and regulates Th1- and Th17-cell differentiation. *Immunity* 26, 579-591 (2007).

71. Asseman, C., Mauze, S., Leach, M.W., Coffman, R.L. & Powrie, F. An essential role for interleukin 10 in the function of regulatory T cells that inhibit intestinal inflammation. *J Exp Med* 190, 995-1004 (1999).

72. Baras, A.S., *et al.* The ratio of CD8 to Treg tumor-infiltrating lymphocytes is associated with response to cisplatin-based neoadjuvant chemotherapy in patients with muscle invasive urothelial carcinoma of the bladder. *Oncoimmunology* 5, e1134412 (2016).

73. Liu, Y.N., *et al.* Sphingosine 1 phosphate receptor-1 (S1P1) promotes tumor-associated regulatory T cell expansion: leading to poor survival in bladder cancer. *Cell Death Dis* 10, 50 (2019).

74. Oh, D.Y., *et al.* Intratumoral CD4(+) T Cells Mediate Anti-tumor Cytotoxicity in Human Bladder Cancer. *Cell* 181, 1612-1625 e1613 (2020).

75. DeNardo, D.G. & Ruffell, B. Macrophages as regulators of tumour immunity and immunotherapy. *Nat Rev Immunol* 19, 369-382 (2019).

76. Mantovani, A., Sozzani, S., Locati, M., Allavena, P. & Sica, A. Macrophage polarization: tumor-associated macrophages as a paradigm for polarized M2 mononuclear phagocytes. *Trends Immunol* 23, 549-555 (2002).

77. Murray, P.J., *et al.* Macrophage activation and polarization: nomenclature and experimental guidelines. *Immunity* 41, 14-20 (2014).

78. Koll, F.J., *et al.* Tumor-associated macrophages and Tregs influence and represent immune cell infiltration of muscle-invasive bladder cancer and predict prognosis. *J Transl Med* 21, 124 (2023).

79. Sun, M., *et al.* Infiltration and Polarization of Tumor-associated Macrophages Predict Prognosis and Therapeutic Benefit

in Muscle-Invasive Bladder Cancer. *Cancer Immunol Immunother* 71, 1497-1506 (2022).

80.   Wang, L., *et al.* Myeloid Cell-associated Resistance to PD-1/PD-L1 Blockade in Urothelial Cancer Revealed Through Bulk and Single-cell RNA Sequencing. *Clin Cancer Res* 27, 4287-4300 (2021).

81.   Xu, D., *et al.* Single-Cell Analyses of a Novel Mouse Urothelial Carcinoma Model Reveal a Role of Tumor-Associated Macrophages in Response to Anti-PD-1 Therapy. *Cancers (Basel)* 14(2022).

82.   Luo, S., *et al.* Chronic Inflammation: A Common Promoter in Tertiary Lymphoid Organ Neogenesis. *Front Immunol* 10, 2938 (2019).

83.   Carragher, D.M., Rangel-Moreno, J. & Randall, T.D. Ectopic lymphoid tissues and local immunity. *Semin Immunol* 20, 26-42 (2008).

84.   Jones, G.W. & Jones, S.A. Ectopic lymphoid follicles: inducible centres for generating antigen-specific immune responses within tissues. *Immunology* 147, 141-151 (2016).

85.   Sarma, K.P. The role of lymphoid reaction in bladder cancer. *J Urol* 104, 843-849 (1970).

86.   Pagliarulo, F., *et al.* Molecular, Immunological, and Clinical Features Associated With Lymphoid Neogenesis in Muscle Invasive Bladder Cancer. *Front Immunol* 12, 793992 (2021).

87.   Pfannstiel, C., *et al.* The Tumor Immune Microenvironment Drives a Prognostic Relevance That Correlates with Bladder Cancer Subtypes. *Cancer Immunol Res* 7, 923-938 (2019).

88.   Silina, K., *et al.* Germinal Centers Determine the Prognostic Relevance of Tertiary Lymphoid Structures and Are Impaired by Corticosteroids in Lung Squamous Cell Carcinoma. *Cancer Res* 78, 1308-1320 (2018).

89.   Lin, R.L. & Zhao, L.J. Mechanistic basis and clinical relevance of the role of transforming growth factor-beta in cancer. *Cancer Biol Med* 12, 385-393 (2015).

90.   Massague, J. TGFbeta in Cancer. *Cell* 134, 215-230 (2008).

91.   Calon, A., *et al.* Stromal gene expression defines poor-prognosis subtypes in colorectal cancer. *Nat Genet* 47, 320-329 (2015).

92.   Flavell, R.A., Sanjabi, S., Wrzesinski, S.H. & Licona-Limon, P. The polarization of immune cells in the tumour environment by TGFbeta. *Nat Rev Immunol* 10, 554-567 (2010).

93.   Benjamin, D.J. & Lyou, Y. Advances in Immunotherapy and the TGF-beta Resistance Pathway in Metastatic Bladder Cancer. *Cancers (Basel)* 13(2021).

94.   Vento, S. & Cainelli, F. Infections in patients with cancer undergoing chemotherapy: aetiology, prevention, and treatment. *Lancet Oncol* 4, 595-604 (2003).

95.   Bracci, L., Schiavoni, G., Sistigu, A. & Belardelli, F. Immune-based mechanisms of cytotoxic chemotherapy: implications for the design of novel and rationale-based combined treatments against cancer. *Cell Death Differ* 21, 15-25 (2014).

96.   Sakai, H., *et al.* Effects of anticancer agents on cell viability, proliferative activity and cytokine production of peripheral blood mononuclear cells. *J Clin Biochem Nutr* 52, 64-71 (2013).

97.   Galluzzi, L., *et al.* Consensus guidelines for the definition, detection and interpretation of immunogenic cell death. *J Immunother Cancer* 8(2020).

98.   Wang, Z., Till, B. & Gao, Q. Chemotherapeutic agent-mediated elimination of myeloid-derived suppressor cells. *Oncoimmunology* 6, e1331807 (2017).

99.   Roselli, M., *et al.* Effects of conventional therapeutic interventions on the number and function of regulatory T cells. *Oncoimmunology* 2, e27025 (2013).

100. Gandhi, L., *et al.* Pembrolizumab plus Chemotherapy in Metastatic Non-Small-Cell Lung Cancer. *N Engl J Med* 378, 2078-

2092 (2018).

101. Paz-Ares, L*., et al.* First-line nivolumab plus ipilimumab combined with two cycles of chemotherapy in patients with non-small-cell lung cancer (CheckMate 9LA): an international, randomised, open-label, phase 3 trial. *Lancet Oncol* 22, 198-211 (2021).

102. Cortes, J*., et al.* Pembrolizumab plus Chemotherapy in Advanced Triple-Negative Breast Cancer. *N Engl J Med* 387, 217-226 (2022).

103. Grasselly, C*., et al.* The Antitumor Activity of Combinations of Cytotoxic Chemotherapy and Immune Checkpoint Inhibitors Is Model-Dependent. *Front Immunol* 9, 2100 (2018).

104. Pfirschke, C*., et al.* Immunogenic Chemotherapy Sensitizes Tumors to Checkpoint Blockade Therapy. *Immunity* 44, 343-354 (2016).

105. Voorwerk, L*., et al.* Immune induction strategies in metastatic triple-negative breast cancer to enhance the sensitivity to PD-1 blockade: the TONIC trial. *Nat Med* 25, 920-928 (2019).

106. Morales, A., Eidinger, D. & Bruce, A.W. Intracavitary Bacillus Calmette-Guerin in the treatment of superficial bladder tumors. *J Urol* 116, 180-183 (1976).

107. Bisiaux, A*., et al.* Molecular analyte profiling of the early events and tissue conditioning following intravesical bacillus calmette-guerin therapy in patients with superficial bladder cancer. *J Urol* 181, 1571-1580 (2009).

108. Ratliff, T.L., Ritchey, J.K., Yuan, J.J., Andriole, G.L. & Catalona, W.J. T-cell subsets required for intravesical BCG immunotherapy for bladder cancer. *J Urol* 150, 1018-1023 (1993).

109. Kates, M*., et al.* Adaptive Immune Resistance to Intravesical BCG in Non-Muscle Invasive Bladder Cancer: Implications for Prospective BCG-Unresponsive Trials. *Clin Cancer Res* 26, 882-891 (2020).

110. Balar, A.V*., et al.* Pembrolizumab monotherapy for the treatment of high-risk non-muscle-invasive bladder cancer unresponsive to BCG (KEYNOTE-057): an open-label, single-arm, multicentre, phase 2 study. *Lancet Oncol* 22, 919-930 (2021).

111. Meghani, K*., et al.* First-in-human Intravesical Delivery of Pembrolizumab Identifies Immune Activation in Bladder Cancer Unresponsive to Bacillus Calmette-Guerin. *Eur Urol* 82, 602-610 (2022).

112. Kirschner, A.N., Wang, J., Rajkumar-Calkins, A., Neuzil, K.E. & Chang, S.S. Intravesical Anti-PD-1 Immune Checkpoint Inhibition Treats Urothelial Bladder Cancer in a Mouse Model. *J Urol* 205, 1336-1343 (2021).

113. Challita-Eid, P.M*., et al.* Enfortumab Vedotin Antibody-Drug Conjugate Targeting Nectin-4 Is a Highly Potent Therapeutic Agent in Multiple Preclinical Cancer Models. *Cancer Res* 76, 3003-3013 (2016).

114. Rosenberg, J*., et al.* EV-101: A Phase I Study of Single-Agent Enfortumab Vedotin in Patients With Nectin-4-Positive Solid Tumors, Including Metastatic Urothelial Carcinoma. *J Clin Oncol* 38, 1041-1049 (2020).

115. Powles, T*., et al.* Enfortumab Vedotin in Previously Treated Advanced Urothelial Carcinoma. *N Engl J Med* 384, 1125-1135 (2021).

116. Krysko, D.V*., et al.* Immunogenic cell death and DAMPs in cancer therapy. *Nat Rev Cancer* 12, 860-875 (2012).

117. Hoimes, C.J*., et al.* Enfortumab Vedotin Plus Pembrolizumab in Previously Untreated Advanced Urothelial Cancer. *J Clin Oncol* 41, 22-31 (2023).

118. Heijden, M.S.V.D*., et al.* Study EV-302: A two-arm, open-label, randomized controlled phase 3 study of enfortumab vedotin in combination with pembrolizumab versus chemotherapy in previously untreated advanced urothelial carcinoma (aUC) (trial in progress). *Journal of Clinical Oncology* 40, TPS589-TPS589 (2022).

119. O'Donnell, P.H*., et al.* Enfortumab vedotin (EV) alone or in combination with pembrolizumab (P) in previously untreated

cisplatin-ineligible patients with locally advanced or metastatic urothelial cancer (la/mUC): Subgroup analyses of confirmed objective response rate (cORR) from EV-103 cohort K. *Journal of Clinical Oncology* 41, 499-499 (2023).

120. van Dijk, N.*, et al.* The Cancer Immunogram as a Framework for Personalized Immunotherapy in Urothelial Cancer. *Eur Urol* 75, 435-444 (2019).

2

CHAPTER 3

Assessment of predictive genomic biomarkers for response to cisplatin-based neoadjuvant chemotherapy in bladder cancer

Alberto Gil-Jimenez*, Jeroen van Dorp*, Alberto Contreras-Sanz, Kristan van der Vos,
Daniel J. Vis, Linde Braaf, Annegien Broeks, Ron Kerkhoven, Kim E.M. van Kessel,
María José Ribal, Antonio Alcaraz, Lodewyk F.A. Wessels, Roland Seiler, Jonathan L. Wright,
Lourdes Mengual, Joost Boormans, Bas W.G. van Rhijn, Peter C. Black, Michiel S. van der Heijden

These authors contributed equally

ABSTRACT

Cisplatin-based neoadjuvant chemotherapy (NAC) followed by radical cystectomy is recommended for patients with muscle-invasive bladder cancer (MIBC). Somatic deleterious mutations in *ERCC2,* gain-of-function mutations in *ERBB2*, and alterations in *ATM*, *RB1*, and *FANCC* have been shown to correlate with pathological response to NAC in MIBC.

The objective of this study was to validate these genomic biomarkers in pre-treatment transurethral resection (TUR) material from an independent retrospective cohort of 165 MIBC patients who had subsequently undergone NAC and radical surgery. Patients with ypT0/Tis/Ta/T1N0 disease after surgery were defined as responders.

Somatic deleterious mutations in *ERCC2* were found in 9/68 (13%) evaluable responders and in 2/95 (2%) evaluable non-responders (p=0.009, FDR=0.03). No correlation was observed between response and alterations in *ERBB2* or in *ATM*, *RB1* or *FANCC* alone or in combination. In an exploratory analysis, no additional genomic alterations discriminated between responders and non-responders to NAC. No further associations were identified between the aforementioned biomarkers and complete pathological complete response (ypT0N0) after surgery.

In conclusion, we observed a positive association between deleterious mutations in *ERCC2* and pathological response to NAC, but not overall survival or recurrence-free survival. Other previously reported genomic biomarkers were not validated.

PATIENT SUMMARY

It is currently unknown which patients will respond to chemotherapy before definitive surgery for bladder cancer. Previous studies described several gene mutations in bladder cancer that correlated with chemotherapy response. This study confirmed that patients with bladder cancer with a mutation in the *ERCC2* gene often respond to chemotherapy.

INTRODUCTION

Neoadjuvant cisplatin-based chemotherapy (NAC) followed by radical cystectomy is recommended for patients with muscle-invasive bladder cancer (MIBC)[1]. Pathological response after treatment with NAC is strongly associated with recurrence-free survival (RFS) and overall survival (OS)[2]. Currently, clinicians are unable to identify which patients will benefit from NAC. Genomic biomarkers have been described to correlate with response to NAC, including somatic deleterious mutations in *ERCC2,* gain-of-function mutations in *ERBB2*, and alterations in *ATM*, *RB1* and *FANCC*[3-7]. However, none of these biomarkers have been validated in larger independent cohorts and are consequently not used in clinical practice[1,8].

Here, we set out to to validate these genomic biomarkers in an independent multicenter retrospective cohort. Pre-treatment tissue derived from five centers was sequenced at the Netherlands Cancer Institute (NKI cohort, n=117) or Vancouver Prostate Centre (Vancouver cohort, n=48, Supplementary Figure 1). All patients were diagnosed with MIBC (cT2-4aN0M0 and/or cT1-4aN1-3M0) by transurethral resection (TUR) and were treated with at least two cycles of cisplatin-based NAC, followed by radical cystectomy. The primary endpoint of this study was pathological response, defined as ypT0/Tis/Ta/T1N0 after surgery[2,9]. Seventy of 165 patients (42%) were categorized as responders. Pathological complete response after surgery, defined as ypT0N0, was used as a secondary endpoint which was observed in 51 of 165 patients (31%).

RESULTS

Baseline age, gender, chemotherapy regimen, and number of cycles of chemotherapy did not differ between response groups, however cT-stage at baseline was higher in the non-responders (Table 1). Furthermore, baseline cT-stage and chemotherapy regimen differed between cohorts (Supplementary Table 1). Tumor DNA extracted from TUR samples obtained prior to NAC was sequenced using a targeted capture-based panel for the NKI cohort and whole exome sequencing for the Vancouver cohort. Somatic variants in *ERCC2*, *ERBB2*, *ATM*, *RB1* and *FANCC* were inferred from population databases (Supplementary Methods). Mutations were predicted to be functional (deleterious or gain-of-function) using the annotation databases OncoKB, ClinVar, SIFT, FATHMM, and PolyPhen-2 (Supplementary Methods). A high concordance between the observed and the TCGA mutation rates was observed (Supplementary Table 2).

After filtering, deleterious mutations in *ERCC2* were found in nine of 68 (13%) evaluable responders and in two of 95 (2%) evaluable non-responders (p=0.009, Figure 1A). We found relevant gain-of-function mutations in *ERBB2* in nine of 69 (13%) evaluable responders and five of 95 (5%) evaluable non-responders (p=0.09, Figure 1A). Twenty-seven of 70 (39%) responders had ≥1 alteration in *ATM*, *RB1* or *FANCC* compared to 25 of 95 (26%) non-responders (p=0.13, Figure

1A). Nine of eleven patients (82%) with a deleterious mutation in *ERCC2* had a pathological response after treatment with NAC, as opposed to 62 of 154 patients (40%) without any relevant mutations in *ERCC2* (Supplementary Table 3). After correction for multiple hypothesis testing (three hypotheses), mutations in *ERCC2* were significantly enriched in responders (FDR=0.03, Figure 1B). The association remained when adjusted for cT-stage in a multivariable logistic regression model (p_{ERCC2}=0.008, p_{cT2}=p_{cT3}=p_{cT4}>0.9), or when patients that received less than 3 cycles of NAC were excluded (Supplementary Figure 2). Baseline clinical difference between *ERCC2* mutated and wild-type patients were not identified (Supplementary Table 3).

Table 1 | Baseline characteristics and response of 165 patients with muscle-invasive bladder cancer treated with neoadjuvant chemotherapy and radical cystectomy.

	NKI		Vancouver		
	Responders (ypT0/Tis/Ta/ T1N0)	Non-responders (≥ypT2N0)	Responders (ypT0/Tis/Ta/ T1N0)	Non-responders (≥ypT2N0)	Significance Responders vs Non-responders (full cohort)[a]
Number of patients	53	64	17	31	-
Median age in years (IQR)	71.0 (61.0, 75.0)	71.0 (61.0, 77.3)	61.2 (56.0, 66.0)	65.5 (58.3, 73.0)	0.2
Male sex (% of pts)	40 (76%)	38 (59%)	15 (88%)	24 (77%)	0.08
cT-stage (% of pts)					0.04
cT1	1 (2%)	0 (0%)	0 (0%)	0 (0%)	
cT2	27 (51%)	19 (30%)	2 (12%)	4 (13%)	
cT3	21 (40%)	26 (40%)	7 (41%)	20 (65%)	
cT4	4 (7%)	19 (30%)	8 (47%)	7 (22%)	
cN-stage (% of pts)					0.6
cN0	31 (59%)	40 (63%)	10 (59%)	12 (39%)	
cN+	22 (41%)	24 (37%)	7 (41%)	19 (61%)	
Chemotherapy regimen (% of pts)					0.16
Cis/Gem	40 (75%)	41 (64%)	14 (82%)	28 (90%)	
MVAC	11 (21%)	23 (36%)	3 (18%)	3 (10%)	
CMV	2 (4%)	0 (0%)	0 (0%)	0 (0%)	
Chemotherapy cycles received (% of pts)					0.8
2	2 (4%)	2 (3%)	0 (0%)	2 (6%)	
3	10 (19%)	13 (20%)	6 (35%)	7 (23%)	
4	39 (74%)	46 (72%)	10 (59%)	17 (55%)	
>4	2 (4%)	3 (5%)	1 (6%)	5 (16%)	
Pathological response (% of pts)					-
ypT0N0 (complete response)	40 (75%)	0 (0%)	13 (76%)	0 (0%)	
ypTis/Ta/T1N0	13 (25%)	0 (0%)	4 (24%)	0 (0%)	
≥ypT2N0 (non-response)	0 (0%)	64 (100%)	0 (0%)	31 (100%)	

[a] Fisher's exact test for binary predictors, t-test for numerical predictors. All the statistical tests were two-sided. No adjustments were made for multiple hypothesis testing. Significant associations are highlighted on bold. *Cis/Gem = cisplatin + gemcitabine; MVAC = methotrexate + vinblastine + docorubicin + cisplatin; CMV = cisplatin + methotrexate + vinblastine; IQR = interquartile range.*

In contrast, alterations in *ERCC2*, *ERBB2*, or in any one of *ATM*, *RB1* or *FANCC* did not associate with a pathological complete response (ypT0N0) after correcting for multiple hypothesis testing (FDR$_{ERCC2}$=0.09, FDR$_{ERBB2}$=0.07, FDR$_{ATM/RB1/FANCC}$=0.07, Supplementary Figure 3).
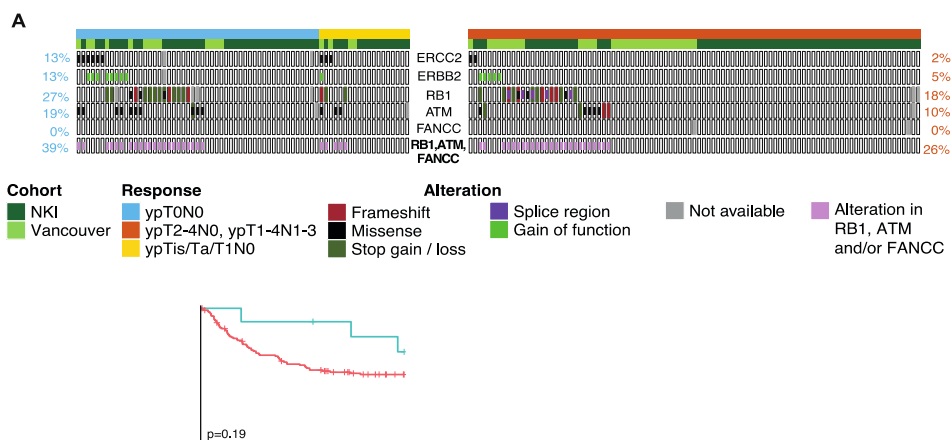
Figure 1 | Somatic mutations in the genes *ERCC2*, *ERBB2*, *ATM*, *RB1* and *FANCC* in patients with muscle-invasive bladder cancer treated with neoadjuvant chemotherapy. A, Overview of relevant mutations for each patient (**Supplementary Methods - Variant calling and inference of somatic and functional variants**). Left panel shows patients with ypT0N0 (light blue, n=51) or ypTis/Ta/T1N0 (yellow, n=19) after neoadjuvant chemotherapy (responders), and right panel shows non-responders (orange, n=95). Percentages represent the number of patients with a relevant mutation relative to the total number of eligible patients for that specific gene for responders (left) and non-responders (right). Patients with an alteration in any one of *ATM*, *RB1* or *FANCC* are indicated in the last row. **B,** Five-year overall survival (OS) for patients with (blue) and without (red) mutations in *ERCC2*. The p-value indicates statistical significance by a log-rank test. **C,** 5-year recurrence-free survival (RFS) for patients with (blue) and without (red) mutations in *ERCC2*. The p-value inside the survival plot indicates statistical significance by a log-rank test. *NKI = patients from the NKI-cohort; wt = wild type; mut = mutant; Not available = gene-coverage below 20 reads.*

The median duration of follow-up for patients using reverse censoring was 7.2 years. The 5-year OS rates for patients with and without mutations in *ERCC2* were 75% (95% confidence interval (CI): 50%-100%) and 52% (95% CI: 45%-62%), respectively (p=0.2, Figure 1C). The 5-year RFS rates were 65% (95% CI: 39%-100%) and 49% (95% CI: 42%-59%), respectively (p=0.2, Figure 1D). Thus, while the Kaplan Meier curves appear to separate according to *ERCC2* mutation status, we could not demonstrate a statistical difference for either OS or RFS, possibly due to the low frequency of *ERCC2* mutations.

Following earlier analyses by Plimack and colleagues[6], we assessed copy number alterations (CNA) for *ATM*, *RB1,* and *FANCC* by shallow whole genome sequencing for patients from the NKI cohort (n=117, Supplementary Methods). CNA on the Vancouver cohort could not be confidently assessed

due to a lack of germline data. We found seven CNA in *ATM*, *RB1* and/or *FANCC* in all evaluable patients. Together with the previously described mutations, 22 of 53 (42%) responders had ≥1 alteration in *ATM*, *RB1* or *FANCC* versus 20 of 64 (31%) non-responders (p=0.052, Supplementary Figure 4).

In a further exploratory analysis, mutations frequently occurring in MIBC were assessed for their correlation with response to NAC (Supplementary Figure 5). This analysis included *FGFR3*, which was previously associated with negative outcome after chemotherapy (Supplementary Figure 6)[10]. No association with response was identified after correction for multiple hypothesis testing (Supplementary Figure 5).

DISCUSSION

There are several limitations to this study. The genomic data were derived using different sequencing technologies at different centers, leading to potential biases in the mutation frequency. Furthermore, we lacked germline data and somatic variants were filtered with the help of population databases to remove benign germline variants. As germline DNA is often unavailable, this approach is common practice and was also used in the original studies of *ERBB2* and *ATM*/*RB1*/*FANCC*[4,6]. Multiple definitions of response have been used in previous studies, thus introducing heterogeneity between studies. Complete pathological response (ypT0N0) and pathological downstaging (ypT0/Tis/Ta/T1N0) are commonly used. Long-term clinical outcome is favorable in both groups, although patients with ypT0/TisN0 may have a modest survival benefit over patients with ypT0/Tis/Ta/T1N0[2,9].

In summary, we attempted to validate mutations in *ERCC2*, *ERBB2*, *ATM*, *RB1* and *FANCC* as predictive markers of pathological response in a cohort of 165 patients treated with NAC. We confirmed a positive association of deleterious mutations in *ERCC2* with pathological response (ypT0/Tis/Ta/T1N0), but not with complete response (ypT0N0), OS or RFS. Prospective evaluation of *ERCC2* mutations as a biomarker for response to NAC is needed to confirm our results.

REFERENCES

1. Witjes, J.A., *et al.* European Association of Urology Guidelines on Muscle-invasive and Metastatic Bladder Cancer: Summary of the 2020 Guidelines. *Eur Urol* 79, 82-104 (2021).

2. Rosenblatt, R., *et al.* Pathologic downstaging is a surrogate marker for efficacy and increased survival following neoadjuvant chemotherapy and radical cystectomy for muscle-invasive urothelial bladder cancer. *Eur Urol* 61, 1229-1238 (2012).

3. Van Allen, E.M., *et al.* Somatic ERCC2 mutations correlate with cisplatin sensitivity in muscle-invasive urothelial carcinoma. *Cancer Discov* 4, 1140-1153 (2014).

4. Groenendijk, F.H., *et al.* ERBB2 Mutations Characterize a Subgroup of Muscle-invasive Bladder Cancers with Excellent Response to Neoadjuvant Chemotherapy. *Eur Urol* 69, 384-388 (2016).

5. Li, Q., *et al.* ERCC2 Helicase Domain Mutations Confer Nucleotide Excision Repair Deficiency and Drive Cisplatin Sensitivity in Muscle-Invasive Bladder Cancer. *Clin Cancer Res* 25, 977-988 (2019).

6. Plimack, E.R., *et al.* Defects in DNA Repair Genes Predict Response to Neoadjuvant Cisplatin-based Chemotherapy in Muscle-invasive Bladder Cancer. *Eur Urol* 68, 959-967 (2015).

7. Miron, B., *et al.* Defects in DNA Repair Genes Confer Improved Long-term Survival after Cisplatin-based Neoadjuvant Chemotherapy for Muscle-invasive Bladder Cancer. *Eur Urol Oncol* 3, 544-547 (2020).

8. Becker, R.E.N., *et al.* Clinical Restaging and Tumor Sequencing are Inaccurate Indicators of Response to Neoadjuvant Chemotherapy for Muscle-invasive Bladder Cancer. *Eur Urol* 79, 364-371 (2021).

9. Ravi, P., *et al.* Optimal pathological response after neoadjuvant chemotherapy for muscle-invasive bladder cancer: results from a global, multicentre collaboration. *BJU Int* 128, 607-614 (2021).

10. Teo, M.Y., *et al.* Fibroblast Growth Factor Receptor 3 Alteration Status is Associated with Differential Sensitivity to Platinum-based Chemotherapy in Locally Advanced and Metastatic Urothelial Carcinoma. *Eur Urol* 78, 907-915 (2020).

3

SUPPLEMENTARY METHODS

STUDY POPULATION / TREATMENT

The full cohort consisted of 165 prospectively collected samples from five different centers. All patients had muscle-invasive bladder cancer (MIBC, cT2-4aN0M0 and/or cT1-4aN1-3M0) diagnosed by transurethral resection (TUR) and treated with at least two cycles of neoadjuvant chemotherapy (NAC) followed by radical cystectomy. NAC consisted of either cisplatin + gemcitabine (cis/gem), methotrexate + vinblastine + doxorubicin + cisplatin (MVAC) or cisplatin + methotrexate + vinblastine (CMV).

Patient cohorts were named after the center in which the sequencing was performed. The NKI cohort (n=117) included retrospectively collected MIBC samples from three centers: Amsterdam (The Netherlands), Rotterdam (The Netherlands), and Barcelona (Spain) and the Vancouver cohort (n=48) included MIBC samples from two institutions: Bern (Switzerland) and Seattle (Washington, USA) were compiled (Supplementary Figure 1, Table 1).

TARGETED DNA SEQUENCING (NKI COHORT)

Formalin-fixed paraffin-embedded (FFPE) tumor blocks from TUR material were collected from the different hospitals and centrally reviewed by an experienced pathologist. Tumor area was marked for every tumor block and DNA was collected from subsequent FFPE slides (10 μm). NanoDrop 2000 spectrophotometer (Thermo Fisher Scientific, Waltham, Massachusetts, USA) was used to quantify the total amount of DNA, and Qubit dsDNA HS Assay Kit (Thermo Fisher Scientific, Waltham, Massachusetts, USA) was used to quantify the amount of double stranded DNA. Covaris Focused ultrasonicator was used to fragment up to 2000 ng of double stranded genomic DNA to get fragment sizes of 200-300 bp (Covaris, Woburn, Massachusetts, USA). 2X AMPure XP PCR purification beads were used to purify samples following the manufacturer's instructions (Beckman Coulter, Indianapolis, Indiana, USA). The sheared DNA samples were qualified and quantified using a BioAnalyzer DNA Analysis 7500 Kit (Agilent Technologies, Santa Clara, California, USA). Library preparation for Illumina sequencing was done using the KAPA HTP Library Preparation Kit (Kapa Biosystems, Roche Sequencing and Life Science, Wilmington, Massachusetts, USA) with an input of maximum 1 μg sheared DNA. Four PCR cycles were done during library amplification to obtain sufficient yield for the exome capture. Libraries were cleaned up using 1X AMPure XP PCR purification beads (Beckman Coulter, Indianapolis, Indiana, USA). The DNA libraries were analyzed on a Bioanalyzer system using the BioAnalyzer DNA Analysis 7500 Kit chips to determine the concentration. With 150 ng of each indexed sample three pools of eight samples were prepared, and 2 μl of Universal blockers - TS Mix (Integrated DNA Technologies, Coralville, Iowa, USA) and 5 μl Human Cot-1 DNA (Thermo Fisher Scientific, Waltham, Massachusetts, USA) was added to the pools. Then, a concentrator was used to dry the pool, and to rehydrate 8.5 μl of Hybridization buffer, 3.4 μl Hybridization component A (SeqCap Hybridization and Wash Kit, Roche, Basel, Switzerland) and 1.1 μl nuclease-free water was added. The pool underwent incubation at room

temperature for 10 minutes, and at 96 °C for 10 minutes. The samples were hybridized with 4 µl of the custom 44 gene bladder cancer panel (which included muscle-invasive bladder cancer driver genes, clinically relevant genes, and frequently mutated genes) at 65 °C for 24 hours. The hybridized sample pool was captured according to the Rapid protocol for DNA probe Hybridization and Target Capture using an Illumina TruSeq or Ion Torrent Library and subsequently amplified using 10 PCR cycles (Integrated DNA Technologies, Coralville, Iowa, USA). The amplified pool was purified using AMPure XP PCR purification beads (Beckman Coulter, Indianapolis, Indiana, USA). The purified pools were quantified on the Agilent BioAnalyzer DNA Analysis 7500 system and one sequence pool was made by equimolar pooling (Agilent Technologies, Santa Clara, California, USA). The sequence pool was diluted to a final concentration of 10 nM and subjected to sequencing with a MID 150 cycle kit for a paired end 75 bp run following manufacturer's instructions on an Illlumina Nextseq 550 machine (Illumina, San Diego, California, USA).

Sequencing reads were aligned against the Human Reference Genome Ghr38 using Burrows-Wheeler aligner v0.7.17-r1188 (Li H. and Durbin R. (2010), Bioinformatics, 25:1754-60). Duplicated reads were marked and removed using GATK MarkDuplicates v4.1.1.0 (Broad Institute, Cambridge, Massachusetts, USA), and base quality score recalibration was done using GATK ApplyBQSR v4.1.1.0 (Broad Institute, Cambridge, Massachusetts, USA). Indel realignment was not performed as per current GATK best practices (June 2021) it is not recommended when performing variant calling with Mutect2.

EXOME DNA SEQUENCING (VANCOUVER COHORT)
To extract DNA from FFPE tumor samples, two FFPE cores per case were used to prepare hematoxylin and eosin-stained slides and a certified pathologist reviewed them for tumor content. Macro-dissection on tumor regions was done to enrich for tumor content. For paraffin removal, tissue re-hydration, tissue digestion and DNA extraction a M220 Focused ultrasonicator and a truXTRAC FFPE DNA microTUBE Kit (both from Covaris, Woburn, Massachusetts, USA) wered used. To quantify DNA the Qubit 2.0 fluorometer (Thermo Fisher Scientific, Waltham, Massachusetts, USA) was used. The DNA quality was assessed by multiplex PCR assay with usable DNA in samples with >400 bp PCR products.

To sequence the samples, 150-200 bp fragments were generated by fragmenting 1 µg of genomic DNA by hydrodynamic shearing using a E210 Focused ultrasonicator (Covaris, Woburn, Massachusetts, USA). DNA fragments were ligated to Illumina barcoded adapters. PCR amplification was used to enrich for adapter ligated fragments. To quantify DNA the Qubit 2.0 fluorometer (Thermo Fisher Scientific, Waltham, Massachusetts, USA) was used. The library was enriched by liquid phase hybridization using Agilent SureSelect XT Human All Exon v6 (Agilent Technologies, Santa Clara, California, USA) according to the manufacturer's recommendations, and amplified by PCR using indexing primers. Captured libraries were cleaned and controlled for quality using the Qubit 2.0 fluorometer (Thermo Fisher Scientific, Waltham, Massachusetts, USA). For clustering

of index-coded samples and sequencing of PE100 libraries an Illlumina HiSeq 4000 machine (Illumina, San Diego, California, USA) was used.

Sequencing reads were aligned against the Human Reference Genome Ghr38 using Burrows-Wheeler aligner v0.7.17-r1188. Duplicated reads were marked and removed using MarkDuplicates v2.23.8, and base quality score recalibration was done using GATK ApplyBQSR v4.1.1.0.

VARIANT CALLING AND INFERENCE OF SOMATIC AND FUNCTIONAL VARIANTS
GATK Mutect2 v4.1.9.0 (Broad Institute, Cambridge, Massachusetts, USA) was used to call single-nucleotide variants (SNVs) and short insertions and deletions (indels) on tumor samples using the 'Tumor-only' mode. Variants were further filtered using GATK FilterMutectCalls v4.1.9.0 (Broad Institute, Cambridge, Massachusetts, USA), and variants with an allele frequency below 5% or an alternate number or reads below 3 were filtered out.

Because the sequencing depth between samples and genes was variable, we annotated regions with a low sequencing coverage. First, we computed the sequencing depth using Samtools v1.9 (Sanger Institute, Hinxton, UK) and estimated the average coverage per-gene. For each sample, we annotated each gene from the oncoplots (i.e. Figure 1A) as '*Not available*' when the average number of gene sequencing coverage was <20 reads. As an exception to this rule, when a relevant (non-germline and pathogenic) variant and with at least 3 alternate reads was detected for a low coverage gene, the variant was subjected to downstream analysis and the '*Not available*' annotation was removed.

For downstream analysis, samples showing low coverage (average <20 reads) in >40% of the studied genes were filtered out, which affected 4 patients from the NKI cohort, and 2 patients from the Vancouver cohort. Variants were processed in R 3.6.0 using the packages VariantAnnotation v1.24.5 (Obenchain, V. et al. (2014), Bioinformatics, 30(14), 2076-2078), ComplexHeatmap v1.17.1 (Gu, Z. et al. (2016), Bioinformatics), tidyverse 1.2.1 (Wickham, H. et al. (2019), Journal of Open Source Software, 4(43)), and ggpubr 0.2.1 (Kassambara, A. (2020), CRAN).

Variants were annotated using SnpEff 4.3t (Cingolani, P. (2012), Fly, 6:80-92) against the Human Reference Genome Ghr38, and using SnpSift (Cingolani, P. (2012), Frontiers in Genetics, 3) against the databases dbSNP (build 151), COSMIC (v85), ClinVar, dbNSFP, GNOMAD (version exomes. r2.1.1.sites), and OncoKB (version MVL2.sorted). To filter out germline variants, only variants annotated as COMMON != 1, CAF <0.05, TOPMED <0.05, GNOMAD dbNSFP_gnomAD_exomes_NFE_ AF <0.05. and dbNSFP_gnomAD_exomes_AF <0.05 were retrieved. To further filter out potential germline variants, we retrieved the germline DNA sequencing data collected from NABUCCO cohort 1, and identified the germline variants FOXQ1 T60P, KMT2D T4629P (mutated in >70% of the patients), which were filtered out from our list.

To retrieve functional variants, we filtered out variants annotated as introns, non-coding, synonymous, downstream gene variant, 3' UTR variant, 5' UTR variant, t' UTR premature start codon gain, sequence feature. Then, we only retrieved variants being annotated with at least one of the following annotations: Pathogenic or Likely Pathogenic on CLNSIG, High Impact, Deleterious on SIFT or FATHMM, Damaging or Probably Damaging on HVAR, or as Oncogenic or Likely Oncogenic on OncoKB. For ERBB2, only variants annotated as Gain of Function by OncoKB were retrieved and reported in the manuscript.

SHALLOW WHOLE-GENOME DNA SEQUENCING FOR COPY NUMBER (NKI COHORT)
For shallow genome sequencing, the protocol up to PCR amplification was analogous to the one indicated in 'DNA sequencing'. The uniquely indexed samples were mixed together by equimolar pooling. Different pools of samples were prepared, consisting of 5 batches of 12 (1 pool, 1 lane), and one batch of 34 samples (1 pool, 3 lanes). The pools were analyzed on the Agilent Technologies 2100 Bioanalyzer (Agilent Technologies, Santa Clara, California, USA). The pools were diluted to 10 nM, and measured using qPCR. Finally, the pools were sequenced in a single-end 65 bp run, following the manufacturer's instructions on an Illumina HiSeq2500 machine (Illumina, San Diego, California, USA).

The low coverage whole genome samples were aligned to GRCh38.78 using the Burrows-Wheeler Aligner mem algorithm (bwa version 0.7.17) (Li H. and Durbin R. (2010), Bioinformatics, 25:1754-60). For every sample, and on segments of 20 kb on the genome, the mapping quality read counts were rated and tiled for 65 base pairs against a similar mapping of all known sequences for genome version GRCh38.78. A non-linear loess fit of mappabilities over 0.8 on autosomes was used to correct per 20 kb for local GC effects. Then a scaling to the slope of a linear fit of the reference mappabilities after GC correction was done on the reference values. where the intercept was forced at the origin. We filtered out the ratios of corrected sample counts and the reference values left out bins with a mappability below 0.2 or overlapped with ENCODE blacklisted regions (ENCODE Project Consortium, Nature, 2012). The pipeline used in the count and log2ratio corrections is available at https://github.com/NKI-GCF/SeqCNV. For male patients, the $\log_2$ ratio was increased by one in genes from Chromosome X. Copy number ratios (CNR) at a gene level (CNR-gene) were estimated using a weighted average copy number ratio per gene. We defined deletions as $\log_2$(CNR-gene) <−0.7, and amplifications as $\log_2$(CNR-gene) >1.

TCGA COHORT
Mutation data from Muscle-invasive bladder cancer patients from the TCGA cohort (n=412, Robertson *et al.*, Comprehensive Molecular Characterization of Muscle-Invasive Bladder Cancer, Cell, 2017) was downloaded as provided on cBioportal on 8th April 2022. Mutation data was aggregated by patient to compute mutation rates, and compared with mutation rates from our cohort by a two-sided Fisher's exact test.

STATISTICAL ANALYSES

Associations between genomic mutations and clinical response were tested using a two-sided Fisher's exact test. We performed multiple hypothesis testing on our original set of 3 hypotheses (*ERCC2*, *ERBB2* and *ATM*, *RB1* or *FANCC*) using the Benjamini-Hochberg method. A 0.05 threshold for both the unadjusted p-values and the false discovery rates was used to define significance. Associations between baseline clinical characteristics and response (**Table 1**) were sought using a Fisher's exact test for binary predictors, and a t-test for numerical predictors. Unless otherwise stated, all the statistical tests were two-sided. The statical analysis was performed using R 3.6.0.

Survival analysis with time to event was performed with a Kaplan-Meier analysis, and statistical significance was tested with a log-rank test. Time to event was computed as the temporal window between the day of cystectomy and either time to death (overall survival, OS) or time to recurrence (recurrence-free survival RFS). For median follow-up estimation, reverse censoring was implemented using the reverse Kaplan-Meier method by reversing the event and censoring labels. For OS and RFS analysis, censoring was implemented for patients lost to follow-up. Hazard ratio testing with a Cox proportional hazards regression model was not performed, due to the proportional hazard assumption being violated for a Cox model of the 5-year OS association with *ERCC2* mutations, in which a significant association between the Cox model residuals and time was identified (p=0.037). Analyses were performed using the R packages survival version 2.44 (Therneau, T. M, CRAN), prodlim version 2019.11.13 (Gerds, T. A., CRAN), and survminer version 0.4.6 (Kassambara, A., CRAN).

SUPPLEMENTARY DATA
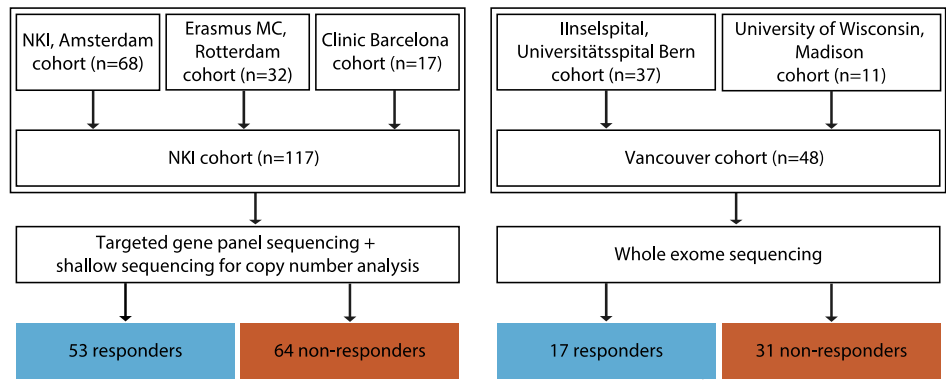
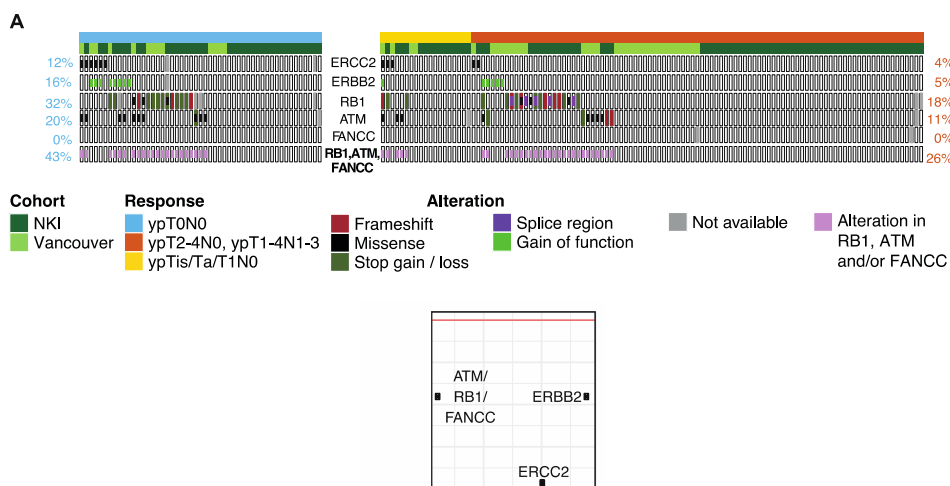**Supplementary Figure 1 | Overview of patient cohorts from 5 different centers.** The patients from Amsterdam (The Netherlands), Rotterdam (The Netherlands) and Barcelona (Spain) (n=117) were sequenced by the NKI using targeted DNA sequencing and shallow whole genome sequencing. Whole-exome sequencing was performed in Vancouver on tumor material from Bern (Switzerland) and Seattle (Washington) (n=48).
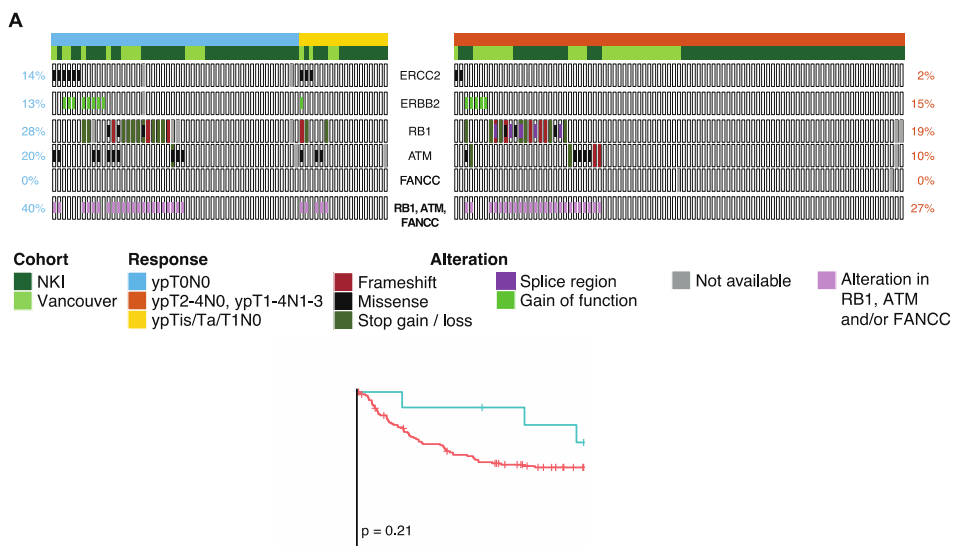
Supplementary Figure 2 | Somatic mutations in the genes *ERCC2*, *ERBB2, ATM, RB1 and FANCC* **in patients with muscle-invasive bladder cancer treated with neoadjuvant chemotherapy with at least 3 NAC cycles.** Six patients that received 2 cycles of chemotherapy were excluded from the analysis. **A,** Overview of relevant mutations for each individual patient. Left panel shows patients with pathological complete response (ypT0N0, light blue, n=50), and right panel shows patients with ypTis/Ta/T1N0 (yellow, n=18) and ≥ypT2N0 (orange, n=91). Percentages represent the number of patients per cohort with a relevant mutation relative to the total number of eligible patients for that specific gene for ypT0N0 (left) and >ypT0N0 (right) patients. Patients with an alteration in any one of *ATM*, *RB1* or *FANCC* are indicated in the last row. **B,** Adjusted p-value versus odds ratio for *ERCC2*, *ERBB2* and any one of *ATM*, *RB1* or *FANCC* between response groups. P-values were calculated by a two-sided Fisher's exact test, and adjusted for multiple hypothesis testing using the Benjamini-Hochberg procedure. The 5-year (**C**) overall survival and (**D**) recurrence-free survival for patients with (blue) and without (red) a mutation in *ERCC2*. The p values indicate statistical significance for a log-rank test. *NKI = patients from the NKI-cohort; Not available = gene-coverage below 20 reads.*

A

Cohort
NKI
Vancouver

Response
ypT0N0
ypT2-4N0, ypT1-4N1-3
ypTis/Ta/T1N0

Alteration
Frameshift
Missense
Stop gain / loss
Splice region
Gain of function
Not available
Alteration in RB1, ATM and/or FANCC
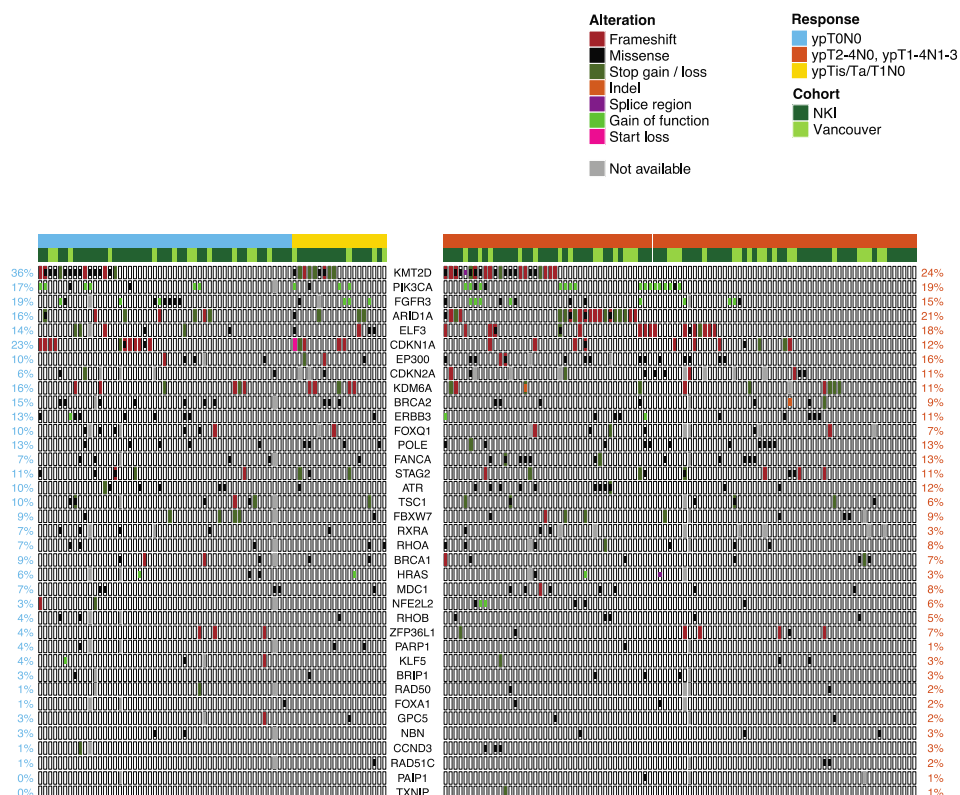
Supplementary Figure 3 | Somatic mutations in the genes *ERCC2, ERBB2, ATM, RB1 and FANCC* in patients with muscle-invasive bladder cancer treated with neoadjuvant chemotherapy related to complete pathological response. A, Overview of relevant mutations for each individual patient. Left panel shows patients with pathological complete response (ypT0N0, light blue, n=51), and right panel shows patients with ypTis/Ta/T1N0 (yellow, n=19) and ≥ypT2N0 (orange, n=95). Percentages represent the number of patients per cohort with a relevant mutation relative to the total number of eligible patients for that specific gene for ypT0N0 (left) and >ypT0N0 (right) patients. Patients with an alteration in any one of *ATM*, *RB1* or *FANCC* are indicated in the last row. **B,** Adjusted p-value versus odds ratio for *ERCC2, ERBB2* and any one of *ATM*, *RB1* or *FANCC* between response groups. P-values were calculated by a two-sided Fisher's exact test, and adjusted for multiple hypothesis testing using the Benjamini-Hochberg procedure. *NKI = patients from the NKI-cohort; Not available = gene-coverage below 20 reads.*
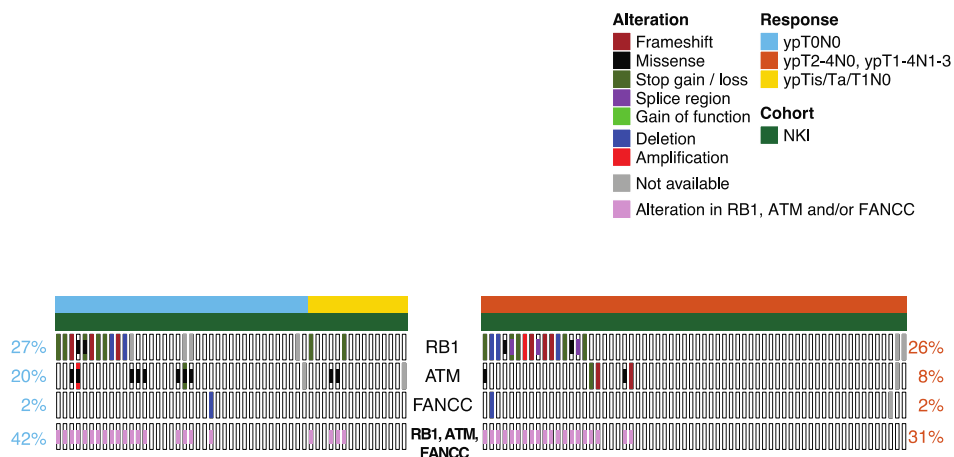
Supplementary Figure 4 | Somatic mutations and copy number alterations in *ERCC2, ERBB2, ATM, RB1* and *FANCC* in patients from the NKI cohort. Overview of relevant mutations and copy number alterations for all patients for whom mutation data and copy number alterations were available (NKI cohort, n=117). Left panel shows responders (ypT0/Tis/Ta/T1N0), and the right panel shows non-responders. Percentages represent the number of patients with a relevant alteration relative to the number of eligible patients for that specific gene for responders (left) and non-responder (right) patients. Patients with an alterations in any one of *ATM, RB1* or *FANCC* are shown separately in the last row. *NKI = patients from the NKI-cohort; Not available = gene-coverage below 20 reads.*

Supplementary Figure 5 | Somatic mutations in oncogenic driver genes and genes frequently-mutated in muscle-invasive bladder cancer. Overview of somatic mutations in driver genes and genes frequently altered in muscle-invasive bladder cancer in responders (ypT0/Tis/Ta/T1N0, left) and in non-responders (right). Adjusted p-value versus odds ratio for the alterations of each gene between response groups. P-values were calculated by a two-sided Fisher's exact test, and adjusted for multiple hypothesis testing using the Benjamini-Hochberg procedure. *NKI = patients from the NKI-cohort; Not available = gene-coverage below 20 reads.*

Supplementary Figure 6 | Somatic mutations in the *FGFR3* gene in patients with muscle-invasive bladder cancer treated with neoadjuvant chemotherapy. A, Overview of relevant *FGFR3* mutations for each patient. Left panel shows patients with ypT0N0 (light blue, n=51) or ypTis/Ta/T1N0 (yellow, n=19) after neoadjuvant chemotherapy (responders), and right panel shows non-responders (orange, n=95). Percentages represent the number of patients with a relevant mutation relative to the total number of eligible patients for that specific gene for responders (left) and non-responders (right). **B,** Five-year overall survival (OS) for patients with (blue) and without (red) somatic mutations in *FGFR3*. The p-value indicates statistical significance by a log-rank test. **C,** 5-year recurrence-free survival (RFS) for patients with (blue) and without (red) somatic mutations in *FGFR3*. The p-value inside the survival plot indicates statistical significance by a log-rank test. *NKI = patients from the NKI-cohort; Not available = gene-coverage below 20 reads*

Supplementary Table 1 | Baseline characteristics and response of 165 patients with muscle-invasive bladder cancer treated with neoadjuvant chemotherapy and radical cystectomy and comparison between cohorts.

	NKI Cohort	Vancouver	Significance NKI vs Vancouver[a]
Number of patients	117	48	-
Median age in years (IQR)	71.0 (61.0, 75.0)	62.1 (57.3, 72.0)	**0.003**
Male sex (% of pts)	78 (67%)	39 (81%)	0.09
cT-stage (% of pts)			**0.002**
cT1	1 (1%)	0 (0%)	
cT2	46 (39%)	6 (13%)	
cT3	47 (40%)	27 (56%)	
cT4	23 (20%)	15 (31%)	
cN-stage (% of pts)			0.09
cN0	71 (61%)	22 (46%)	
cN+	46 (39%)	26 (54%)	
Chemotherapy regimen (% of pts)			**0.03**
Cis/Gem	81 (69%)	42 (88%)	
MVAC	34 (29%)	6 (13%)	
CMV	2 (2%)	0 (0%)	
Chemotherapy cycles received (% of pts)			0.15
2	4 (3%)	2 (4%)	
3	23 (20%)	13 (27%)	
4	85 (73%)	27 (56%)	
>4	5 (4%)	6 (13%)	
Pathological response (% of pts)			0.5
ypT0N0 (complete response)	38 (32%)	13 (27%)	
ypTis/Ta/T1N0	15 (13%)	4 (8%)	
≥ypT2N0 (non-response)	64 (55%)	31 (65%)	
Nodal response (% of pts)			0.7
ypN0	81 (69%)	32 (67%)	
≥ypN1	34 (29%)	16 (33%)	
ypN unavailable	2 (2%)	0 (0%)	

[a] Fisher's exact test for binary predictors, t-test for numerical predictors. All the statistical tests were two-sided. No adjustments were made for multiple hypothesis testing. Significant associations are highlighted on bold.
Cis/Gem = cisplatin + gemcitabine; MVAC = methotrexate + vinblastine + docorubicin + cisplatin; CMV = cisplatin + methotrexate + vinblastine; IQR = Interquartile range; pts = patients.

3

Supplementary Table 2 | Comparison of mutation rates against TCGA Bladder Urothelial Carcinoma (n=412).

Gene	NKI/Vancouver mutation rate (%)	TCGA mutation rate (%)	Significance TCGA vs NKI/Vancouver[a]	Significance (false-discovery rate)[a]
KDM6A	13	33	0.0005	0.02
FANCA	10	4	0.01	0.16
CDKN1A	16	9	0.01	0.16
POLE	13	7	0.02	0.16
TXNIP	1	5	0.02	0.16
FOXQ1	8	3	0.02	0.17
MDC1	8	4	0.06	0.4
ARID1A	19	30	0.15	0.6
ELF3	16	13	0.18	0.6
ATR	11	8	0.19	0.6
FANCC	0	1	0.19	0.6
PAIP1	1	3	0.19	0.6
RHOA	7	5	0.22	0.6
RB1	22	19	0.23	0.6
BRCA1	8	5	0.24	0.6
ERBB2	9	13	0.24	0.6
CDKN2A	9	7	0.28	0.7
CCND3	2	1	0.28	0.7
ERCC2	7	10	0.33	0.7
PIK3CA	18	26	0.36	0.8
KLF5	4	6	0.41	0.8
STAG2	11	15	0.41	0.8
FOXA1	2	3	0.42	0.8
FGFR3	17	15	0.44	0.8
GPC5	2	4	0.46	0.8
BRIP1	3	5	0.50	0.8
BRCA2	11	10	0.54	0.8
NFE2L2	5	7	0.56	0.9
RHOB	5	7	0.69	0.9
EP300	14	17	0.70	0.9
RAD51C	2	1	0.72	0.9
FBXW7	9	8	0.73	0.9
ERBB3	12	11	0.77	0.9
RAD50	2	3	0.77	0.9
NBN	3	3	0.78	0.9
RXRA	5	6	0.84	1
KMT2D	29	34	0.92	1
ATM	14	15	1	1
HRAS	4	4	1	1
PARP1	2	3	1	1
TSC1	8	9	1	1
ZFP36L1	6	6	1	1

[a] Fisher's exact test for frequency of somatic mutations between TCGA and NKI/Vancouver cohorts. P-values were adjusted for multiple hypothesis testing by the Benjamini-Hochberg method.

Supplementary Table 3 | Baseline characteristics and response rates of 163 patients with muscle-invasive bladder cancer treated with neoadjuvant chemotherapy and radical cystectomy and comparison between *ERCC2* mutation status.

	$ERCC2_{mut}$	$ERCC2_{wt}$	Significance $ERCC2_{mut}$ vs $ERCC2_{wt}$ [a]
Number of patients	11	152	
Median age in years (IQR)	57.0 (53.2, 74.0)	69.0 (60.9, 75.0)	0.12
Male sex (% of pts)	8 (72%)	107 (70%)	1
cT-stage (% of pts)			0.7
cT1	0 (0%)	1 (1%)	
cT2	2 (18%)	49 (32%)	
cT3	6 (55%)	67 (44%)	
cT4	3 (27%)	35 (23%)	
cN-stage (% of pts)			0.4
cN0	8 (73%)	84 (55%)	
cN+	3 (27%)	68 (45%)	
Chemotherapy regimen (% of pts)			0.8
Cis/Gem	9 (82%)	112 (74%)	
MVAC	2 (18%)	38 (25%)	
CMV	0 (0%)	2 (1%)	
Chemotherapy cycles received (% of pts)			0.5
2	0 (0%)	6 (4%)	
3	4 (36%)	32 (21%)	
4	6 (54%)	104 (68%)	
>4	1 (9%)	10 (7%)	
Pathological response (% of pts)			0.009
ypT0N0 (complete response)	6 (54%)	43 (28%)	
ypTis/Ta/T1N0	3 (27%)	16 (11%)	
≥ypT2N0 (non-response)	2 (18%)	93 (61%)	

[a] Fisher's exact test for binary predictors. t-test for numerical predictors. All the statistical tests were two-sided. No adjustments were made for multiple hypothesis testing. Significant associations are highlighted on bold.
Cis/Gem = cisplatin + gemcitabine; MVAC = methotrexate + vinblastine + docorubicin + cisplatin; CMV = cisplatin + methotrexate + vinblastine; mut = mutant; wt = wild-type; IQR = Interquartile range; pts = patients.

CHAPTER 4

Platinum-based chemotherapy induces opposing effects on immunotherapy response-related spatial and stromal biomarkers in the bladder cancer microenvironment

Jeroen van Dorp, Maksim Chelushkin, Sandra van Wilpe, Iris M. Seignette, Jan-Jaap J. Mellema,
Maartje Alkemade, Alberto Gil-Jimenez, Dennis Peters, Wim Brugman, Chantal F. Stockem,
Erik Hooijberg, Annegien Broeks, Bas W.G. van Rhijn, Laura S. Mertens,
Antoine G. van der Heijden, Niven Mehra, Maurits L. van Montfoort, Lodewyk F. A. Wessels,
Daniel J. Vis, and Michiel S. van der Heijden

ABSTRACT

PURPOSE

Platinum-based chemotherapy and immune checkpoint inhibitors are key components of systemic treatment for muscle-invasive and advanced urothelial cancer. The ideal integration of these two treatment modalities remains unclear as clinical trials have led to inconsistent results. Modulation of the tumor-immune microenvironment by chemotherapy is poorly characterized. We aimed to investigate this modulation, focusing on potential clinical implications for immune checkpoint inhibitor response.

EXPERIMENTAL DESIGN

We assessed immune cell densities, spatial relations, and tumor/stromal components from 116 urothelial bladder cancer patients (paired data for 95 patients), before and after platinum-based chemotherapy.

RESULTS

Several published biomarkers for immunotherapy response changed upon chemotherapy-treatment. The intratumoral $CD8^+$ T-cell percentage increased after treatment and was associated with increased TNFα-via-NFκB signaling. The percentage of PD-L1$^+$ immune cells was higher after chemotherapy. An increase in chemo-induced changes that potentially inhibit an anti-tumor immune response was also observed, including increased fibroblast-based TGF-β signaling and distances from immune cells to the nearest cancer cell. The latter two parameters correlated significantly in post-treatment samples, suggesting that TGF-β signaling in fibroblasts may play a role in spatially separating immune cells from cancer cells. We examined specific chemotherapy regimens and found that treatment with methotrexate, vinblastine and adriamycin was associated with an increase in the macrophage cell percentage. Gemcitabine-containing chemotherapy were associated with upregulation of fibroblast TGF-β signaling.

CONCLUSIONS

The opposing effects of platinum-based chemotherapy on the immune cell composition and stromal context of the tumor-immune microenvironment may explain the inconsistent results of clinical trials investigating chemotherapy and immune checkpoint inhibitor combinations in bladder cancer.

TRANSLATIONAL RELEVANCE

In various tumor types, successful synergy of chemotherapy and immune checkpoint inhibitors (ICI) has been established, but in muscle-invasive bladder cancer (MIBC), clinical trials yielded inconsistent results. Therefore, understanding chemotherapy-induced changes in the tumor-immune microenvironment (TIME) of MIBC is highly relevant. To investigate them, we collected and analyzed a large dataset of paired pre- and post-platinum-treatment tumor samples. We demonstrate that platinum-based neoadjuvant chemotherapy (NAC) is associated with promoting TIME characteristics previously shown to relate to both ICI response and resistance. The latter includes fibroblast-based TGF-β signaling and median distances from CD8+ T-cells and macrophages to their nearest cancer cells. This suggests that responses to ICI in MIBC after platinum-based NAC might be improved by adding TGF-β inhibitors or bispecific antibodies promoting spatial rearrangements of immune and cancer cells. Finally, our data suggests differences between MVAC and gemcitabine-containing platinum-based regimens in their effects on the bladder TIME.

INTRODUCTION

Cisplatin-based neoadjuvant chemotherapy (NAC) followed by radical cystectomy is recommended for patients with muscle-invasive bladder cancer (MIBC)[1]. Accelerated methotrexate, vinblastine, adriamycin and cisplatin (MVAC) and cisplatin-gemcitabine are the two most commonly used NAC regimens for MIBC[2]. Despite a pathological complete pathological response rate (pCR) of 25-42%, cisplatin-based NAC is associated with only a 5-8% absolute increase in 5-year overall survival (OS) when compared to radical cystectomy alone[3,4,5]. Recently, the CheckMate-274 trial showed that adjuvant treatment with nivolumab (PD-1 inhibitor) significantly increased disease-free survival (DFS) for patients with residual MIBC or lymph node involvement[6]. Exploratory analyses revealed a notable improvement of DFS for patients who were previously treated with cisplatin-based NAC (hazard ratio (HR): 0.52; 95% CI: 0.38-0.71 for nivolumab vs. placebo), while those who did not receive NAC appeared to have limited benefit (HR: 0.92; 95% CI: 0.69-1.21).

In the metastatic setting, improved clinical outcomes have been observed in patients treated with avelumab (PD-L1 inhibitor) maintenance therapy after platinum-based chemotherapy, similarly suggesting a benefit of sequential treatment with chemo- and immunotherapy[7]. Clinical trials exploring concurrent chemotherapy and immune checkpoint inhibitors (ICI) have shown mixed results. In the IMvigor130 trial, atezolizumab, combined with platinum-based chemotherapy as first-line treatment for advanced urothelial cancer, improved progression-free survival (PFS) compared to chemotherapy alone, although the improvement in OS (final 1-sided p-value=0.023) did not reach statistical significance (final OS efficacy boundary: *P*=0.021)[8,9]. In an exploratory analysis, a more pronounced effect of atezolizumab on OS (and PFS) was observed in the cisplatin-treated

subgroup (HR for OS: 0.73; 95% CI: 0.54-0.98) versus the carboplatin-treated subgroup (HR for OS: 0.91; 95% CI: 0.75-1.10)[10]. The CheckMate-901 study specifically tested the addition of nivolumab to cisplatin-based chemotherapy, reporting positive results for the primary endpoints OS (HR=0.78) and PFS (HR=0.72)[11]. These findings suggest that the combination of ICI with cisplatin-based chemotherapy may be more effective than with carboplatin-based chemotherapy. Conversely, the addition of pembrolizumab to first-line platinum-based chemotherapy in the KEYNOTE 361 study did not significantly improve PFS or OS by central review in the unselected population per the prespecified p-value boundaries[12]. However, hazard-ratios for PFS were 0.78 (95% CI: 0.65–0.93) in the total population and 0.67 (95% CI: 0.51–0.89) in the choice-of-cisplatin subgroup[12]. Although clinical trials suggest potential synergy between platinum-based chemotherapy and ICI (either sequential or concurrent), results have not been unequivocally positive. Additionally, the positive results may partly be explained by earlier ICI initiation, as only a subset of patients (25-48%) in the standard arms of the chemo-immunotherapy trials in the advanced urothelial cancer setting received ICI as subsequent therapy[7,8,11,12]. Given the disappointing results in several trials testing concurrent platinum-based chemotherapy and ICI, particularly when combining carboplatin-based chemotherapy with ICI, a negative interaction between chemotherapy and ICI (e.g. by immune suppression) in a subset of patients cannot be excluded[8,12].

Here, we investigate the changes in the bladder cancer tumor microenvironment (TIME) induced by platinum-based NAC, focusing on potential implications for immunotherapy treatment. For this purpose, we collected and analyzed RNA-seq, multiplex immunofluorescence (mIF), and immunohistochemistry (IHC) data of tumor tissue from MIBC patients before and after treatment with platinum-based chemotherapy.
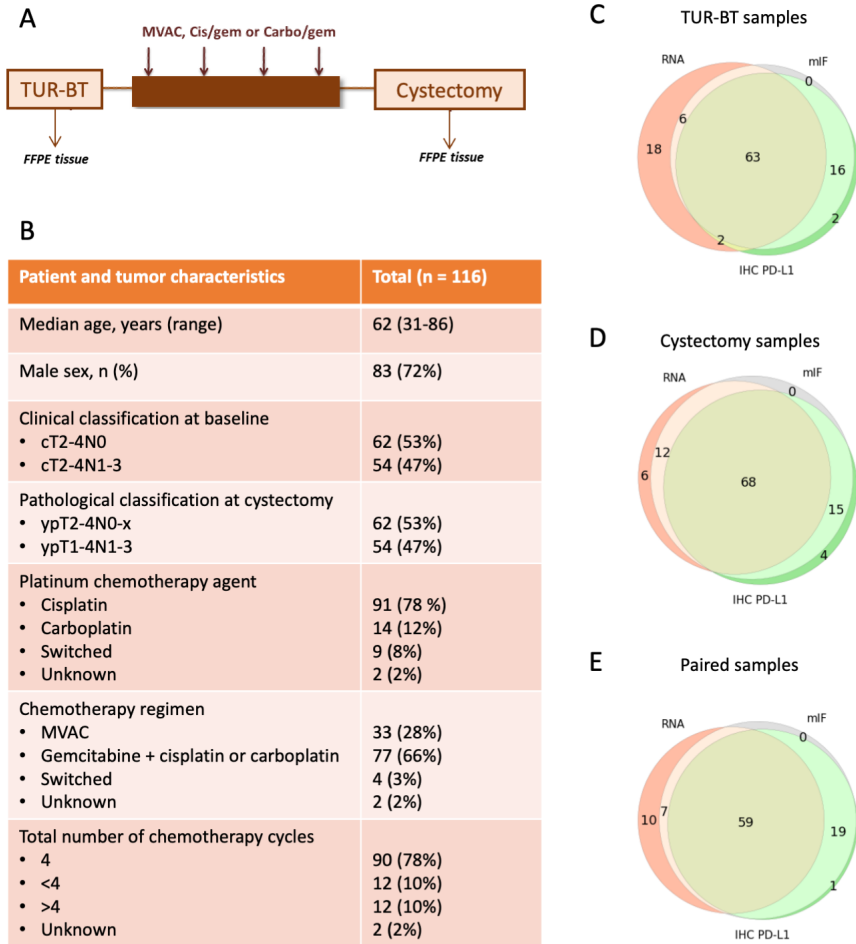
RESULTS

COHORT AND DATA DESCRIPTION

We retrospectively included 183 MIBC patients treated with platinum-based NAC followed by radical cystectomy (Supplementary Fig. 1, Methods). Patients achieving a pCR to NAC have a favorable clinical outcome and are therefore less likely to benefit from additional ICI treatment; these patients were not included in the various adjuvant ICI studies for this reason[6]. Furthermore, as all tumor cells will have been eliminated in patients with a pCR after neoadjuvant chemotherapy and prior to tissue collection, a reliable TIME analysis cannot be conducted in these patients. Therefore, regardless of nodal status, only patients with remaining viable tumor tissue at cystectomy (≥ypT1) were included (Supplementary Fig. 1). Tissue samples from 130 patients were subjected to analysis. We collected pre-treatment transurethral resection of the bladder tumor (TUR-BT) tissue at diagnosis (baseline) and post-treatment cystectomy tissue (resected tumor bulk) from each patient (Fig. 1A). In total 116 unique patients represented by at least one sample of one data type (mIF, IHC, RNA-seq) were included in our dataset. Sixty-two (53%) patients

had clinically node-negative disease at baseline (cT2-4aN0), and fifty-four (47%) patients were clinically node-positive (cT2-4aN1-3, Fig. 1B). Cisplatin was the most frequently used platinum-based treatment agent (78% of patients). Other patients were treated with carboplatin (12%) or switched their platinum agent during neoadjuvant treatment due to toxicity (8%). Of note, whereas cisplatin-based chemotherapy is the standard treatment in the neoadjuvant setting, some locoregionally advanced cis-ineligible patients were treated with carboplatin-based induction therapy and had consolidative surgery in case of a clinical response. As the active metabolites between these platinum-agents are similar[13] and questions regarding a potential difference in immune-induction remain to be answered, we included both platinum agents. Besides platinum, the treatment regimen included gemcitabine (in 66% of patients) or methotrexate, vinblastine, and doxorubicin (MVAC, 28%), or both at different time points (3%). The majority of patients (78%) received four cycles of NAC, while a subset received fewer (10%) or more (10%) than four cycles (Fig. 1B). The processed sample counts for each experimental technique and timepoint are shown in Fig. 1 C and D. Due to failed quality control, not all patients had both TUR-BT and cystectomy samples processed successfully. The final numbers of paired samples included 85 pairs of multiplex immunofluorescence (mIF), 76 pairs of RNA-sequencing, and 79 pairs of PD-L1 immunohistochemistry (IHC). In 59 patients, all three analyses could be performed on paired samples (Fig. 1E).

CHEMOTHERAPY-INDUCED CHANGES IN ICI RESPONSE BIOMARKERS

Abundance of tumor-infiltrating $CD8^+$ T-cells, PD-L1 expression, and gene signatures related to T-cell immunity (e.g., IFNγ and effector $CD8^+$ T-cell gene signatures) are biomarkers commonly associated with ICI response in cancer, including MIBC[14,15,16]. In our cohort, the $CD8^+$ T-cell percentage (mIF) increased in the tumor area (P=0.015) and adjacent stroma (P=0.017; Methods) as well as in their combined area (P=0.00076; Fig. 2A-C) upon chemotherapy treatment. The percentage of PD-L1 positive immune cells (IC), determined by IHC, increased after treatment (P=0.00033; Fig. 2D), while the percentage of PD-L1 positive tumor cells (TC) and the PD-L1 combined positivity score (CPS) remained unchanged (Fig. 2E, F). A fibroblast-based TGF-β signaling gene signature was previously associated with ICI resistance in MIBC in subsets of patients[14,15,17]. The single-sample gene set enrichment analysis (ssGSEA) score of this signature increased upon chemotherapy treatment in our cohort (P=1.2 * 10^{-8}; Fig. 2G). No difference in IFNγ and effector $CD8^+$ T-cell gene signatures between pre- and post-chemotherapy tumor tissue were detected (Fig. 2 H, I). These results demonstrate that features both positively ($CD8^+$ T-cell percentage, PD-L1 IC score) and negatively (TGF-β signaling in fibroblasts) associated with ICI response in MIBC increased upon platinum-based chemotherapy.

A

MVAC, Cis/gem or Carbo/gem

TUR-BT → Cystectomy

FFPE tissue   FFPE tissue

B

Patient and tumor characteristics	Total (n = 116)
Median age, years (range)	62 (31-86)
Male sex, n (%)	83 (72%)
Clinical classification at baseline • cT2-4N0 • cT2-4N1-3	62 (53%) 54 (47%)
Pathological classification at cystectomy • ypT2-4N0-x • ypT1-4N1-3	62 (53%) 54 (47%)
Platinum chemotherapy agent • Cisplatin • Carboplatin • Switched • Unknown	91 (78 %) 14 (12%) 9 (8%) 2 (2%)
Chemotherapy regimen • MVAC • Gemcitabine + cisplatin or carboplatin • Switched • Unknown	33 (28%) 77 (66%) 4 (3%) 2 (2%)
Total number of chemotherapy cycles • 4 • <4 • >4 • Unknown	90 (78%) 12 (10%) 12 (10%) 2 (2%)

**C** TUR-BT samples

D Cystectomy samples

E Paired samples

Figure 1 | Patient cohort characteristics and collected data. A, Treatment scheme. **B**, Patient and tumor characteristics. **C**, Availability of pre-treatment (TUR-BT) data by type. **D**, Availability of post-treatment (cystectomy) data by type. **E**, Number of sample pairs (TUR-BT-cystectomy from the same patient) available.

COMPREHENSIVE ASSESSMENT OF TIME CHANGES UPON CHEMOTHERAPY TREATMENT

Next, we aimed to better understand the effect of platinum-based chemotherapy on the bladder cancer TIME in a more comprehensive and unsupervised manner. We assessed alterations in the cellular immune cell composition by mIF and transcriptional changes through RNA-sequencing data by comparing pre- vs post-chemotherapy samples. Because we used different sample types for our analyses, which are transurethral resection (TUR-BT) samples as pre-chemotherapy tissue and radical cystectomy samples after chemotherapy, we aimed to identify and mitigate possible biases in the mIF data analysis. After finding a difference in the total cell density between the sample types (Supplementary Fig. 2A), we proceeded with cell percentages instead of raw densities to minimize a possible confounding effect of the sample type. Comparison of TIME cell percentages assessed by mIF analysis (normalized densities) showed that, besides the CD8^{+} T-cell percentage increase after chemotherapy, the macrophage cell percentage increased as well (adj. P=0.016; Fig. 3A). Boxplots showing cell percentages and raw densities of all cell types identified by our mIF panel between TUR-BT and cystectomy sample sets are shown in Supplementary Fig. 3. Gene set enrichment analysis (GSEA) performed with the Hallmark gene sets[18] on the differentially expressed genes before and after treatment showed (among others) a strong upregulation of epithelial-mesenchymal transition (EMT; adj. P=5.5 * 10^{-27}) and TNFα-via-NFκB signaling (adj. P=3.0 * 10^{-33}; Fig. 3B). Of note, EMT signaling was previously associated with ICI resistance in urothelial cancer[19]. We recently showed that a shorter distance from macrophages and CD8^{+} T-cells to their first-nearest neighboring (1-NN) cancer cells at baseline was positively associated with pre-operative combination ICI response in an analysis of the NABUCCO (MIBC) and IMCISION (head and neck cancer) trials[17,20,21]. Following the same approach, we quantified the median 1-NN distances for each spatial relationship as identified by our mIF panel (refer to the Methods section for more details). To identify a possible bias between the sample types, we analyzed the cell-type-agnostic 1-NN median distances and established that they were similar between TUR-BTs and cystectomies (Methods, Supplementary Fig. 2B), suggesting no bias in the analysis of 1-NN median distances.

A comparison of paired cystectomies and TUR-BTs showed that all five immune cell types tested (CD8 T-cells, macrophages, Tregs, helper T-cells, and B-cells) were, on average, further away from their 1-NN cancer cells after chemotherapy treatment compared to the pre-treatment sample (Fig. 3C), including CD8^{+} T-cells (adj. P=1.6 * 10^{-5}) and macrophages (adj. P=1.5 * 10^{-5}; Fig. 3D). Thus, whereas the percentages of cells with potential anti-tumor immune activity increased upon chemotherapy, immune cells were (on average) further from the nearest neighboring cancer cells. This increased distance suggests that their anti-tumor activity may be impeded. Fold changes in CD8^{+} T-cell percentages did not correlate to the fold changes in median distances from CD8^{+} T-cells to 1-NN cancer cells (Supplementary Fig. 4). Therefore, in many sample pairs, only one of the two characteristics increased (Supplementary Fig. 4, examples in Fig. 3E, F). Still, in some sample pairs, both characteristics became higher (Supplementary Fig. 4, examples in Fig. 3G).
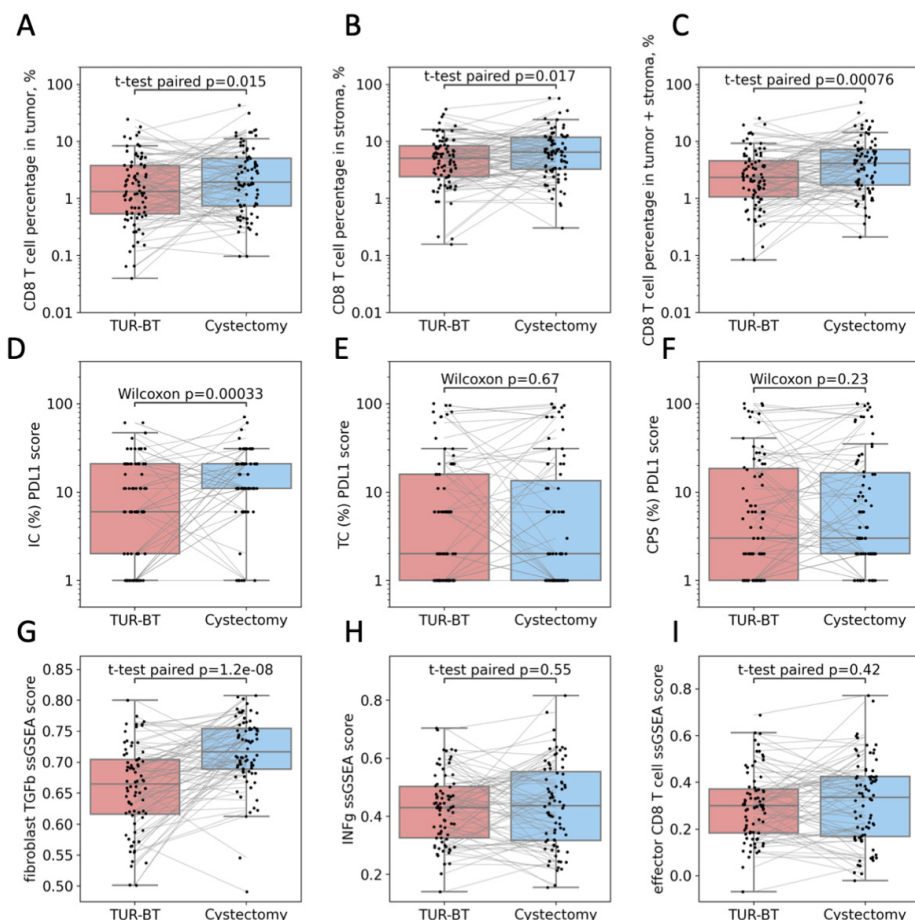
Figure 2 | Changes associated with platinum-based chemotherapy. A-C, CD8^{+} T-cell percentage determined by mIF in the tumor (A), stromal areas (B) and full analyzed area (C). **D**, Percentage of PD-L1 positive immune cells (IC) determined by IHC. **E**, Percentage of PD-L1 positive tumor cells (TC) determined by IHC. **F**, PD-L1 combined positivity score (CPS) determined by IHC. **G**, ssGSEA score of the fibroblast-based TGF-β signaling gene signature from[14]. **H, I**, ssGSEA score of Interferon gamma and CD8^{+} T-cells effector gene signatures. ssGSEA, single-sample gene set enrichment analysis. *IQR: interquartile range*.

CORRELATION ANALYSES SUGGEST DIFFERENT TIME RESPONSE PATTERNS TO CHEMOTHERAPY

Next, we investigated whether changes in stromal (fibroblast TGF-β and EMT) and inflammation-related (TNFα-via-NFκB) signatures correlated with specific changes in the TIME immune cell composition upon treatment with chemotherapy. For this analysis, we considered immune cell percentages and distances that changed after chemotherapy treatment, i.e., CD8^{+} T-cell and macrophage percentages and all five immune-to-cancer cell distances (Fig. 3 A, C), as well as the PD-L1-positive immune cell percentage (Fig. 1D). For the correlation analysis, we used the Kendall

τ-*b* correlation coefficient (because of ties in the PD-L1 data). Results of Pearson correlation analysis excluding PD-L1 IC data are shown in Supplementary Fig. 5 A-C. We found an association between the increase in CD8^{+} T-cell percentage and upregulation of TNFα-via-NFκB signaling upon chemotherapy (τ-*b* = 0.29, *P*=0.00048; Fig. 4A, Supplementary Fig. 6A). The TNFα-via-NFκB signature and CD8^{+} T-cell percentage also correlated significantly after chemotherapy, i.e., within the cystectomy sample set (τ-*b* = 0.23, *P*=0.0021; Fig. 4B, Supplementary Fig. 6B) and before chemotherapy, i.e., within the TUR-BT sample set (τ-*b* = 0.24, *P*=0.0042; Fig. 4C, Supplementary Fig. 6C). These results suggest that a subset of patients experienced an induction of T-cell immunity upon platinum-based chemotherapy, e.g., patients with a higher than median change in TNFα-via-NFκB signaling showed a higher fold change in CD8^{+} T-cell infiltration (*P*=0.014; Fig. 4D). On the other hand, the fibroblast-based TGF-β signaling positively correlated with higher distances (but not densities) from each immune cell type to their nearest cancer cell within post-treatment samples (Fig. 4B, F). Also, a negative correlation was observed between these distances and the PD-L1 IC score (Fig. 4B). Furthermore, we investigated the correlation between PD-L1 IC and fibroblast TGF-β signaling, and found a significantly negative correlation (Supplementary Fig. 6D, □-*b* = -0.27, *P*=0.0022). When comparing high vs. low PD-L1 IC in post-treatment samples as assessed by the median PD-L1 IC score (11%), the IC-low subset showed a higher fibroblast-derived TGF-β signaling score (Fig. 4E, right) and larger distances from immune cells to their nearest cancer cells (regardless of their density; Fig. 4G, right). This was not observed when comparing TUR-BT samples split by the baseline PD-L1 IC median (6%; Fig. 4 E, G, left).

In our previous work with NABUCCO samples, we found a negative correlation between pathologic response to pre-operative immunotherapy and both fibroblast TGF-β signaling[17] and 1-NN CD8^{+} T-cell-cancer cell distances[21]. Therefore, we expect the TIME in patients belonging to the subset having post-chemotherapy high TGF-β signaling and 1-NN CD8-cancer cell distance and low PD-L1 IC score to be less likely to support response to ICI. The associations found between TGF-β, PD-L1 IC positivity, and immune-to-cancer cell distances in the post-treatment set appeared to be weaker or absent before treatment (Fig. 4C). We formally tested which correlations changed upon treatment using Fisher's z-transformation of the equivalent Pearson correlations (Methods) and found a statistically significant change (FDR < 10%) for the immune cell distances to 1-NN cancer cells and PD-L1 IC positivity (Supplementary Fig. 7, an example for CD8 T-cells and IC is shown on Supplementary Fig. 6E, F). Although the correlation coefficient between the macrophage-to-cancer-cell distance and PD-L1 IC score increased significantly (with FDR level < 5%), it was the pair with the weakest resulting correlation in the cystectomy set (Fig. 4B). These results suggest that the percentage of PD-L1 positive cells among immune cells is higher when they are closer to their nearest neighboring cancer cells, and this relation appears only after chemo-treatment. For CD8^{+} T-cell-to-cancer-cell distances, this is illustrated in Fig. 4G with the PD-L1 IC score binarized by medians. distance between groups of TUR-BT and cystectomy samples with the PD-L1 IC score lower and higher than the TUR-BT median and the cystectomy median correspondingly.

4
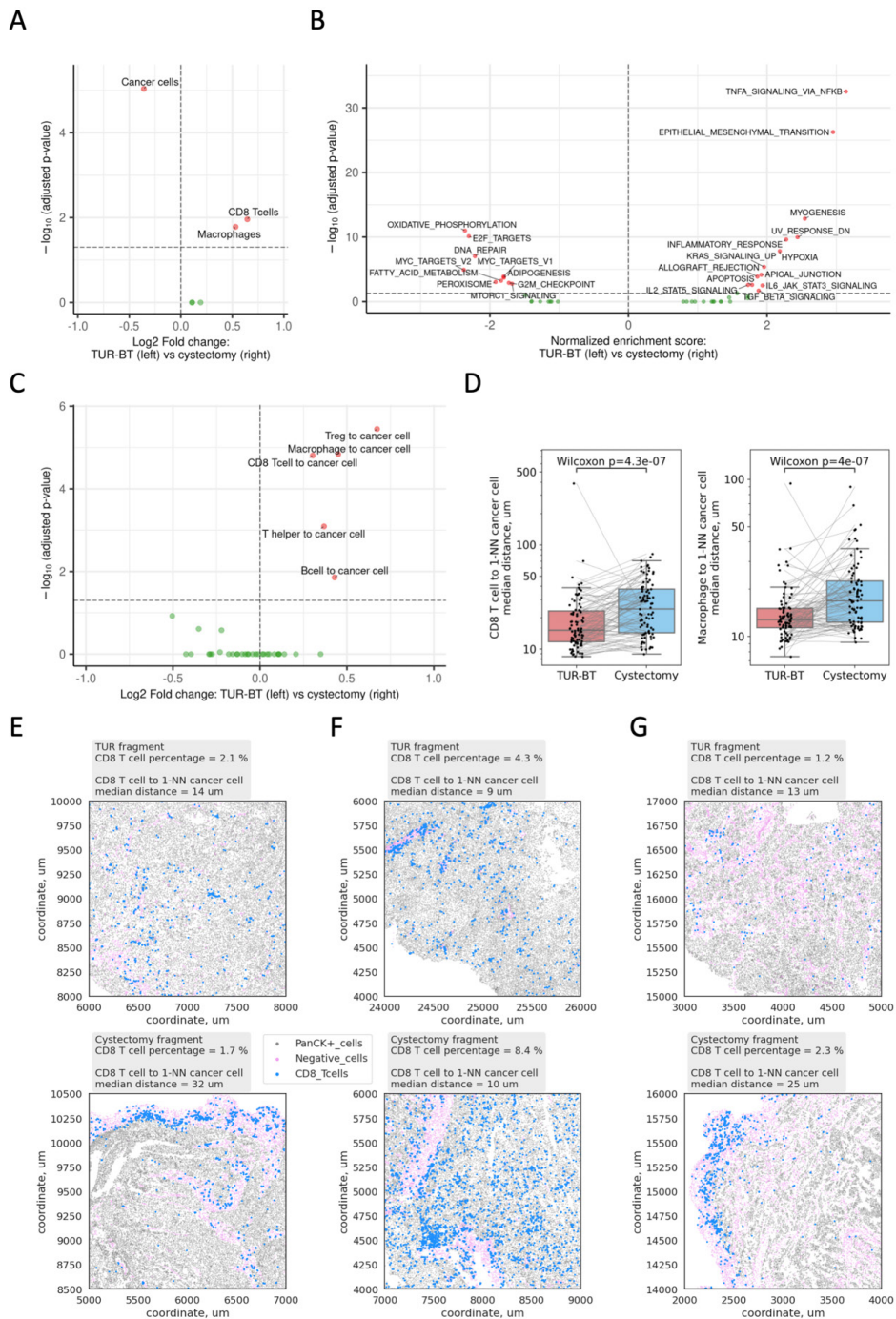
Figure 3 | A, mIF-based cell percentages compared between post- and pre-treatment. **B**, GSEA results for hallmark gene signatures. **C**, 1-NN median distances calculated from fitting Weibull distribution to the mIF data and compared between post- and pre-treatment. **D**, Comparison of median distances from CD8^{+}

T-cells to 1-NN cancer cells and from macrophages to 1-NN cancer cells between post- and pre-treatment. **E-G,** Examples of slide fragments for corresponding TUR-BT and cystectomy samples recreated based on cell coordinates and labels. Only CD8⁺ T-cells (blue), cancer cells (grey), and DAPI-positive cells negative with the other markers (purple) are shown. P-values shown in A and C are Wilcoxon test p-values adjusted with Bonferroni correction for multiple testing.
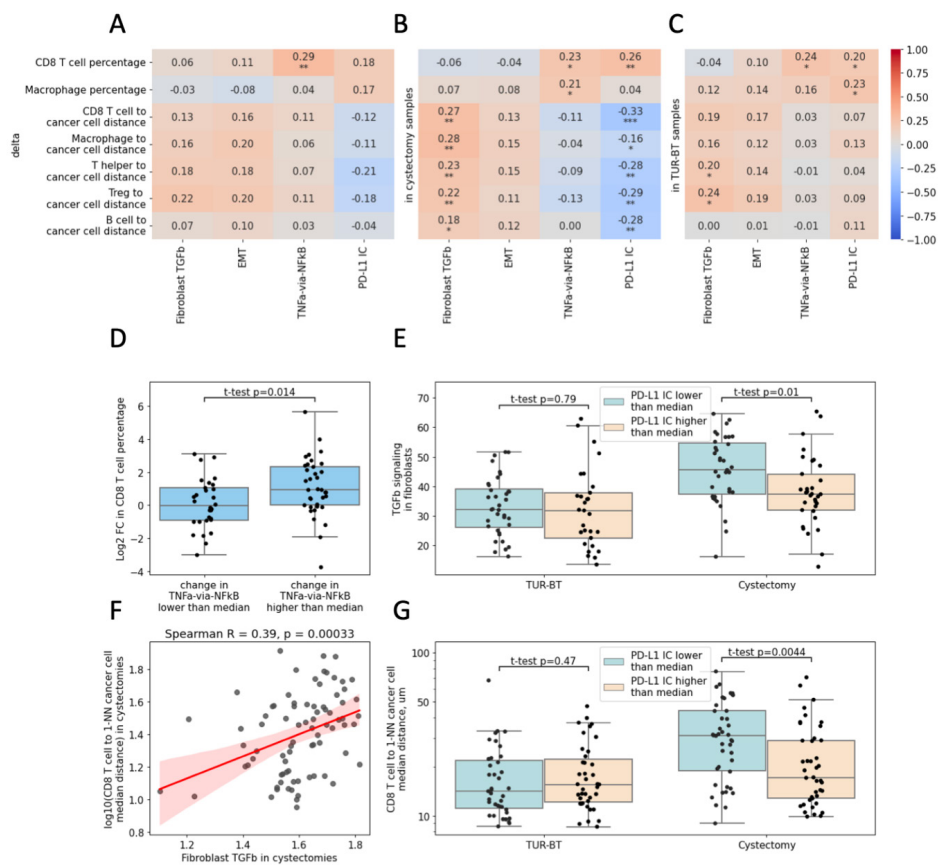
Figure 4 | A-C, Correlation analysis of parameters altered by the chemo-treatment between different data modalities. RNA-Seq and IHC are shown on the x-axis and mIF is shown on the y-axis. Kendall τ-b correlation coefficients are shown and indicated by colors. Stars denote p-values for the correlation coefficients to be non-zero assessed by the distribution of τ (two-sided test): *: p<0.05, **: p<0.01, ***: p<0.001. P-values are FDR-adjusted for multiple testing within each column. A, Correlations between changes ("deltas"). B, Correlations within cystectomy samples (post-treatment). C, Correlations within TUR-BT samples (pre-treatment). D, CD8⁺ T-cell percentage (mIF) fold change upon chemo-treatment between patient groups with the change in TNFα-via-NFκB gene signature score (RNA) below and higher than a median change. E, Fibroblast-derived TGF-β gene signature score (RNA) between groups of TUR-BT and cystectomy samples with the PD-L1 IC score lower and higher than the TUR-BT median and the cystectomy median correspondingly. F, Correlation between the fibroblast-derived TGF-β gene signature score (RNA) and CD8⁺-T-cell-to-cancer-cell 1-NN median distance (mIF) in cystectomy samples. G, CD8⁺-T-cell-to-cancer-cell 1-NN median

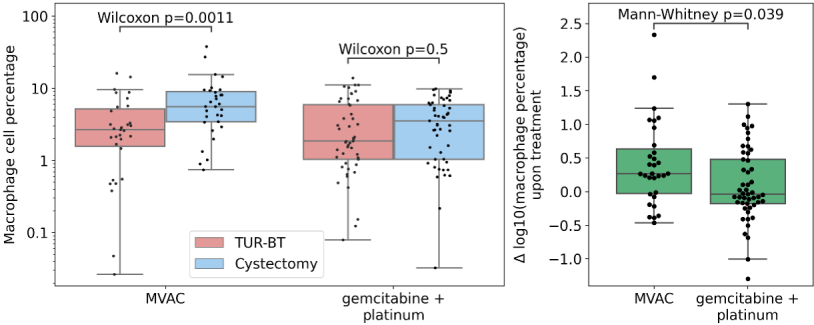## MVAC AND GEMCITABINE-CONTAINING PLATINUM-BASED REGIMENS WERE ASSOCIATED WITH DISTINCT CHANGES TO THE TIME

While all patients received platinum-based chemotherapy, the specific chemotherapeutic regimens varied (Fig. 1B). To assess the impact of these regimens on TIME changes, we explored differences between MVAC versus gemcitabine-containing platinum-based regimens. We used robust analogues of a mixed ANOVA with between-subject variable "chemo regimen" and within-subject variable "timepoint", i.e., TUR-BT (pre-treatment) or cystectomy (post-treatment; Methods, Statistical analysis). We performed this analysis with each of the target variables, which are the TIME characteristics changed upon chemotherapy (CD8^{+} T-cell and macrophage cell percentages: Fig. 3A; PD-L1 IC, fibroblast TGF-β: Fig 2 D, G; CD8^{+} T-cell-to-cancer median 1-NN distance, and macrophage-to-cancer median 1-NN distance: Fig. 3C). Besides significant coefficients for the timepoint term in all models (in line with the overall changes shown in Fig. 2 and 3), our analyses showed significant statistical interaction between the timepoint and chemo regimen variables in the models for the macrophage cell percentage and fibroblast TGF-β signaling (Fig. 5A). These results suggest that the change in macrophage cell percentage and fibroblast TGF-β signaling depended on the regimen, whereas the changes in CD8^{+} T-cell density, PD-L1 IC, CD8^{+} T-cell-to-cancer cell, and macrophage-to-cancer cell median 1-NN distances were the same for both regimens. The post-hoc analysis showed a more pronounced increase in the macrophage cell percentage upon MVAC than upon gemcitabine-containing chemotherapy (Fig. 5B). Conversely, fibroblast TGF-β signaling increased more upon the gemcitabine-containing platinum-based regimen (Fig. 5C). We did not find associations with the type of platinum agent (cisplatin versus carboplatin) for the six TIME characteristics analyzed before in the context of MVAC and gemcitabine-containing platinum-based regimens (Supplementary Fig. 8). However, the analysis for the platinum agent had less statistical power and a more unbalanced design due to the low number of carboplatin-treated patients (8 patients with paired mIF and 11 patients with paired RNA data) compared to the number of cisplatin-treated patients (68 patients with paired mIF and 57 patients with paired RNA data). pre- and post-treatment within groups of patients who received different chemotherapy regimens. The right panels show comparison between changes ("deltas") upon the distinct regimens.

In summary, our results show that platinum-based chemotherapy can induce changes that are potentially either pro-immunogenic (increased CD8^{+} T-cell percentage, TNFα-via-NFκB signaling, IC PD-L1 score) or immune-inhibitory (larger distance of immune-to-cancer cells, stromal signatures).

A

Target variable	CD8+ T cell fraction (mIF)	Macrophage cell fraction (mIF)	PD-L1 IC	Fibroblast-derived TGFb signaling (ssGSEA score)	CD8+ T cell to cancer cell median 1-NN distance	Macrophage to cancer cell median 1-NN distance
Method	mixed ANOVA based on the trimmed means	F1-LD-F1 non-parametric model, ANOVA	F1-LD-F1 non-parametric model, ANOVA	mixed ANOVA based on the trimmed means	F1-LD-F1 non-parametric model, ANOVA	F1-LD-F1 non-parametric model, ANOVA
Chemo regimen, p-value	0.85	0.074	0.013	0.13	0.83	0.35
Time point, p-value	0.0056	0.00012	$1.0 * 10^{-5}$	$1.0 * 10^{-6}$	$3.2*10^{-7}$	$1.4*10^{-6}$
Chemo regimen: Time point, interaction p-value	0.66	**0.023**	0.13	**0.025**	0.84	0.66
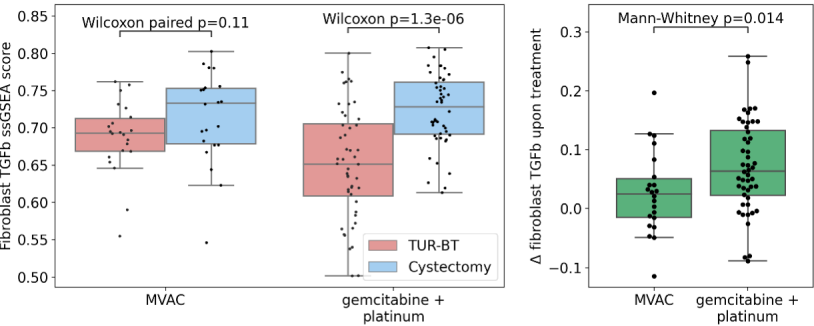
Figure 5 | Analysis of changes in the TIME characteristics upon MVAC and gemcitabine-containing platinum-based chemotherapy regimens. A, P-values of robust mixed ANOVA analogues are chosen depending on the data normality for each combination of the ANOVA design factors (Methods, Statistical analysis). Significant statistical interactions between the regimen and timepoint are highlighted as bold. **B,C**, Post-hoc analysis of changes in macrophage cell percentage (B) and fibroblast-derived TGF-β signaling (C). The left panels show comparison between pre- and post-treatment within groups of patients who received different chemotherapy regimens. The right panels show comparison between changes ("deltas") upon the distinct regimens.

DISCUSSION

The efficacy of concurrent chemotherapy and ICI has been established in lung, head-and-neck, triple-negative breast, gastric, and esophageal cancers[22]. In urothelial cancer, clinical trials yielded inconsistent results[6,7,8,11,12,23]. In this study, we comprehensively assessed the TIME in urothelial bladder cancer following platinum-based chemotherapy. To do so, we have collected and analyzed a large dataset of paired pre- and post-platinum-treatment bladder tumor samples analyzed with different experimental techniques.

In our cohort of MIBC patients treated with platinum-based chemotherapy, several parameters indicative of T-cell immunity increased. This included an increase in the CD8^{+} T-cell percentage, as determined by mIF; the percentage of PD-L1^{+} immune cells, determined by immunohistochemistry, and an upregulation of TNFα-via-NFκB, as shown in differential gene expression analysis. The macrophage (CD68^{+}) percentage increased as well, which appeared to be specifically associated with the MVAC treatment regimen.

Several preclinical studies suggested an association between cisplatin chemotherapy and increased CD8^{+} T-cell infiltration or activation[24,25,26]. Single-cell RNA-seq analysis of peripheral blood immune cells of participants in the IMvigor130 trial at baseline and on chemotherapy demonstrated that cisplatin (and not carboplatin; both with gemcitabine) induced immune and inflammatory transcriptional programs in circulating monocytes including TNFα-via-NFκB and genes encoding proteins associated with antigen presentation and T-cell priming[10]. Seiler *et al.* found specific post-chemotherapy molecular subtypes in MIBC, some of which were characterized by higher immune signatures and CD8^{+} T-cell immune infiltration[27]. In contrast, a recent study in human bladder cancer showed no association between neo-adjuvant platinum-based chemotherapy and CD8^{+} T-cell infiltration assessed by mIF[28]. However, the sample size in the latter study (33 patients) was smaller than in our cohort and the comparison was made with raw cell densities (cells per mm[2]) rather than percentages, potentially amplifying confounding signals from the different sample types (see Methods). Conversely, induction chemotherapy consisting of docetaxel, a platinum-containing agent and 5-fluorouracil induced PD-L1 expression and CD8^{+} T-cell infiltration in patients with head and neck squamous cell carcinoma[29]. A similar effect was observed in connection to NAC with 5-fluorouracil and cisplatin in esophageal squamous cell carcinoma[30]. Further, in ovarian cancer, platinum- and taxane-based NAC regimens were associated with an increased T-cell infiltration and T-cell receptor (TCR) oligoclonal expansion both assessed via TCR-sequencing[31]. In triple-negative breast cancer, an induction therapy with doxorubicin was associated with an increase in inflammatory signatures, including TNFα-via-NFκB signaling[32].

In contrast to these alterations related to an enhanced immune presence in the tumor, potentially indicative of a favorable ICI response, several parameters previously connected to ICI resistance

increased upon chemotherapy. Expression of a fibroblast-derived TGF-β gene signature was enhanced after chemotherapy. Its upregulation was significantly higher in the tumors of patients treated with a gemcitabine-containing platinum-based regimen (in contrast to MVAC). In line with our results, a recent report suggests that platinum chemotherapy drug accumulation in cancer-associated fibroblasts intensified TGF-β activity and associated with increased cancer aggressiveness in colorectal cancer[33]. Additionally, median distances from CD8+ T-cells and macrophages to their nearest neighboring cancer cell increased upon chemotherapy and were significantly correlated with the fibroblast-based TGF-β signaling in post-treatment samples. Interestingly, spatial analysis of triple-negative breast cancer in mice showed that quiescent cancer cells expressing chemotherapy resistance genes form niches which exclude immune infiltrates locally and contain immune-suppressive fibroblasts[34]. In our approach, local exclusion corresponds to the increase in 1-NN distances from immune cells to cancer cells.

Our findings may point to the importance of a balance between pro-immunogenic and anti-immunogenic aspects of the bladder cancer TIME, ultimately determining the response to ICI treatment. The importance of such opposing forces in the TIME was previously suggested by Wang et al.[19], showing that in patients with T-cell infiltrated tumors, higher EMT/stroma-related gene expression is associated with lower clinical benefit to nivolumab in advanced urothelial cancer. Similarly, Mariathasan et al[14] showed that a TGF-β in fibroblast-related signature was inversely associated with response to atezolizumab, specifically in immune-excluded tumors. Our findings suggest that platinum-based chemotherapy can modulate this balance, either in a positive or negative way.

The chemotherapy-associated TIME alterations discussed above suggest several potential avenues to improve benefit from chemotherapy and immunotherapy combinations. The addition of TGF-β inhibitors to ICI regimens after platinum-based NAC, especially in regimens containing gemcitabine, may potentially improve immunotherapeutic responses in MIBC. Combinations of ICI and TGF-β inhibitors have been tested in phase 1 and 2 clinical trials in various cancer types, including urothelial cancer[35]. However, while preclinical studies exploring the combination of TGF-β and PD-1/PD-L1 inhibition showed uniformly positive results, the addition of TGF-β inhibitors in clinical trials has often failed to show a meaningful benefit beyond the current generation of ICIs alone[35]. Administering agents promoting spatial rearrangement of immune cells to achieve closer proximity to cancer cells, e.g., bispecific antibodies, might be another treatment option specifically in the setting of ICI after platinum-based NAC. Several bispecific antibodies targeting cancer cells and T-cells have been tested in clinical urothelial cancer trials (e.g., Orlotamab (CD3×B7-H3)[36] and Catumaxomab (CD3 × EpCAM)[37]. Interestingly, therapeutic co-administration of TGF-β inhibitors and PD-L1 inhibitors in a mouse mammary carcinoma model recapitulating an immune-excluded phenotype was shown to facilitate T-cell penetration into the center of tumors and provoke tumor regression, while therapeutic blockade of PD-L1 or TGF-β alone had little or no effect[14].

This study has several limitations. First, we used different sample types for our analyses, which are transurethral resection (TUR-BT) samples as pre-chemotherapy tissue and radical cystectomy samples after chemotherapy. In our methods, we aimed to identify and mitigate possible biases in the mIF data analysis by comparing the total cell densities and the cell-type-agnostic 1-NN median distances between sample types and using cell percentages instead of raw densities. Another limitation is the heterogeneity in the chemotherapy regimens (Fig. 1B). Although the inclusion of different regimens could have allowed us to study divergent effects on the TIME by cisplatin vs. carboplatin, only 12% of patients were treated with carboplatin, while 78% received cisplatin. This complicated detecting TIME-related changes associated with the specific platinum agent, which are probable based on the recent findings from the translational analysis of the data from the IMvigor130 participants[10]. Further, although our ultimate interest was motivated by establishing potential synergy or antagonism between chemo- and immunotherapies, patients in our cohort did not receive immunotherapy peri-operatively. A dataset consisting of a pre- and post-NAC comprehensive TIME assessment and clinical data on additional peri-operative immunotherapy treatment does not exist currently. However, clinical studies randomizing between NAC with or without checkpoint inhibition are currently ongoing and tumor tissue collected in these trials may provide a source for further validation[38]. Finally, our study does not provide information whether the TIME modulation by chemotherapy is stable in time and affects the immune response to ICI at the time of its administration.

In conclusion, neo-adjuvant platinum-based chemotherapy for MIBC is associated with promoting TIME characteristics previously shown to relate to both ICI response (CD8^{+} T-cell percentage, PD-L1^{+} immune cell percentage) and ICI resistance (fibroblast-based TGF-β signaling, median distances from CD8^{+} T-cells and macrophages to their nearest cancer cells). Additionally, our data suggests there may be biological differences between MVAC and gemcitabine-containing platinum-based chemo regimens in their effects on the bladder TIME. A better understanding of chemotherapy-induced changes in the bladder TIME and their implications for immunotherapy warrants further investigation. Future studies could test our hypotheses by analyzing data from patients randomized between NAC with and without concurrent ICI, with several ongoing phase 3 studies expected to provide relevant insights.

METHODS

PATIENT POPULATION

We retrospectively included patients that were treated with neoadjuvant chemotherapy followed by radical cystectomy for MIBC (cT2-4N0-3). Only patients with remaining viable tumor tissue after cystectomy were included (≥ypT1), regardless of nodal status. Exclusion criteria were prior pelvic radiotherapy and non-urothelial primary histology. Urothelial carcinoma with squamous and/or glandular differentiation was allowed. Patients underwent radical cystectomy between 1995 and 2021. Follow-up was performed according to local guidelines. Data were collected in accordance with institutional and national ethical guidelines; the project was approved by the NKI institutional review board (IRBm20-296).

TISSUE COLLECTION AND RNA ISOLATION

Pre-treatment TUR-BT and post-treatment cystectomy material was stored as formalin-fixed paraffin embedded (FFPE) tissue blocks in The Netherlands Cancer Institute. Tumor material from patients that had their TUR-BT or cystectomy in a different hospital was requested as tissue blocks and subsequently stored at The Netherlands Cancer Institute. An experienced uro-pathologist assessed all available tissue blocks and the most representative tissue block was selected. Tumor area and tumor cell percentage was determined by an experienced uro-pathologist. RNA was isolated from baseline tumor material (5-10x 10 μm slides) using the using the Qiagen AllPrep FFPE DNA/RNA Kit.

RNA SEQUENCING

Quality and quantity of the total RNA were assessed using the 2100 Bioanalyzer and a Nano chip (Agilent). The percentage of RNA fragments with > 200-nucleotide fragment distribution values (DV200) were determined using the region analysis method according to the manufacturer's instructions manual (Illumina, technical-note-470-2014-001). Strand-specific libraries were generated using the TruSeq RNA exome library prep kit (Illumina) according to the manufacturer's instructions (Illumina, 1000000039582v01). Briefly, total RNA was random primed and reverse transcribed using SuperScript II reverse transcriptase (Invitrogen, 18064-014) with the addition of actinomycin D. Second strand synthesis was performed using polymerase I and RNaseH with the replacement of dTTP for dUTP. The generated cDNA fragments were 3'-end adenylated and ligated to Illumina (batch 1, 140 samples) or Integrated DNA Technologies xGen UDI(10bp)-UMI(9bp; batch 2, 35 samples) paired-end sequencing adapters and subsequently amplified by 15 cycles of PCR. The libraries were validated on a 2100 Bioanalyzer using a 7500 chip (Agilent) followed by a 1-4 plex library pooling containing up to 200 ng of each sample. The pooled libraries were enriched for target regions using the probe Coding Exome Oligos set (CEX, 45MB) according to the manufactures instruction (Illumina, 1000000039582v01). Briefly, cDNA libraries and biotin- labeled capture probes were combined and hybridized using a denaturation step of 95°C for 10 minutes and an incubation step from 94 °C to 58 °C with a ramp of 18 cycles, a 1-minute incubation and 2

°C per cycle. The hybridized target regions were captured using streptavidin magnetic beads and subjected to two stringency washes, an elution step and a second round of enrichment followed by a cleanup using AMPure XP beads (Beckman, A63881) and PCR amplification of 10 cycles. The target enriched pools were analyzed on a 2100 Bioanalyzer using a 7500 chip (Agilent), diluted and subsequently pooled equimolar into a multiplex sequencing pool. The libraries from 140 samples originated from 74 patients (batch 1) were sequenced with 65-bp single-end reads on a HiSeq 2500 using V4 chemistry (Illumina). The libraries from additional 35 samples (from the other 25 patients, batch 2) were sequenced with 54-bp paired-end reads on a NovaSeq 6000 using an SP Reagent Kit v1.5 (100cycles; Illumina).

IMMUNOHISTOCHEMISTRY AND MULTIPLEX IMMUNOFLUORESCENCE

Immunohistochemistry of the FFPE tumor samples was performed on a BenchMark Ultra autostainer (Ventana Medical Systems). Briefly, paraffin sections were cut at 3 um, heated at 75°C for 28 minutes and deparaffinized in the instrument with EZ prep solution (Ventana Medical Systems). Heat-induced antigen retrieval was carried out using Cell Conditioning 1 (CC1, Ventana Medical Systems) for 48 minutes at 95°C. PD-L1 was detected using clone 22C3 (1/40 dilution, 1 hour at RT, Agilent/DAKO). Bound antibody was detected using the OptiView DAB Detection Kit (Ventana Medical Systems). Slides were counterstained with Hematoxylin and Bluing Reagent (Ventana Medical Systems). A PANNORAMIC® 1000 scanner from 3DHISTECH was used to scan the slides at a 40x magnification. After scanning, PD-L1 and hematoxylin and eosin slides were uploaded to Slide Score (www.slidescore.com) for manual scoring. An experienced uro-pathologist determined the percentage of PD-L1 positive tumor cells (TC), the percentage of PD-L1 positive immune cells (IC) and the combined positivity score (CPS). Analysis of tumor immune cell infiltrates (anti-CD3 (1:400 dilution Clone P7, Thermo Fisher Scientific), anti-CD8 (1:100 dilution Clone C8/144B, Dako), anti-CD68 (1:500 dilution Clone KP1, Dako), anti-FoxP3 (1:50 dilution Clone 236A/47, Abcam), anti-CD20 (1:500 dilution Clone L26, Dako) and anti-PanCK (1:100 dilution Clone AE1AE3, Thermo Fisher Scientific) was performed by multiplex immunofluorescence technology on a Ventana Discovery Ultra automated stainer using PerkinElmer opal seven-color dyes. In short, 3 μm FFPE sections were cut and heated at 75 °C for 28 minutes and subsequently deparaffinized in EZ Prep solution (Ventana Medical Systems). Using Cell Conditioning 1 (CC1, Ventana Medical Systems), heat-induced antigen retrieval was conducted at 95 °C for 32 minutes. Further analysis was done by VECTRA image acquisition (Akoya Biosciences, v3.0) and HALO (Indica Labs, v2.3) image analysis. Tumor and stroma regions were classified by HALO automated tissue segmentation primarily based on PanCK expression. Adjacent stroma was defined as all tissue surrounding the tumor area within 150 μm. Cell segmentation was performed using a pre-trained nuclear segmentation AI module in HALO. Marker thresholds were set manually for each sample. Data was analyzed separately for tumor and stroma regions and subsequently exported. Immune cell classification was based on marker expression, as shown in the table below. When a cell was positive for two or more mutually exclusive markers, the cell was classified according to the highest relative intensity of the respective markers.

Marker positivity[a]	Cell type
PanCK^{+}	Cancer cell
CD8^{+} FoxP3^{-}	CD8^{+} T-cell
CD8^{-} FoxP3^{+}	Treg
CD3^{+}CD8^{-}FoxP3^{-}	T-helper
CD68^{+}	Macrophage
CD20^{+}	B-cell

[a] all cells are DAPI positive

COMPUTATIONAL ANALYSIS OF MULTIPLEX IMMUNOFLUORESCENCE DATA

Final classification of cells into tumor and stromal regions and quantification of these regions' areas was performed by the method we previously published[21] with the modification to take into account immune cells in addition to the negative cells while computing stroma-related kernel density estimation (KDE). Initially, cell densities were obtained from the output of this step by dividing cell counts over the corresponding area. The density of the total cells (regardless of their label) was significantly higher in TUR-BT samples than in cystectomy (Supplementary Fig. 2A). To minimize the possible bias related to the sample type, we switched to cell percentages by dividing each cell density over the total cell density. We quantified spatial relationships by using the first-nearest neighbor statistics. After quantifying distances between the first nearest neighboring cells of differenT-cell types in the full analyzed area (tumor plus adjacent stroma), we fitted the Weibull distribution to these data using the generalized linear mixed effect models for each of 49 cell phenotype combination in our mIF data following[21]. The scale and shape parameters were used to calculate medians of the Weibull distribution. Before analyzing the medians, we performed the same analysis with the cell labels removed and compared the medians between the two sample types to control for a possible bias. These overall medians were the same between the sample types (Supplementary Fig. 2B).

RNA-SEQ COMPUTATIONAL ANALYSIS

Gene expressions were quantified with Kallisto (v0.46.1) with the Gencode reference transcriptome v40 (basic annotation). Gene TPM values were filtered according to the gene biotype from the GTF (General Transfer Format) transcriptome annotation file, renormalized to 1 million in total, and used for ssGSEA (Gseapy v0.10.7). The following types of genes (according to the Gencode GTF basic annotation, v40) were retained in the expression files: 'protein_coding', 'processed_pseudogene', 'transcribed_processed_pseudogene','TEC', 'polymorphic_pseudogene', 'pseudogene', 'IG_C_gene','TR_C_gene','translated_processed_pseudogene', 'IG_C_pseudogene'. Transcript counts were summarized to the gene level and used for differential expression with DESeq2 (v1.36.0) and GSEA with Fgsea (v1.22.0) and Msigdbr (v7.5.1). The dataset included two batches with differences in the library preparation protocol and sequencing. The batch correction procedure was performed with the Limma R package (v3.52.4, function removeBatchEffect) on logarithmed gene TPM expressions.

STATISTICAL ANALYSIS

Pandas v1.3.3 and NumPy v1.20.0 were used for data handling. Seaborn v0.12.2, Matplotlib v3.7.3, statannotations 0.4.2, and EnhancedVolcano v1.14.0 were used for plotting. Basic statistical tests were implemented from Scipy v1.8.1 and Statsmodels v0.13.1. Before comparison, Kendall τ-*b* correlation coefficients were transformed to the equivalent Pearson R using Kendall's formula[39]. Function r.test from R package Psych (v2.3.9) was used to perform z-test of the difference of the Fisher's z-transformed correlations divided by the standard error of the difference. For the analysis of association between different chemotherapy regimens and changes in the TIME, we used robust analogues of a mixed ANOVA: a rank-based nonparametric method for longitudinal data in factorial experiments (F1-LD-F1 design[40], R package nparLD, v2.2) and the robust mixed ANOVA based on the trimmed means[41] (R package WRS2, v1.1.5). For the variables violating the assumption of normality within each combination of the ANOVA model factors (macrophage cell percentage, CD8+ T-cell/macrophage to cancer cell median 1-NN distances, and PD-L1 IC), we applied the non-parametric method. The normality was tested with Shapiro-Wilk test implemented in R package Rstatix (v0.7.2).

DATA AVAILABILITY

RNA sequencing data have been deposited in the European Genome-phenome Archive under the accession code EGASXXX and will be made available upon reasonable request for academic use and within the limitations of the provided informed consent by the corresponding author upon acceptance. Every request will be reviewed by the institutional review board of the Netherlands Cancer Institute; the researcher will need to sign a data access agreement with the Netherlands Cancer Institute after approval. Multiplex immunofluorescence primary data used for this study will be made available upon reasonable academic request within the limitations of informed consent by the corresponding author upon acceptance.

REFERENCES

1. Witjes JA, Bruins HM, Cathomas R, Compérat EM, Cowan NC, Gakis G, et al. European Association of Urology Guidelines on Muscle-invasive and Metastatic Bladder Cancer: Summary of the 2020 Guidelines. Eur Urol. 2021 Jan;79(1):82-104.

2. Powles T, Bellmunt J, Comperat E, De Santis M, Huddart R, Loriot Y, et al.; ESMO Guidelines Committee. Bladder cancer: ESMO Clinical Practice Guideline for diagnosis, treatment and follow-up. Ann Oncol. 2022 Mar;33(3):244-258.

3. Yin M, Joshi M, Meijer RP, Glantz M, Holder S, Harvey HA, et al. Neoadjuvant Chemotherapy for Muscle-Invasive Bladder Cancer: A Systematic Review and Two-Step Meta-Analysis. *Oncologist* 2016;21: 708-15.

4. Pfister C, Gravis G, Fléchon A, Soulié M, Guy L, Laguerre B, et al.; VESPER Trial Investigators. Randomized Phase III Trial of Dose-dense Methotrexate, Vinblastine, Doxorubicin, and Cisplatin, or Gemcitabine and Cisplatin as Perioperative Chemotherapy for Patients with Muscle-invasive Bladder Cancer. Analysis of the GETUG/AFU V05 VESPER Trial Secondary Endpoints: Chemotherapy Toxicity and Pathological Responses. Eur Urol. 2021 Feb;79(2):214-221.

5. Advanced Bladder Cancer (ABC) Meta-analysis Collaboration. Neoadjuvant chemotherapy in invasive bladder cancer: update of a systematic review and meta-analysis of individual patient data advanced bladder cancer (ABC) meta-analysis collaboration. Eur Urol. 2005 Aug;48(2):202-5; discussion 205-6.

6. Bajorin DF, Witjes JA, Gschwend JE, Schenker M, Valderrama BP, Tomita Y, et al. Adjuvant Nivolumab versus Placebo in Muscle-Invasive Urothelial Carcinoma. N Engl J Med. 2021 Jun 3;384(22):2102-2114. Erratum in: N Engl J Med. 2021 Aug 26;385(9):864.

7. Powles T, Park SH, Voog E, Caserta C, Valderrama BP, Gurney H, et al. Avelumab Maintenance Therapy for Advanced or Metastatic Urothelial Carcinoma. N Engl J Med. 2020 Sep 24;383(13):1218-1230.

8. Galsky MD, Arija JÁA, Bamias A, Davis ID, De Santis M, Kikuchi E, et al.; IMvigor130 Study Group. Atezolizumab with or without chemotherapy in metastatic urothelial cancer (IMvigor130): a multicentre, randomised, placebo-controlled phase 3 trial. Lancet. 2020 May 16;395(10236):1547-1557.

9. Galsky M, Arija J, De Santis M, Davis I, Bamias A, Kikuchi E, et al. Atezolizumab (atezo) + platinum/gemcitabine (plt/gem) vs placebo + plt/gem for first-line (1L) treatment (tx) of locally advanced or metastatic urothelial carcinoma (mUC): Final OS from the randomized Phase 3 IMvigor130 study. Journal of Clinical Oncology 2023 41:6_suppl, LBA440.

10. Galsky MD, Guan X, Rishipathak D, Rapaport AS, Shehata HM, Banchereau R, et al. Immunomodulatory effects and improved outcomes with cisplatin- versus carboplatin-based chemotherapy plus atezolizumab in urothelial cancer. Cell Rep Med. 2024 Feb 20;5(2):101393.

11. van der Heijden MS, Sonpavde G, Powles T, Necchi A, Burotto M, Schenker M, et al.; CheckMate 901 Trial Investigators. Nivolumab plus Gemcitabine-Cisplatin in Advanced Urothelial Carcinoma. N Engl J Med. 2023 Nov 9;389(19):1778-1789.

12. Powles T, Csőszi T, Özgüroğlu M, Matsubara N, Géczi L, Cheng SY, et al.; KEYNOTE-361 Investigators. Pembrolizumab alone or combined with chemotherapy versus chemotherapy as first-line therapy for advanced urothelial carcinoma (KEYNOTE-361): a randomised, open-label, phase 3 trial. Lancet Oncol. 2021 Jul;22(7):931-945.

13. Go, Ronald S., and Alex A. Adjei. "Review of the comparative pharmacology and clinical activity of cisplatin and carboplatin." *Journal of Clinical Oncology* 17.1 (1999): 409-409.

14. Mariathasan S, Turley SJ, Nickles D, Castiglioni A, Yuen K, Wang Y, et al. TGFβ attenuates tumour response to PD-L1 blockade by contributing to exclusion of T cells. Nature. 2018 Feb 22;554(7693):544-548.

15. Powles T, Kockx M, Rodriguez-Vida A, Duran I, Crabb SJ, Van Der Heijden MS, et al. Clinical efficacy and biomarker analysis of neoadjuvant atezolizumab in operable urothelial carcinoma in the ABACUS trial. Nat Med. 2019 Nov;25(11):1706-

1714. Erratum in: Nat Med. 2020 Jun;26(6):983. Erratum in: Nat Med. 2023 Dec;29(12):3271.

16.   Ayers M, Lunceford J, Nebozhyn M, Murphy E, Loboda A, Kaufman DR, et al. IFN-γ-related mRNA profile predicts clinical response to PD-1 blockade. J Clin Invest. 2017 Aug 1;127(8):2930-2940.

17.   van Dijk N, Gil-Jimenez A, Silina K, Hendricksen K, Smit LA, de Feijter JM, et al. Preoperative ipilimumab plus nivolumab in locoregionally advanced urothelial cancer: the NABUCCO trial. Nat Med. 2020 Dec;26(12):1839-1844.

18.   Liberzon A, Birger C, Thorvaldsdóttir H, Ghandi M, Mesirov JP, Tamayo P. The Molecular Signatures Database (MSigDB) hallmark gene set collection. Cell Syst. 2015 Dec 23;1(6):417-425.

19.   Wang L, Saci A, Szabo PM, Chasalow SD, Castillo-Martin M, Domingo-Domenech J, et al. EMT- and stroma-related gene expression and resistance to PD-1 blockade in urothelial cancer. Nat Commun. 2018 Aug 29;9(1):3503.

20.   Vos JL, Elbers JBW, Krijgsman O, Traets JJH, Qiao X, van der Leun AM, et al. Neoadjuvant immunotherapy with nivolumab and ipilimumab induces major pathological responses in patients with head and neck squamous cell carcinoma. Nat Commun. 2021 Dec 22;12(1):7348.

21.   Gil-Jimenez A, van Dijk N, Vos JL, Lubeck Y, van Montfoort ML, Peters D, et al. Spatial relationships in the urothelial and head and neck tumor microenvironment predict response to combination immune checkpoint inhibitors. bioRxiv 2023.05.25.542236.

22.   Larroquette M, Domblides C, Lefort F, Lasserre M, Quivy A, Sionneau B, et al. Combining immune checkpoint inhibitors with chemotherapy in advanced solid tumours: A review. Eur J Cancer. 2021 Oct 13;158:47-62.

23.   Bellmunt J, Hussain M, Gschwend JE, Albers P, Oudard S, Castellano D, et al.; IMvigor010 Study Group. Adjuvant atezolizumab versus observation in muscle-invasive urothelial carcinoma (IMvigor010): a multicentre, open-label, randomised, phase 3 trial. Lancet Oncol. 2021 Apr; 22(4):525-537.

24.   Wakita D, Iwai T, Harada S, Suzuki M, Yamamoto K, Sugimoto M. Cisplatin Augments Antitumor T-Cell Responses Leading to a Potent Therapeutic Effect in Combination With PD-L1 Blockade. Anticancer Res (2019) 39:1749–60.

25.   Markasz L, Skribek H, Uhlin M, Otvos R, Flaberg E, Eksborg S, et al. Effect of frequently used chemotherapeutic drugs on cytotoxic activity of human cytotoxic T-lymphocytes. J Immunother. 2008 Apr;31(3):283-93.

26.   Beyranvand Nejad E, van der Sluis TC, van Duikeren S, Yagita H, Janssen GM, van Veelen PA, et al. Tumor Eradication by Cisplatin Is Sustained by CD80/86-Mediated Costimulation of CD8+ T Cells. Cancer Res. 2016 Oct 15;76(20):6017-6029.

27.   Seiler R, Gibb EA, Wang NQ, Oo HZ, Lam HM, van Kessel KE, et al. Divergent Biological Response to Neoadjuvant Chemotherapy in Muscle-invasive Bladder Cancer. Clin Cancer Res. 2019 Aug 15;25(16):5082-5093.

28.   van Wilpe S, Sultan S, Gorris MAJ, Somford DM, Kusters-Vandevelde HVN, Koornstra RHT, et al. Intratumoral T cell depletion following neoadjuvant chemotherapy in patients with muscle-invasive bladder cancer is associated with poor clinical outcome. Cancer Immunol Immunother. 2023 Jan;72(1):137-149.

29.   Leduc C, Adam J, Louvet E, Sourisseau T, Dorvault N, Bernard M, et al. TPF induction chemotherapy increases PD-L1 expression in tumour cells and immune cells in head and neck squamous cell carcinoma. ESMO Open. 2018 Jan 9;3(1):e000257.

30.   Fukuoka E, Yamashita K, Tanaka T, Sawada R, Sugita Y, Arimoto A, et al. Neoadjuvant Chemotherapy Increases PD-L1 Expression and CD8+ Tumor-infiltrating Lymphocytes in Esophageal Squamous Cell Carcinoma. Anticancer Res. 2019 Aug;39(8):4539-4548.

31.   Jiménez-Sánchez A, Cybulska P, Mager KL, Koplev S, Cast O, Couturier DL, et al. Unraveling tumor-immune heterogeneity in advanced ovarian cancer uncovers immunogenic effect of chemotherapy. Nat Genet. 2020 Jun;52(6):582-593.

32.   Voorwerk L, Slagter M, Horlings HM, Sikorska K, van de Vijver KK, de Maaker M, et al. Immune induction strategies in

metastatic triple-negative breast cancer to enhance the sensitivity to PD-1 blockade: the TONIC trial. Nat Med. 2019 Jun;25(6):920-928.

33. Linares J, Sallent-Aragay A, Badia-Ramentol J, Recort-Bascuas A, Méndez A, Manero-Rupérez N, et al. Long-term platinum-based drug accumulation in cancer-associated fibroblasts promotes colorectal cancer progression and resistance to therapy. Nat Commun. 2023 Feb 10;14(1):746.

34. Baldominos P, Barbera-Mourelle A, Barreiro O, Huang Y, Wight A, Cho JW, et al. Quiescent cancer cells resist T cell attack by forming an immunosuppressive niche. Cell. 2022 May 12;185(10):1694-1708.e19.

35. Metropulos AE, Munshi HG, Principe DR. The difficulty in translating the preclinical success of combined TGFβ and immune checkpoint inhibition to clinical trial. EBioMedicine. 2022 Dec;86:104380.

36. Blanco B, Domínguez-Alonso C, Alvarez-Vallina L. Bispecific Immunomodulatory Antibodies for Cancer Immunotherapy. *Clin Cancer Res*. 2021; 27(20): 5457–5464.

37. Ruf P, Bauer HW, Schoberth A, Kellermann C, Lindhofer H. First time intravesically administered trifunctional antibody catumaxomab in patients with recurrent non-muscle invasive bladder cancer indicates high tolerability and local immunological activity. *Cancer Immunol Immunother*. 2021; 70(9): 2727–2735.

38. Sonpavde G, Necchi A, Gupta S, Steinberg GD, Gschwend JE, Van Der Heijden MS, et al. ENERGIZE: a Phase III study of neoadjuvant chemotherapy alone or with nivolumab with/without linrodostat mesylate for muscle-invasive bladder cancer. Future Oncol. 2020 Jan;16(2):4359-4368.

39. Kendall, M. G. (1970). Rank correlation methods (4th ed.). London: Charles Griffin & Co. Page 126.

40. Noguchi, K., Gel, Y. R., Brunner, E., & Konietschke, F. (2012). nparLD: An R Software Package for the Nonparametric Analysis of Longitudinal Data in Factorial Experiments. Journal of Statistical Software, 50(12), 1–23.

41. Mair P, Wilcox RR (2020). "Robust Statistical Methods in R Using the WRS2 Package." *Behavior Research Methods*, 52, 464–488.

4

SUPPLEMENTARY DATA
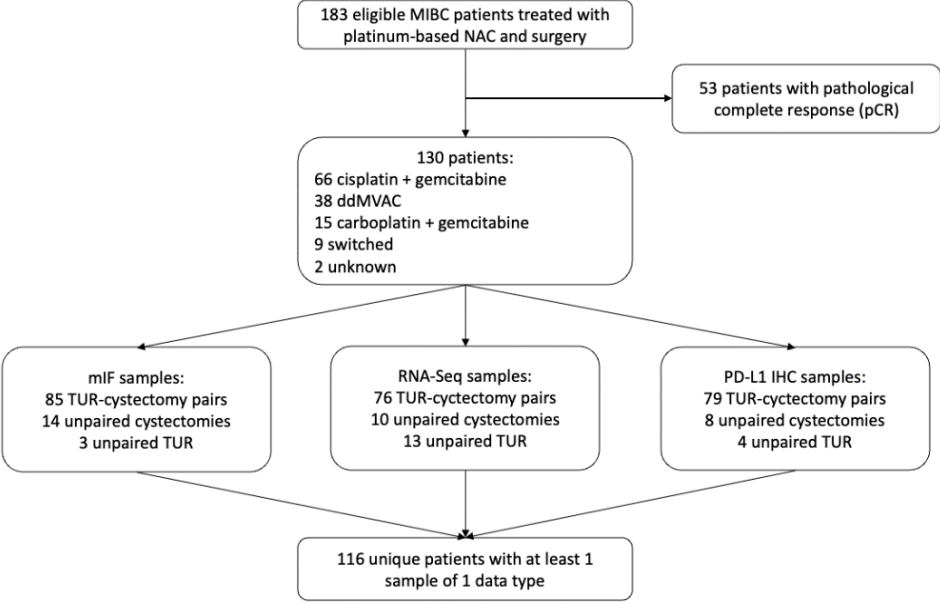
Supplementary Figure 1 | Consort diagram.
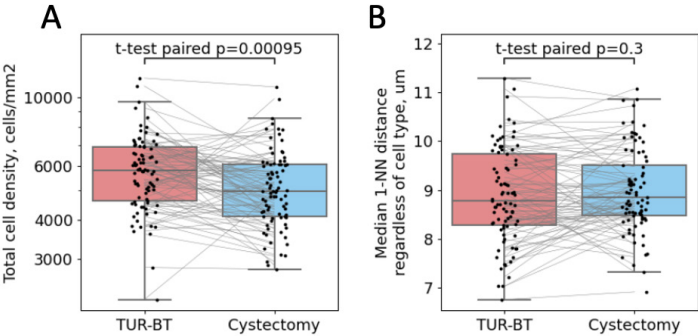
Supplementary Figure 2 | Evaluating the sample-type-related bias in the mIF data. A, Comparison of the total cell density between the sample types. **B**, Comparison of the median 1-NN distances between cells regardless of their type.
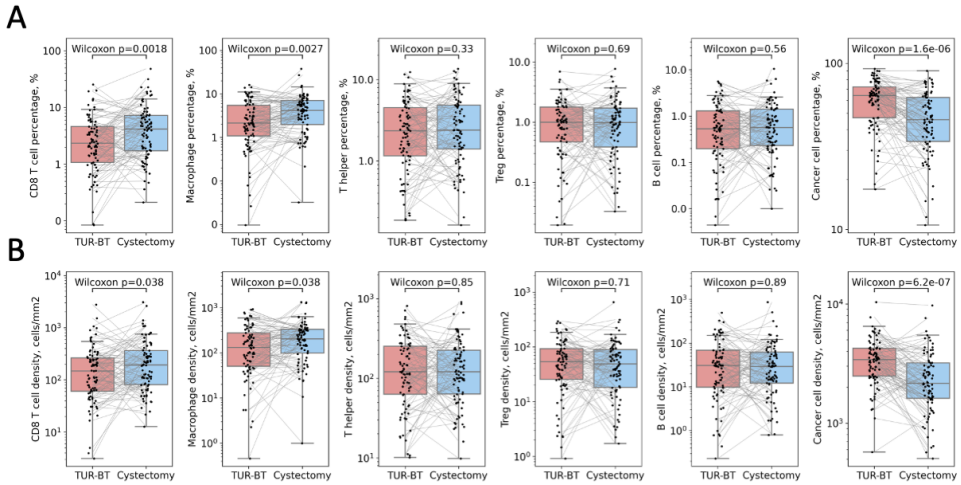
Supplementary Figure 3 | Changes in cell percentages. **A**, and cell densities **B**, associated with platinum-based chemotherapy for all cell types identified by our mIF panel (Methods).
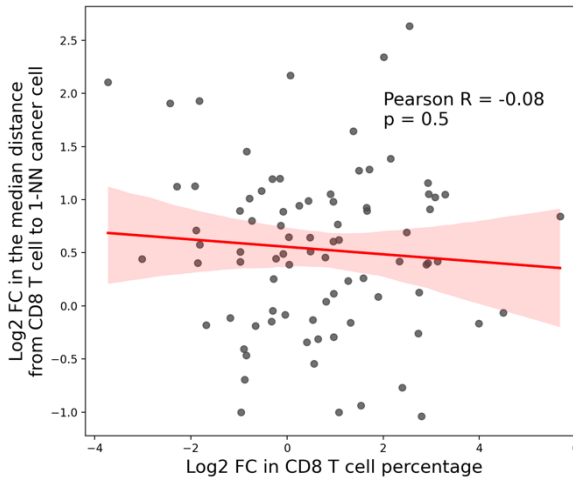
Supplementary Figure 4 | Correlation between Log2 fold changes in CD8$^+$ T cell percentage and in the median distance from CD8$^+$ T cells to their 1-NN cancer cells upon chemotherapy. One extreme distance outlier (higher than Q3 + 3IQR, where Q3 is the third quartile and IQR is the interquartile range) was excluded due to containing only two CD8$^+$ T cells.
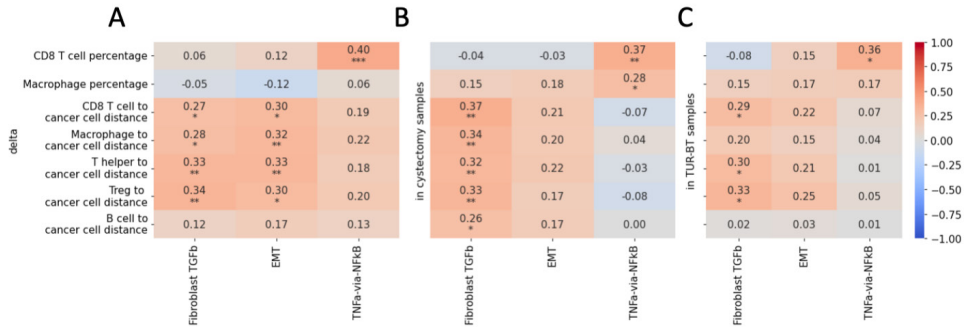
Supplementary Figure 5 | Correlation analysis of parameters altered by the chemo-treatment between different data modalities. RNA-Seq is shown on x-axis; mIF and IHC are shown on y-axis. Pearson correlation coefficients are shown. Stars denote p-values for the correlation coefficients to be non-zero assessed by the distribution of ☐ (two-sided test): $P<0.05$ (*); $P<0.01$ (**); $P<0.001$ (***). P-values are FDR-adjusted for multiple testing within each column. **A**, Correlations between changes ("deltas"). **B**, Correlations within cystectomy samples (post-treatment). **C**, Correlations within TUR-BT samples (pre-treatment).
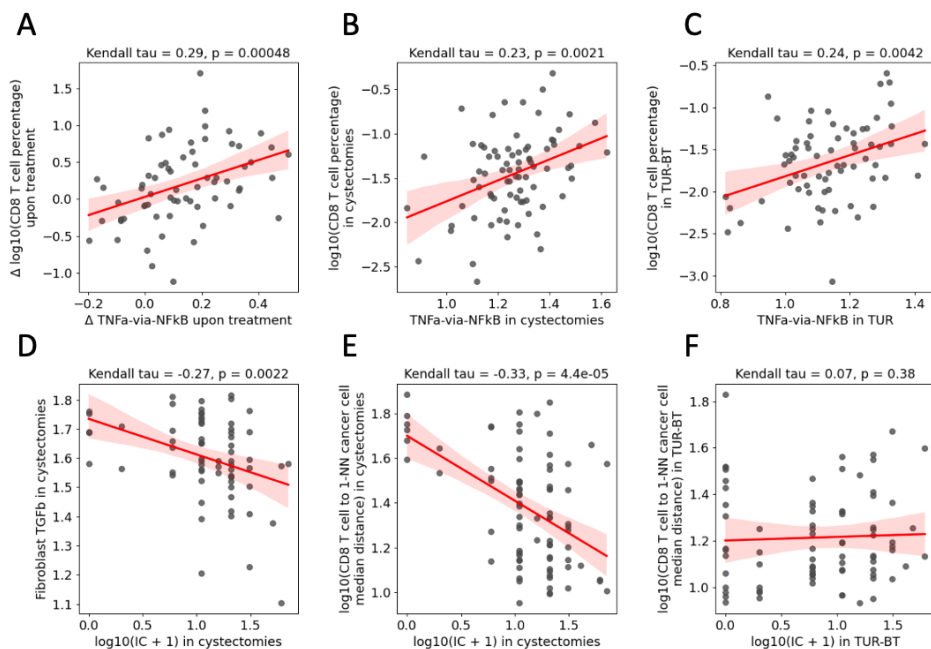
Supplementary Figure 6 | Correlations of the selected TME characteristics altered by chemo-treatment. **A-C**, Correlations between CD8 T-cell percentage (mIF) and TNFα-via-NFκB gene signature score (RNA) for changes, cystectomy samples, and TUR-BT samples. **D**, Correlation between PD-L1^{+} immune cell percentage and fibroblast-derived TGF-β signaling in cystectomy samples. **E,F**, Correlations between CD8^{+} T-cell-to-cancer-cell 1-NN median distance and PD-L1^{+} immune cell percentage for cystectomy and TUR-BT samples.

4
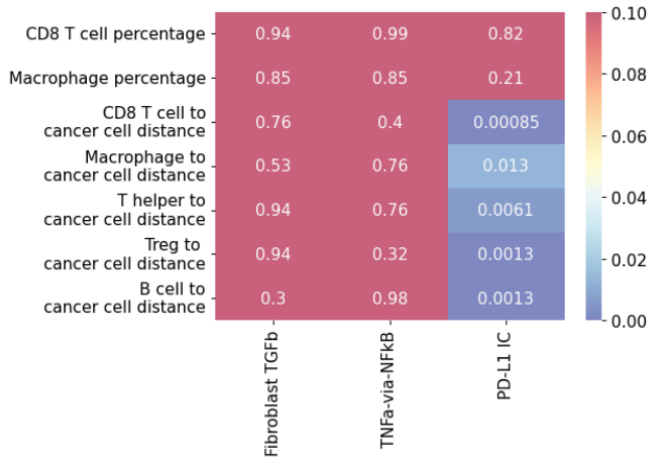
Supplementary Figure 7 | FDR-corrected p-values for comparison of Kendall ☐ correlation coefficients (Methods, Statistical analysis) between cystectomy and TUR-BT sample sets.

Target variable	CD8+ T cell fraction (mIF)	Macrophage cell fraction (mIF)	PD-L1 IC	Fibroblast-derived TGFb signaling (ssGSEA score)	CD8+ T cell to cancer cell median 1-NN distance	Macrophage to cancer cell median 1-NN distance
Method	mixed ANOVA based on the trimmed means	F1-LD-F1 non-parametric model, ANOVA	F1-LD-F1 non-parametric model, ANOVA	F1-LD-F1 non-parametric model, ANOVA	F1-LD-F1 non-parametric model, ANOVA	F1-LD-F1 non-parametric model, ANOVA
Platinum agent, p-value	0.09	0.0019	0.80	0.68	0.84	0.78
Time point, p-value	0.009	0.0069	$2.3 * 10^{-6}$	$1.6 * 10^{-9}$	$2.0*10^{-6}$	$2.6*10^{-9}$
Platinum agent: Time point, interaction p-value	0.12	0.61	0.39	0.15	0.50	0.11

Supplementary Figure 8 | Analysis of changes in the TME characteristics upon chemotherapy with cisplatin and carboplatin. P-values of mixed ANOVA or its robust analogues (depending on the violation of the default mixed ANOVA assumptions of normality, homoscedasticity, and homogeneity of covariances).

4

4

CHAPTER 5

High- or low-dose preoperative ipilimumab plus nivolumab in stage III urothelial cancer: the phase 1B NABUCCO trial

Jeroen van Dorp, Christodoulos Pipinikas, Britt B.M. Suelmann, Niven Mehra,
Nick van Dijk, Giovanni Marsico, Maurits L. van Montfoort, Sophie Hackinger, Linde M. Braaf,
Tauanne Amarante, Charlaine van Steenis, Kirsten McLay, Antonios Daletzakis,
Daan van den Broek, Maaike W. van de Kamp, Kees Hendricksen, Jeantine M. de Feijter,
Thierry N. Boellaard, Richard P. Meijer, Antoine G. van der Heijden, Nitzan Rosenfeld,
Bas W.G. van Rhijn, Greg Jones, Michiel S. van der Heijden

ABSTRACT

Cohort 1 of the phase 1B NABUCCO trial showed high pathological complete response (pCR) rates with preoperative ipilimumab plus nivolumab in stage III urothelial cancer (UC). In cohort 2, the aim was dose adjustment to optimize responses. Additionally, we report secondary endpoints including efficacy and tolerability in cohort 2, and the association of presurgical absence of circulating tumor DNA (ctDNA) in urine and plasma with clinical outcome in both cohorts. Thirty patients received two cycles of either ipilimumab 3 mg/kg plus nivolumab 1 mg/kg (cohort 2A) or ipilimumab 1 mg/kg plus nivolumab 3 mg/kg (cohort 2B), both followed by nivolumab 3 mg/kg. We observed a pCR in six (43%) patients in cohort 2A, and a pCR in one (7%) patient in cohort 2B. Absence of urinary ctDNA correlated with pCR in the bladder (ypT0Nx), but not with progression-free survival (PFS). Absence of plasma ctDNA correlated with pCR (odds ratio (OR): 45.0; 95% confidence interval (CI): 4.9-416.5) and PFS (hazard ratio (HR): 10.4; 95% CI: 2.9-37.5). Our data suggest that high-dose ipilimumab plus nivolumab is required in stage III UC and that absence of ctDNA in plasma can predict PFS. ClinicalTrials.gov registration: NCT03387761.

5

INTRODUCTION

Cisplatin-based chemotherapy followed by radical cystectomy is recommended for patients with muscle-invasive UC[1,2]. pCR (defined as ypT0N0) has been observed in 24-42% of patients and is associated with modestly improved long-term survival[2,3]. However, some patients are ineligible to receive cisplatin-based chemotherapy and the prognosis of UC patients remains poor. To improve this outlook, we have treated patients with locoregionally advanced UC (stage III; cT3-4aN0 or cT1-4aN1-3) with ipilimumab 3 mg/kg (anti-CTLA-4) plus nivolumab (anti-PD-1) in cohort 1 of the NABUCCO trial (Extended Data Fig. 1)[4]. The trial met its primary endpoint of surgical resection within 12 weeks after initiation of preoperative treatment. Moreover, we observed a pCR in eleven (46%) patients, and no residual muscle-invasive disease (ypT0/Tis/Ta/T1N0) in fourteen (58%) patients[4]. Due to immunotherapy-related adverse events, six (25%) patients missed the third treatment cycle (nivolumab 3 mg/kg), resulting in a relatively low exposure to nivolumab (one cycle of nivolumab 1 mg/kg)[4]. In other cancer types, encouraging efficacy with acceptable tolerability was observed using a lower dose of preoperative ipilimumab (1 mg/kg instead of 3 mg/kg)[5-7].

In NABUCCO cohort 2, we aimed to further optimize preoperative treatment with ipilimumab plus nivolumab in terms of efficacy and tolerability. Patients were randomized to receive either two cycles of ipilimumab 3 mg/kg plus nivolumab 1 mg/kg (cohort 2A) or two cycles of ipilimumab 1 mg/kg plus nivolumab 3 mg/kg (cohort 2B), in both cohorts followed by a third cycle of nivolumab 3 mg/kg (Extended Data Fig. 1). Similar to NABUCCO cohort 1, we included patients with cT3-4aN0 or cT1-4aN1-3 UC, who were ineligible to receive cisplatin-based chemotherapy or refused (Study Protocol in Supplementary Information)[4]. Feasibility in cohort 1 (surgery <12 weeks) was the primary endpoint of the trial[4]. Efficacy - defined as pCR rate - was a secondary endpoint of the trial and the main objective in cohort 2. Other secondary endpoints reported here include immunotherapy-related adverse events (irAEs) and the association between absence of ctDNA pre-surgery and pathological response and PFS. For biomarker purposes, patients with ypT0/Ta/Tis/T1N0 were considered responders[8].

RESULTS

Thirty patients were randomized (1:1) to cohort 2A and 2B between December 5, 2019 and April 13, 2021. Baseline characteristics can be found in Supplementary Table 1; cohort 1 patients are included for reference. Twenty-six (87%) patients received all treatment cycles; the other four (13%) patients missed one or two cycles due to irAEs. Twenty-six (87%) patients underwent radical surgery. One patient progressed on-treatment and was no longer eligible for surgery (non-responder). Three patients refused radical surgery, one of whom had a transurethral resection of the bladder and a lymph node dissection showing a nodal micrometastasis (ypTxN3). This

patient was also considered a non-responder. The two remaining patients who refused surgery were considered non-evaluable in terms of pathological response (Fig. 1a), both patients are recurrence-free after 11 and 23 months.

We observed a pCR in six (43%) evaluable patients treated with ipilimumab 3 mg/kg plus nivolumab 1 mg/kg (2A; 95% CI: 21-67%) and in one (7%) patient treated with ipilimumab 1 mg/kg plus nivolumab 3 mg/kg (2B; 95% CI: 0-34%; P=0.08; Fig. 1a-c). The pCR rate in cohort 2A was similar to cohort 1 (P=1.00; Fig. 1b,c). In contrast, the pCR rate in cohort 2B was significantly lower compared to cohort 1 (P=0.03; Fig. 1b,c). Eight (57%) patients treated with ipilimumab 3 mg/kg plus nivolumab 1 mg/kg (2A; 95% CI: 33-79%) and four (29%) patients treated with ipilimumab 1 mg/kg plus nivolumab 3 mg/kg (2B; 95% CI: 11-55%) had no residual muscle-invasive disease after surgery (ypT0/Tis/Ta/T1N0; Fig. 1a-c).

Treatment details and clinical follow-up for patients in cohort 2A and 2B (data cut-off: March 31, 2022) can be found in Extended Data Fig. 2. IrAEs were comparable to previous preoperative studies with ipilimumab plus nivolumab (Fig. 1c and Supplementary Table 2)[5-7]. Surgery was postponed in one patient due to irAEs (>12 weeks since start of therapy). Of note, the proportion of patients with a grade ≥3 irAE was significantly lower in cohort 2B (ipilimumab 1 mg/kg plus nivolumab 3 mg/kg) compared to cohort 1 (cohort 1: 58%, cohort 2B: 20%; P=0.026, two-sided Fisher's Exact test).

Radical cystectomy is a surgical procedure with significant morbidity and mortality[9]. Given the high rate of pCR after treatment with ipilimumab plus nivolumab, resection may not always be necessary and a bladder-sparing approach could be feasible in a subset of patients. However, current diagnostic tools cannot accurately predict a pathological response upon neoadjuvant therapy[10]. Recently, ctDNA in plasma was correlated with clinical outcome in MIBC patients treated with preoperative and adjuvant atezolizumab[11,12]. To evaluate the effect of preoperative treatment with ipilimumab and nivolumab in patients with locoregionally advanced MIBC, we assessed ctDNA in urine and plasma before and during therapy, and prior to surgery, using the commercially available RaDaR assay (Supplementary Fig. 1)[13].

Based on whole-exome sequencing of tumor and germline material, we identified tumor-specific genetic variants for all patients in NABUCCO cohort 1 (n=24) and isolated cell-free DNA from plasma and urine samples (Extended Data Fig. 3, Supplementary Table 3-6 and Methods)[13]. The mean estimated variant allele frequency (eVAF%) in urine was not statistically different between responders (ypT0/Tis/Ta/T1N0) and non-responders (≥ypT2 or N+) at any time point (Extended Data Fig. 4a)[8]. We observed no correlation between absence of ctDNA in urine prior to surgery and pathological response (P=0.39; Extended Data Fig. 4a-c). When comparing patients with and without a pCR in the bladder (ypT0Nx) specifically, we observed a correlation with absence of urinary ctDNA prior to surgery (P<0.01; Extended Data Fig. 4a-c). As some patients with absence of urinary ctDNA prior to surgery had ypT0N+ disease, there was no correlation with pCR (ypT0N0;

P=0.08) or clinical outcome (Extended Data Fig. 4b-d and 5), making urinary ctDNA a suboptimal biomarker for clinical decision-making.

Figure 1 | Treatment and response details for patients in cohort 2. a, Patient details for cohort 2A and 2B. Patients are organized based on response. cTNM-stage before treatment and ypTNM-stage after surgery are shown above and below the plot, respectively. **b,** Bar chart showing pathological responses for all cohorts. Cohort 1 vs 2A: P=1.00; cohort 1 vs 2B: P=0.03; cohort 2A vs 2B: P=0.08. P-values: two-sided Fisher's Exact test comparing pCR rate (ypT0N0) between cohorts. **c,** Table showing pathological responses for evaluable patients and immunotherapy-related adverse events. *Ipi: ipilimumab, Nivo: nivolumab, TURBT: transurethral resection of the bladder tumor, LND: lymph node dissection.*
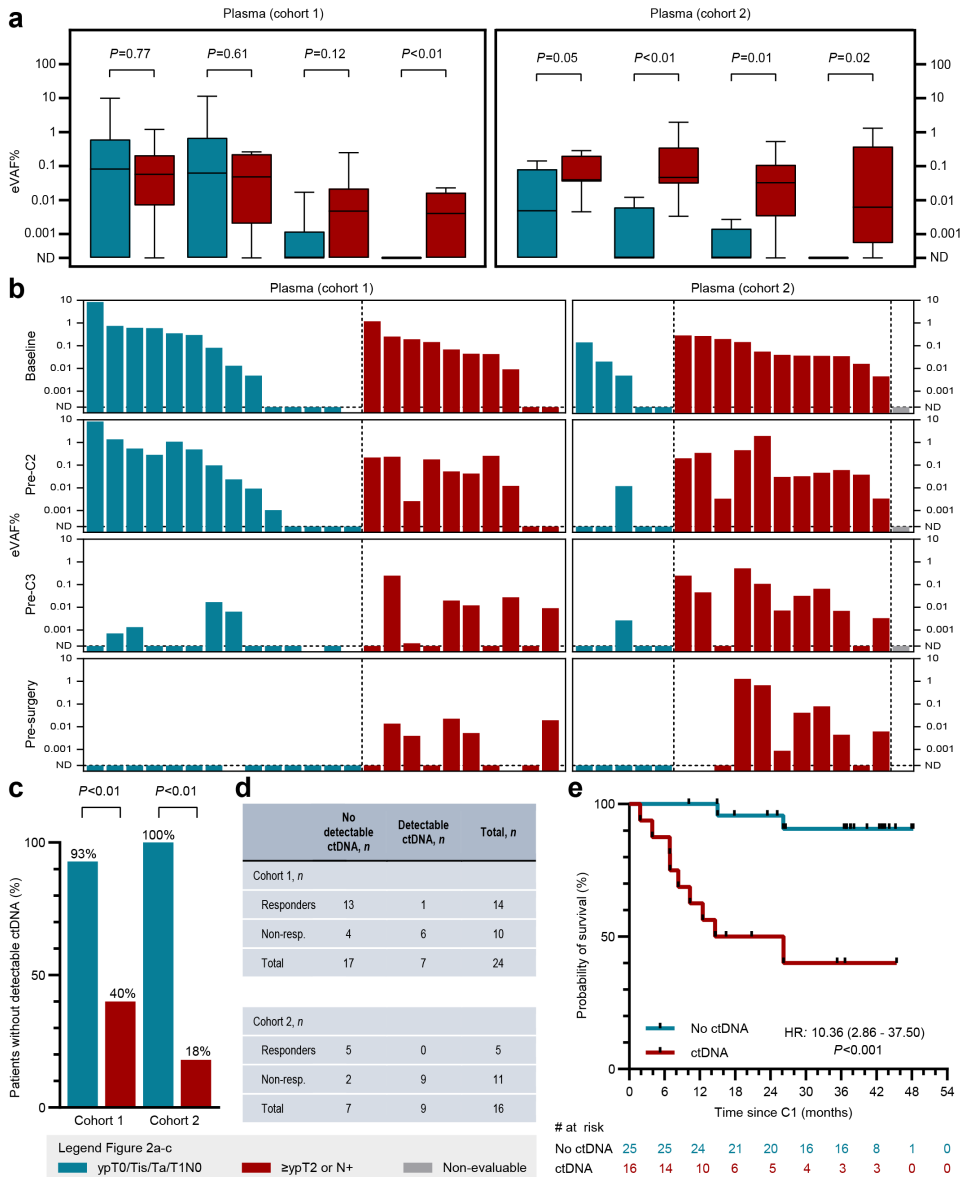
In plasma, the mean eVAF% was not statistically different between responders and non-responders at baseline. We observed a significantly lower mean plasma eVAF% prior to surgery in responders compared to non-responders (P<0.01; Fig. 2a). ctDNA was not detectable in the latest available plasma sample prior to surgery in thirteen (93%) responders and in four (40%) non-responders (P<0.01; Fig. 2b-d). To validate these observations, we also assessed plasma ctDNA collected from patients treated in the Netherlands Cancer Institute in cohort 2A and 2B (n=17; Supplementary Table 3-6 and Extended Data Fig. 6). CtDNA was not detectable in plasma prior to surgery in five (100%) responders and in two (18%) non-responders (P<0.01; Fig. 2b-d) showing a similar correlation between absence of ctDNA in plasma prior to surgery and pathological response as observed in cohort 1. Taken together, the OR for cohort 1+2 combined was 45.0 (95% CI: 4.9-416.5; Fig. 2b-d). Finally, we analyzed PFS for patients (n=24+17) with and without detectable ctDNA in the latest available plasma sample. We observed a strong association between absence of ctDNA and PFS (HR: 10.4; 95% CI: 2.9-37.5; Fig. 2e and Extended Data Fig. 5).

DISCUSSION

There are several limitations to our findings. Most importantly, the sample size was relatively small. Although the response rate was significantly different between cohort 1 and cohort 2B, suggesting a difference in pCR between high and low ipilimumab schedules, we could not show a statistical difference in response rates between cohort 2A and 2B. Still, given the magnitude of the difference in pCR rate between the cohorts and the results of the CheckMate-032 trial, favoring ipilimumab 3 mg/kg plus nivolumab over ipilimumab 1 mg/kg plus nivolumab in the metastatic setting[14], we decided against a further expansion of our study. Ultimately, the efficacy of preoperative ipilimumab 3 mg/kg in combination with nivolumab in urothelial cancer will need to be confirmed in a randomized trial. The underlying biological mechanism of the context-dependent dose-response association for anti-CTLA-4 therapy is currently unknown.

The precise value of urinary ctDNA as a biomarker for response was not fully addressed in our study, as it was assessed in a limited number of samples (only cohort 1). Whereas our results suggest absence of urinary ctDNA after preoperative therapy is unable to accurately predict PFS or OS, it may provide a useful biomarker to assess bladder-specific pCR (ypT0). Interestingly, some patients having a pCR in the bladder still had detectable urinary ctDNA, which could potentially be derived from residual non-viable tumor tissue. Assessment of ctDNA in plasma and urine in larger studies, including later time points, may provide additional granularity on ctDNA dynamics and help to build personalized strategies to de-escalate

a

Plasma (cohort 1)

Plasma (cohort 2)

b

Plasma (cohort 1)

Plasma (cohort 2)

c

d

	No detectable ctDNA, n	Detectable ctDNA, n	Total, n
Cohort 1, n			
Responders	13	1	14
Non-resp.	4	6	10
Total	17	7	24
Cohort 2, n			
Responders	5	0	5
Non-resp.	2	9	11
Total	7	9	16

e

HR: 10.36 (2.86 - 37.50)
$P<0.001$

at risk

No ctDNA	25	25	24	21	20	16	16	8	1	0
ctDNA	16	14	10	6	5	4	3	3	0	0

Legend Figure 2a-c
ypT0/Tis/Ta/T1N0   ≥ypT2 or N+   Non-evaluable

5

Figure 2 | ctDNA assessment in plasma and relation to outcome. a-c, Data for patients in cohort 1 (left, *n*=24) and cohort 2 (right, *n*=17). Blue bars: responders (ypT0/Tis/Ta/T1N0), red bars: non-responders (≥ypT2 and/or N+), grey bars: non-evaluable patients, missing bars: missing samples. Non-evaluable patients were excluded in responders versus non-responders comparisons. Undetectable values are plotted as 0.0002. **a,** Mean eVAF% in plasma for responders and non-responders before (cohort 1: *P*=0.77; cohort 2: *P*=0.05) and during treatment, and pre-surgery (cohort 1: *P*<0.01; cohort 2: *P*=0.02). Boxplots show median value and 25th and 75th percentiles. Whiskers show minimum/maximum values. *P*-values: two-sided Mann-Whitney test. **b,** Individual eVAF% in plasma before and during treatment, and pre-surgery. **c,** Percentage of patients with no detectable ctDNA in latest available plasma sample pre-surgery for responders and non-responders per cohort. Cohort 1: *P*<0.01; cohort 2: *P*<0.01. *P*-values: two-sided Fisher's Exact test comparing patients with detectable ctDNA pre-surgery in responders to non-responders for cohort 1 and 2 separately. **d,** Number of

patients with and without detectable ctDNA in latest available plasma sample pre-surgery for responders and non-responders per cohort. **e,** Progression-free survival for patients with and without detectable ctDNA in latest available plasma sample pre-surgery. Hazard ratio: 10.36; 95% confidence interval: 2.86-37.50; *P*<0.001 using a two-sided Log-rank (Mantel-Cox) test. *ND: not detectable, Pre-C2/3: prior to second/third treatment cycle.*

UC treatment. Clinical strategies could include a wait-and-see approach with longitudinal ctDNA monitoring in patients having absence of ctDNA in both plasma and urine after preoperative therapy.

In conclusion, we confirmed in an independent cohort that preoperative treatment with ipilimumab 3 mg/kg - in combination with nivolumab - leads to high pCR rates in stage III UC, whereas ipilimumab 1 mg/kg appeared less effective. The absence of pre-surgery ctDNA in plasma predicts pathological response and PFS and could potentially guide clinical decision-making to select patients for bladder-sparing strategies after treatment with ipilimumab plus nivolumab. The ongoing INDIBLADE trial (ClinicalTrials.gov registration: NCT05200988) will assess the efficacy of preoperative ipilimumab plus nivolumab followed by chemoradiation therapy as a bladder-sparing strategy.

REFERENCES

1. Witjes, J.A., *et al.* European Association of Urology Guidelines on Muscle-invasive and Metastatic Bladder Cancer: Summary of the 2020 Guidelines. *Eur Urol* 79, 82-104 (2021).

2. Advanced Bladder Cancer Meta-analysis, C. Neoadjuvant chemotherapy in invasive bladder cancer: update of a systematic review and meta-analysis of individual patient data advanced bladder cancer (ABC) meta-analysis collaboration. *Eur Urol* 48, 202-205; discussion 205-206 (2005).

3. Pfister, C., *et al.* Randomized Phase III Trial of Dose-dense Methotrexate, Vinblastine, Doxorubicin, and Cisplatin, or Gemcitabine and Cisplatin as Perioperative Chemotherapy for Patients with Muscle-invasive Bladder Cancer. Analysis of the GETUG/AFU V05 VESPER Trial Secondary Endpoints: Chemotherapy Toxicity and Pathological Responses. *Eur Urol* 79, 214-221 (2021).

4. van Dijk, N., *et al.* Preoperative ipilimumab plus nivolumab in locoregionally advanced urothelial cancer: the NABUCCO trial. *Nat Med* 26, 1839-1844 (2020).

5. Rozeman, E.A., *et al.* Identification of the optimal combination dosing schedule of neoadjuvant ipilimumab plus nivolumab in macroscopic stage III melanoma (OpACIN-neo): a multicentre, phase 2, randomised, controlled trial. *Lancet Oncol* 20, 948-960 (2019).

6. Chalabi, M., *et al.* Neoadjuvant immunotherapy leads to pathological responses in MMR-proficient and MMR-deficient early-stage colon cancers. *Nat Med* 26, 566-576 (2020).

7. Vos, J.L., *et al.* Neoadjuvant immunotherapy with nivolumab and ipilimumab induces major pathological responses in patients with head and neck squamous cell carcinoma. *Nat Commun* 12, 7348 (2021).

8. Rosenblatt, R., *et al.* Pathologic downstaging is a surrogate marker for efficacy and increased survival following neoadjuvant chemotherapy and radical cystectomy for muscle-invasive urothelial bladder cancer. *Eur Urol* 61, 1229-1238 (2012).

9. Stimson, C.J., *et al.* Early and late perioperative outcomes following radical cystectomy: 90-day readmissions, morbidity and mortality in a contemporary series. *J Urol* 184, 1296-1300 (2010).

10. Becker, R.E.N., *et al.* Clinical Restaging and Tumor Sequencing are Inaccurate Indicators of Response to Neoadjuvant Chemotherapy for Muscle-invasive Bladder Cancer. *Eur Urol* 79, 364-371 (2021).

11. Powles, T., *et al.* ctDNA guiding adjuvant immunotherapy in urothelial carcinoma. *Nature* 595, 432-437 (2021).

12. Szabados, B., *et al.* Final Results of Neoadjuvant Atezolizumab in Cisplatin-ineligible Patients with Muscle-invasive Urothelial Cancer of the Bladder. *Eur Urol* 82, 212-222 (2022).

13. Flach, S., *et al.* Liquid BIOpsy for MiNimal RESidual DiSease Detection in Head and Neck Squamous Cell Carcinoma (LIONESS)-a personalised circulating tumour DNA analysis in head and neck squamous cell carcinoma. *Br J Cancer* 126, 1186-1195 (2022).

14. Sharma, P., *et al.* Nivolumab Alone and With Ipilimumab in Previously Treated Metastatic Urothelial Carcinoma: CheckMate 032 Nivolumab 1 mg/kg Plus Ipilimumab 3 mg/kg Expansion Cohort Results. *J Clin Oncol* 37, 1608-1616 (2019).

METHODS

Study design and population

NABUCCO (ClinicalTrials.gov: NCT03387761) is a multicenter investigator-initiated, prospective phase 1B trial which was conducted in two subsequent phases. In the first phase (NABUCCO cohort 1) 24 patients with resectable locoregionally advanced urothelial cancer (UC; stage III; cT3-4aN0 or cT1-4aN1-3) were enrolled at the Netherlands Cancer Institute and treated with preoperative ipilimumab 3 mg/kg (day 1), ipilimumab 3 mg/kg plus nivolumab 1 mg/kg (day 22) and nivolumab 3 mg/kg (day 43), followed by cystectomy or nephroureterectomy with lymph node dissection[4]. In the second phase (NABUCCO cohort 2A and 2B) 30 patients with resectable locoregionally advanced UC were enrolled at the Netherlands Cancer Institute, the University Medical Center Utrecht and the Radboud University Medical Center between December 5, 2019 and April 13, 2021. Patients were randomized (1:1, open-label) and treated with either (2A) ipilimumab 3 mg/kg plus nivolumab 1 mg/kg (day 1 and 22) and nivolumab 3 mg/kg (day 43), or (2B) ipilimumab 1 mg/kg plus nivolumab 3 mg/kg (day 1 and 22) and nivolumab 3 mg/kg (day 43), both followed by cystectomy or nephroureterectomy with appropriate lymph node dissection (Extended Data Fig. 1). Disease staging was performed according to American Joint Committee on Cancer guidelines. Patients were ≥18 years of age and were either ineligible for cisplatin or refused cisplatin-based chemotherapy, have not received prior treatment with anti-CTLA-4, anti-PD-1 or anti-PD-L1 agents, had a World Health Organization performance score of 0–1, and had diagnostic transurethral resection bladder tumor (TURBT) blocks available (or other baseline tumor material in case of upper tract tumors). Key exclusion criteria included documented severe autoimmune disease, chronic infectious disease and use of systemic immunosuppressive medications. All patients provided written informed consent. No financial compensation was offered to patients except to cover travel expenses to and from the hospital. Surgery was scheduled in weeks 9–12 from the first drug infusion. Baseline staging was based on diagnostic pathology and thorax/abdomen/pelvis computed tomography (CT). CT-based response assessment occurred in weeks 8–10. Additional baseline and on-treatment pelvic magnetic resonance imaging (MRI) assessment was optional. All adverse events and immunotherapy-related adverse events were graded and reported throughout the study according to CTCAE v5.0. The sponsor of the trial was the Netherlands Cancer Institute. Bristol-Myers Squibb provided the study drugs and funding for the trial (CA209-9Y4). The trial is part of the Dutch Uro-Oncology Study Group. A data safety monitoring board was established, consisting of Thomas Powles (medical oncologist, Barts Cancer Centre) and Joost Boormans (urologist, Erasmus Medical Centre). This study was approved by the institutional review board (IRB) of the Netherlands Cancer Institute (METC-AVL, currently named NedMEC) and was executed in accordance with the protocols and Good Clinical Practice Guidelines defined by the International Conference on Harmonization and the principles of the Declaration of Helsinki. For more information, refer to the study protocol (Study Protocol in Supplementary Information).

CLINICAL DATA ACQUISITION AND INTERPRETATION

Clinical data was collected in electronic Case Report Forms (eCRF) using Tenalea (version 18.1) at the Netherlands Cancer Institute, University Medical Center Utrecht and Raboud University Medical Center and further processed and analyzed in the Netherlands Cancer Institute. Clinical follow-up visits were planned for all patients at 1, 4 and 8 weeks after surgery. CT-scans and follow-up visits were planned according to local protocol but at a minimum included CT scans 12 and 24 months after surgery. The date of the first treatment cycle (C1) was used as date of reference to determine progression-free and overall survival. Data cut-off was done on March 31, 2022. All eligible patients were contacted prior to this date and last date of contact was used as date of reference to determine progression-free and overall survival. Progression was defined as the first evident sign of recurrence of disease through clinical, radiological and/or pathological assessment. Patients who were alive and had no evident signs of progression were censored on the last day of contact before the data cut-off date for progression-free and overall survival analysis. All deceased patients - regardless of cause of death - were considered an event for overall survival analysis and were censored on the date of death for progression-free survival analysis if there were no evident signs of progression.

DNA ISOLATION AND SEQUENCING

TURBT, cystectomy and/or nephroureterectomy material was stored as formalin-fixed, paraffin embedded (FFPE) tissue blocks in The Netherlands Cancer Institute after surgery. Additional tumor material from participating hospitals was requested as FFPE tissue blocks or as cut slides from University Medical Center Utrecht, Radboud University Medical Center or other referring hospitals.

Tumor area and tumor cell percentage for every specimen was assessed by a trained pathologist. DNA was isolated from baseline tumor material (5-10x 10 µm slides) using the AllPrep FFPE DNA/RNA Kit (Qiagen), using the QIAcube according to manufacturer's protocol. Germline DNA was extracted from peripheral blood mononuclear cells from every patient prior to start of treatment (baseline) using the QIAsymphony DSP DNA Midi kit (Qiagen). DNA sequencing was carried out following the Human IDT Exome Target Enrichment Protocol. Covaris shearing was used to fragment the DNA to 200–300 base pairs. KAPA Hyper DNA Library Kit (KAPA Biosystems) was used for library preparation. IDT Human Exome capture v2.0 (xGen Exome Research Panel v2.0) was used for exome enrichment. Libraries were sequenced with 100 base pairs paired-end reads using the Novaseq 6000 (Illumina) with a high output mode PE 100.

RAW TUMOR DNA SEQUENCING DATA ANALYSIS

Raw whole exome sequencing (WES) data were transferred to Inivata as BAM files and converted to FASTQ file format. A custom analytical pipeline based on the GATK best practices was used to process the FASTQ files by first aligning the sequencing reads to the human genome (hg38) using bwa mem (version 0.7.17) and marking duplicates by Picard (version 2.23.8), followed by a

proprietary algorithm performing somatic variant calling. Germline variants were removed using information available from public single nucleotide polymorphism (SNP) databases and variants were filtered and prioritized based on multiple parameters including allele frequency and depth. Patient WES data were subjected to full quality control by assessing key sequencing metrics (Supplementary Table 4). A matched germline genomic DNA sample available from all patients was also subjected to WES to ensure that germline variants were filtered out. The median read depth per sample based on usable (i.e. not duplicated, on-target) reads was 72 (range: 8-107) for tumor WES compared to a median of 71 (range: 46-113) for germline WES. The estimated purity of the tumor material was a median fraction of 0.41 (range: 0.18-0.70).

RADAR PATIENT-SPECIFIC ASSAY DESIGN AND PANEL QUALIFICATION

RaDaR is a multiplex PCR, next generation sequencing (NGS) liquid biopsy assay built on the InVision® platform[15] that uses a tumor-informed approach for the sensitive detection of circulating tumor DNA (ctDNA) in a patient's blood circulation. Refer to the paragraph below (*RaDaR assay analytical validation*) for more details. Tumor WES-derived somatic variants (single nucleotide variants (SNPs) and indels) were prioritized using a proprietary algorithm to build patient-specific primer panels of up to 48 primer pairs each capturing at least one somatic variant. Variant prioritization and selection criteria take into consideration the variant set most suitable for the sensitive detection of plasma ctDNA in the patient for whom the assay was designed for as well as ensuring that the selected primer pairs are well suited for multiplex PCR allowing the efficient amplification of the target ctDNA. Each designed RaDaR panel was synthesized (Integrated DNA Technologies, Coralville, IA) and combined with a fixed primer panel of common population-specific SNPs for quality control purposes during the NGS testing. Panel qualification involved NGS testing of a reference DNA standard, a negative amplification control and FFPE tumor tissue DNA on iSeq100 (Illumina). Panels with 8 or more tumor-confirmed variants detected at sufficient read depth were considered as qualified. RaDaR is an US, EU and UK registered trademark of Inivata, Ltd.

PLASMA AND URINE COLLECTION AND PROCESSING

Serial blood samples (*n*=159) from 41 patients were collected by standard phlebotomy techniques in 2x10mL K2-EDTA tubes from up to 4 different time points, namely prior to start of treatment (day 1, baseline), prior to each subsequent treatment cycle (day 22 and 43) and prior to surgery. Blood samples were processed to plasma within two hours after collection with an initial centrifugation at 380x g for 20 min followed by a second centrifugation of isolated plasma aliquots at 20,000x g for 10 min to remove any remaining cellular debris and stored at -80 °C. Urine samples (*n*=93) were collected together with plasma samples for patients in cohort 1 (*n*=24). Urine samples were spun down to remove any cells and cellular debris processed at 380x g for 20 min and stored at -80 °C.

CFDNA EXTRACTION AND QUANTIFICATION

Plasma and urine samples were sent to Inivata (Cambridge, UK) for further processing and

analysis. Cell-free DNA (cfDNA) was isolated from 3-4 mL plasma using a solid phase reverse immobilization magnetic bead protocol on a Hamilton Microlab STAR automated platform. A *no-template* control sample was included in each extraction batch to monitor for contamination. cfDNA was isolated from 8 mL urine supernatant using the QIAsymphony SP protocol following the manufacturer's instructions (Qiagen). The isolated cfDNA was quantified on a QX200 ddPCR system (BioRad, Hercules, CA) using a custom 108 bp digital droplet PCR assay (ddPCR) measuring the amplification of the RPP30 gene (ribonuclease P/MRP subunit P30). The primers and probes used were as follows:

- Forward = 5'-GGAGGTGGAGGAGGAGGATA-3';
- Reverse = 5'-ACGGAATACAGAACCCATGACT-3';
- Probe = 5'-FAM/AGCCTTGAG/ZEN/ AGACGAGAACCTGT/IABkF Q-3'[16].

CFDNA RADAR PROFILING

Following panel qualification, personalized RaDaR assays were used in multiplex PCR amplification of plasma and urine cfDNA. For plasma, median input as measured by ddPCR was 6,900 amplifiable copies per sample (range: 2,000 to 20,224 copies). For urine, median input was 20,020 amplifiable copies per sample (range: 200-25,224). In plasma, sequencing depth was a median value of 241,930 reads per variant per sample (range: 81,661 to 1,506,623) and a total median of 11,743,870 reads per sample across all variants (range: 4,001,393 to 72,317,915). In urine, sequencing depth was a median value of 238,805 reads per variant per sample (range: 874 to 953,341) and a total median of 11,512,230 reads per sample across all variants (range: 37,594 to 46,713,722). Control DNA was also tested to ensure that germline variants and confounding signals derived from age-related CHIP somatic variants (clonal hematopoiesis of indeterminate potential) were filtered out. The amplicon products were then barcoded and the resulting libraries were pooled, combined with PhiX and subjected to ultra-deep sequencing on the Illumina NovaSeq 6000 platform (Illumina Inc., San Diego, USA) to allow sensitive detection of low ctDNA levels.

RADAR DATA ANALYSIS, VARIANT FILTERING AND CTDNA STATUS CALLING

RaDaR data were analyzed in a multistep process. Raw sequencing base calls were converted to FASTQ format and then demultiplexed using bcl2fastq2 (version 2.20) before being aligned to the human reference genome using bwa mem. Proprietary software was used to identify primer pairs and count mutant and reference bases for each variant. Individual variants were subjected to strict quality control and only those detected in the tumor DNA sequencing but absent in the control genomic DNA sequencing using the RaDaR panel were considered in the process of calling plasma samples ctDNA positive or negative. Variants absent in tumor DNA when tested with the personalized panel were filtered as these are typically WES false positives or variants that have failed to amplify, sequence or align to the target region. The median number of tumor confirmed variants was 47 (range: 18 to 51), corresponding to a median of 98% confirmed variants (range: 35%-100%), with 83% of samples having at least 40 confirmed variants (Supplementary Table 4 and 6).

To obtain evidence for the presence or absence of ctDNA at the sample level, the statistical significance of the observed mutant counts for each of the remaining variants was assessed using a statistical framework incorporating the entire set of personalized variants passing the above filter. This framework compared the sequencing counts of each variant to a model of noise for each individual variant and was locked prior to the analyses described in this study. A sample was classified as "ctDNA positive" when its cumulative statistical score was above a pre-set threshold defined during the assay's analytical development and validation of the locked assay[13]. Refer to the paragraph below (*RaDaR assay analytical validation*) for more details. Further in-depth details of the statistical model to determine the ctDNA status of each sample, the pre-set statistical thresholds and the process of calculating the estimated variant allele frequency are all core part of the proprietary code and fully IP-protected and as such cannot be disclosed.

The tumor fraction for each sample was estimated and reported as the "estimated variant allele frequency" (eVAF; Supplementary Table 5). The estimated 95% limit of detection (LoD95, column "Est. lod" in Supplementary Table 5) for each sample has been assessed using linear interpolation of pre-tabulated assay validation data for 2,000 and 20,000 input copies for different number of variants: the estimated LoD per sample had a median value of 57 ppm (0.0057%) and a range of 11.4 to 120 ppm (0.0011 to 0.0120 %). In this study, plasma detection and quantification of these variants by RaDaR was used as a proxy to assess ctDNA dynamics during preoperative treatment and evaluate response to treatment and correlation with progression-free survival.

RADAR ASSAY ANALYTICAL VALIDATION

The RaDaR assay was analytically validated in Inivata's CLIA laboratory (RTP, North Carolina) by trained operators. Personalized RaDaR assays were designed and synthesized for 5 lung cancer patient samples and 2 breast cancer (HCC1395 & HCC1954) and 1 colon cancer (SW480) cell lines. The lung cancer patients were part of the INI-001 study (ClinicalTrials.gov: NCT02906852). All patients had had ctDNA previously detected in their blood using InVisionFirst-Lung®. To determine analytical specificity, the 8 personalized RaDaR panels were tested against 69 blood samples from 18 healthy donors drawn into Streck cfDNA blood collection tubes. No calls were made in any of the 69 samples. A further 20 blood samples from 5 of the same healthy donors were drawn into EDTA tubes and run against the breast and colon cancer cell line RaDaR assays and again no calls were made, thereby demonstrating 100% specificity (Supplementary Fig. 1a).

LoD of the RaDaR assay was tested using the two breast cancer and one colon cancer cell lines. Cell line-derived DNA was diluted into normal DNA to produce contrived samples mimicking ctDNA at a range of levels near the target LoD of the RaDaR assay. To achieve this, each of the cell lines along with normal DNA from the Genome in a Bottle sample NA12878 was sheared to approximately 160 bp in length to mimic cfDNA fragmentation. NA12878 was selected as it has been extensively characterized with other sequencing methods. The fragmented DNA was quantified in copies per microliter by digital PCR (copies/µl) to enable accurate dilution. DNA was then serially diluted into

normal DNA samples from 0.008%, 0.004%, 0.002% to 0.001% variant allele fraction respectively. Each cell line dilution was analyzed in duplicate on 5 separate runs using 20,000 amplifiable copies of the genome as measured by digital PCR. The runs were performed by two operators with two reagent lots (Supplementary Fig. 1b). In total, each dilution was assessed 30 times (10 replicates of each cell line). Sensitivity of the RaDaR assay was measured using Probit-based analysis. Using this approach, the LoD95 (the limit where 95% of samples are detected) of the RaDaR assay is 0.0011% variant allele fraction. Good reproducibility was also observed between runs, operators, and reagent lots.

To assess the impact of the number of available variants on the LoD, results from the cell line dilution study were randomly sub-sampled (bootstrapped) removing different numbers of variants before calling. As the number of variants decreases, the sensitivity decreased in a predictable fashion (Supplementary Fig. 1c). For example, the LoD with 48 variants (0.0011%) is close to half the LoD when using half the number of variants (24 variant LoD95 = 0.0023%). This showed that targeting 48 variants improves sensitivity of the RaDaR assay. Furthermore, this demonstrated that in instances where less than 48 variants are available, the assay is still very sensitive, and this sensitivity is predictable based on the number of variants.

STATISTICAL ANALYSIS

Information on statistical methodology related to individual figure panels can be found in the corresponding figure legends. General statistical methodology is discussed in this subsection. The interpretation of the secondary endpoint of pCR in cohort 2 was mainly exploratory to support further expansion or a randomized trial. Nevertheless, a power calculation was done to support patient numbers. We assumed a comparator pCR rate for chemotherapy of 21% in this population. Based on the results in cohort 1, we presumed a target of 55% pCR for cohort 2A and 2B, which is higher than the observed pCR rate in cohort 1, as we hypothesized that introducing both ipilimumab and nivolumab from the start of treatment may increase response rates. With 15 patients per treatment arm, cohort 2A and 2B would have a power of 82% to exclude a pCR rate of 21%, with a two-sided alpha of 0.05. All 95% confidence intervals for pCR rate for the separate cohorts were calculated by modified Wald method. ctDNA measurements shown in Figure 2 and Extended Data Fig. 4 are based on a single measurement per time point per patient, as described in the RaDaR sequencing analysis subheading. All statistical tests described are two-sided. No corrections for multiple hypothesis testing have been conducted. No tests for normality of data were performed. Statistical tests were performed using R (version 4.2.0) and GraphPad Prism (version 9.0.2).

METHODS REFERENCES

15.   Plagnol, V., *et al.* Analytical validation of a next generation sequencing liquid biopsy assay for high sensitivity broad molecular profiling. *PLoS One* **13**, e0193802 (2018).
16.   Gale, D., *et al.* Development of a highly sensitive liquid biopsy platform to detect clinically-relevant cancer mutations at low allele fractions in cell-free DNA. *PLoS One* **13**, e0194630 (2018).
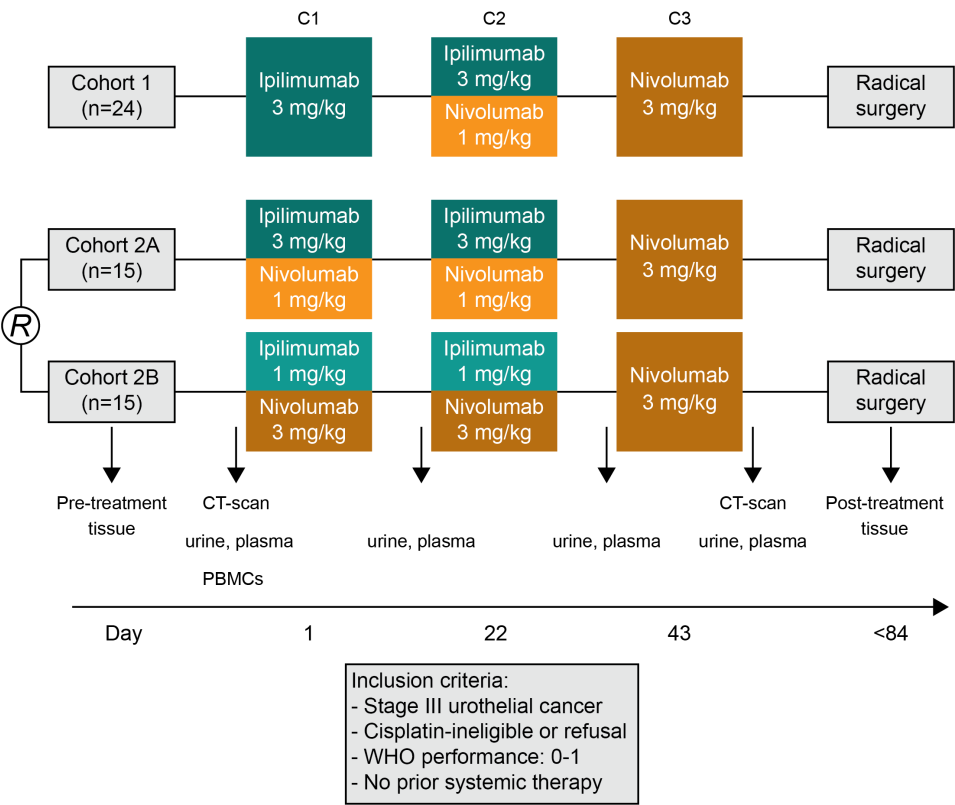
Extended Data Figure 1 | NABUCCO study design. Cohort 1 is shown at the top, cohort 2A and cohort 2B are shown at the bottom. Arrows correspond with timing of study procedures and apply to all cohorts. Peripheral blood mononuclear cells (PBMCs), urine and plasma samples were collected <24 hours prior to corresponding treatment cycle or radical surgery. *C1/2/3: first, second and third treatment cycle.*
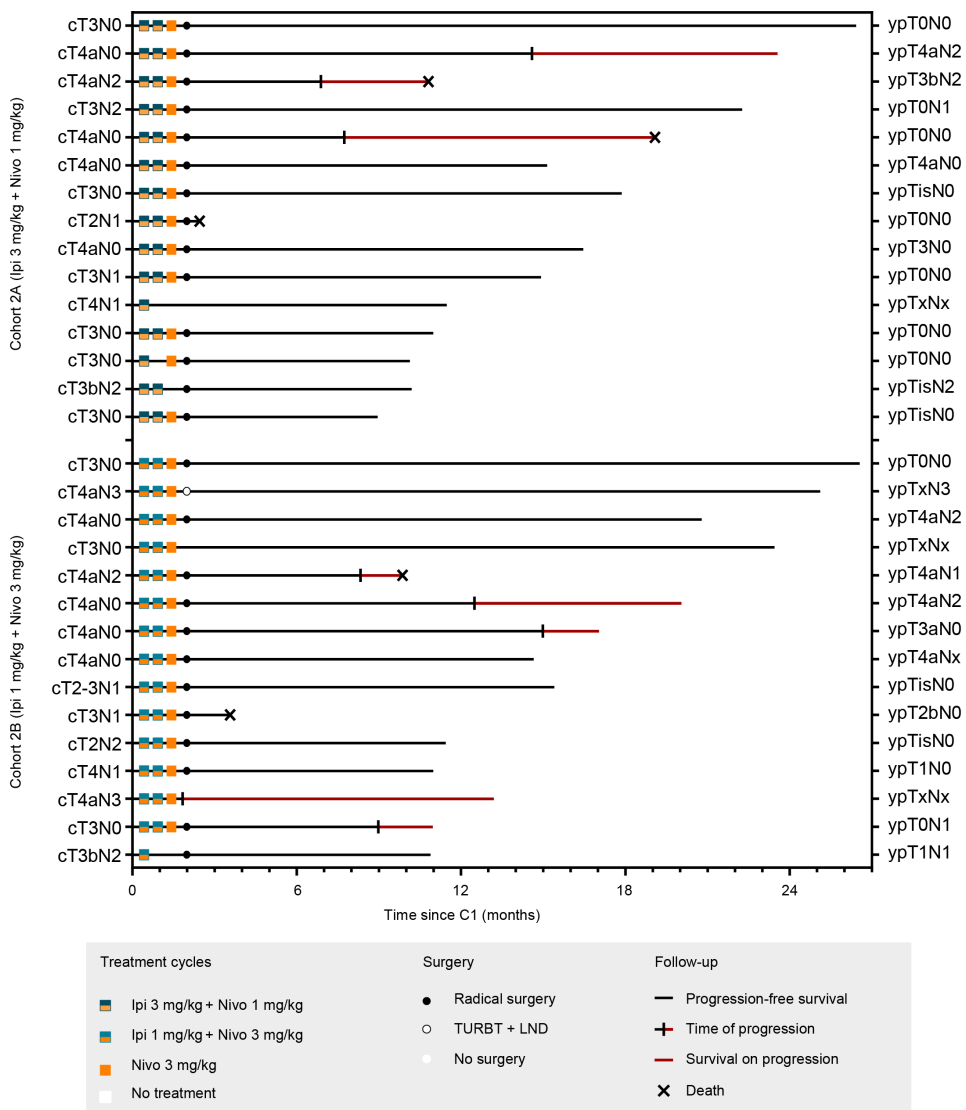
Extended Data Figure 2 | Treatment, response and follow-up details for every patient treated in cohort 2A and 2B. Swimmer plot with treatment and follow-up details for every patient in cohort 2A and 2B. Patients are organized per cohort and based on inclusion date. Time is relative to the date of first treatment of ipilimumab plus nivolumab (C1). Clinical TNM-stage prior to start of treatment is shown on the left side of the plot. Pathological TNM-stage after surgery is shown on the right side of the plot. Orange and green boxes represent treatment cycles administered. Black dots represent radical surgery. Open circles represent alternative surgery (transurethral resection bladder tumor and pelvic lymph node dissection). Black horizontal lines represent progression-free survival. Vertical lines indicate disease progression. Red horizontal lines represent survival after disease progression. Black cross indicates death. Two fatal surgery-related adverse events occurred within 90 days after surgery, both hemorrhage after an intra-operative complication. After extensive review, no relation with ipilimumab and/or nivolumab was established. *Ipi: ipilimumab, Nivo: nivolumab, TURBT: transurethral resection of the bladder tumor, LND: lymph node dissection, C1: first treatment cycle.*
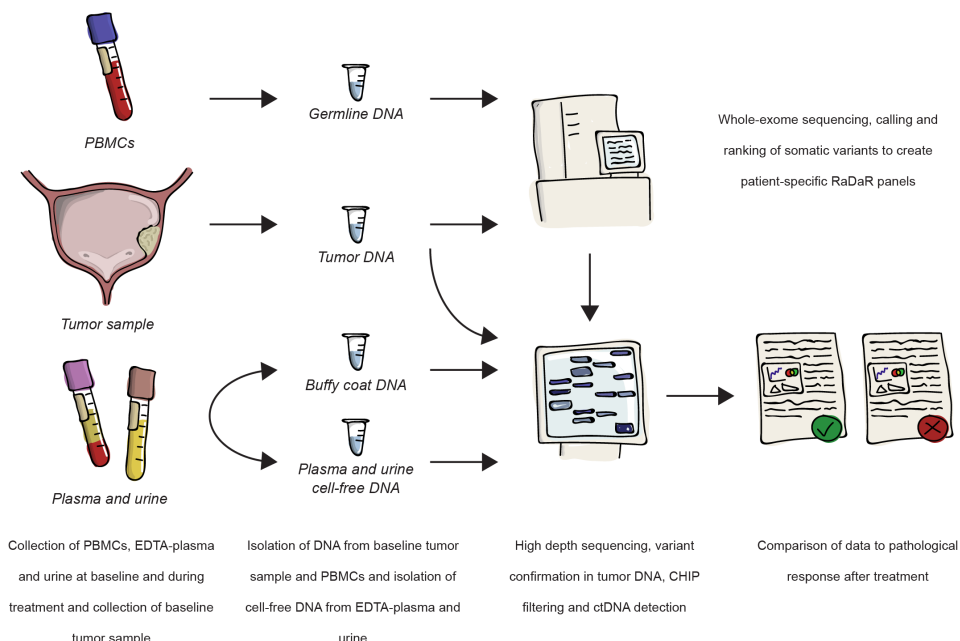
Extended Data Figure 3 | Workflow of RaDaR panel generation and ctDNA assessment in plasma and urine. DNA was isolated from baseline tumor sample and from PBMCs and used for whole-exome sequencing to identify tumor-specific somatic mutations. A personalized ctDNA assay was developed for each patient. Cell-free DNA and buffy coat DNA from EDTA-plasma and urine samples were analyzed together with tumor DNA using the personalized assays to confirm somatic mutations and perform CHIP filtering. *PBMCs: peripheral blood mononuclear cells, ctDNA: circulating tumor DNA, CHIP: clonal hematopoiesis of indeterminate potential.*

5
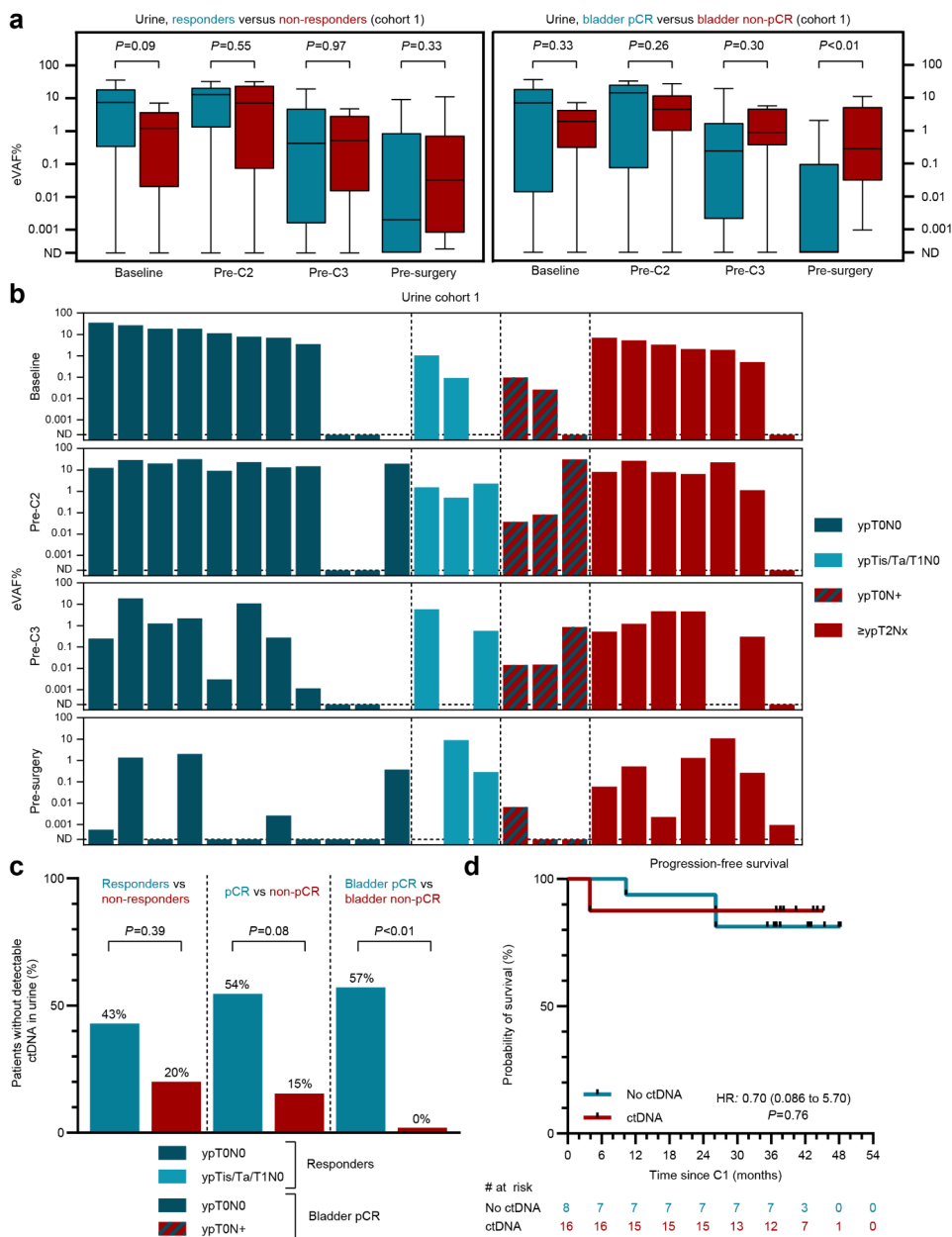
Extended Data Figure 4 | ctDNA assessment in urine and relation to outcome. Urine was assessed in patients in cohort 1 (*n*=24). **a,** Mean eVAF% in urine before and during treatment, and pre-surgery for responders and non-responders (left; baseline: P=0.09; pre-surgery: P=0.33) and for patients with and without a pathological complete response in the bladder (ypT0Nx versus ypTis/Ta/T1-4aNx) (right; baseline: P=0.33; pre-surgery: P<0.01). Boxplots show median value and 25th and 75th percentiles. Whiskers show minimum/ maximum values. P-values: two-sided Mann-Whitney test. **b,** Individual data points for eVAF% in urine before and during treatment, and pre-surgery. Dark blue bars: patients with a pathological complete response (pCR, ypT0N0), light blue bars: patients with no residual muscle-invasive disease (ypTis/Ta/T1N0), red bars: patients

with muscle-invasive disease in the bladder (≥ypT2Nx), Mixed dark blue and red bars: patients with a pCR in the bladder and lymph node metastases (ypT0N+), missing bars: missing samples. Undetectable values are plotted as 0.0002. **c,** Percentage of patients with no detectable ctDNA in urine at latest available sample pre-surgery for patients categorized in different ways. Responders vs non-responders: P=0.39; pCR vs non-pCR: P=0.08; bladder pCR vs bladder non-pCR: P<0.01. P-values: two-sided Fisher's Exact test comparing the proportion of patients with detectable ctDNA pre-surgery in responders (ypTis/Ta/T1N0) compared to non-responders (left), patients with or without a pCR (ypT0N0; middle) and patients with or without a pathological complete response in the bladder (ypT0Nx; right). **d,** Progression-free survival for patients with and without detectable ctDNA in urine measured at latest available sample pre-surgery. Hazard ratio (HR) and P-value: Hazard ratio: 0.70; 95% confidence interval: 0.086-5.70; P=0.76 using a two-sided Log-rank (Mantel-Cox) test. *ND: not detectable, Pre-C2/3: prior to second or third treatment cycle.*

Urine (cohort 1)

Baseline Pre-C2 Pre-C3 Pre-surgery Follow-up

Plasma (cohort 1+2)

Baseline Pre-C2 Pre-C3 Pre-surgery Follow-up

ctDNA measurements (Baseline, Pre-C2, Pre-C3, Pre-surgery)

- Detectable ctDNA
- No detectable ctDNA
- No ctDNA measurement

Follow-up

- No disease progression
- Disease progression
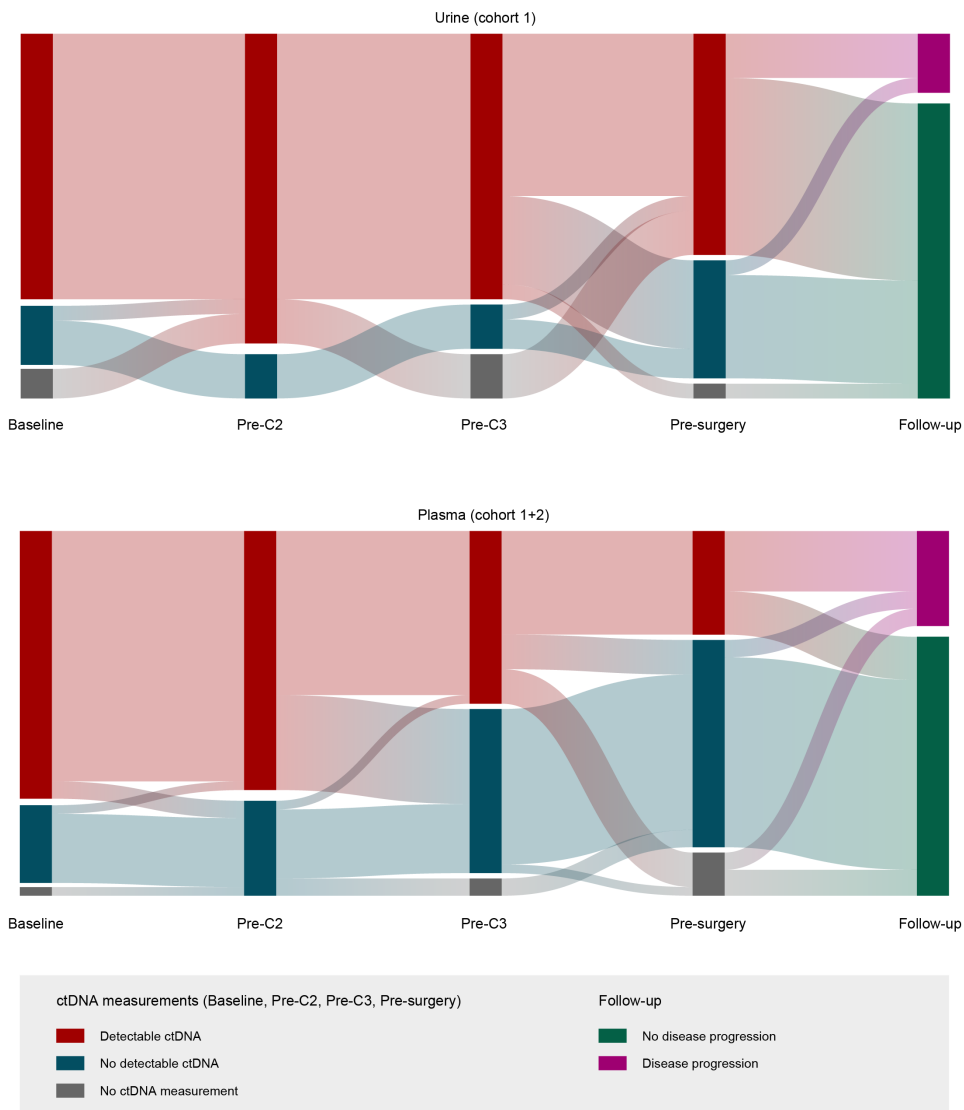
Extended Data Figure 5 | Sankey Diagrams showing the ctDNA dynamics and relation with outcome. Top: ctDNA in urine in patients in cohort 1 (*n*=24). Bottom: ctDNA in plasma in patients in cohort 1 and 2 combined (*n*=41). Red, blue and grey bars represent the number of patients with detectable, undetectable or missing ctDNA measurements, respectively, at different timepoints (Baseline, Pre-C2, Pre-C3 or Pre-surgery). In follow-up, red and blue bars represent the number of patients with and without disease progression, respectively. *Pre-C2/3: prior to second or third treatment cycle.*

5
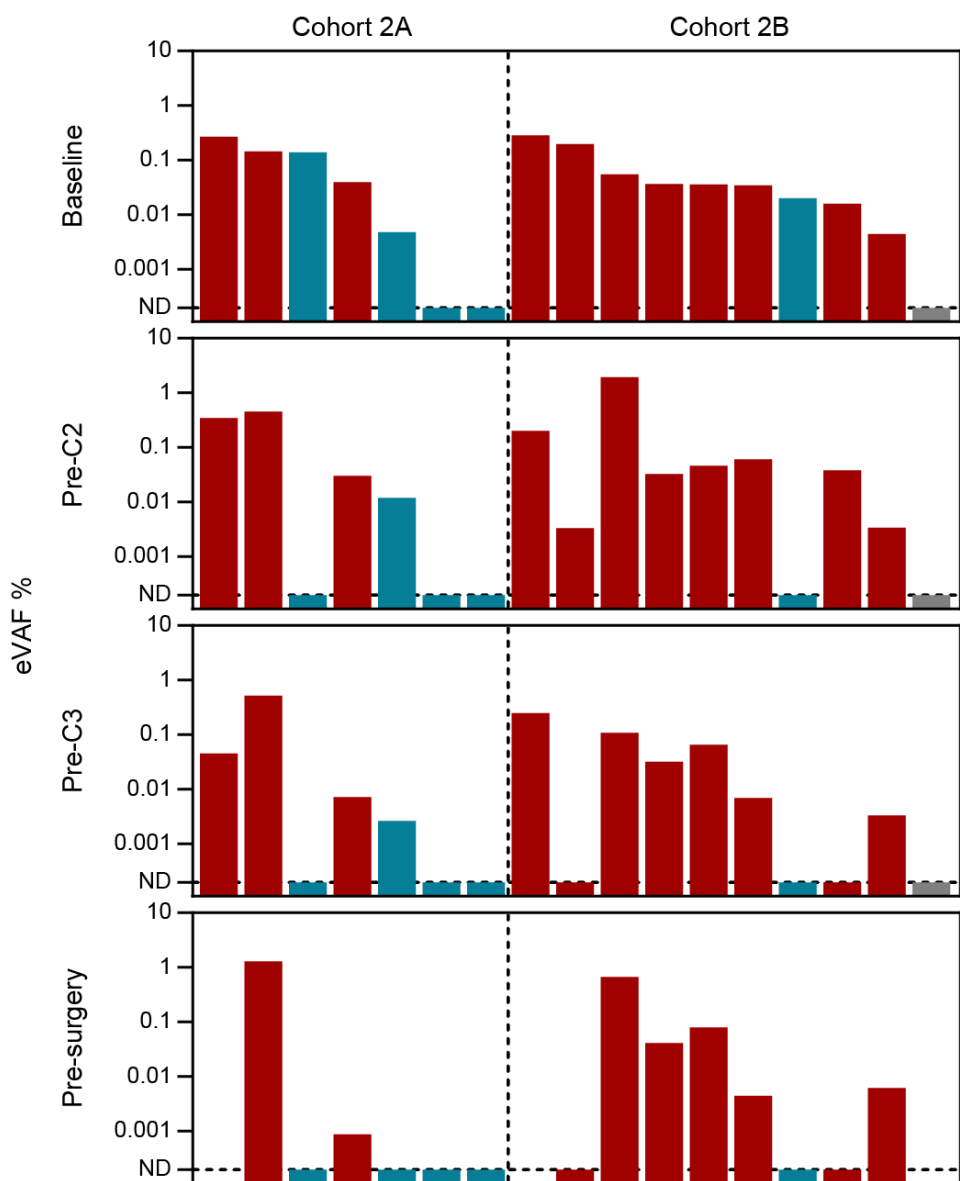
Extended Data Fig. 6 | ctDNA assessment in plasma in cohort 2A and 2B. ctDNA assessment in plasma in cohort 2A and 2B.

SUPPLEMENTARY DATA

Supplementary Table 4-6 and NABUCCO study protocol are available online only.

a

Tube type	Panel	Healthy donor blood tubes	Successfully tested	Detected n (%)
EDTA	HCC1395	8	8	0 (0%)
EDTA	HCC1954	8	8	0 (0%)
EDTA	SW480	4	4	0 (0%)
Streck	HCC1395	20	20	0 (0%)
Streck	HCC1954	20	20	0 (0%)
Streck	SW480	9	9	0 (0%)
Streck	5 NSCLC patients	20	20	0 (0%)

b
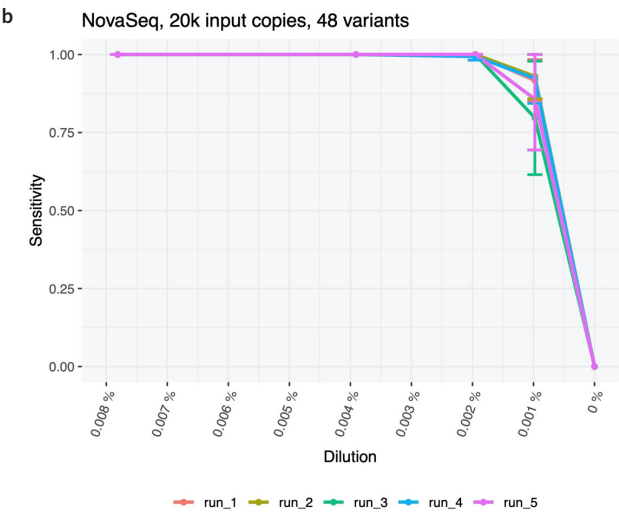
c

Number of variants	LoD$_{95}$ VAF
48	0.00114%
44	0.00128%
40	0.00138%
36	0.00152%
32	0.00172%
28	0.00190%
24	0.00228%
20	0.00276%
16	0.00336%
12	0.00438%
8	0.00640%

Supplementary Figure 1 | RaDaR assay analytical validation. a, Summary of the samples and panels used to determine RaDaR assay specificity. **b**, Dilution-based analysis of RaDaR sensitivity using two breast cancer and one colon cancer cell line. Each line represents the result of an independent RaDaR run performed

in the lab with the three different cell lines, all analyzed in duplicate (n=2x3). Each line shows the mean and standard deviation (SD) of the sensitivity values of the three cell lines (n=5 separate experiments). **c**, Analysis of the impact of the number of variants on the limit of detection (LoD). Variants were randomly for all three cell lines removed before calling was performed and Probit was used to determine LoD with these sub-sampled data sets.

Supplementary Table 1 | Baseline characteristics. Baseline characteristics for patients from cohort 1, 2A and 2B. *P*-values: two-sided Chi-square tests for all parameters except *age*, for which the *P*-value is calculated using a two-sided ANOVA test. No correction for multiple hypothesis testing has been conducted.

Baseline characteristics	Cohort 1 (*n*=24)	Cohort 2A (*n*=15)	Cohort 2B (*n*=15)	Statistics
Median age, years (IQR)	66 (64-71)	70 (65-73)	68 (64-72)	*P*=0.59
Male sex, *n* (%)	18/24 (75%)	11/15 (73%)	12/15 (80%)	*P*=0.90
Clinical T-stage, *n* (%)				*P*=0.50
cT3-4aN0M0	14/24 (58%)	8/15 (53%)	7/15 (47%)	
cT1-4aN1-3M0	10/24 (42%)	7/15 (47%)	8/15 (53%)	
Cisplatin-eligibility status *n* (%)				*P*=0.45
Cisplatin-ineligible[a]	13/24 (54%)	10/15 (67%)	11/15 (73%)	
Refusal of cisplatin-based chemotherapy	11/24 (46%)	5/15 (33%)	4/15 (27%)	
WHO performance score, *n* (%)				*P*=0.13
WHO 0	21/24 (88%)	9/15 (60%)	12/15 (80%)	
WHO 1	3/24 (12%)	6/15 (40%)	3/15 (20%)	
Primary tumor localization				*P*=0.97
Lower tract	24/24 (100%)[b]	14/15 (93%)	15/15 (100%)	
Upper tract	1/24 (4%)	1/15 (7%)	0/15 (9%)	

[a] *Cisplatin-ineligible according to Galsky criteria*
[b] *1 patient in cohort 1 had combined upper and lower tract involvement*

Supplementary Table 2 | Immunotherapy-related adverse events. Table showing the frequency of all adverse events, the frequency of immunotherapy-related adverse events (i.e. with a 'possible', 'likely' or very likely' relation with ipilimumab plus nivolumab), and the frequency of specific immunotherapy-related adverse events. Data is shown separately for cohort 1, 2A and 2B and for 'any grade' events and 'grade ≥3 events'.

Adverse events	Cohort 1 (*n*=24)		Cohort 2A (Ipi 3 mg/kg + Nivo 1 mg/kg, *n*=15)		Cohort 2B (Ipi 1 mg/kg + Nivo 3 mg/kg, *n*=15)	
	All grade	Grade ≥3	All grade	Grade ≥3	All grade	Grade ≥3
Any adverse event, *n* (%)	24/24 (100%)	22/24 (92%)	15/15 (100%)	9/15 (60%)	14/15 (93%)	9/15 (60%)
Any immunotherapy-related adverse event, *n* (%)	23/24 (96%)	14/24 (58%)	15/15 (100%)	6/15 (40%)	11/15 (73%)	3/15 (20%)
Immunotherapy-related adverse events, *n* (%)						
Lipase increased	8/24 (33%)	6/24 (25%)	5/15 (33%)	2/15 (13%)	0/15 (0%)	0/15 (0%)
Diarrhea	5/24 (21%)	3/24 (13%)	4/15 (27%)	1/15 (7%)	3/15 (20%)	1/15 (7%)
Alanine aminotransferase increased	5/24 (21%)	3/24 (13%)	3/15 (20%)	0/15 (0%)	3/15 (20%)	1/15 (7%)
GGT increased	3/24 (13%)	2/24 (8%)	3/15 (20%)	1/15 (7%)	4/15 (27%)	1/15 (7%)
Colitis	3/24 (13%)	2/24 (8%)	1/15 (7%)	0/15 (0%)	1/15 (7%)	0/15 (0%)
Fatigue	6/24 (25%)	1/24 (4%)	6/15 (40%)	0/15 (0%)	3/15 (20%)	1/15 (7%)
Aspartate aminotransferase increased	4/24 (17%)	1/24 (4%)	4/15 (27%)	0/15 (0%)	2/15 (13%)	1/15 (7%)
Alkaline phosphatase increased	3/24 (13%)	1/24 (4%)	3/15 (20%)	0/15 (0%)	4/15 (27%)	1/15 (7%)
Bilirubin increased	1/24 (4%)	1/24 (4%)	0/15 (0%)	0/15 (0%)	1/15 (7%)	0/15 (0%)
Cardiomyopathy	1/24 (4%)	1/24 (4%)	0/15 (0%)	0/15 (0%)	0/15 (0%)	0/15 (0%)
Hemolysis	1/24 (4%)	1/24 (4%)	0/15 (0%)	0/15 (0%)	0/15 (0%)	0/15 (0%)
Hyperglycemia	1/24 (4%)	1/24 (4%)	0/15 (0%)	0/15 (0%)	0/15 (0%)	0/15 (0%)
Peripheral motor neuropathy	1/24 (4%)	1/24 (4%)	0/15 (0%)	0/15 (0%)	0/15 (0%)	0/15 (0%)
Toxicodermia	1/24 (4%)	1/24 (4%)	0/15 (0%)	0/15 (0%)	0/15 (0%)	0/15 (0%)
Hyperthyroidism	3/24 (13%)	0/24 (0%)	3/15 (20%)	1/15 (7%)	3/15 (20%)	0/15 (0%)
Dermatitis	0/24 (0%)	0/24 (0%)	3/15 (20%)	1/15 (7%)	1/15 (7%)	0/15 (0%)
Hyponatremia	0/24 (0%)	0/24 (0%)	1/15 (7%)	1/15 (7%)	1/15 (7%)	0/15 (0%)
Hypopituitarism	0/24 (0%)	0/24 (0%)	1/15 (7%)	1/15 (7%)	0/15 (0%)	0/15 (0%)
COVID-19 infection	0/24 (0%)	0/24 (0%)	0/15 (0%)	0/15 (0%)	1/15 (7%)	1/15 (7%)
Renal insufficiency	0/24 (0%)	0/24 (0%)	0/15 (0%)	0/15 (0%)	1/15 (7%)	1/15 (7%)
Maculo-papular rash	4/24 (17%)	0/24 (0%)	2/15 (13%)	0/15 (0%)	1/15 (7%)	0/15 (0%)
Erythema multiforme	4/24 (17%)	0/24 (0%)	0/15 (0%)	0/15 (0%)	0/15 (0%)	0/15 (0%)
Pruritis	3/24 (13%)	0/24 (0%)	4/15 (27%)	0/15 (0%)	3/15 (20%)	0/15 (0%)
Amylase increased	3/24 (13%)	0/24 (0%)	4/15 (27%)	0/15 (0%)	0/15 (0%)	0/15 (0%)
Headache	3/24 (13%)	0/24 (0%)	2/15 (13%)	0/15 (0%)	0/15 (0%)	0/15 (0%)
Endocrine disorders, unspecified	3/24 (13%)	0/24 (0%)	0/15 (0%)	0/15 (0%)	0/15 (0%)	0/15 (0%)
Hypothyroidism	2/24 (8%)	0/24 (0%)	4/15 (27%)	0/15 (0%)	1/15 (7%)	0/15 (0%)
Adrenal insufficiency	2/24 (8%)	0/24 (0%)	1/15 (7%)	0/15 (0%)	0/15 (0%)	0/15 (0%)
Dry skin	2/24 (8%)	0/24 (0%)	1/15 (7%)	0/15 (0%)	0/15 (0%)	0/15 (0%)
Nausea	2/24 (8%)	0/24 (0%)	0/15 (0%)	0/15 (0%)	1/15 (7%)	0/15 (0%)
Flu-like symptoms	2/24 (8%)	0/24 (0%)	0/15 (0%)	0/15 (0%)	0/15 (0%)	0/15 (0%)
Infusion-related reaction	1/24 (4%)	0/24 (0%)	2/15 (13%)	0/15 (0%)	1/15 (7%)	0/15 (0%)

Supplementary Table 2 | Continued.

Adverse events	Cohort 1 (*n*=24)		Cohort 2A (Ipi 3 mg/kg + Nivo 1 mg/kg, *n*=15)		Cohort 2B (Ipi 1 mg/kg + Nivo 3 mg/kg, *n*=15)	
	All grade	Grade ≥3	All grade	Grade ≥3	All grade	Grade ≥3
Conjunctivitis	1/24 (4%)	0/24 (0%)	1/15 (7%)	0/15 (0%)	0/15 (0%)	0/15 (0%)
Dry mouth	1/24 (4%)	0/24 (0%)	1/15 (7%)	0/15 (0%)	0/15 (0%)	0/15 (0%)
Alopecia	1/24 (4%)	0/24 (0%)	0/15 (0%)	0/15 (0%)	0/15 (0%)	0/15 (0%)
Arthralgia	1/24 (4%)	0/24 (0%)	0/15 (0%)	0/15 (0%)	0/15 (0%)	0/15 (0%)
Infections, unspecified	1/24 (4%)	0/24 (0%)	0/15 (0%)	0/15 (0%)	0/15 (0%)	0/15 (0%)
Mucosal infection	1/24 (4%)	0/24 (0%)	0/15 (0%)	0/15 (0%)	0/15 (0%)	0/15 (0%)
Muscle weakness in lower extremity	1/24 (4%)	0/24 (0%)	0/15 (0%)	0/15 (0%)	0/15 (0%)	0/15 (0%)
Rash	1/24 (4%)	0/24 (0%)	0/15 (0%)	0/15 (0%)	0/15 (0%)	0/15 (0%)
Skin exanthema	1/24 (4%)	0/24 (0%)	0/15 (0%)	0/15 (0%)	0/15 (0%)	0/15 (0%)
Skin induration	1/24 (4%)	0/24 (0%)	0/15 (0%)	0/15 (0%)	0/15 (0%)	0/15 (0%)
Urinary incontinence	1/24 (4%)	0/24 (0%)	0/15 (0%)	0/15 (0%)	0/15 (0%)	0/15 (0%)
Dysgeusia	0/24 (0%)	0/24 (0%)	2/15 (13%)	0/15 (0%)	1/15 (7%)	0/15 (0%)
Malaise	0/24 (0%)	0/24 (0%)	2/15 (13%)	0/15 (0%)	1/15 (7%)	0/15 (0%)
Fever	0/24 (0%)	0/24 (0%)	2/15 (13%)	0/15 (0%)	0/15 (0%)	0/15 (0%)
Back pain	0/24 (0%)	0/24 (0%)	1/15 (7%)	0/15 (0%)	1/15 (7%)	0/15 (0%)
Dry eye	0/24 (0%)	0/24 (0%)	1/15 (7%)	0/15 (0%)	1/15 (7%)	0/15 (0%)
Abdominal pain	0/24 (0%)	0/24 (0%)	1/15 (7%)	0/15 (0%)	0/15 (0%)	0/15 (0%)
Edema in extremity	0/24 (0%)	0/24 (0%)	1/15 (7%)	0/15 (0%)	0/15 (0%)	0/15 (0%)
Eosinophils increased	0/24 (0%)	0/24 (0%)	1/15 (7%)	0/15 (0%)	0/15 (0%)	0/15 (0%)
Eye disorders, unspecified	0/24 (0%)	0/24 (0%)	1/15 (7%)	0/15 (0%)	0/15 (0%)	0/15 (0%)
Gastrointestinal symptoms, unspecified	0/24 (0%)	0/24 (0%)	1/15 (7%)	0/15 (0%)	0/15 (0%)	0/15 (0%)
Hypophysitis	0/24 (0%)	0/24 (0%)	1/15 (7%)	0/15 (0%)	0/15 (0%)	0/15 (0%)
LDH increased	0/24 (0%)	0/24 (0%)	1/15 (7%)	0/15 (0%)	0/15 (0%)	0/15 (0%)
Leukocytosis	0/24 (0%)	0/24 (0%)	1/15 (7%)	0/15 (0%)	0/15 (0%)	0/15 (0%)
Muscle and joint stiffness	0/24 (0%)	0/24 (0%)	1/15 (7%)	0/15 (0%)	0/15 (0%)	0/15 (0%)
Pain, unspecified	0/24 (0%)	0/24 (0%)	1/15 (7%)	0/15 (0%)	0/15 (0%)	0/15 (0%)
Platelets increased	0/24 (0%)	0/24 (0%)	1/15 (7%)	0/15 (0%)	0/15 (0%)	0/15 (0%)
Skin disorders, unspecified	0/24 (0%)	0/24 (0%)	1/15 (7%)	0/15 (0%)	0/15 (0%)	0/15 (0%)
Skin hypopigmentation	0/24 (0%)	0/24 (0%)	1/15 (7%)	0/15 (0%)	0/15 (0%)	0/15 (0%)
Subcutaneous lesions in upper extremity	0/24 (0%)	0/24 (0%)	1/15 (7%)	0/15 (0%)	0/15 (0%)	0/15 (0%)
Thyroiditis	0/24 (0%)	0/24 (0%)	1/15 (7%)	0/15 (0%)	0/15 (0%)	0/15 (0%)
Anemia	0/24 (0%)	0/24 (0%)	0/15 (0%)	0/15 (0%)	1/15 (7%)	0/15 (0%)
Hepatitis	0/24 (0%)	0/24 (0%)	0/15 (0%)	0/15 (0%)	1/15 (7%)	0/15 (0%)
Hypercalcemia	0/24 (0%)	0/24 (0%)	0/15 (0%)	0/15 (0%)	1/15 (7%)	0/15 (0%)
Investigations, unspecified	0/24 (0%)	0/24 (0%)	0/15 (0%)	0/15 (0%)	1/15 (7%)	0/15 (0%)
Myositis	0/24 (0%)	0/24 (0%)	0/15 (0%)	0/15 (0%)	1/15 (7%)	0/15 (0%)
Pain in extremity	0/24 (0%)	0/24 (0%)	0/15 (0%)	0/15 (0%)	1/15 (7%)	0/15 (0%)
Peripheral sensory neuropathy	0/24 (0%)	0/24 (0%)	0/15 (0%)	0/15 (0%)	1/15 (7%)	0/15 (0%)
Urticaria	0/24 (0%)	0/24 (0%)	0/15 (0%)	0/15 (0%)	1/15 (7%)	0/15 (0%)

Supplementary Table 3 | Baseline characteristics for patients with and without ctDNA assessment.
Baseline characteristics for patients in the primary ctDNA cohort (all from cohort 1), from the validation cohort (all from cohort 2A and 2B), and for patients for which ctDNA was not assessed (all from cohort 2A and 2B).

Baseline characteristics	Primary cohort (plasma and urine assessment, n=24)	Validation cohort (plasma assessment only, n=17)	Remaining patients (no ctDNA assessment, n=13)
Institute, n (%)			
Netherlands Cancer Institute	24/24 (100%)	17/17 (100%)	1/13 (7%)
University Medical Center Utrecht	0/24 (0%)	0/17 (0%)	10/13 (77%)
Radboud University Medical Center	0/24 (0%)	0/17 (0%)	2/13 (15%)
Median age, years (IQR)	66 (64-71)	68 (61-73)	68 (67-72)
Male sex, n (%)	18/24 (75%)	14/17 (82%)	9/13 (69%)
Clinical T-stage, n (%)			
cT3-4aN0M0	14/24 (58%)	12/17 (71%)	3/13 (23%)
cT1-4aN1-3M0	10/24 (42%)	5/17 (29%)	10/13 (77%)
Cisplatin-eligibility status, n (%)			
Cisplatin-ineligible[a]	13/24 (54%)	14/17 (82%)	7/13 (54%)
Refusal of cisplatin-based chemotherapy	11/24 (46%)	3/17 (18%)	6/13 (46%)
WHO performance score, n (%)			
WHO 0	21/24 (88%)	14/17 (82%)	7/13 (54%)
WHO 1	3/24 (12%)	3/17 (18%)	6/13 (46%)
Primary tumor localization			
Lower tract	24/24 (100%)[b]	17/17 (100%)	12/13 (92%)
Upper tract	1/24 (4%)	0/17 (0%)	1/13 (8%)

[a] Cisplatin-ineligible according to Galsky criteria
[b] 1 patient in cohort 1 had combined upper and lower tract involvement

5

CHAPTER 6

A serendipitous preoperative trial of combined ipilimumab plus nivolumab For localized prostate cancer

Jeroen van Dorp, Maurits L. van Montfoort, Nick van Dijk, Ingrid Hofland,
Jeantine M. de Feijter, Andries M. Bergman, Kees Hendricksen, Henk G. van der Poel,
Bas W.G. van Rhijn, Michiel S. van der Heijden

ABSTRACT

INTRODUCTION

Encouraging results have been observed by treating castration-resistant metastatic prostate cancer (PCa) patients with combined ipilimumab plus nivolumab. In other malignancies, pre-operative treatment with immune checkpoint inhibitors (ICIs) in the localized setting is associated with excellent responses.

In the NABUCCO trial, n=24 locally advanced muscle-invasive bladder cancer patients were treated with ipilimumab plus nivolumab, followed by radical surgery. This trial offered the unique opportunity to investigate the effect of these agents in PCa incidentally found at cystoprostatectomy.

PATIENTS AND METHODS

NABUCCO patients were evaluated for the presence of PCa and histopathological features of response to ICIs. Findings were compared to PCa incidentally found in a control cohort of bladder cancer patients. Representative PCa tissue sections from NABUCCO and control patients were stained for CD3, CD8 and CD45.

RESULTS

PCa was observed in 9/16 (56%) of eligible NABUCCO patients, compared with 48/121 (40%) in the control cohort. No histopathological features of response to ipilimumab plus nivolumab were observed. The number of CD8+-cells, CD3+-cells and CD45+-cells in the PCa area was not statistically different between NABUCCO and control patients.

CONCLUSION

Taking several limitations of this retrospective study into consideration, we found no evidence for a major effect of ipilimumab plus nivolumab on incidental localized PCa.

CLINICAL PRACTICE POINTS
- Incidental prostate cancer was found in cystoprostatectomy specimens in 9 out of 16 patients treated in the NABUCCO trial.
- This was not statistically different from incidental prostate cancer observed after cystoprostatectomy in a control cohort.
- Based on histopathological analysis and immunohistochemistry, we found no evidence for response to ipilimumab and nivolumab in incidental prostate cancer in the NABUCCO trial.

INTRODUCTION

Immune checkpoint inhibition (ICI) has demonstrated impressive results in multiple malignancies[1-3]. However, the first trials with ICI monotherapy in prostate cancer (PCa) showed only limited clinical benefit[4,5]. Recently, more encouraging results in PCa were observed by combining nivolumab (anti-PD-1) and ipilimumab (anti-CTLA-4) in the CheckMate-650 trial, showing an overall response rate of 25.0% in chemotherapy-naïve metastatic castration-resistant PCa patients[6].

In other malignancies, excellent results have been observed by treating patients with combined ICI in the localized, pre-operative setting[7,8]. This is also observed in cancer types where response to ICI is rare in the metastatic setting, such as microsatellite-stable colon cancer[9].

In the NABUCCO trial, locally advanced muscle-invasive bladder cancer (MIBC) patients were treated with ipilimumab plus nivolumab, followed by radical surgery[10]. As part of the surgical template in male patients, the prostate is removed (cystoprostatectomy). This presents a unique opportunity to investigate the effect of combined ipilimumab plus nivolumab on (incidental) PCa in the localized, pre-operative setting.

MATERIALS AND METHODS

NABUCCO STUDY DESIGN
NABUCCO is a prospective, single-arm trial testing the feasibility of pre-operative ipilimumab 3 mg/kg (day 1), ipilimumab 3 + nivolumab 1 mg/kg (day 22), and nivolumab 3 mg/kg (day 43) followed by resection with appropriate lymph node dissection in stage III (cT3-4aN0M0 and cT1-4aN1-3M0) resectable MIBC patients (*n*=24). For more information on the NABUCCO trial, refer to *Van Dijk et al., Nat Med, 2020*[10] and ClinicalTrials.gov:NCT03387761.

CONTROL COHORT PATIENT SELECTION
Patients that underwent radical surgery for bladder cancer in the Netherlands Cancer Institute from 2016 – 2019 were included in the control cohorts. Exclusion criteria were female sex, prior diagnosis of PCa, prostate-sparing surgery, previous systemic anticancer therapy except neo-adjuvant chemotherapy for MIBC, or previous radiotherapy in the pelvic area. Clinical data for eligible patients was collected from an institutional database in accordance with national and institutional ethical guidelines and approved under IRBdm20-092.

IMMUNOHISTOCHEMISTRY AND IMMUNE CELL QUANTIFICATION
Immunohistochemistry of formalin-fixed paraffin embedded tumor samples was performed on a BenchMark Ultra autostainer or Discovery Ultra autostainer (beta-2 Microglobulin). Briefly, paraffin

sections were cut at 3µm and deparaffinised. Antibodies used were CD3 clone SP7 (1/100 dilution, Spring/ITK), CD8 clone C8/144B (1/200 dilution, DAKO/Agilent), CD45 Clone 2B11PD7/26 (Ventana Medical Systems) and PSA, a polyclonal antibody (1/8000 dilution, DAKO). Bound antibody was detected using the OptiView and Ultraview DAB Detection Kits (Ventana Medical Systems). Slides were counterstained with Hematoxylin and Bluing Reagent (Ventana Medical Systems) and uploaded in SlideScore (https://www.slidescore.com/). Up to five randomly selected fields (0.8mm^2, magnification 20x) were generated in the PCa tumor area for each slide. Cells were counted manually by an experienced uropathologist (MvM) together with JvD. PCa tumors with a very small tumor focus (<0.8mm^2) were considered as '0' positive cells. The reported cell count for each patient is the mean for each of the five quantitated fields. For details concerning the multiplex immunofluorescent images (DAPI, PanCK, CD3, CD8, CD20, CD68 and FoxP3), see *Van Dijk et al., Nat Med, 2020*[10].

STATISTICAL ANALYSIS

All graphs and statistics were generated in GraphPad Prism 7.0.3. Illustrations were created in Adobe Illustrator CS6 (v. 16.0.3).
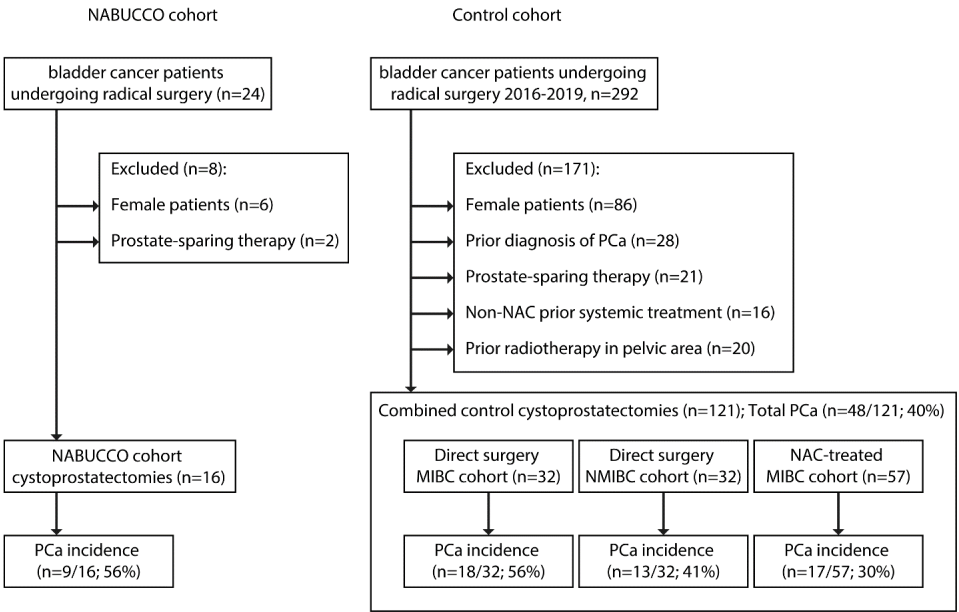
Figure 1 | Inclusion of patients. Left: All NABUCCO patients that underwent a cystectomy were included for analysis. Female patients and patients with prostate-sparing surgery were excluded. Right: All patients that underwent a cystectomy (2016 – 2019) were included for analysis. For the control cohort, we excluded female patients, patients with a prior diagnosis of PCa or prostate-sparing surgery, patients that were treated with systemic therapy before surgery other than platinum-based neo-adjuvant chemotherapy for MIBC, and patients that received prior radiotherapy in the pelvic area. Patients with prior local treatment for NMIBC were included. The remaining patients were subdivided over three cohorts: NMIBC patients, MIBC patients treated with neo-adjuvant platinum-based chemotherapy, and MIBC patients treated with a direct cystectomy.

RESULTS

In total, 24 stage III MIBC patients were treated with ipilimumab plus nivolumab in the NABUCCO trial[10]. As part of the eligibility criteria, only patients without prior diagnosis of PCa or with low-risk PCa were included. The presence of PCa was not actively excluded by prostate biopsies during screening, though prostate biopsies were obtained in patients undergoing prostate-sparing surgery. 16/24 patients underwent a cystoprostatectomy and were eligible for histological examination (Table 1; Figure 1, left). In 9/16 (56%) patients, incidental PCa was found. The majority of cases were low-grade PCa with a Gleason Score (Gleason) 3+3=6 in 7/9 cases and ≤pT2 in 8/9 cases (Table 1). Two patients were diagnosed with a clinically significant Gleason 4+4=8 PCa, including one patient with PCa metastases in multiple pelvic lymph nodes (Table 1).

We reassessed all prostate tissue sections from the NABUCCO cohort and compared these to the MIBC tissue sections. As described previously, response of MIBC to ipilimumab plus nivolumab was characterized by fields of fibrosis and necrosis, infiltration of immune cells, and formation of tertiary lymphoid structures (Figure 2A)[10]. 5/16 patients had a complete pathological response of MIBC (31%, ypT0N0) and 8/16 showed major pathological downstaging of MIBC (50%, <ypT2N0), often exhibiting a prominent immune infiltrate in the tumor bed[10]. No correlation was found between the response of MIBC to ipilimumab plus nivolumab and the occurrence of PCa. In addition, there was no fibrosis, necrosis or other histopathological features of response to ICI in any of the nine PCa specimens (Figure 2B).

Without a full pre-treatment diagnostic work-up for PCa, it is possible that we underestimate the response to ipilimumab plus nivolumab in PCa. To this end, we retrospectively collected data from control patients treated with a radical cystoprostatectomy in our hospital from 2016 – 2019 to compare the incidence and characteristics of PCa to our findings in the NABUCCO cohort (Figure 1, right). Baseline data was collected for three cohorts: MIBC patients treated by direct cystoprostatectomy (without prior systemic treatment, n=32), for three cohorts: MIBC patients treated by direct cystoprostatectomy (without prior systemic treatment, n=32), MIBC patients treated with neo-adjuvant platinum-based chemotherapy followed by cystoprostatectomy (n=57) and non-muscle-invasive bladder cancer (NMIBC) patients (n=32) (Table 1; Figure 1, right). Incidental PCa was found in 48 of the 121 patients in the control cohorts, which was not significantly different from the NABUCCO cohort (40% versus 56%; p=0.28; Table 1). This was also comparable to previously published cohorts[11,12]. Gleason 3+3=6 was found in 33/48 (69%) cases in the combined control cohorts versus 7/9 (78%) cases in the NABUCCO cohort (p=0.71). pT-stage for PCa was ≤pT2 in 44/48 (89%) cases in the other cohorts versus 8/9 (89%) cases in the NABUCCO cohort (p=1.00; Table 1; Figure 2C). In summary, when comparing PCa in the NABUCCO cohort against a control cohort, no significant differences in terms of incidence, Gleason score or disease stage were found. This suggests that we are not underestimating response to ipilimumab plus nivolumab in PCa in NABUCCO patients.

Table 1 | Patient characteristics in urothelial cancer cohorts

	NABUCCO patients	Direct surgery MIBC patients	NAC-treated MIBC patients	NMIBC patients	Statistics
Number of patients eligible	16	32	57	32	
Mean age in years (std)[a]	69.4 (6.8)	70.7 (9.3)	65.3 (9.0)	67.2 (9.4)	p=0.38[b] p≥0.26[c]
Mean PSA at baseline in µg/l (std)	3.40 (3.45)	3.14 (3.30)	2.28 (3.04)	2.48 (2.04)	p=0.30[d] p≥0.42[e]
number of patients with incidental prostate cancer (% of eligible patients)	9 (56)	18 (56)	17 (30)	13 (41)	p=0.28[f] p=1.00[g]
Gleason score (% of PCa)					p=0.71[h] p=0.67[i]
3+3=6	7 (78)	11 (61)	12 (71)	10 (77)	
3+4=7	0 (0)	4 (22)	5 (29)	3 (23)	
4+3=7	0 (0)	3 (16)	0 (0)	0 (0)	
4+4=8	2 (22)	0 (0)	0 (0)	0 (0)	
T-stage PCa (% of PCa)					p=1.00[j] p=0.64[k]
pT1	0 (0)	0 (0)	0 (0)	0 (0)	
pT2	8 (89)	14 (78)	17 (100)	13 (100)	
pT3a	0 (0)	3 (22)	0 (0)	0 (0)	
pT3b	1 (11)	1 (6)	0 (0)	0 (0)	
N-stage for PCa					
pN0	8 (89)	18 (100)	17 (100)	13 (100)	
pN1	1 (11)	0 (0)	0 (0)	0 (0)	
Pre-treatment clinical TNM stage for bladder cancer (% of eligible patients)					
<cT2N0	0 (0)	0 (0)	0 (0)	32 (0)	
cT2N0	0 (0)	21 (65)	4 (7)	0 (0)	
cT2N+	0 (0)	1 (3)	7 (12)	0 (0)	
cT3N0	7 (44)	8 (25)	21 (37)	0 (0)	
cT3N+	5 (31)	2 (6)	12 (21)	0 (0)	
cT4aN0	4 (25)	0 (0)	6 (11)	0 (0)	
cT4aN+	0 (0)	0 (0)	7 (12)	0 (0)	

[a] Mean age at time of cystectomy for all eligible patients;
[b] two-tailed t-test, mean age in NABUCCO versus all control cohorts combined;
[c] 1-way ANOVA followed by Dunnet's multiple comparisons test, mean age for NABUCCO cohort versus all control cohorts separately;
[d] two-tailed t-test, mean PSA in NABUCCO versus all control cohorts combined;
[e] 1-way ANOVA followed by Dunnet's multiple comparisons test, mean age for NABUCCO cohort versus all control cohorts separately;
[f] Fisher's exact test, comparing incidence of PCa in NABUCCO versus all control cohorts combined;
[g] Fisher's exact test, comparing incidence of PCa in NABUCCO versus MIBC cohort treated with direct cystectomy;
[h] Fisher's exact test, comparing GS ≤3+3=6 versus >3+3=6 in NABUCCO versus all control cohorts combined;
[i] Fisher's exact, comparing GS ≤3+3=6 versus >3+3=6 in NABUCCO versus MIBC cohort treated with direct cystectomy;
[j] Fisher's exact test, comparing ≤T2 versus >T2 in NABUCCO versus all control cohorts combined;
[k] Fisher's exact, comparing ≤T2 versus >T2 in NABUCCO versus MIBC cohort treated with direct cystectomy;
(N)MIBC = (Non-)Muscle-invasive bladder cancer; NAC = Neo-adjuvant chemotherapy; PSA = Prostate-specific antigen; PCa = Prostate cancer
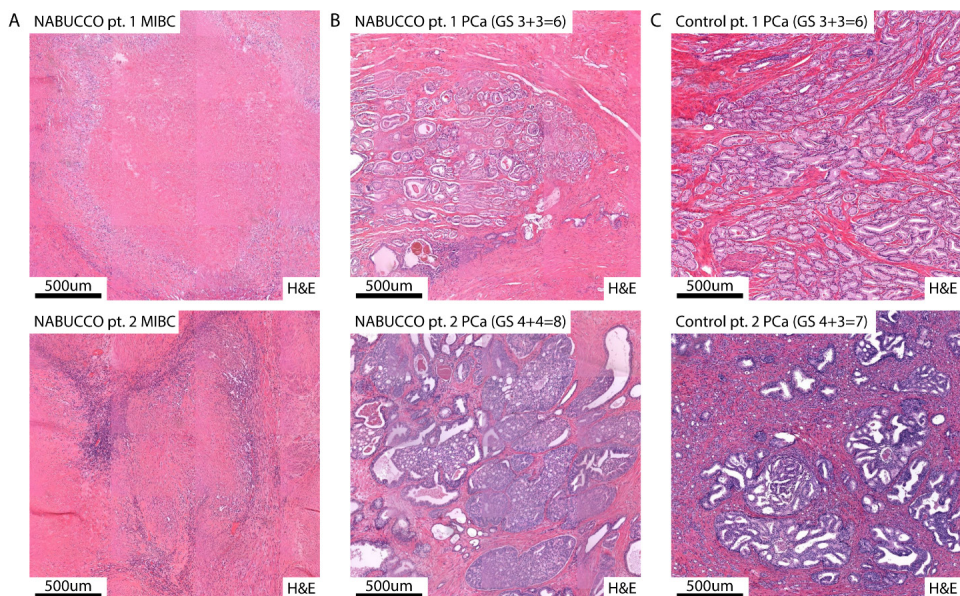
Figure 2 | Histological features of bladder cancer and prostate cancer observed in NABUCCO compared to patients treated with a direct cystectomy without prior neo-adjuvant treatment. A, H&E stainings of representative slides of the MIBC tumor bed in two NABUCCO patients showing extensive necrosis and fibrosis, surrounded by immune infiltrate (top panel: pt#1; ypT0N0, bottom panel, pt#2; ypT3bN0). **B,** H&E stainings of representative slides of PCa in the same NABUCCO patients as in (A), showing a PCa focus with vital tumor cells without any histopathological features of response (top panel: pt#1, GS3+3=6. pT2a; bottom panel: pt#2, GS4+4=8, pT3b). **C,** H&E stainings of representative slides of PCa in two MIBC patients without neo-adjuvant treatment showing a PCa focus with vital tumor cells (top panel: pt#1, GS3+3=6, pT2a; bottom panel: pt#2, GS4+3=7, pT3a).

Despite the absence of histological features related to response in PCa in NABUCCO patients, it is still possible that treatment with ICI results in the recruitment of effector T-cells into the PCa microenvironment, as described previously for pre-operative treatment with sipuleucel-T[13]. We assessed infiltrating immune cells in the prostate tumor microenvironment as a result of treatment with ipilimumab plus nivolumab versus a control cohort. To exclude potential effects from neo-adjuvant chemotherapy or previous treatment for NMIBC, we compared NABUCCO patients to MIBC patients who underwent cystoprostatectomy without any neo-adjuvant systemic treatment. Representative PCa tissue sections were stained for CD3, CD8 and CD45. We found no statistical difference in cells per mm^2 in the PCa tumor area in control patients and NABUCCO patients for any of the immune cell markers (CD3: 110 versus 124 cells per mm^2 p=0.80; CD8: 25 versus 15 cells per mm^2 p=0.25; CD45: 74 versus 80 cells per mm^2 p=0.85, Figure 3). Based on these data, we found no evidence for recruitment of effector T-cells in the PCa microenvironment as a result of treatment with ipilimumab plus nivolumab.

DISCUSSION

Treatment with combined ICI has shown impressive results in multiple malignancies. Superior results have been observed in the localized, pre-operative setting, as demonstrated for MIBC in the NABUCCO trial[10]. Given the encouraging results with ipilimumab plus nivolumab in metastatic PCa, we expected to find a similar response in localized PCa. Surprisingly, the PCa incidence, pT-stage, Gleason score and infiltration of immune cells was comparable between the NABUCCO cohort and the control cohorts. Thus, in sharp contrast to the high activity against MIBC in this cohort, we found no evidence that ipilimumab plus nivolumab induces a meaningful anti-cancer immune response in localized PCa.

There are several potential explanations why ICI would not be effective in localized PCa. The Checkmate-650 trial observed a higher response rate in metastatic PCa patients with a higher tumor mutational burden[6]. On average, patients with locoregional PCa have a lower tumor mutational burden compared to patients with metastatic PCa[14]. In addition, the prostate tumor microenvironment could potentially disrupt the function of ICI antibody molecules or prevent access to relevant immune cells. However, one particular patient in the NABUCCO cohort with MIBC invasion of the prostate showed an impressive response in the bladder and in MIBC invading the prostate (Figure 4A and 4B), whereas no histopathological signs of response were observed in the concurrent primary Gleason 4+4=8 PCa or in three PCa lymph node metastases (Figure 4B and 4C).

This retrospective study has several limitations. As a pre-treatment PCa diagnosis was not actively investigated in patients who were planned for cystoprostatectomy, there may have been patients having a PCa with a complete pathological response to ipilimumab plus nivolumab. In addition, PCa found in our analysis was mostly low-risk disease and would generally not have required treatment. In conclusion, in contrast to other cancer types, we find no evidence for a major effect of ipilimumab plus nivolumab on incidental, localized PCa.
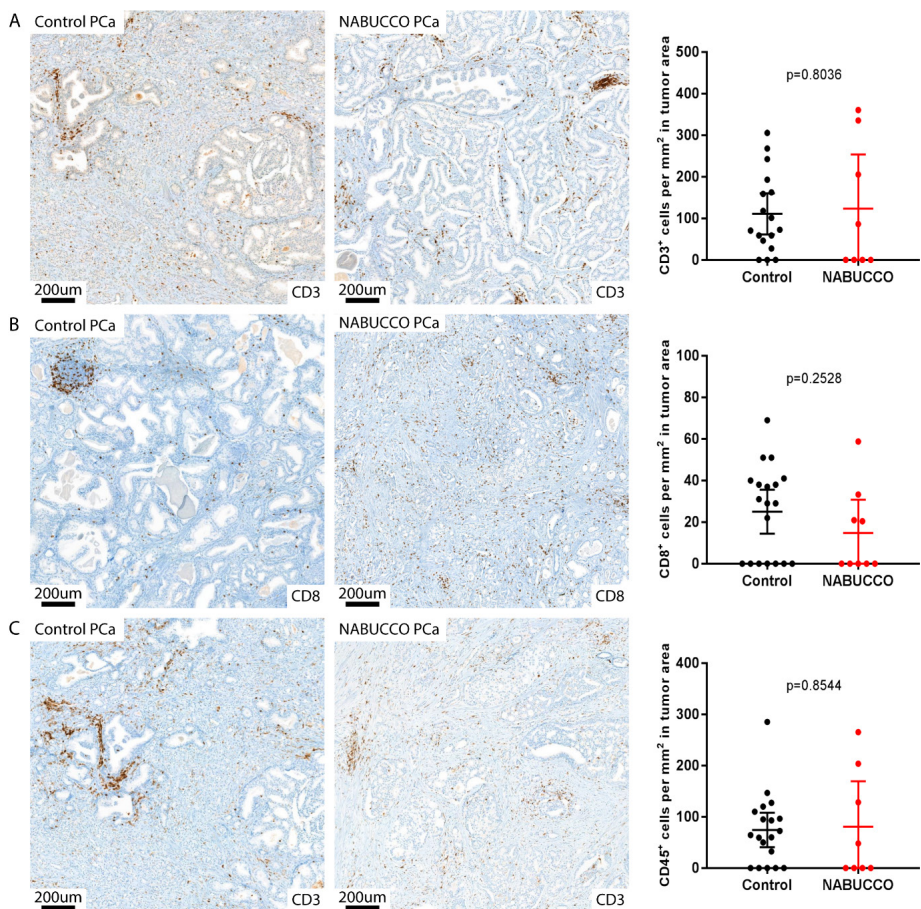
Figure 3 | Expression of CD3, CD8 and CD45 in prostate cancer in NABUCCO cohort and control cohort treated with direct cystectomy. Representative images of CD3 (**A**), CD8 (**B**) and CD45 (**C**) IHC for PCa in a MIBC patient without neo-adjuvant treatment (left) and PCa in a NABUCCO-patient (middle). Graphs (right) show the number of positive cells per mm^2 in the PCa tumor area per cohort per cell surface marker. P-value is given for unpaired t-test, error bars show 95% CI.

6
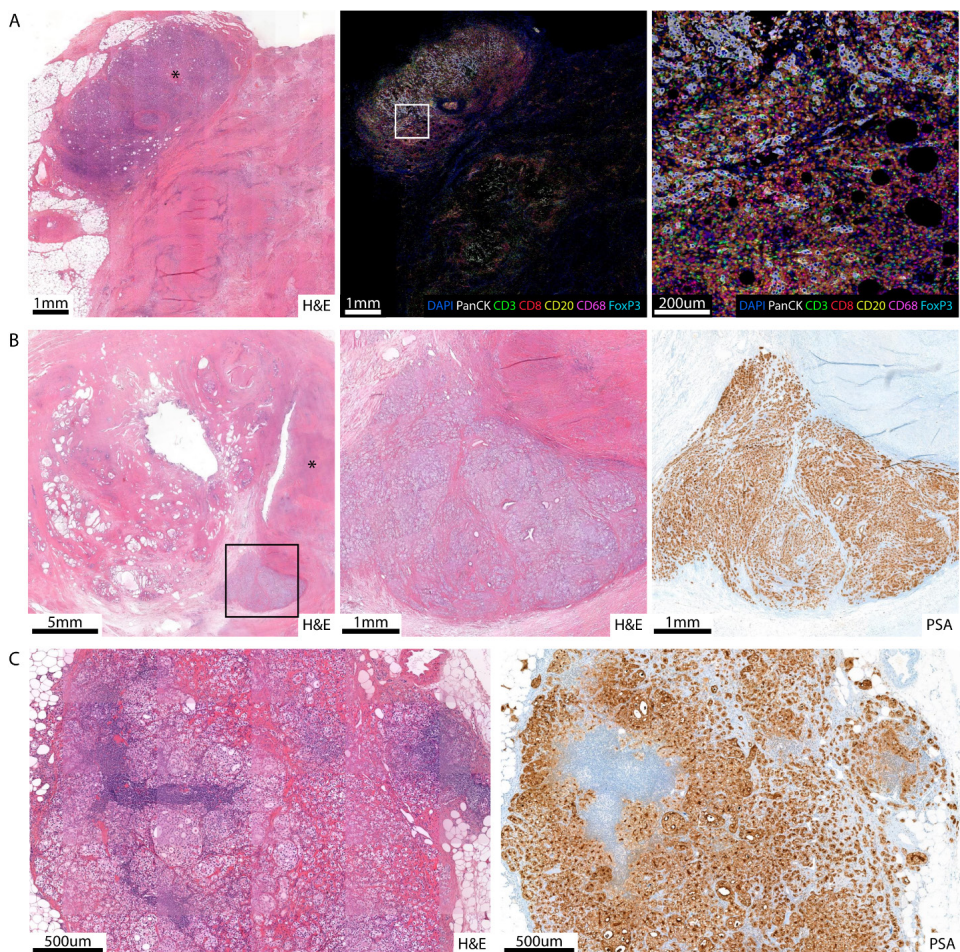
Figure 4 | NABUCCO patient with pT3bN1 incidental PCa. A, Left panel, H&E staining: bladder tumor area with central field of necrosis, indicative of response to ipilimumab plus nivolumab. In the topleft area in the panel, a vital tumor remnant is visible, marked by an asterisk (*). Middle panel, multiplex immunofluorescent staining: Comparable tumor area as visible in the left panel. The white square marks the area that is visible in the right panel. Right panel, multiplex immunofluorescent staining: Close-up shows individual tumor cells (PanCK^{+}), surrounded by T-cells (CD3^{+}CD8^{+/-}), B-cells (CD20^{+}) and macrophages (CD68^{+}). **B,** Left panel, H&E staining: Prostate with field of necrotic bladder tumor on the right, marked by an asterisk (*). The black square marks the area that is visible in the middle and right panel. Middle and right panel: Close-up shows field of PCa (middle: H&E, right: PSA). **C,** PCa cells in local lymph node (left: H&E, right: PSA).

REFERENCES

1. Postow, M.A., Callahan, M.K. & Wolchok, J.D. Immune Checkpoint Blockade in Cancer Therapy. *J Clin Oncol* 33, 1974-1982 (2015).

2. Hodi, F.S.*, et al.* Improved survival with ipilimumab in patients with metastatic melanoma. *N Engl J Med* 363, 711-723 (2010).

3. Borghaei, H.*, et al.* Nivolumab versus Docetaxel in Advanced Nonsquamous Non-Small-Cell Lung Cancer. *N Engl J Med* 373, 1627-1639 (2015).

4. Antonarakis, E.S.*, et al.* Pembrolizumab for Treatment-Refractory Metastatic Castration-Resistant Prostate Cancer: Multicohort, Open-Label Phase II KEYNOTE-199 Study. *J Clin Oncol* 38, 395-405 (2020).

5. Beer, T.M.*, et al.* Randomized, Double-Blind, Phase III Trial of Ipilimumab Versus Placebo in Asymptomatic or Minimally Symptomatic Patients With Metastatic Chemotherapy-Naive Castration-Resistant Prostate Cancer. *J Clin Oncol* 35, 40-47 (2017).

6. Sharma, P.*, et al.* Nivolumab Plus Ipilimumab for Metastatic Castration-Resistant Prostate Cancer: Preliminary Analysis of Patients in the CheckMate 650 Trial. *Cancer Cell* 38, 489-499 e483 (2020).

7. Rozeman, E.A.*, et al.* Identification of the optimal combination dosing schedule of neoadjuvant ipilimumab plus nivolumab in macroscopic stage III melanoma (OpACIN-neo): a multicentre, phase 2, randomised, controlled trial. *Lancet Oncol* 20, 948-960 (2019).

8. Versluis, J.M., Long, G.V. & Blank, C.U. Learning from clinical trials of neoadjuvant checkpoint blockade. *Nat Med* 26, 475-484 (2020).

9. Chalabi, M.*, et al.* Neoadjuvant immunotherapy leads to pathological responses in MMR-proficient and MMR-deficient early-stage colon cancers. *Nat Med* 26, 566-576 (2020).

10. van Dijk, N.*, et al.* Preoperative ipilimumab plus nivolumab in locoregionally advanced urothelial cancer: the NABUCCO trial. *Nat Med* (2020).

11. Bruins, H.M.*, et al.* Incidental prostate cancer in patients with bladder urothelial carcinoma: comprehensive analysis of 1,476 radical cystoprostatectomy specimens. *J Urol* 190, 1704-1709 (2013).

12. Winkler, M.H., Livni, N., Mannion, E.M., Hrouda, D. & Christmas, T. Characteristics of incidental prostatic adenocarcinoma in contemporary radical cystoprostatectomy specimens. *BJU Int* 99, 554-558 (2007).

13. Fong, L.*, et al.* Activated lymphocyte recruitment into the tumor microenvironment following preoperative sipuleucel-T for localized prostate cancer. *J Natl Cancer Inst* 106(2014).

14. Ryan, M.J. & Bose, R. Genomic Alteration Burden in Advanced Prostate Cancer and Therapeutic Implications. *Front Oncol* 9, 1287 (2019).

6

CHAPTER 7

Summary and general discussion

SUMMARY AND GENERAL DISCUSSION

This thesis focuses on systemic preoperative treatment strategies for muscle-invasive bladder cancer (BC). In **Chapter 2** we reviewed the recent advancements in treatment with immune checkpoint inhibitors (ICI) in BC and the relation between its relation with the tumor immune micro-environment (TIME). In **Chapter 3** we have looked primarily at predicting pathological response after neoadjuvant platinum-based chemotherapy based on genomic biomarkers. In **Chapter 4** we retrospectively investigated the effects of neoadjuvant platinum-based chemotherapy on the tumor-immune microenvironment in muscle-invasive BC patients. In **Chapter 5** we have looked in detail at the results from cohort 2 of the NABUCCO trial, where patients were randomized to receive either of two different dosing regimens of ipilimumab and nivolumab. In addition, we set out to predict pathological response and clinical outcome based on circulating tumor DNA (ctDNA) in plasma and urine. In **Chapter 6** we retrospectively assessed the prostate tissue that was part of the radical cystoprostatectomy specimens from NABUCCO cohort 1.

CHAPTER 2 – THE BLADDER CANCER IMMUNE MICRO-ENVIRONMENT IN THE CONTEXT OF RESPONSE TO IMMUNE CHECKPOINT INHIBITION

In Chapter 2 we reviewed the current scientific progress on the BC immune micro-environment in the context of response to ICI. We evaluated recent and current clinical trials that are using ICI and included various aspects and parameters of the tumor immune micro-environment in our review. In addition, we reviewed different methods to modulate the tumor-immune microenvironment to potentially improve the effect of ICI, including the encouraging results with enfortumab vedotin, an antibody-drug conjugate.

Enfortumab vedotin is directed against nectin-4, a protein which is highly expressed in urothelial cancer cells[1]. Encouraging results have been observed when this drug was used as monotherapy in pretreated mUC in the EV-301 trial[2]. In addition, it was recently shown in the EV-302 trial that enfortumab vedotin combined with pembrolizumab led to a significant increase in PFS and OS compared to standard first-line platinum-based chemotherapy in previously untreated mUC patients. Median PFS was 12.5 months for patients treated with enfortumab vedotin combined with pembrolizumab and only 6.3 months for patients treated with platinum-based chemotherapy. Likewise, median OS improved from 16.1 months to 31.5 months[3]. In the preoperative setting, it was shown in the EV-103 trial that patients treated with enfortumab vedotin followed by radical surgery had a pathological complete response rate (ypT0N0) of 34% and pathological downstaging (ypT0/Tis/Ta/T1N0) in 42% of patients [4]. These data support the ongoing phase 3 programs evaluating enfortumab vedotin in combination with pembrolizumab in muscle-invasive BC (KEYNOTE-905/EV-303, KEYNOTE-B15/EV304)[5,6]. Taken together, enfortumab vedotin has

shown some very promising results and it will be very interesting to witness how these treatments will eventually influence the landscape of BC.

CHAPTER 3 – ASSESSMENT OF PREDICTIVE GENOMIC BIOMARKERS FOR RESPONSE TO CISPLATIN-BASED NEO-ADJUVANT CHEMOTHERAPY IN BLADDER CANCER

In Chapter 3 we have looked primarily at predicting pathological response after neoadjuvant cisplatin-based chemotherapy based on genomic biomarkers. We assessed a large cohort of 165 patients treated in 5 different hospitals and found primarily that deleterious mutations in *ERCC2* are associated with a pathological response after neoadjuvant treatment with cisplatin-based chemotherapy. However, mutations in other genes were not related to pathological response. While the conclusion from this work is robust, there are some methodological caveats that require some discussion.

Firstly, it should be noted that a different sequencing approach has been used in the different hospitals where the samples were analyzed. In the NKI-AVL, we performed panel-based deep sequencing and shallow whole-genome sequencing. In Vancouver, whole-exome sequencing was performed (Chapter 3, Supplementary Figure 1). The two cannot be combined without further consideration, with the risk of over- or underestimating the frequency of certain genomic alterations. We have chosen to present the data separately for the NKI-AVL patients including the shallow whole-genome sequencing data in Chapter 3, Supplementary Figure 4, which we believe is the most appropriate approach. Preferably, all samples should have been processed and sequenced in the same center to avoid potential discrepancies and batch effects.

The frequency of genomic alterations in the genes that were assessed in this study are comparable to what has been observed in other cohorts (Chapter 3, Supplementary Table 2).[7,8] However, the absolute number of genomic alterations is relatively low. Potentially, this could lead to a lack of statistical power to assess correlations between genomic alterations and outcome after cisplatin-based chemotherapy. Indeed, we observed a numerically higher mutation rate for *ERBB2*, *ATM* and *RB1* in responders compared to non-responders (Chapter 3, Figure 1). We cannot exclude that mutations in these genes were significantly associated with pathological response if we had assessed a sufficiently large number of patients.

The trend for improved progression-free survival (PFS) and overall survival (OS) for mutations in *ERCC2* is compelling and it would be interesting to assess a larger number of patients to see if this trend is significant. However, a possible prognostic effect of *ERCC2* cannot be excluded here. To further investigate this potential prognostic effect, it would be necessary to compare PFS and OS for patients with mutations in *ERCC2* that are either treated with cisplatin-based chemotherapy

followed by radical cystectomy or with a direct radical cystectomy (and no neoadjuvant cisplatin-based chemotherapy).

Finally, with no approved alternative preoperative treatment options currently available, it is debatable what the current clinical impact is of the findings described in this paper. The main case where it could be useful is when there is doubt about whether to treat a patient with neoadjuvant chemotherapy and sequencing data is available for *ERCC2* (or, to a lesser degree, any of the other markers that were investigated). When a relevant mutation is found, this would be an argument in favor of pre-treating patients with neoadjuvant chemotherapy, if the mutation is absent, the choice should be based on clinical parameters instead, as patients without an *ERCC2* mutation still can respond to neoadjuvant cisplatin-based chemotherapy. However, with new encouraging neoadjuvant treatment strategies becoming available, there is an unmet need to select the optimal treatment for every individual patient. To help in this endeavor, (genomic) biomarkers to predict pathological response and clinical outcome might become more appealing.

CHAPTER 4 – PLATINUM-BASED CHEMOTHERAPY INDUCES OPPOSING EFFECTS ON IMMUNOTHERAPY RESPONSE-RELATED SPATIAL AND STROMAL BIOMARKERS IN THE BLADDER CANCER MICROENVIRONMENT

In Chapter 4 we collected paired tumor tissue before and after neoadjuvant platinum-based chemotherapy from 116 muscle-invasive BC patients. We used RNA sequencing, multiplex immunofluorescence and immunohistochemistry on the pre- and post-treatment tissue samples to assess the effect of platinum-based chemotherapy on the TIME in a comprehensive manner. Primarily, we were interested in potential implications for subsequent response to ICI, as the results of the CheckMate 274 trial suggested that BC patients treated with neoadjuvant platinum-based chemotherapy and radical surgery benefit from adjuvant nivolumab[9]. We found that the percentage of PD-L1^{+} immune cells and the percentage of intratumoral CD8^{+} T-cells increased after neoadjuvant treatment. Conversely, we also observed an increase in fibroblast-based TGF-β signaling and an increase in distance from immune cells to the nearest cancer cell after treatment.

We have included patients with ypT1-4aNx after treatment with neoadjuvant chemotherapy and radical surgery. We opted to exclude patients without invasive BC after treatment, as the TIME in those patients would per definition not contain any vital tumor cells and would consist of only necrotic tissue, fibrosis and immune cells. Consequently, we have only included non-responding patients in our cohort and based our conclusions on this subpopulation of patients. However, this population is particularly relevant as it could potentially benefit from adjuvant nivolumab as has been shown in the CheckMate 274.

There are multiple parameters in the manuscript that are used as surrogate markers for potential benefit of subsequent ICI treatment, mostly based on historic data. Unfortunately, there are very few patients in our cohort that have received adjuvant treatment with ICI. It would be of interest to assess the patients that have been treated with neoadjuvant chemotherapy and adjuvant nivolumab in the CheckMate 274 and compare the patients that responded to adjuvant nivolumab to those patients that did not respond. However, defining response for adjuvant treatment is not as straightforward as it is for neoadjuvant treatment. Disease-free survival is presumably the most sensible outcome measure but this is also dependent on pathological response after radical surgery. Regardless, when comparing radical surgery specimens from patients that responded to nivolumab versus those that did not respond to nivolumab, biomarkers could emerge that are truly predictive of response to adjuvant treatment. It would be especially interesting if tissue parameters can be identified in transurethral resection of the bladder tumor (TUR-BT) samples obtained prior to neoadjuvant platinum-based chemotherapy that correlate with immune-induction and would benefit from adjuvant nivolumab. One could imagine a treatment-naïve phenotype that is not necessarily prone to respond to neoadjuvant platinum-based chemotherapy, but is indeed 'pushed' by this treatment towards a phenotype that is prone to respond to adjuvant nivolumab.

It is currently still unclear how platinum-based chemotherapy and ICI interact with each other in the context of bladder cancer. In this study we have found arguments that support combining platinum-based chemotherapy, such as increased intratumoral CD8^{+} T-cells and increased expression of PD-L1 on immune cells. However, we have also found an increase in TGF-β signaling and an increase in distance from immune cells to the nearest cancer cell after treatment, which could suggest there is an antagonistic relationship between these two treatment strategies. These observations may explain conflicting results in first-line metastatic studies, where positive results for the addition of nivolumab to cisplatin-based chemotherapy in the CheckMate 901[10] were recently published after two earlier negative trials. It is likely that we should be specific when discussing the interaction between chemotherapy and ICI, as not all chemotherapy and ICI treatments are interchangeable and show the same results when used in combination. Nivolumab (PD-1 inhibitor) in particular seems to synergize with prior cisplatin-based chemotherapy specifically[9,10], whereas atezolizumab and pembrolizumab did not synergize with carboplatin-based regimens[11,12]. The next challenge will be to differentiate the different treatment strategies and find out why certain specific combinations work better when combined.

CHAPTER 5 – HIGH- OR LOW-DOSE PREOPERATIVE IPILIMUMAB PLUS NIVOLUMAB AND PREDICTING OUTCOME USING CTDNA IN THE NABUCCO TRIAL

In Chapter 5 we have looked in detail at the results from cohort 2 of the NABUCCO trial. In this trial, thirty patients were randomized to receive either two cycles of ipilimumab 3 mg/kg plus

nivolumab 1 mg/kg (cohort 2A) or two cycles of ipilimumab 1 mg/kg plus nivolumab 3 mg/kg (cohort 2B), followed in both cohorts by a third cycle of nivolumab 3 mg/kg. We found that 6/14 (43%) patients treated in cohort 2A had a pathological complete response, whereas only 1/14 (7%) patient in cohort 2B had a pathological complete response. In addition, we set out to predict pathological response and clinical outcome based on ctDNA in plasma and urine in patients treated in NABUCCO cohort 1 and 2 and found a strong correlation between the absence of ctDNA in plasma before radical surgery and pathological response and OS in all cohorts.

OPTIMAL DOSE OF COMBINED IPILIMUMAB PLUS NIVOLUMAB

When comparing the efficacy between the three separate NABUCCO cohorts, we observe a similar pathological complete response rate of 46% in cohort 1 and 43% in cohort 2A (*P*=1.00, Chapter 5, Figure 1). In contrast, cohort 2B only shows a complete pathological response rate of 7%, which is statistically different compared to cohort 1 (*P*=0.03, Chapter 5, Figure 1). However, we did not observe a statistically significant difference in pathological response rate between cohort 2A and 2B (*P*=0.08). The apparent difference in efficacy between the three cohorts could be explained by the higher dose of ipilimumab (3 mg/kg) that is used in cohort 1 and 2A, whereas a lower dose of ipilimumab (1 mg/kg) is used in cohort 2B. This would then suggest that a higher dose of ipilimumab (combined with nivolumab) leads to a higher efficacy and better overall results compared to a lower dose of ipilimumab (combined with nivolumab) in muscle-invasive BC. However, as mentioned before, there is no statistically significant difference when comparing pathological complete response rates between cohort 2A and 2B. In addition, while the high dose of ipilimumab is a common denominator between cohorts 1 and 2A, the two cohorts are not identical, with the main difference being the addition of nivolumab 1 mg/kg to the first treatment cycle in cohort 2A. Regardless, we believe differences in immunotherapy-related toxicity and observations from other studies support our hypothesis that a higher dose of ipilimumab (combined with nivolumab) leads to a higher efficacy and better overall results compared to a lower dose of ipilimumab (combined with nivolumab) in muscle-invasive BC.

CORRELATION BETWEEN DOSE, TOXICITY AND EFFICACY FOR COMBINED IPILIMUMAB PLUS NIVOLUMAB

We observed a numerically higher rate of all grade immunotherapy-related adverse events in cohort 1 and 2A in compared to cohort 2B (cohort 1: 96%; cohort 2A: 100%; cohort 2B: 73%, Chapter 5, Supplementary Table 2). Likewise, we also observed a numerically higher rate of grade ≥3 immunotherapy-related adverse events (cohort 1: 58%; cohort 2A: 40%; cohort 2B: 20%; Chapter 5, Supplementary Table 2). A dose-efficacy as well as a dose-toxicity relation has been described for ipilimumab as monotherapy in metastatic melanoma[13,14]. These data suggest that there would also be a correlation between toxicity and efficacy. A similar dose-toxicity relation has been described for ipilimumab in combination with nivolumab in multiple studies that tested the efficacy and/or tolerability of ipilimumab 3 mg/kg plus nivolumab 1 mg/kg compared to ipilimumab 1 mg/kg plus nivolumab 3 mg/kg directly[15-22]. However, the dose-efficacy relation of

ipilimumab in combination with nivolumab is less clear and is potentially dependent on tumor type and disease stage. However, regardless of tumor type, ipilimumab 3 mg/kg was at least as efficious compared to ipilimumab 1 mg/kg in all studies mentioned. This could suggest a correlation between efficacy and toxicity for ipilimumab in combination with nivolumab.

OPTIMAL DOSE OF IPILIMUMAB AND NIVOLUMAB IN OTHER STUDIES
In the CheckMate 032 trial, patients with advanced BC were treated with either nivolumab monotherapy, or in combination with ipilimumab with different dose combinations[20]. While this trial was not properly powered to detect a statistical difference in objective response rate or OS, both these outcome measures were numerically better in patients treated with plus 3 mg/kg ipilimumab plus 1 mg/kg nivolumab compared to patients treated with 1 mg/kg ipilimumab plus 3 mg/kg nivolumab or nivolumab monotherapy[20]. Notably, a similar trend was also observed in esophageal cancer and recurrent small-cell lung carcinoma in the same trial[17,18]. However, no difference in efficacy was observed in stage III melanoma patients that were treated with either a high dose of ipilimumab (3 mg/kg) plus nivolumab or a low dose of ipilimumab (1mg/kg) plus nivolumab in the OpACIN-neo trial[16]. Thus, it should be concluded that the trend for increased efficacy for a high dose of ipilimumab compared to a low dose (in combination with nivolumab) does not hold true for all cancer types and/or disease stages. While the precise underlying mechanism is not completely understood, we hypothesize that a higher dose of ipilimumab helps to recruit additional naïve T-cells to the tumor micro-environment, which are subsequently activated due to the effect of nivolumab. Potentially, tumors like stage III melanoma that are prone to respond to preoperative ipilimumab 1 mg/kg (in combination with nivolumab) are already prone to respond to checkpoint inhibitors to such an extent that a higher dose of ipilimumab (in combination with nivolumab) confers no additional benefit in terms of efficacy.

PREOPERATIVE COMBINED IMMUNOTHERAPY VERSUS NEOADJUVANT CISPLATIN-BASED CHEMOTHERAPY
The results from the NABUCCO trial and from other preoperative immunotherapy trials suggest that preoperative (ICI) followed by radical surgery could be a promising alternative for patients with muscle-invasive BC unfit to receive cisplatin-based chemotherapy, for whom there are currently no approved preoperative treatment strategies available. However, with pathological complete response rates approaching 50% for patients treated with high dose ipilimumab combined with nivolumab, it would be interesting to directly compare this treatment to standard cisplatin-based neoadjuvant chemotherapy in a randomized trial.

Previously, we retrospectively analyzed all patients with muscle-invasive BC (cT3-4aNx or cT1-4aN1-3) that were treated in the NKI-AvL during the period of inclusion of the first cohort of the NABUCCO trial[23]. We compared patients that were treated with preoperative ipilimumab plus nivolumab in NABUCCO to patients that were treated with neoadjuvant (or induction) cisplatin-based chemotherapy. Pathological complete response rate in the latter group was 22% (compared

to 46% in NABUCCO). Both PFS and OS was superior for the patients treated in NABUCCO[23]. As discussed prior, cT2-4aN0 BC patients were treated with dose-dense MVAC in the VESPER trial leading to a pathological complete response in 42% of patients[24]. However, the study population consisted primarily of cT2N0 patients (197/218), and patients with lymph node metastases were excluded[24]. Another study investigated cT3-4aN0 patients treated with dose-dense MVAC and observed a pathological complete response rate of 28%[25].

In the CheckMate 274 trial, improved disease-free survival was observed in patients treated with adjuvant nivolumab, in particular in patients that were previously treated with neoadjuvant cisplatin-based chemotherapy and with a high expression of PD-L1 on tumor cells[9]. This has led to approval of nivolumab as adjuvant treatment for muscle-invasive BC by the FDA in 2021. At an extended data analysis presented at ASCO GU 2023 it was shown that the 24-month disease-free survival rate for patients treated with adjuvant nivolumab was 48.4% compared to 38.8% for the placebo group. By comparison, the 24-months disease-free survival rate for NABUCCO cohort 1 is 92%. Note that patients with a complete pathological response after neoadjuvant treatment were not included in the CheckMate 274, which would probably have improved the disease-free survival rates presented in this trial. Moreover, it should be noted that there are currently no published data on OS for the CheckMate 274 trial. This is important, as disease-free survival does not necessarily translates to an OS benefit, potentially only delaying recurrence. If patients recur, they might have fewer treatment options in the metastatic setting. Despite this caveat, the combination of dose-dense MVAC for muscle-invasive BC, followed by radical cystectomy and adjuvant nivolumab for patients with residual muscle-invasive disease or lymph node metastases can be considered the current optimal treatment for patients with muscle-invasive BC. It should be noted that trials assessing novel treatments such as enfortumab vedotin as preoperative treatment for muscle-invasive BC are expected to impact the treatment landscape[26]. For that reason, it is difficult to define a robust state-of-the-art treatment to compare novel treatments against that will not be outdated when a new trial has run its course. However, this should not be a reason to disregard findings from new encouraging developments.

MACBETH TRIAL: A PHASE III TRIAL OF PREOPERATIVE DOSE-DENSE METHOTREXATE, VINBLASTINE, DOXORUBICIN, AND CISPLATIN FOLLOWED BY ADJUVANT NIVOLUMAB COMPARED TO PREOPERATIVE IPILIMUMAB PLUS NIVOLUMAB FOR LOCALLY ADVANCED UROTHELIAL CANCER

As part of the discussion of this thesis, I would like to propose a randomized phase 3 trial where we compare preoperative dose-dense MVAC followed by adjuvant nivolumab (standard arm) versus combined preoperative ipilimumab (3 mg/kg) plus nivolumab as is described in NABUCCO cohort 2A, with adjuvant cisplatin-based chemotherapy in case of residual muscle-invasive disease or lymph node metastases after radical surgery (experimental arm, Figure 1). The recommended standard-of-care for eligible patients is cisplatin-based neoadjuvant chemotherapy followed by radical surgery, however, especially in the context of ICI, we believe adding adjuvant nivolumab

for eligible patients is presumably the optimal choice, as discussed prior[27]. The main inclusion criteria will include a WHO performance score 0-1, cT3-4aN0M0 or cT1-4aN1-3M0 urothelial cancer, including upper tract tumors. All patients should be cisplatin-eligible and be eligible to receive ipilimumab and nivolumab. Primary outcome will be pathological complete response after radical surgery for the intention-to-treat population and OS after 24 months. Secondary outcomes will include complete pathological downstaging after surgery (ypTa/Tis/T1N0), toxicity and extended OS and PFS.

Based on the results of the trials that tested dose-dense MVAC, we assume a pathological complete response rate of 30% for the standard arm. This is lower than the 42% observed in the VESPER trial, however, as discussed prior, this trial mainly included cT2N0 patients[24]. We estimate >28% pathological complete response rate (as was observed in the retrospective trial in cT3-4a patients) since our patients will be relatively good condition, WHO 0-1 and eligible to receive either combination treatment. We assume a pathological complete response rate of 43% for the patients treated with combined ipilimumab plus nivolumab, as was also observed in NABUCCO cohort 2A. We also assume an α of 0.05 and a power of 80% (β = 0.2). This results in a total population size of N=428, divided equally over 2 cohorts.

The 24-month PFS and OS rates for patients treated in NABUCCO cohort 1 is 92%. The 24-month PFS and OS data for patients treated in NABUCCO cohort 2A is still currently being analyzed. Three cases of disease progression and three cases of death have been reported as of 31 March 2022, the data cut-off date used for the manuscript (Chapter 5, Extended Data Figure 2). Taken together, we conservatively estimate that the eventual PFS and OS will be around 82% for both cohort 1 and 2A combined after 24 months. The 24-month PFS rate for patients treated with adjuvant nivolumab in the CheckMate 274 is 48.4%. When we proportionally include follow-up for fictive patients with locally advanced disease that would have had a pathological complete response or complete pathological downstaging after neoadjuvant or induction cisplatin-based chemotherapy, we get to a total of 62% PFS after 24 months (based on the data presented by Einerhand *et al.*, assuming 34% pathological complete downstaging of which 88% will have shown no progression and adjuvant therapy for all patients with residual muscle-invasive disease)[23]. As no OS data is available for the CheckMate 274, and similar rates for PFS and OS have been found in both NABUCCO cohort 1 and 2a, we will assume 62% and 82% as surrogate numbers for the sake of addressing whether we would have sufficient statistical power in our study to detect a difference. Based on an α of 0.05 and a power of 80% (β = 0.2), this results in a total required number of participants of N=156, divided equally over 2 cohorts. In conclusion, a total study population of 428 will have the statistical power to address both a difference in pathological complete response and an eventual difference in OS.

7
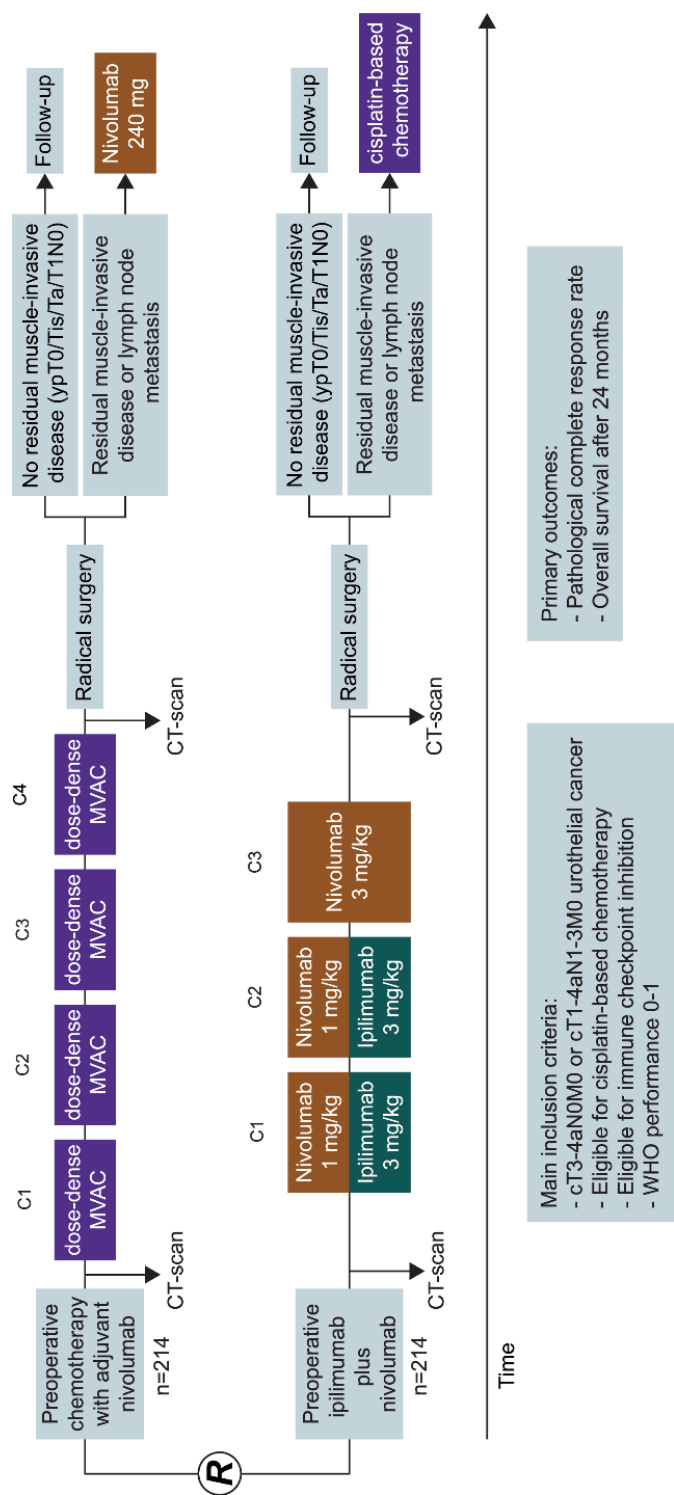
Figure 1 | Graphic overview of MacBeth Trial. Eligible patients are randomized equally (1:1) over two arms. Patients in the first arm will receive either four doses of dose-dense MVAC chemotherapy followed by radical surgery and adjuvant nivolumab for up to one year, as described for the CheckMate 274 trial. In the experimental arm, patients will receive ipilimumab and nivolumab as described for cohort 2A in the NABUCCO trial, followed by adjuvant cisplatin-based chemotherapy according to standard practices.

CTDNA IN PLASMA TO PREDICT PATHOLOGICAL RESPONSE AND CLINICAL OUTCOME

We found a strong correlation between the presence of ctDNA in plasma prior to radical surgery and pathological response and clinical outcome. In patients in cohort 1 and 2 of NABUCCO combined we found that ctDNA was no longer detectable in the last plasma measurement prior to surgery in seventeen (94%) patients that had no residual muscle-invasive disease after surgery (responders). In contrast, ctDNA was no longer detectable in the last plasma measurement prior to surgery in only six (29%) patients that had residual muscle-invasive disease or lymph node metastases after treatment (non-responders). While statistically significant, the clinical relevance of this biomarker is particularly apparent by looking at the outliers. There was no plasma sample available prior to surgery for one responder. The final available sample (taken before the third treatment cycle) still showed detectable ctDNA. However, there are four other responders that still did show detectable ctDNA prior to the third treatment cycle, of which all had no detectable ctDNA prior to surgery. In addition, none of the non-responders that had detectable ctDNA prior to the third cycle had subsequent undetectable ctDNA prior to surgery. Following this trend, it could be expected that the patient with detectable ctDNA prior to the third treatment cycle would have shown undetectable ctDNA if a sample prior to surgery would have been available.

When looking specifically at the six non-responders that have no detectable ctDNA prior to surgery, we find that four of these patients did not show any signs of disease recurrence during follow-up. Three of these patients had a single lymph node micrometastasis, and one other had residual muscle-invasive disease. However, two other patients with residual muscle-invasive disease did show disease recurrence, which are shown as events in patients with no detectable ctDNA prior to surgery (blue line) in Chapter 5, Figure 2a. Overall, the positive predictive value for the presence of ctDNA and disease recurrence is 59% (10/17). The negative predictive value, ie. the number of patients with absence of ctDNA prior to surgery and no disease recurrence is 92% (22/24). We can compare this to the predictive value of pathological response after surgery. For this comparison we can include the patients from other centers which were not included in the ctDNA analysis as these samples had not been analyzed. When interpreting these numbers, it should be noted that radical surgery is not a diagnostic procedure by itself and very likely influences the chance of disease recurrence, which is in contrast to blood withdrawal for the analysis of ctDNA in plasma. Overall, the positive predictive value for the presence of muscle-invasive disease and/or lymph node metastasis (non-responders) and disease recurrence is 42% (11/26). The negative predictive value for absence of muscle-invasive disease and/or lymph node metastasis (responders) and no disease recurrence is 96% (25/26). Based on these results, we could argue that the presence of ctDNA rivals pathological response after radical surgery to predict PFS after preoperative treatment with combined ipilimumab and nivolumab in muscle-invasive BC. Indeed, a recent study on ctDNA in urothelial cancer patients treated with neoadjuvant chemotherapy followed by surgery also concluded that ctDNA status before surgery and ctDNA dynamics during neoadjuvant chemotherapy both outperformed pathologic downstaging in predicting treatment efficacy and patient outcomes after radical cystectomy[28].

7
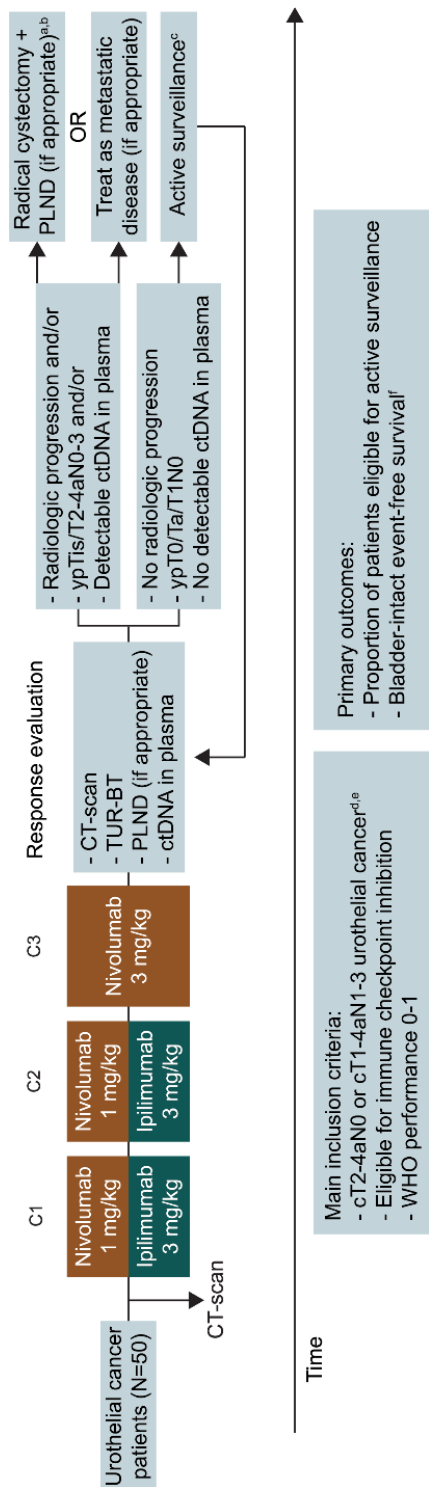
Figure 2 | Graphic overview of the Night's Dream Trial. Eligible patients receive ipilimumab and nivolumab as described for cohort 2A in the NABUCCO trial, followed by a response evaluation. Based on the outcome, patients will be followed with active surveillance or treated with radical cystectomy with a pelvic lymph node dissection if appropriate. Depending on the on the response evaluation outcome, patients will be treated with BCG or as metastatic disease instead. a) Alternatively, eligible patients can be treated with chemoradiation; b) Alternatively, eligible patients with CIS can be treated with BCG; c) Active surveillance will include regular cystoscopies, CT-scans and ctDNA in plasma; d) A maximum of 50% of cT2N0 patients will be permitted; e) Patients with lymph node metastasis at baseline will be treated with a PLND during response evaluation in addition to TUR-BT. *TUR-BT: Transurethral resection of the bladder tumor, ctDNA: circulating tumor DNA, PLND: Pelvic lymph node dissection*

CTDNA IN URINE TO PREDICT PATHOLOGICAL RESPONSE IN THE BLADDER

In contrast to ctDNA in plasma, ctDNA in urine was not predictive for pathological response or PFS. When looking at the data in detail, a number of observations can be made. Primarily, when looking at the graph in Chapter 5, Extended Data Figure 6a, we observe that a number of patients with a pathological complete response still show detectable ctDNA in urine prior to surgery. This could be explained by residual non-vital tumor that is being degraded and is still actively or passively shedding cell-free DNA. In addition, ctDNA is also detected prior to surgery in patients with residual non-muscle-invasive disease (Chapter 5, Extended Data Figure 6). Finally, we have one example of patient with a complete pathological response in the bladder and a single lymph node metastasis that showed rapid disease progression after treatment. This patient showed clearance of ctDNA in the urine prior to surgery, but did show increasing levels of ctDNA in plasma over the course of treatment. This exemplifies that urine possibly reflects the bladder micro-environment but does not reflect the systemic presence of ctDNA which is probably more relevant in terms of disease progression.

RECENT DEVELOPMENTS FOR BLADDER-SPARING TREATMENT IN MUSCLE-INVASIVE BLADDER CANCER

Radical cystectomy is a surgical procedure with significant morbidity and mortality[29]. In NABUCCO, three patients refused radical surgery, one of whom was treated with transurethral resection of the bladder tumor and a lymph node dissection. Two patients refused surgery altogether and are currently in follow-up. None of these patients did show any signs of disease recurrence.

Another recent trial (HCRN GU16-257) investigated the feasibility of cisplatin plus gemcitabine plus nivolumab in cT2-4N0M0 urothelial cancer patients without standard consolidating treatment[30]. After initial treatment and clinical restaging, 33 patients (43%) achieved a clinical complete response and opted to forego direct radical cystectomy. Nine of these patients developed a local recurrence and were treated with a salvage radical cystectomy. Of these 33 patients, two developed distant metastases during follow-up[30]. Given these encouraging results and the high rate of pathological complete response after treatment with ipilimumab plus nivolumab in NABUCCO, we would argue that foregoing consolidating treatment could also be feasible in a subset of patients treated with ipilimumab and nivolumab.

NIGHT'S DREAM TRIAL: A PHASE 2 TRIAL OF COMBINED NIVOLUMAB PLUS IPILIMUMAB FOLLOWED BY ACTIVE SURVEILLANCE FOR LOCALIZED OR LOCALLY ADVANCED UROTHELIAL CANCER

As part of the discussion of this thesis, I would like to propose a phase 2 trial to assess the feasibility of treating patients with combined ipilimumab (3 mg/kg) plus nivolumab as is described in NABUCCO cohort 2A, followed by clinical restaging based on radiological imaging, pathological assessment of the bladder tumor by TUR-BT and measuring ctDNA in plasma. The predictive value of ctDNA in plasma prior to surgery might aid to properly select patients that could safely forego

or postpone radical cystectomy. Patients with no signs of radiologic progression, no evidence of muscle-invasive disease (or carcinoma *in situ*) after transurethral resection of the bladder tumor and no detectable ctDNA in plasma after treatment with ipilimumab and nivolumab will not receive any consolidating treatment but instead will be regularly monitored with radiological imaging, cystoscopy and ctDNA measurements. Patients with evidence of residual muscle-invasive disease (or carcinoma *in situ*) after transurethral resection, detectable ctDNA in plasma and/or radiologic progression will be treated with radical cystectomy including removal of the locoregional lymph nodes. Patients with ypTisN0 will be counseled for treatment with BCG or radical cystectomy accordingly. Alternatively, patients will be treated with chemoradiation treatment if eligible. Patients with local recurrence during active surveillance will be treated accordingly with a re-TUR-BT, BCG, radical cystectomy (with PLND) or chemoradiation treatment. Patients with lymph node positive disease will be eligible for the study as we have observed complete pathological responses in NABUCCO in these patients. However, these patients will be treated with a pelvic lymph node dissection in addition to the transurethral resection of the bladder tumor. Patients with cT2N0 tumors will also be eligible for this study as these patients have an *a priori* lower chance of disease recurrence after treatment and will benefit from a bladder-sparing treatment. However, this patient category will be limited to have a sufficient number of patients with locally advanced disease participating. Patients with upper tract tumors will not be eligible in this trial.

Overall, this trial will include patients with cT2-4aN0M0 or cT1-4aN1-3M0 BC. All patients should be eligible to receive ipilimumab and nivolumab and should have a WHO performance score of 0-1. Primary outcome will be proportion of patients eligible for active surveillance meaning no signs of radiologic progression, no evidence of muscle-invasive disease (or carcinoma *in situ*) after transurethral resection of the bladder tumor, no vital lymph node metastasis in case of a PLND and no detectable ctDNA in plasma. Bladder-intact event-free survival for active surveillance-eligible patients will be monitored as a co-primary endpoint as recommended[31]. Events are defined as muscle-invasive recurrence in the bladder or in the distal ureter, nodal or distant recurrence, death related to disease progression or related to treatment and/or radical cystectomy. Secondary outcomes will include immune-related toxicity, changes in ctDNA as measured in plasma during treatment with, rate of non-muscle invasive recurrence, PFS and OS for the population as a whole and pathological complete response (ypT0Nx) and residual non-muscle-invasive disease (ypTa/Tis/T1Nx) for those patients undergoing radical cystectomy, Forty-seven percent of patients In NABUCCO cohort 1 and 2A combined had no residual muscle-invasive disease or carcinoma *in situ* after radical cystectomy. In addition, a total of 6 patients (16%) showed disease progression during follow-up in NABUCCO 1 and 2A combined. Taking these numbers into account, we will enroll a total of 50 patients in this trial, including a maximum of 50% (n=25) patients with cT2N0 tumors. We assume a pathological response rate (ypT0/Ta/T1N0) of around 50% (n=25). Survival outcomes for this population will be compared to results from NABUCCO cohort 1 and 2A and from the INDIBLADE study.

CHAPTER 6 – A SERENDIPITOUS PRE-OPERATIVE TRIAL OF COMBINED IPILIMUMAB PLUS NIVOLUMAB FOR LOCALIZED PROSTATE CANCER

In chapter 6, we examined the incidence and characteristics of prostate cancer in sixteen patients treated with ipilimumab and nivolumab followed by radical cystoprostatectomy in NABUCCO cohort 1. In addition, we compared the findings from NABUCCO to a control cohort consisting of 121 patients treated with muscle-invasive BC that were treated with neoadjuvant chemotherapy followed by radical cystoprostatectomy or treated with a direct radical cystoprostatectomy. Surprisingly, the incidence of prostate cancer, pT-stage, Gleason score and infiltration of immune cells were all comparable between the NABUCCO cohort and the control cohort. In conclusion, we found no evidence that ipilimumab plus nivolumab induces a meaningful anti-cancer immune response in localized prostate cancer.

It is currently not well understood why localized prostate cancer does not respond well to immunotherapy. This study does provide some insights into this phenomenon. Firstly, we observe no correlation between (lack of) response in muscle-invasive BC and the incidence of prostate cancer, supporting the idea that the patient immune system is still intact and not suppressed due to the presence of prostate cancer. In addition, the prostate tumor microenvironment could potentially disrupt the function of ICI antibody molecules or prevent access to relevant immune cells. However, one particular patient in the NABUCCO cohort with invasion of muscle-invasive BC into the prostate showed an impressive response in the bladder and also in part of the bladder tumor that was invading the prostate (Chapter 6, Figure 4). In contrast, no histopathological signs of treatment response were observed in the concurrent prostate tumor or in three prostate cancer lymph node metastases (Chapter 6, Figure 4). This suggests that the prostate micro-environment is not necessarily detrimental for the effect of ICI.

Tumor mutational burden might also explain why prostate cancer does not respond well to treatment with ICI. It has been found that the average tumor mutational burden is lower in prostate cancer compared to tumor types that are more prone to respond to treatment with ICI, such as melanoma, non-small cell lung cancer and BC[32]. In addition, a correlation between response rate and tumor mutational burden in metastatic prostate cancer patients treated with ipilimumab plus nivolumab in the Checkmate 650 trial[33]. Finally, it has been observed that patients with localized prostate cancer have a lower tumor mutational burden compared to patients with metastatic prostate cancer[34].

As the diagnosis of prostate cancer was not actively investigated in patients who were planned for cystoprostatectomy, no adequate pre-treatment prostate cancer information is available. This excludes the possibility to properly compare pre- and post-treatment prostate cancer characteristics, which could be considered necessary to properly evaluate the treatment effect of

ipilimumab and nivolumab on localized prostate cancer. Potentially, there may have been patients with prostate cancer with a partial or complete response after treatment with ipilimumab and nivolumab that was no longer detectable at the time of radical cystoprostatectomy. However, we observed that the incidence and grade of prostate cancer was not statistically different between the different cohorts. Of note, the incidence of prostate cancer was numerically slightly higher in the patients treated with ipilimumab and nivolumab, and this cohort also included the single patient with prostate cancer-related lymph node metastases.

In conclusion, there is only limited evidence for the efficacy of ICI in prostate cancer, which is in sharp contrast other cancer types. In our study we also did not find any evidence for a relevant effect of ipilimumab plus nivolumab on incidental, localized prostate cancer. More research is required to find out if there are other immune-related (combination) treatments that will improve the treatment of prostate cancer.

CLOSING WORDS

For many years, cisplatin-based chemotherapy followed by radical surgery was the only option for patients with locally advanced BC and provided only a marginal benefit. In the last years, a plethora of new treatment options and combinations thereof have become available including ICI and enfortumab vedotin. In addition, with improved efficacy of neoadjuvant treatment strategies, bladder-sparing treatments are currently becoming a valid alternative treatment for an increasing number of patients.

As we conclude this exciting chapter of research, let us not only celebrate the advancements made but also acknowledge the ongoing journey ahead. With continued dedication and collaboration, we can pave the way for a future where bladder cancer treatment is not just about managing the disease but about achieving enduring remission and improved quality of life for all those affected.

REFERENCES

1. Challita-Eid, P.M., *et al.* Enfortumab Vedotin Antibody-Drug Conjugate Targeting Nectin-4 Is a Highly Potent Therapeutic Agent in Multiple Preclinical Cancer Models. *Cancer Res* 76, 3003-3013 (2016).

2. Powles, T., *et al.* Enfortumab Vedotin in Previously Treated Advanced Urothelial Carcinoma. *N Engl J Med* 384, 1125-1135 (2021).

3. Powles, T.B., *et al.* LBA6 EV-302/KEYNOTE-A39: Open-label, randomized phase III study of enfortumab vedotin in combination with pembrolizumab (EV+P) vs chemotherapy (Chemo) in previously untreated locally advanced metastatic urothelial carcinoma (la/mUC). *Annals of Oncology* 34, S1340 (2023).

4. Sridhar, S., *et al.* 2365MO Study EV-103 cohort L: Perioperative treatment w/ enfortumab vedotin (EV) monotherapy in cisplatin (cis)-ineligible patients (pts) w/ muscle invasive bladder cancer (MIBC). *Annals of Oncology* 34, S1203 (2023).

5. Necchi, A., *et al.* Phase 3 KEYNOTE-905/EV-303: Perioperative pembrolizumab (pembro) or pembro + enfortumab vedotin (EV) for muscle-invasive bladder cancer (MIBC). *Journal of Clinical Oncology* 41, TPS585-TPS585 (2023).

6. Hoimes, C.J., *et al.* KEYNOTE-B15/EV-304: Randomized phase 3 study of perioperative enfortumab vedotin plus pembrolizumab versus chemotherapy in cisplatin-eligible patients with muscle-invasive bladder cancer (MIBC). *Journal of Clinical Oncology* 39, TPS4587-TPS4587 (2021).

7. Cancer Genome Atlas Research, N. Comprehensive molecular characterization of urothelial bladder carcinoma. *Nature* 507, 315-322 (2014).

8. Robertson, A.G., *et al.* Comprehensive Molecular Characterization of Muscle-Invasive Bladder Cancer. *Cell* 171, 540-556 e525 (2017).

9. Bajorin, D.F., *et al.* Adjuvant Nivolumab versus Placebo in Muscle-Invasive Urothelial Carcinoma. *N Engl J Med* 384, 2102-2114 (2021).

10. van der Heijden, M.S., *et al.* Nivolumab plus Gemcitabine-Cisplatin in Advanced Urothelial Carcinoma. *N Engl J Med* 389, 1778-1789 (2023).

11. Powles, T., *et al.* Pembrolizumab alone or combined with chemotherapy versus chemotherapy as first-line therapy for advanced urothelial carcinoma (KEYNOTE-361): a randomised, open-label, phase 3 trial. *Lancet Oncol* 22, 931-945 (2021).

12. Galsky, M.D., *et al.* Atezolizumab with or without chemotherapy in metastatic urothelial cancer (IMvigor130): a multicentre, randomised, placebo-controlled phase 3 trial. *Lancet* 395, 1547-1557 (2020).

13. Ascierto, P.A., *et al.* Ipilimumab 10 mg/kg versus ipilimumab 3 mg/kg in patients with unresectable or metastatic melanoma: a randomised, double-blind, multicentre, phase 3 trial. *Lancet Oncol* 18, 611-622 (2017).

14. Wolchok, J.D., *et al.* Ipilimumab monotherapy in patients with pretreated advanced melanoma: a randomised, double-blind, multicentre, phase 2, dose-ranging study. *Lancet Oncol* 11, 155-164 (2010).

15. Lebbe, C., *et al.* Evaluation of Two Dosing Regimens for Nivolumab in Combination With Ipilimumab in Patients With Advanced Melanoma: Results From the Phase IIIb/IV CheckMate 511 Trial. *J Clin Oncol* 37, 867-875 (2019).

16. Rozeman, E.A., *et al.* Identification of the optimal combination dosing schedule of neoadjuvant ipilimumab plus nivolumab in macroscopic stage III melanoma (OpACIN-neo): a multicentre, phase 2, randomised, controlled trial. *Lancet Oncol* 20, 948-960 (2019).

17. Janjigian, Y.Y., *et al.* CheckMate-032 Study: Efficacy and Safety of Nivolumab and Nivolumab Plus Ipilimumab in Patients With Metastatic Esophagogastric Cancer. *J Clin Oncol* 36, 2836-2844 (2018).

18.	Antonia, S.J*., et al.* Nivolumab alone and nivolumab plus ipilimumab in recurrent small-cell lung cancer (CheckMate 032): a multicentre, open-label, phase 1/2 trial. *Lancet Oncol* 17, 883-895 (2016).

19.	Hammers, H.J*., et al.* Safety and Efficacy of Nivolumab in Combination With Ipilimumab in Metastatic Renal Cell Carcinoma: The CheckMate 016 Study. *J Clin Oncol* 35, 3851-3858 (2017).

20.	Sharma, P*., et al.* Nivolumab Alone and With Ipilimumab in Previously Treated Metastatic Urothelial Carcinoma: CheckMate 032 Nivolumab 1 mg/kg Plus Ipilimumab 3 mg/kg Expansion Cohort Results. *J Clin Oncol* 37, 1608-1616 (2019).

21.	Yau, T*., et al.* Efficacy and Safety of Nivolumab Plus Ipilimumab in Patients With Advanced Hepatocellular Carcinoma Previously Treated With Sorafenib: The CheckMate 040 Randomized Clinical Trial. *JAMA Oncol* 6, e204564 (2020).

22.	Wolchok, J.D*., et al.* Overall Survival with Combined Nivolumab and Ipilimumab in Advanced Melanoma. *N Engl J Med* 377, 1345-1356 (2017).

23.	Einerhand, S.M.H*., et al.* Survival after neoadjuvant/induction combination immunotherapy vs combination platinum-based chemotherapy for locally advanced (Stage III) urothelial cancer. *Int J Cancer* (2022).

24.	Pfister, C*., et al.* Randomized Phase III Trial of Dose-dense Methotrexate, Vinblastine, Doxorubicin, and Cisplatin, or Gemcitabine and Cisplatin as Perioperative Chemotherapy for Patients with Muscle-invasive Bladder Cancer. Analysis of the GETUG/AFU V05 VESPER Trial Secondary Endpoints: Chemotherapy Toxicity and Pathological Responses. *Eur Urol* 79, 214-221 (2021).

25.	Zargar, H*., et al.* Neoadjuvant Dose Dense MVAC versus Gemcitabine and Cisplatin in Patients with cT3-4aN0M0 Bladder Cancer Treated with Radical Cystectomy. *J Urol* 199, 1452-1458 (2018).

26.	Flaig, T.W*., et al.* Study EV-103: Neoadjuvant treatment with enfortumab vedotin monotherapy in cisplatin-ineligible patients (pts) with muscle invasive bladder cancer (MIBC): Updated results for Cohort H. *Journal of Clinical Oncology* 41, 4595-4595 (2023).

27.	Kamat, A.M*., et al.* Definitions, End Points, and Clinical Trial Designs for Bladder Cancer: Recommendations From the Society for Immunotherapy of Cancer and the International Bladder Cancer Group. *J Clin Oncol* 41, 5437-5447 (2023).

28.	Lindskrog, S.V*., et al.* Circulating Tumor DNA Analysis in Advanced Urothelial Carcinoma: Insights from Biological Analysis and Extended Clinical Follow-up. *Clin Cancer Res* 29, 4797-4807 (2023).

29.	Stimson, C.J*., et al.* Early and late perioperative outcomes following radical cystectomy: 90-day readmissions, morbidity and mortality in a contemporary series. *J Urol* 184, 1296-1300 (2010).

30.	Galsky, M.D*., et al.* Gemcitabine and cisplatin plus nivolumab as organ-sparing treatment for muscle-invasive bladder cancer: a phase 2 trial. *Nat Med* 29, 2825-2834 (2023).

31.	Balar, A.V*., et al.* Pembrolizumab monotherapy for the treatment of high-risk non-muscle-invasive bladder cancer unresponsive to BCG (KEYNOTE-057): an open-label, single-arm, multicentre phase 2 study. *Lancet Oncol* 22, 919-930 (2021).

32.	Chalmers, Z.R*., et al.* Analysis of 100,000 human cancer genomes reveals the landscape of tumor mutational burden. *Genome Med* 9, 34 (2017).

33.	Sharma, P*., et al.* Nivolumab Plus Ipilimumab for Metastatic Castration-Resistant Prostate Cancer: Preliminary Analysis of Patients in the CheckMate 650 Trial. *Cancer Cell* 38, 489-499 e483 (2020).

34.	Ryan, M.J. & Bose, R. Genomic Alteration Burden in Advanced Prostate Cancer and Therapeutic Implications. *Front Oncol* 9, 1287 (2019).

7

7

APPENDICES

Nederlandse samenvatting
Curriculum vitae
List of publications
Acknowledgements

NEDERLANDSE SAMENVATTING

Urotheelcarcinoom van de blaas, of blaaskanker is een veelvoorkomende vorm van kanker. Zodra er doorgroei in de spierlaag van de blaas wordt geconstateerd, is er sprake van spierinvasieve ziekte waarbij de prognose drastisch verslechterd en er een reële kans bestaat dat de ziekte uitbreidt naar de lymfeklieren of naar andere organen. De standaardbehandeling van spierinvasieve blaaskanker is een operatie waarbij de gehele blaas wordt verwijderd en er een urinestoma wordt aangelegd. Om de overlevingskansen te verbeteren worden patiënten voorafgaand aan de operatie veelal behandeld met cisplatin-bevattende chemotherapie. Helaas zijn er nog veel patiënten die ondanks deze intensieve behandeling op korte termijn uitzaaiingen ontwikkelen en niet meer te genezen zijn.

Immuuntherapie is een vorm van behandeling waarbij het immuunsysteem van de patiënt wordt ingezet om actief kankercellen op te sporen en te elimineren. Gezonde cellen hebben van nature een manier om te voorkomen dat zij worden herkend door het immuunsysteem. Kankercellen kunnen deze methode misbruiken om deze herkenning door het immuunsysteem te voorkomen. Immuuntherapie grijpt in op deze interactie waardoor de kankercellen alsnog kunnen worden herkend en geëlimineerd. Immuuntherapie gericht op de eiwitten PD-1, PD-L1 en CTLA-4 wordt sinds een aantal jaar toegepast in blaaskanker met bemoedigende resultaten. Daarnaast wordt het optimale gebruik van deze middelen uitgebreid onderzocht in studieverband.

In **Hoofdstuk 2** hebben we de huidige stand van zaken met betrekking tot de complexe wisselwerking tussen immuuntherapie en de directe omgeving van kankercellen in kaart gebracht. Met nieuwe behandelmogelijkheden komt de vraag wat voor elke individuele patiënt de optimale behandeling is. Daarnaast is het de vraag hoe we behandelingen zo effectief mogelijk kunnen combineren. Ook de komst van nieuwe middelen zoals enfortumab vedotin maakt het behandellandschap van blaaskanker meer divers en complex, maar uiteindelijk hopelijk vooral ook beter.

In **Hoofdstuk 3** hebben wij onderzocht of er bepaalde genetische afwijkingen in blaaskankercellen voorkomen die deze cellen meer gevoelig maken voor cisplatin-bevattende chemotherapie. Hiertoe hebben wij retrospectief een groot aantal patiënten bestudeerd dat werd behandeld met cisplatin-bevattende chemotherapie gevolgd door het verwijderen van de blaas. Wij hebben genetisch onderzoek verricht op het weefsel dat was verkregen voorafgaand aan het starten van de cisplatin-bevattende chemotherapie. Wij vonden dat patiënten met blaaskakercellen met een mutatie in het gen *ERCC2* een grotere kans had om goed te reageren op de cisplatin-bevattende chemotherapie. In eerdere studies werd gevonden dat afwijkingen in een aantal andere genen in blaaskankercellen mogelijk ook de kans zou vergroten om goed te reageren op cisplatin-bevattende chemotherapie. Hiervoor vonden wij in deze studie echter geen sterk bewijs. Al met al kunnen deze resultaten ertoe leiden dat patiënten met spierinvasieve blaaskanker beter

&

geselecteerd kunnen worden voor het wel of niet behandelen met chemotherapie voorafgaand aan het verwijderen van de blaas.

Bij patiënten met blaaskanker die met cisplatin-bevattende chemotherapie worden behandeld gevolgd door het verwijderen van de blaas, worden in veel gevallen nog vitale kankercellen aangetroffen bij het pathologisch onderzoek. Een recente studie heeft laten zien deze patiënten vermoedelijk baat hebben bij een aanvullende behandeling met nivolumab, een antilichaam gericht tegen het PD-1 eiwit. Dit doet vermoeden dat de chemotherapie die aanvankelijk wordt gegeven voorafgaand aan het verwijderen van de blaas al een bepaalde invloed heeft op de kankercellen zodat deze in tweede instantie een hogere kans hebben om te reageren op de immuuntherapie. Dit fenomeen wordt ook in andere vormen van kanker gezien. In **Hoofdstuk 4** hebben we onderzocht welke veranderingen er optreden in de kankercellen en hun directe omgeving als gevolg van cisplatin-bevattende chemotherapie. Hiertoe hebben wij weefsel onderzocht dat is verkregen voorafgaand aan de behandeling met chemotherapie en weefsel dat is verkregen na het verwijderen van de blaas. Vervolgens hebben wij de kankercellen en hun directe omgeving uit deze weefsel uitgebreid genetisch en immunohistochemisch onderzocht en de veranderingen in kaart gebracht. Wij vonden een toename was van CD8$^+$ lymfocyten na behandeling met chemotherapie, wat veelal wordt geassocieerd met een actieve immuunreactie tegen kankercellen. Echter, we vonden ook een toename in de TGF-β signaalcascade. Dit wordt geassocieerd met het remmen van de immuunreactie tegen de kankercellen. Wat precies de wisselwerking tussen chemotherapie en immuuntherapie is in de praktijk, en van welke factoren deze precies afhankelijk is, staat daarmee nog ter discussie.

In plaats van immuuntherapie te geven ná het verwijderen van de blaas, wordt er in studieverband ook onderzocht of immuuntherapie al voor de blaasoperatie kan worden gegeven. In de NABUCCO-studie hebben wij eerder gevonden dat een behandeling met immuuntherapie met zowel ipilimumab (antilichaam gericht tegen CTLA-4) als nivolumab (antilichaam gericht tegen PD-1) uitstekende resultaten oplevert, waarbij er bij ongeveer de helft van de patiënten geen vitale kankercellen meer worden gevonden bij het pathologisch onderzoek na het verwijderen van de blaas. In **Hoofdstuk 5** bespreken we de resultaten van het tweede cohort van de NABUCCO-studie. Hier hebben wij onderzocht wat de optimale dosering is van ipilimumab en nivolumab voorafgaand aan het verwijderen van de blaas. Net als in het eerste cohort vonden wij dat een behandeling met een relatief hoge dosering ipilimumab in combinatie met nivolumab uitstekende resultaten oplevert. Echter, we zagen ook dat een behandeling met een relatief lage dosering ipilimumab in combinatie met nivolumab minder goede resultaten opleverde. Omdat een deel van de patiënten zo'n goede reactie liet zien na de behandeling met gecombineerde immuuntherapie, dachten we dat het wellicht mogelijk zou zijn om voor geselecteerde patiënten het verwijderen van de blaas achterwege te laten. Om beter te kunnen voorspellen bij welke patiënten dit verantwoord zou zijn, hebben we voorafgaand aan de operatie onderzocht of er nog vrij DNA afkomstig van de blaaskankercellen meetbaar was in het bloed. We vonden dat bij de patiënten bij wie dit niet

&

meer te detecteren was, vrijwel allemaal ook geen vitale kankercellen waren terug te vinden bij het pathologisch onderzoek na het verwijderen van de blaas. Potentieel zouden deze patiënten wellicht de operatie achterwege kunnen laten en in plaats daarvan intensiever gecontroleerd kunnen worden.

Hoewel ons onderzoek primair gericht is op blaaskanker, hebben wij ook prostaatkanker onderzocht. Vergeleken met blaaskanker komt prostaatkanker zeer veel voor, maar wordt het ook vaak per toeval gevonden en verder ontwikkelt deze vorm van kanker zich vaak langzaam. Studies naar de effectiviteit van immuuntherapie bij prostaatkanker hebben tot nog toe niet veel opgeleverd, in tegenstelling tot studies in blaaskanker en in andere vormen van kanker. Bij het verwijderen van de blaas vanwege blaaskanker wordt bij mannen ook de prostaat verwijderd. Bij een aanzienlijk deel van deze mannen wordt daarbij ook per toeval prostaatkanker gevonden. In **Hoofdstuk 6** hebben we de unieke gelegenheid aangegrepen om te onderzoeken wat het effect is van een behandeling met gecombineerde immuuntherapie op prostaatkanker die toevalligerwijs werd gevonden na en het verwijderen van de blaas in de NABUCCO-studie. Hoewel we bij het pathologisch onderzoek van de blaas uitgebreide tekenen zagen van een reactie op immuuntherapie, zagen we geen enkele verandering in de prostaatkanker bij de patiënten waarbij dit werd geconstateerd. Zelfs na het vergelijken van deze groep patiënten met een groep die níet werd voorbehandeld met immuuntherapie, zagen we geen verschillen.

In de discussie blikken we uitgebreid terug op de onderzoeken die zijn gedaan, en wat we hierbij achteraf anders of beter hadden kunnen doen. Op basis van de resultaten van de NABUCCO-trial doen we daarnaast nog een fictief voorstel voor een tweetal klinische trials. In de *MacBeth* trial willen we onderzoeken of gecombineerde immuuntherapie gevolgd het verwijderen van de blaas wellicht even goed of zelfs beter is dan de standaardbehandeling met cisplatin-bevattende chemotherapie gevolgd door het verwijderen van de blaas. In de *Night's Dream* trial onderzoeken we met behulp van DNA afkomstig van blaaskankercellen in het bloed of we voor een selecte groep patiënten wellicht het verwijderen van de blaas achterwege kunnen laten en in plaats daarvan meer intensieve controles kunnen doen. Deze fictieve trials dienen vooral om te illustreren hoeveel er de laatste jaren is veranderd in het onderzoek naar blaaskanker.

&

CURRICULUM VITAE

Jeroen van Dorp was born on 8 August 1991 in Vlaardingen, The Netherlands. After graduating from the Groen van Prinsterer Lyceum in 2009, he started his medical training at the Erasmus Medical Center in Rotterdam. In his second year of the bachelor program, he got accepted into the Molecular Medicine research master program. After finishing his bachelor degree in Medicine, he continued with the research master program and joined the lab of Catherine Robin at the Hubrecht Institute in Utrecht. After finishing this internship, he continued his medical training at the Erasmus Medical Center where he developed a keen interest for urology and did his final medical internship at the urology department in the Erasmus Medical Center after which he obtained his first master's degree in Medicine in 2016. He then continued at the lab of Guido Jenster at the department of Experimental Urology in the Erasmus Medical Center and focused on prostate cancer metastasis in xenograft mouse models. With that, he obtained his secondary master's degree in Molecular Medicine in 2017. He then applied for a position as a PhD candidate in the Group of Michiel van der Heijden at the Netherlands Cancer Institute in Amsterdam focusing on neoadjuvant treatment for muscle-invasive bladder cancer, the results of which are presented in this thesis. He then started to work as a clinician at the urology department in the Alrijne Hospital in Leiden and got accepted into residency in 2023 to become an urologist. He aspires to keep combining urological patient care with scientific research to ultimately improve care for patients with urological cancer.

LIST OF PUBLICATIONS

Maksim Chelushkin & Jeroen van Dorp *et al.*, Platinum-based chemotherapy induces opposing effects on immunotherapy response-related spatial and stromal biomarkers in the bladder cancer microenvironment. *Submitted to Clinical Cancer Research.*

Jeroen van Dorp and Michiel S. van der Heijden, The bladder cancer immune micro-environment in the context of response to immune checkpoint inhibition. *Frontiers of Immunonology (2023)*.

Jeroen van Dorp *et al.*, Nabucco Cohort 2: Hoog Versus Laag Gedoseerd Ipilimumab In Combinatie Met Nivolumab Als Preoperatieve Therapie Voor Lokaal Gevorderd Urotheelcarcinoom. *Nederlands Tijdschrift voor Oncologie (2023)*

Sarah M.H. Einerhand, Jeroen van Dorp *et al*., Re: Neoadjuvant PD-L1 plus CTLA-4 Blockade in Patients with Cisplatin-ineligible Operable High-risk Urothelial Carcinoma. *European Urology (2023)*.

Jeroen van Dorp *et al*., High- or low-dose preoperative ipilimumab plus nivolumab in stage III urothelial cancer: the phase 1B NABUCCO trial. *Nature Medicine (2023)*.

Alberto Gil-Jimenez & Jeroen van Dorp *et al.*, Assessment of Predictive Genomic Biomarkers for Response to Cisplatin-based Neoadjuvant Chemotherapy in Bladder Cancer. *European Urology (2023)*.

Sarah M.H. Einerhand, Jeroen van Dorp *et al*., Survival after neoadjuvant/induction combination immunotherapy vs combination platinum-based chemotherapy for locally advanced (Stage III) urothelial cancer. *International Journal of Cancer (2022)*.

Anne-Gaëlle Goubet, Jeroen van Dorp *et al.*, Escherichia coli-Specific CXCL13-Producing TFH Are Associated with Clinical Efficacy of Neoadjuvant PD-1 Blockade against Muscle-Invasive Bladder Cancer. *Cancer Discovery (2022)*.

Jeroen van Dorp *et al.*, A Serendipitous Preoperative Trial of Combined Ipilimumab Plus Nivolumab for Localized Prostate Cancer. *Clinical Genitouriny Cancer (2022)*.

Sander A.L. Palit, Jeroen van Dorp, *et al.*, A kinome-centered CRISPR-Cas9 screen identifies activated BRAF to modulate enzalutamide resistance with potential therapeutic implications in BRAF-mutated prostate cancer. *Scientific Reports (2021)*.

&

ACKNOWLEDGEMENTS

Michiel, bedankt voor de fantastische tijd die ik heb gehad als promovendus in het NKI; het was een groot genoegen om met je samen te werken en ik heb veel van je kunnen leren. Ik hoop van harte dat onze paden blijven kruisen in de toekomst.

Bas, ontzettend bedankt voor de input in vrijwel alle projecten waar ik aan heb gewerkt heb. Ik kijk er naar uit om over te zijner tijd weer samen te werken tijdens mijn differentiatiestage in het NKI.

John, Leila, Lodewyk and Marleen, thanks a lot for your guidance and input during the OOA meetings.

Chantal, ik ben heel dankbaar voor de periode die we samen hebben doorgebracht op het NKI. Heel mooi om te zien dat jij nu het werk omtrent de NABUCCO-trial voortzet.

Sarah, bedankt voor de tijd die we samen hebben doorgebracht in het NKI en vooral ook dat je de ICRA van mij hebt overgenomen.

Nick, bedankt je me de eerste jaren wegwijs hebt gemaakt in de groep van Michiel.

Alberto, I really enjoyed working together and am proud of the manuscript that we wrote on together, which is part of this thesis. I hope we will stay in touch.

Maksim, I enjoyed working together on the pre- and post-treatment data from the neoadjuvant chemotherapy cohort. It took several detours, but we are now close to publishing this manuscript, thanks for all the hard work.

Sander, dank dat je me de eerste periode wegwijs hebt gemaakt op B7 en in het NKI. Ik heb heel veel van je geleerd en ik vond het ontzettend leuk om samen te werken aan de genetic screen die uiteindelijk onderdeel is geworden van jouw proefschrift.

Daniel, dank voor je bijdrage aan de projecten over neoadjuvante chemotherapie waar ik met Alberto en Maksim aan heb gewerkt.

Živa, João, Fleur, Antonio and Robin, Despite never really working together, I really enjoyed being a PhD student on B7 and having you around as colleagues and friends. I hope we will stay in touch.

Patty, dank voor alle hulp tijdens mijn tijd op B7. Met name voor het versturen van post naar andere ziekenhuizen en de hulp voor het in orde maken van alle verplichte cursussen.

&

Rene, dank voor de periode op B7, ik heb me hier altijd welkom gevoeld. Daarnaast ook bedankt dat ik mee mocht naar Toscane en de befaamde jaarlijkse lunches bij Loetje.

Annemieke, Arnout, Astrid, Ben, Cor, Elke, Gabriele, Haojie, Johan, Kathy, Katrien, Koen, Kristan, Liqin, Marieke, Marielle, Matheus, Mengnuo, Roderick, Rodrigo, Sara, Silvana, thanks for the unforgettable years as part of B7. I have felt very much at home there, despite spending most of the time outside of the lab. Thanks for the help and guidance at the lab with the few experiments that I conducted there. I cherish the memories of the conversations and small-talk with all of you.

Alle collega's van het CFMPB, met name Annegien, Erik, Iris, Dennis, Rens, Wouter, Maartje, Linde en Ingrid bedankt voor alle hulp met het verzamelen van weefsel, het isoleren van DNA en RNA en het verwerken van alle kleuringen. Jullie hebben een onmisbare bijdrage geleverd aan dit proefschrift. Iris, dank voor al je hulp bij het annoteren en analyseren van alle multiplex immunofluorescentie data. Zonder jouw hulp was dit nooit gelukt.

Alle collega's van de GCF, met name Wim, Charlaine, Ron en Roderick bedankt voor het sequencen van DNA en RNA in veel van onze projecten, en daarnaast al het technisch advies hieromtrent.

Maurits en Joyce, bedankt voor jullie hulp met het beoordelen van alle kleuringen van het patiëntmateriaal voor zowel de NABUCCO als de projecten met neodjuvante chemotherapie.

Iedereen betrokken bij de NABUCCO-trial, met name Jeantine, Kees, Maaike, Thierry, Elsbeth, Anoesjka, Jolanda, Britt, Richard, Niven en Toine bedankt voor jullie bijdrage aan de NABUCCO-trial.

Nitzan and Chris, thanks for the opportunity to collaborate in the NABUCCO-trial.

Dank aan alle patiënten die hebben deelgenomen aan de NABUCCO-trial, dank voor jullie bijdrage aan de wetenschap, dankzij jullie hebben wij een innovatieve behandeling voor patiënten met gevorderde blaaskanker kunnen onderzoeken.

Lieve Jet, jij hebt dit hele avontuur met mij van dichtbij meegemaakt. Je hebt alle hoogtepunten met me kunnen vieren en bood een luisterend oor bij alle dieptepunten en onzekerheden. Dit proefschrift is net zo goed jouw prestatie als de mijne. Tijdens deze reis hebben wij onze plek gevonden in Delft en zijn we getrouwd. Ik kan niet wachten om dit avontuur verder voort te zetten met jou naast me.

&

&